Monoclonal antibody (mAb) purification by Counter Current Chromatography (CCC)

A thesis submitted to Brunel University

for the degree of

Doctor of Philosophy

by

Samantha Fernando

Institute for Bioengineering, Brunel University, London

December 2011

Abstract

Counter current chromatography (CCC) is a form of liquid liquid chromatography, which the Brunel Institute for Bioengineering (BIB) team have developed to process scale. In this thesis, its application has been successfully extended to the rapid, scalable purification of monoclonal antibodies (mAb) from mammalian cell culture, using aqueous two-phase systems (ATPS) of inorganic salts and polymer. A polyethylene glycol (PEG) and sodium citrate system was found to be the most appropriate by robotic phase system selection. The search for an economical alternative to protein A HPLC is a substantial bioprocessing concern; in this work CCC has been investigated.

Initial studies showed that unpredictably, despite separation from impurities being achieved, some loss in the IgG's ability to bind to Protein A was seen, as confirmed by Protein A BiaCore analysis. CCC machines were seen to adversely affect IgG functionality. This led to a systematic investigation of the effect of CCC phase mixing on IgG functionality in a number of different CCC instruments, allowing direct comparisons of modes of CCC (hydrodynamic and hydrostatic CCC) and their associated mixing (wave-like and cascade, respectively). The varying g forces produced within the CCC column were determined using a recently developed model to calculate g force range. The effect of interfacial tension was also studied using a custom built 'g' shaker.

The optimum CCC mode was identified to be the non synchronous CCC, operated in a hydrodynamic mode but allowing bobbin to rotor speed (Pr ratio) to be controlled independently. In a normal synchronous J type centrifuge a Pr of 1 is fixed, this is where the bobbin and rotor speed are identical I.e. one bobbin rotation (where mixing occurs) to one rotor revolution (where settling occurs). Constraints were seen with this 1:1 ratio and the separation of mAb using ATPS. This work has shown with the use of the non synchronous CCC at a Pr of 0.33, mixing is reduced and rotor rotations increased. Consequently the associated g force range is decreased. Furthermore, by the extension of settling time, the clear separation of the mAb from impurities has been achieved with retention of biological activity.

This thesis demonstrates the importance of settling time for ATPS in phase separation and documents the fundamental requirements for the successful separation of biologics. Purified non synchronous CCC samples have additionally undergone rigorous quality control testing at Lonza Biologics by their purification

scientists. This work has ultimately showed that with optimisation, the non synchronous CCC can be used to produce biological samples that are of industry standard.

Table of contents

Acknowledgements

Firstly, I would like to acknowledge all my supervisors for giving me the opportunity to accomplish a personal ambition with the studying of a PhD. Foremost I would like to thank my first supervisor Dr Ian Garrard, for all his invaluable support, ideas, enthusiasm, encouragement and advice. It was a real pleasure to work alongside him and I immensely enjoyed his company on a personal level too. I would like to thank Professor Derek Fisher for his expertise, insight, scientific support and tuition on biochemistry aspects.

A deepest of thank you is extended to my industrial sponsor Dr Lee Allen and his team for their help. I thank Dr Lee Allen for all his knowledge, approachability, promptness and general manner, which has made this collaboration so beneficial to me. For all the industrial insight and laboratory skills I have acquired, I am very grateful. In particular, I would like to greatly thank Mr Samit Patel for all his expertise, experience and training within the laboratory. Most specifically for the entire QC testing he personally conducted and his continual willingness to help or add clarity.

Great thanks and appreciation is given to all my colleagues at the Brunel Institute for Bioengineering. In particular, to Mr Lukasz Grudzien for his experimental advice, training, assistance within the laboratory at times of difficulty (leaks, machine blockages, pumps breakages etc!), scientific discussion and most of all friendship. Professor Ian Sutherland (for invaluable insight and engineering advice on all CCC machines), Dr Remco van den Heuvel (for experimental advice and the use of his g force program), Mrs Caroline Kenealy (for ordering and organisation of numerous conferences so efficiently) and Mr Tony Bunce (for making the custom built shaker).

I wish to extend a heartfelt thank you to all the other PhD students at BIB, who have now become great friends. Mostly for all the camaraderie, entertainment, and laughter we have shared, through what has been an extremely challenging time.

Within the Division of Biosciences at Brunel I thank Professor Robert Evans for the use of his laboratories and also knowledge and advice regarding protein chemistry. I also thank Dr Ian Boluton, for the training and insight into the Biacore technology.

To my fiancé, Chris, I sincerely thank him for all his infinite patience, personal support and love, without which this journey would have been so much harder.

Finally I dedicate this thesis to my parents without whom this would not have been possible. In particular for all the unconditional love and financial support they have tirelessly and unfalteringly given me. I thank my mother for her endless support and persistent encouragement at the hardest of times. I thank my father, for his constant reassurance and reasoning.

Abbreviations

ATPS	Aqueous two phase system
BCA	Bicinchoninic acid
BIB	Brunel Institute for Bioengineering
CCC	Counter current chromatography
CCD	Counter-current distribution
CCS	Cell culture supernatant
CDR	Complementarily determining regions
CEX	Cation exchange chromatography
CHO	Chinese Hamster Ovary
CPC	Centrifugal partitioning chromatography
DNA	Deoxyribonucleic acid
ELISA	Enzyme linked immunosorbent assay
Fab	Fragment of antigen binding
Fc	Constant fragment
FDA	Food and Drug Administration
HCP	Host cell proteins
HPLC	High pressure liquid chromatography
HIC	Hydrophobic interaction chromatography
IgG	Immunoglobulin G
K	Partition coefficient
kDa	Kilodalton
mAb	Monoclonal antibody
PA	Protein A
PEG	Polyethylene glycol
Pr	Planetary drive ratio
PTFE	Polytetrafluoroethylene
QC	Quality control
qPCR	Quantitative polymerase chain reaction

rpm	Revolutions per minute
SDS PAGE	Sodium dodecyl sulfate polyacrylamide gel electrophoresis
Sf	Stationary phase retention
TC CCC	Toroidal coil counter current chromatography
VH	Heavy chain variable domain
VL	Light chain variable domain

The following abbreviations have been used to ease representation in phase system composition:

K citrate	Potassium citrate and citric acid
KPO_4	di-Potassium monohydrogen phosphate and potassium dihydrogen phosphate
Na citrate	Sodium citrate and citric acid
$NaPO_4$	di-Sodium monohydrogen phosphate and sodium dihydrogen phosphate
$NaSO_4$	Sodium sulphate
NH_4PO_4	di-Ammonium hydrogen orthophosphate and ammonium di-hydrogen orthophosphate
NH_4SO_4	Ammonium sulphate

CHAPTER 1: Aims and objectives and literature review

1.1.1 Monoclonal antibody discovery

Monoclonal antibodies (mAbs) are therapeutic proteins, naturally manufactured by the body's B cells, with a typical molecular weight of 150kDa. They were discovered in 1975 by Kohler and Milstein using hybridoma technology. A hybridoma is defined as a biologically constructed hybrid of a mortal antibody producing lymphoid cell with a malignant or immortal myeloma cell (Marx *et al.*, 1997). Hybridoma technology has allowed the limitless production of antibodies from a single clone, thereby named monoclonal antibodies. All resulting antibodies were thus identical and highly specific, creating a major advance in biotherapeutics. Initially, in *vivo* production of mAbs was in mice and rats. The immune system of the animals was primarily suppressed, a hybridoma was injected and multiplication occurred in the peritoneal cavity. Ascetic fluids produced were rich in secreted antibody. Following an appropriate incubation interval, the animal was killed and ascites drained. Despite very high antibody yields being produced in the range of 1-20mg/ml, ethical concerns were raised due to the manner of their production. Additionally, as mAbs were produced in animals, they showed reduced immunoreactivity of around 60-70% (Marx *et al.*, 2007) in humans, lowering their ability to induce human responses (Figure 1.1.1).

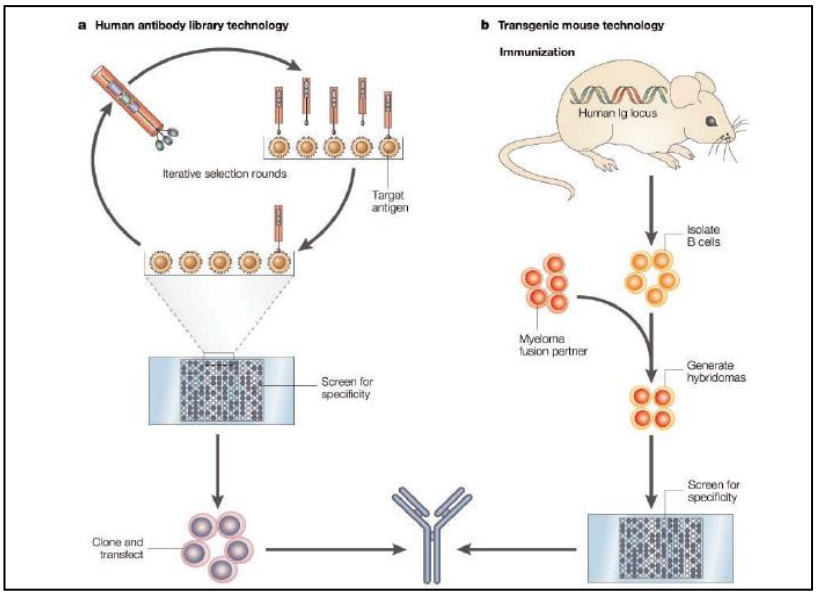

Figure 1.1.1: In vitro and in vivo human antibody production. b) Primarily based on hybridoma technique, monoclonal antibodies were produced using mouse models. These genetically engineered mouse produce humanized immunoglobulins, immortalization is by fusion with the myeloma cell line. A) Due to the demand for human antibodies, libraries can now be used to improve specificity by irrelative selection using a specific target antigen. The library of antibodies can be panned against a target. Antibodies are amplified with Escherichia coli and selection rounds continue until the antibody of correct specificity is obtained (Brekke et al., 2003).

Investigations showed the F_C constant region of the IgG structure was murine in origin, therefore affecting dosing in humans. Patients were seen to develop human-antimouse antibodies (HAMAs) which adversely complexed with murine mAbs, leading to unwanted sickness e.g. acute anaphylactic (Binyamin *et al.*, 2006). Research was prompted into a transition from mouse monoclonal antibodies to mouse-human chimaeras (Weiner et al, 2010). Previous immunogenicity issues were overcome by substitution of mouse constant domains with that of human heavy constant domains (Baker, 2005; Trikha *et al*., 2002).

As the necessity and demand for mAbs has increased, sufficient pressure has been placed on the large scale production of humanized monoclonal antibodies. The majority of monoclonal antibodies now produced use mammalian cell expression systems, for example Lonza uses Chinese Hamster Ovary (CHO) cells. The CHO cell line is typically used due to its relative similarity to the human glycolyasation pattern and stability as an expression system. Cell line stability of an expression system is critical in the production of the desired protein. Generation of the product is only possible when cells accept foreign DNA, in which all antibody information is stored (Sommerfield *et al*., 2005). Due to the need for the highest possible production rate by the cells, an amplification system is typically used. At Lonza (Lonza Biologics, Slough, UK, this company is particularly referred to as they are the industrial sponsors of the CASE studentship) they use the glutamine synthetase (GS) system (Birch *et al.*, 2006; Birch *et al*., 2005).

1.1.2 mAb cell culture production

Cell productivity has greatly increased over the past decade, generating high yields of mAbs. Batch feeding with nutrient fortification has been a major factor in achieving these titres (Trebak *et al.*, 1999) (Figure 1.1.2.1). Serum, which is of animal origin, is generally used to provide essential nutrients for growth. Although cutting edge mammalian cell culture proteins are serum free and use chemically defined media. This simplifies purification and reduces regulatory concerns about potential pathogens. Batch feeding has been found to maximise final mAb yield by increasing cell culture longevity and mAb secretion rate (Bibila *et al.*, 1995).

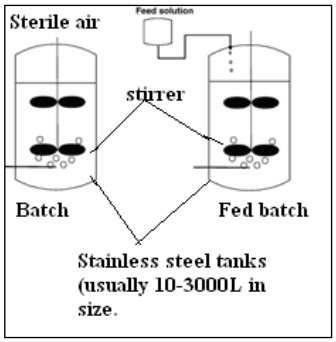

Figure 1.1.2.1: Representation of batch feeding which has resulted in hugely improved cell culture titres. Improvements have been made to previous batch culture (left), where no nutrients were supplemented. In fed-batch culture, nutrients are fed at specific time intervals during the fermentation process (Birch et al., 2006).

Purification of mAbs that follows the fermentation process requires the removal of a variety of protein products secreted by the cells into the fermentation broth (Figure 1.1.2.2). Additionally cell culture medium e.g. amino acids, inorganic salts, vitamins and supplements added for example calf serum must be separated from the product protein. Also DNA, viruses and lipids present in fermentation broth as by products from cell lysis must be removed along with host cell proteins. A vast range of proteins are required to be separated from the protein of interest (mAb), making purification extremely challenging (Somerfield *et al.*, 2005).

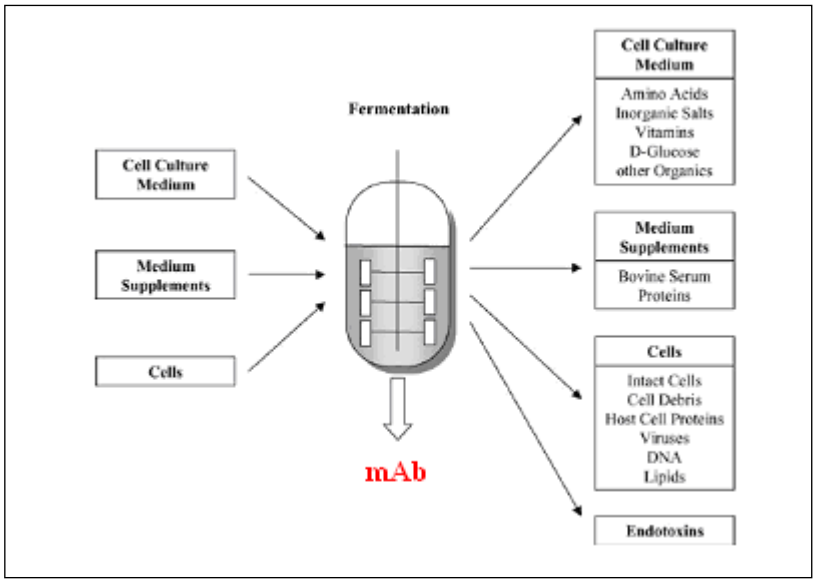

Figure 1.1.2.2: Fermentation tank. On the left hand side all components needed to produce mAb are shown. By-products from cell lysis and the fermentation process must also be removed. Also the mAb must be removed from other proteins, making purification extremely challenging (Sommerfeld et al., 2005).

1.1.3 Mab structure

Antibodies (IgG) are therapeutic molecules with a well defined biochemical structure. Their structure is the major determinant of their resulting specificity to a range of targets (Shukla *et al.*, 2007). Immunoglobulins are defined by four covalently linked polypeptide chains, which are subject to varying degrees of glycosylation. Two distinct functional units make up an antibody; these are known as the fragment of antigen binding (Fab) and the constant fragment (Fc). Of these four polypeptide chains, two chains are heavy and two chains are light and are held together by an intermolecular disulfide bonds (Hinge). All chains are folded into immunoglobulin domains. The Fab contains the variable domains, consisting of three hypervariable complementarily determining regions (CDRs) at the amino terminal part of the molecule. These CDRs form the antigen binding site of the antibody. The binding site is formed where light chain variable domain (VL) and heavy chain variable domain (VH) meet, and antigen specificity and resulting affinity is conferred here (Weiner et al, 2010). The light chain has one constant domain (CL) and one variable domain (VL). The heavy chain, however, has one variable domain (VH) and three constant domains (CH1,CH2,CH3) (Tabrizi *et al.*, 2006). The remaining part of the antibody is composed of a 'constant domain', which varies only between classes and serves to bind varying effector molecules (Brekke *et al.*, 2002). The heavy and light chains are held together by a combination of non covalent and covalent interactions to the disulfide hinge region (Figure 1.1.3.1).

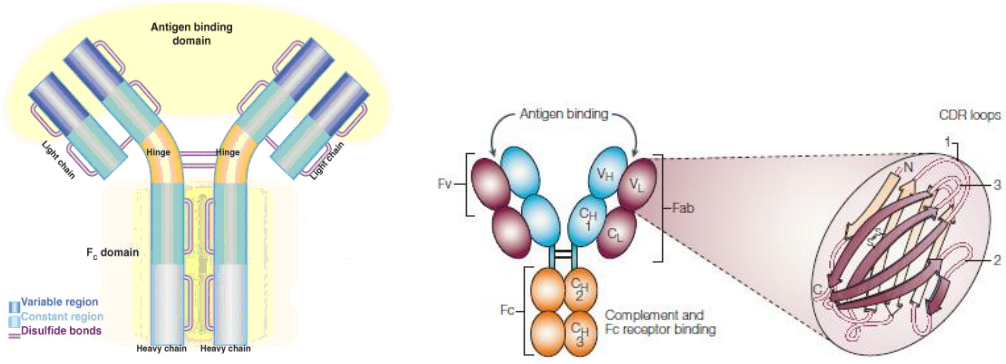

Figure 1.1.3.1: The 4 chain basic structure of Immunoglobulins is shownn (left). Heavy and light chain produce a complete molecule of 150 kDa (Steinmeyer et al., 2008). On the right hand side, Fc and Fab portions are labelled. The resulting inter-chain disulfide bonds and non-covalent interactions can be seen. Specificity is conferred in the CDR loops of the variable region. (Brekke et al., 2002).

There are five different classes of antibodies that exist: IgA, IgD, IgE, IgG and IgM, which are distinguished by the type of heavy chain they contain. It is this difference in heavy chain polypeptide that gives rise to differing structure and therefore biological activity of the classes. The difference is found within the Fc fragment; in addition to this some classes such as IgG, can be further divided into subclasses e.g. IgG1, IgG2, IgG3 and IgG4. The IgG monomer is the most abundant class in human serum; and is the only class to cross the placenta in humans during birth (Figure 1.1.3.2). IgGs are usually used as therapeutics due to the biological response they elicit. Both its abundance and specificity make it an extremely attractive molecule for both research and clinical diagnostics (Pierce scientific).

Molecular weight	150kDa Total size 55kDa for each heavy chain 25kDa for each light chain
Serum concentration	10-16 mg/ml
Percent total Ig	75%

Figure 1.1.3.2: Table summarising IgG properties

1.1.4 Monoclonal antibody market

Monoclonal antibodies due to their specificity represent a multibillion pound industry (Reichert *et al.*, 2008). The therapeutic properties of mAbs for the treatment of a range of diverse diseases have established them as the biggest selling biotherapeutics, known as a blockbuster. mAbs are an equally attractive molecule for diagnostics and are used in a number of differing assays e.g. virus assays. Over 20 mAbs have currently been FDA approved as shown in Figure 1.1.4.1. Their unique selling point of specificity has allowed their applications to grow from biotechnology and diagnostics to most recently the human proteome (Roque *et al.*, 2007). It has been reported, that 3200 pharmacological target in the body out of a possible 5200 in the human genome are susceptible to protein intervention (Steinmryer *et al.*, 2009).

Product	Company	Indication	Category	Year
OKT-3	Johnson & Johnson	Transplant rejection	mMAB	1986
ReoPro	Johnson & Johnson	Percutaneous transluminal coronary angioplasty (PCTA)	cMAB	1993
Rituxan	IDEC/Genentech	B-cell lymphoma	mMAB	1997
Herceptin	Genentech/Roche	Breast cancer	hzMAB	1998
Remicade	Johnson & Johnson	Rheumatoid arthritis/Crohn's disease	cMAB	1998
Simulect	Novartis	Transplant rejection	cMAB	1998
Synagis	Abbott/MedImmune	Respiratory syncytial virus	hzMAB	1998
Zenapax	Roche/PDL	Transplant rejection	hzMAB	1998
Mylotarg	Celltech/AHP	Acute myeloid leukemia	hzMAB	2000
Campath	Millenium/Ilex/Baxter	Chronic lymphocytic leukemia	hzMAB	2001
Zevalin	IDEC	Non-Hodgkin's leukemia	cMAB	2002
Humira	Abbott	Rheumatoid arthritis	humMAB	2003
Xolair	Genentech/Novartis	Allergic asthma	humMAB	2003
Bexxar	Corixa/GlaxoSmithKline	Non-Hodgkin's leukemia	mMAB	2003
Raptiva	Genentech/Xoma	Moderate to severe psoriasis	hzMAB	2003
Erbitux	ImClone/BMS/Merck	Various cancers	cMAB	2004
Avastin	Genentech/Roche	Various cancers	hzMAB	2004
Tysabri	Biogen Crop.	Multiple sclerosis	hzMAB	2004
Enbrel	Immunex	Rheumatoid arthritis/active ankylosing spondylitis	Fus. Prot	1998
Amevive	Biogen Corp.	Chronic plaque psoriasis	Fus. Prot	2003

Figure 1.1.4.1: mAb currently FDA approved and their corresponding indications. (Sommerfield et al., 2005).

The therapeutic indications for mAbs are growing and now encompass oncology, arthritis, infectious disease and immune and inflammatory disorders (AIID) (Reichert *et al.*, 2004). More recently they have been seen to provide customised affinity against drug abuse e.g. prevention of relapse for nicotine addiction (Peterson *et al.*, 2006). Moreover, due to their incredible specificity and limited side effects they remain popular in cancer therapy (Alkan, 2004). Other cancer therapies are well known for their inability to distinguish healthy cells from those of the target tumour cells, hence resulting in toxicity to the patients. Minimal toxicity is seen with mAbs as they can be designed to selectively target the tumour cells and elicit anti-tumour effects. Their mode of action is either by complement mediated cytolysis, cytotoxicity, delivery of radiation or blocking receptors or growth factors (Zhang *et al.*, 2007). The targets used by mAbs in oncology treatment are shown in Figure 1.1.4.2.

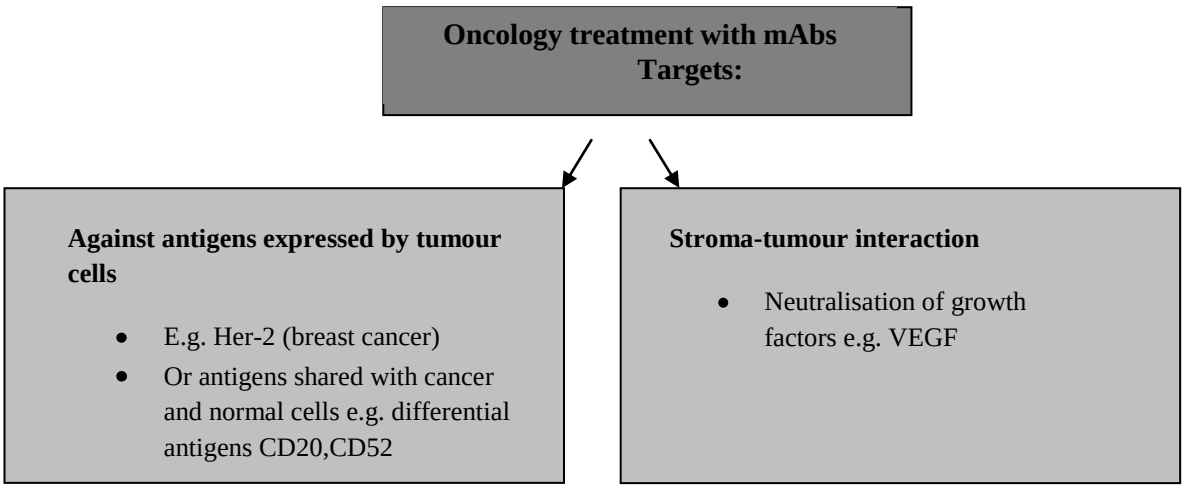

Figure 1.1.4.2: Overview of oncology treatment targets with the use of mAbs

1.1.5 Modes of action

The ultimate aim of mAbs is to eliminate or neutralise infection or to treat disease targets. It is this biological activity that is exploited therapeutically.

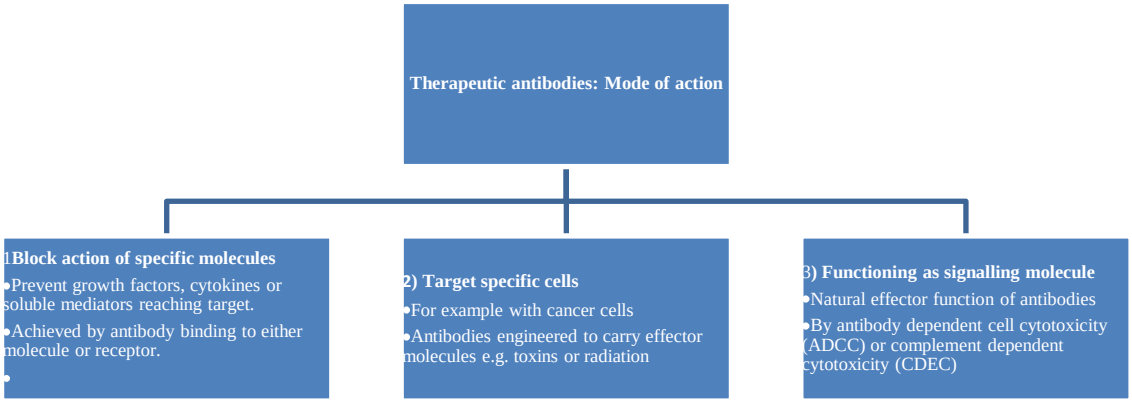

Figure 1.1.5.1: Overview of mAb therapeutic modes of action. Characterized into three modes: (1) blockage of specific molecules,(2) targeting of specific cells or (3) functioning as signalling molecules.

1.1.6 Upstream/ Downstream processing of mAbs

The standard commercial purification protocol for mAbs is shown in Figure 1.1.6.1. The principle purification step used is Protein A (PA) chromatography and this platform approach will be discussed further in later sections.

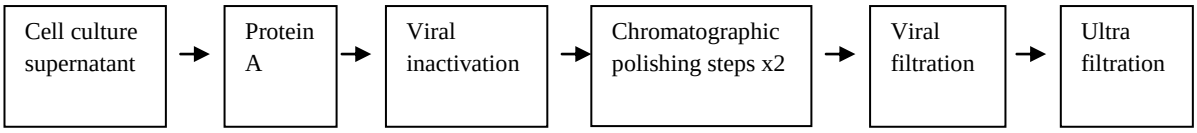

Figure 1.1.6.1: Platform approach typical used in mAb purification using Protein A purification Cell culture supernatant is typically purified by the capture step Protein A chromatography. . In order to remove all contaminates post Protein A capture and to obtain purity to regulatory compliance, two additional chromatographic polishing steps are employed.

Vast improvements upstream in cell culture titres have been achieved; however this has not been directly translated into downstream success, creating a processing bottleneck. Upstream productivity has increased greatly due to previous challenges of bioreactor size, cell culture cycle time and low expression level being overcome. Significant improvements in growth medium and feeding strategies have been made (Swinnen *et al.,* 2007) (Figure 1.1.6.2). Further improvements upstream are still being investigated and include the manipulation of genotypes to produce more stable cell lines and also the use of differing expression systems as opposed to mammalian cells. Recent work has suggested future trends will involve the use of *E.Coil* and yeast with a less expensive and less complex processing time (Birch *et al.*, 2006; Farid *et al.*, 2007; Jiang *et al.*, 2010)

Concerns, however, have shifted downstream; high titres of mAbs now produced by cell culture cannot be processed downstream at the equivalent rates. Downstream processing accounts for 50-80% of total manufacturing costs. The need for a balance between upstream and downstream processing has never been so important. The following costs are encompassed in downstream processing: equipment, consumables, labour, waste treatment, raw material and disposal. Of these costs, the PA resin accounts for 80%, due to its high cost. Despite platform approaches being seen as advantageous in terms of streamlining and costs, manufacturing constraints can still be a problem. Due to the price of the PA resin companies routinely use smaller columns with repeat cycling, increasing the time to process (Low *et al.*, 2007). A need for a replacement that is economically viable, therefore allowing future sustainability, is a major bioprocessing issue. Industrial priorities have now shifted from not only replacing Protein A, but also

reducing unit operations. Integration is required that will reduce loss in yield between each unit operation (Somerfield *et al.*, 2005).

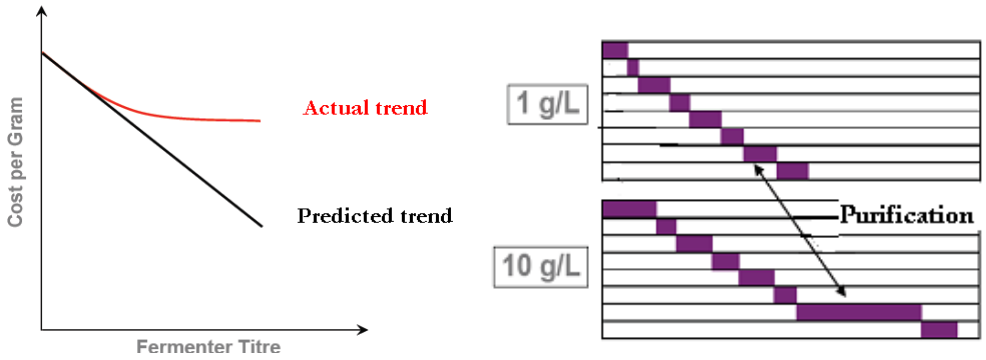

Figure 1.1.6.2: Bioprocessing bottleneck created by mAb purification by Protein A. As fermentation titres have increased, the cost per gram of mAbs would have been predicted to decrease in a linear manner. Plant throughput issues due to cost and processing constraints by PA have resulted in the cost per gram of mAbs to plateau off (Left graph). With the production of mAbs (steps represented by single purple boxes) an increase in titres has significantly increased plant purification time (Right graph). Pictures courtesy of Lonza biologics.

1.1.7 Protein A: Structure

The natural affinity between Protein A and IgG forms the basis of Protein A purification. Protein A is derived from gram-positive bacterium *Staphylococcus aureus*. It is a cell wall associated protein domain that resides on the bacterium surface. Sequencing of the staphylococcus protein A (SPA) was conducted by Uhleh *et al* (1984) this was to predict the gene encoding Protein A was composed of three distinct regions. These being: S for signal sequence, five homologous IgG binding domains, E, D, A, B and C, and a cell wall anchoring region XM (Hober *et al.*, 2007) (Figure 1.1.7.1). It is the five IgG binding domains which allow affinity binding of the Fc portion of IgG1, IgG2 and IgG4.

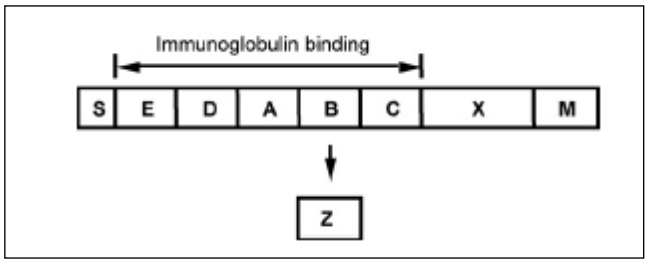

Figure 1.1.7.1: Protein A structure. Protein A has a molecular weight of around 42kDa. Domains E,D,A,B,C define the Fc binding site to the mAb. Specificity offered by protein A to IgG has made it a hugely studied molecule. An engineered domain termed 'z' has been produced and is used in affinity resins (e.g. Mabselect SURE). (Hober et al., 2007).

1.1.8 Protein A chromatography

Monoclonal antibody purification by Protein A is the gold standard capture method in biopharmaceutical manufacturing. It is used due to its incredible specificity. Due to the affinity interaction of the mAb with protein A, a reduced level of non specific binding is seen, thereby increasing operational yields. The ability of protein A to tolerate crude extracts from the cell culture starting supernatant, allows a one step purification to a specificity of > 99.5%. Polishing steps remove host cell proteins, DNA and aggregated IgG to an acceptable level. The uniform platform approach offered by Protein A purification allows manufacturing harmonization, where all additional steps have been investigated to allow efficient mAb production (Follman *et al.*, 2004).

Cuatrecasas et al in 1968 introduced this form of affinity chromatography for antibody purification. Protein A ligands are covalently immobilised onto a solid (agarose) support and packed into a chromatographic column. Cell culture supernatant is loaded onto the column and IgG is retained by its interaction with protein A. Further washing allows unbound non specific species to be washed away with other impurities. Final elution is with a low pH elution buffer, which causes the protonation of histidine residues on the mAb and PA, which are next to each other in the binding area. This leads to charge-charge repulsion and elution (Figure 1.1.8.1). The column is then regenerated for further use.

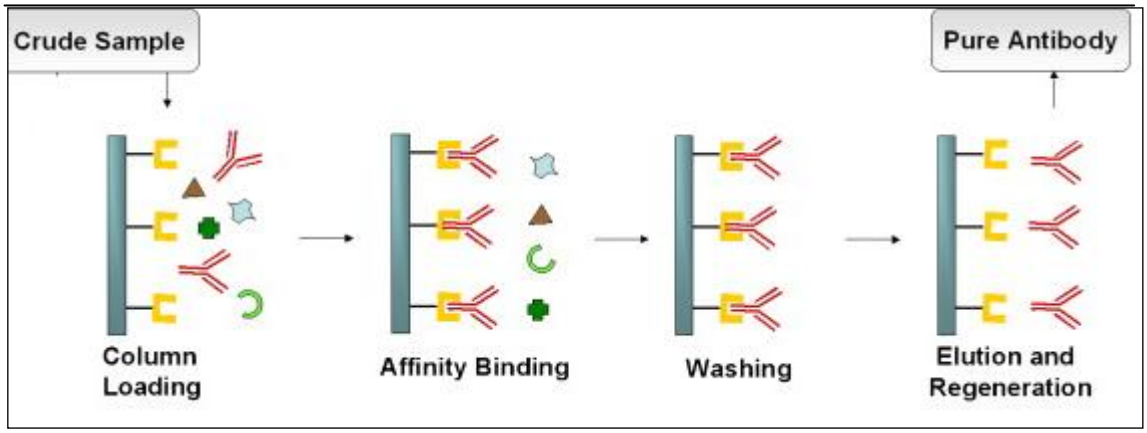

Figure 1.1.8.1: Schematic of protein A HPLC purification. The Protein A ligand is immobilised on to the column. Following crude sample loading, the mAb is retained by affinity binding to protein A. Washing is employed to remove non specific binding. Elution of the mAb is with a low pH elution buffer. (Roque et al., 2007).

Additional chromatographic modes are subsequently employed to allow a final level of acceptable pharmaceutical purity to be reached. Polishing steps are conducted in an orthogonal mode. Hydrophobic interaction chromatography (HIC) and anion exchange chromatography are routinely used based on their differing removal specifications. Anion exchange allows the removal of DNA and endotoxins following Protein A capture, whilst, HIC allows the final removal of aggregates post purification.

1.1.9 Protein A purification issues

The low pH column elution needed for IgG elution from Protein A can cause protein aggregation issues. The need for low pH is due to complementary histidyl residues on both the Protein A and IgG that must be protonated to allow IgG release. Structural changes occur in the Fc region of the IgG and can result in a high weight molecular aggregate content. In turn this affects column eluate turbidity and ultimately creates immunogenicity concerns, hence the need for additional polishing steps. The pH required for elution can be raised by the addition of NaCl (0.1-1M) thereby reducing the adverse effects of using a low pH elution in Protein A purification, but this can reduce yield from the column. Ethylene glycol can also be used to reduce strong hydrophobic interaction between Protein A and IgG, increasing the elution pH required (Shukla *et al.*, 2007).

Protein A leaching is also a serious issue in mAb purification. The Protein A ligand has been seen to co-elute with the antibody, as it dissociated from the column. Additional polishing steps are thus critical for the removal of this leached Protein A which must be cleared for regulatory acceptance. Carter-Franklin *et al* (2007) reported that leaching could possibly be reduced by the addition of EDTA, suggesting that proteinases may be a factor. Cleaning in place and column saturation with Protein A is also an issue; the ligand cannot withstand harsh alkaline conditions. In order to remedy this, high concentrations of chaotropes i.e. urea are used, which pose an environmental removal challenge. The engineered two domains can be used with 0.1M NaOH, Mabselect SURE is used at Lonza.

However, the major disadvantage of Protein A is its high cost, which is non comparable to any other chromatographic resin. Possible solutions have been the design of small molecule ligands with a similar binding affinity of mAbs to Protein A. Hober *et al* 2007, detailed how less sensitive *Staphylococcus aureus* Protein A molecules have been designed where sensitive amino acids are replaced, allowing cleaning in place to therefore

be conducted. However, this resin is even more expensive that normal PA. Ligands to mimic binding pockets of Protein A for Fc region interaction have also been developed. These protein mimetic resins (Mabsorbent A1p) have been seen to be effective; however they have a much lower affinity than Protein A and are not widely used in industry.

1.2 Chromatographic alterative to Protein A

The need to find an alternative to Protein A purification has previously been highlighted (Lyddiatt, 2002). Ideal features for protein chromatographic separation are high selectivity, high binding capacity, low nonspecific absorption, reusability and low cost (Jungbauer *et al.*, 2005). Follman *et al* in 2004 demonstrated that a platform approach can be successfully applied with the use of three chromatographic steps, which do not include Protein A affinity chromatography. Previously, direct technology comparisons have been made with Protein A purification and differing technologies. Other technologies simply cannot compete with the incredible specificity offered by Protein A (>99% impurity removal directly from cell culture supernatant). As this group highlighted there is a need to ensure that following complete purification (all three individual steps) adequate purification is reached and each step should not be viewed as a single entity. By varying combinations of the methods of cation exchange, anion exchange, hydrophobic charge induction and small molecule ligand resin chromatography, host cell proteins (HCPs) could be removed from CHO-derived monoclonal antibodies, to a level comparable to Protein A purification. The order in which chromatographic steps were performed was seen of significant importance. Capture steps that removed the highest amount of HCPs from the cell culture starting material (e.g. mixed mode) did not ultimately yield the lowest HCP level. It was hypothesised that binding competition between HCP species was evident with overloading of initial capture chromatographic steps that would ultimately affect overall HCP removal. The most appropriate chromatographic step combination in terms of removal of the highest amount of HCPs was demonstrated as hydrophobic interaction chromatography, anion exchange chromatography and finally mixed mode ion exchange.

1.2.1 Cation exchange chromatography

The chromatographic capture step which has been seen with the greatest potential to rival protein A purification of mAbs is cation exchange chromatography (CEX). It has been demonstrated with the commercially available mAbs Synagis (Medimmune) and Humira (Abbott). The robustness of cation exchangers, prevention of ligand leaching and

relatively lower costs when compared to Protein A purification, makes it an attractive option. Strong cation exchangers developed by Merck known as Fractogel have shown yields and host cell removal that are comparable to Protein A purification (Stein *et al.*, 2007).

CEX utilizes the basic isoelectric point of mAbs and allows the removal of negatively charged impurities i.e. residual DNA and some host cell proteins. Futhermore it has the ability to discriminate varying antibody variants from target proteins. Previously, elution using CEX was with acidic conditions using sodium chloride which required dilution and moreover was implicated in metal corrosion issues during manufacturing. Zhou *et al* (2007) showed the development of a pH-conductivity hybrid gradient elution with a cation exchange column. Elution was possible without the need for large concentrations of inorganic salts. It was seen that with the use of selected pH values and sodium acetate as a buffering salt, hybrid gradient CEX exhibited host cell protein removal data comparable to PA purification. Furthermore, scalability to 200L was possible, where resolution and separation were not compromised (Zhou *et al.*, 2007).

Work by Clausen *et al* (1999) again used a linear salt gradient CEX but focused on the use of Zicronia, creating a novel ion-exchange matrix. Zicronia with its incredible chemical stability relative to other silica and polymer supports, allowed harsh cleaning procedures to be used. Ethylenediamine-N, N'tetra (methylene phosphoric) (EDTPA) acid was used to modify zicronia based columns, preventing any nonspecific binding at Lewis acid sites on Zirconia surface. A purity of >95% and a yield of 92-98% from cell culture supernatant was achieved. A disadvantage with this technique however comes with scalability. It is predicted that as EDTPA modified Zirconia particle size are increased, decreased column efficiency would result.

Most recently Muller-Spath *et al*, (2010) have investigated the use of cation-exchange chromatographic capture in a continuous mode. By the use of linear gradient interconnected columns are able to recycle side products. High yield and high purity of single variant mAbs have been produced (Muller-Spath *et al.*, 2009). Continuous mAb loading, with cell feeding and also cleaning in place have been demonstrated. Huge benefits have been seen which include time saving, reduction in mAb variants for regulatory approval and a continuous mode of operation. Moreover a model was recently

proposed (Muller-Spath *et al.*, 2011) that showed great potential to rival Protein A purification. At present however, host cell protein removal data has not been considered.

A patented technology known as countercurrent tangential chromatography has also been described. It avoids complications seen with packed bed columns by the use of resins that are flowed through mixers and membranes. The membrane retains target molecules and is then eluted with an elution buffer. Separation has been investigated with Myoglobin and Bovine serum albumin to a purity of > 99% and 94% recovery (Shinkazh *et al.*, 2010). Continuous operation mode is possible, which again has a distinct advantage to PA affinity purification that can only be operated in batch mode.

The downside of ion exchange chromatography however, is the requirement for the samples to be of a low ionic strength before loading. An additional buffer exchange step in most cases is hence required. Due to the large amount of salts used, corrosion of the metal instruments can also be a problem, therefore there is a requirement for buffer exchange prior to samples being used in any biological assay (Stanton, 2003). Uncontrolled pH during elution can also affect protein stability and cause precipitation. With the use of CCC however, despite the need for buffer exchange prior to assays being conducted, no high pH elution is required, hence the conditions offered by the high water content in the phase system is predicted to be much milder.

1.2.2 Hydrophobic interaction chromatography

Another alterative chromatographic method that could possibly be used for the purification of mAbs is hydrophobic interaction chromatography (HIC). Due to the low concentration of mAbs in cell culture supernatant, separation by membrane hydrophobic interaction chromatography has been investigated. The benefit of HIC is selectivity due to high anti-chaotropic salt concentrations required. Ghosh *et al*, (2006) showed the separation of humanised monoclonal antibody from mammalian cell culture using HIC membranes, composed of a stack of microporous polyvinylidine (PVDF) pore size 0.1µm to a purity and recovery of >97%. Further attempts to improve HIC for mAb capture have focussed on increasing resin pore size to maximise mAb transport. Novel hydrophobic charge induction (HCIC) mixed mode ligands have also been used to allow possible capture of mAbs under low salt conditions. The need for high salt has been seen to cause manufacturing concerns, which are exacerbated at larger scale. An ideal alternative

to Protein A would allow desorption under milder conditions and binding without the use of large quantities of salt. The HCIC technique works based on these fundamentals and by the use a pH dependent ionisable ligand. Schwartz *et al* (2001) showed by the use of an antibody selective ligand, binding by HCIC was possible, with lyotrophic salts and desorption at a mild pH 4. Chen *et al*, (2007) further demonstrated the use of HCIC mercapto-Ethyl-Pyridine (MEP) resin which allowed capture comparable to Protein A.

1.2.3 Affinity chromatography

In addition to PA HPLC there are other affinity chromatography methods that can be used; these are desired due to the specificity they offer. A downside however seen with affinity chromatography is the clogging of column matrices with complex feeds. Work using expanded bed affinity chromatography, monolithic chromatography and stabilized fluidized bed has hence been conducted (Hober *et al.*, 2007; Holschuh *et al.*, 2005; Huse *et al*., 2006). All these options are with the objective of increasing cell titre loading and resulting reusability of the resin. Alternative affinity ligands include other bio affinity ligands, which are naturally occurring and bind to antigens and lectins etc. Protein G and L have the ability to bind to immunoglobulin but not to the same degree or specificity as Protein A. They do however withstand the harsh sanitation condition needed in production plants. Lectin (jacalin agarose) affinity chromatography has been used for the purification of IgA with the benefits of elution at a neutral pH. However, as Jacalin is a biologically active lectin its implications in immune responses need to be highly regulated, and leaching cannot be tolerated.

Pseudo specific ligands, as opposed to naturally occurring ligands (lectin, Protein A,G,L etc), are tailor made and mimic natural ligands. They are alternatives to natural ligands with reduced binding affinity. Harsh elution conditions are hence not required to release molecules. Disadvantages and advantages can be seen with this technique. With the use of these pseudo specific ligands, problems associated with biological ligands are avoided whilst specificity to the IgG is high. However, this has been outweighed by low scale up potential, high production costs and the continual issue of ligand leaching (Roque *et al.*, 2006).

Hydrophobic, thiophilic, hydroxyapatite, chelating metal ion and mixed mode affinity ligands can all be used for mAb purification (Roque *et al.*, 2007) (Table 1.2.3.1).

Type of Pseudo biospecfic ligand	Name	Mode of action	Purity achievable
Thiophilic absorbents	T-gel	• Absorption at neutral pH with high lyotrophic salt. • Elution by lowering the salt concentration.	100% recovery of entire immunoglobulin fragment from the crude extract.
Hydroxyapatite	Hydroxyapatite crystals	• Positively charged proteins retained by hydroxyapatite stationary phase. • Increasing ionic strength gradient used for the release.	Used only after PA HPLC, recovery of >80%.
Chelating metal ions	IDA-Ni2+ (IMAC)	• Iminodiacetic acid covalently bound onto solid support to trap nickel ions (affinity ligands for proteins).	>95% IgG recovery from goat serum.
Mixed mode ligands	MEP HyperCel	• Ligand has a hydrophobic core with hydrophilic groups attached. • Elution is by a pH change.	• 85% process yield from crude cell culture. • Optimisation however required: by pH and conductivity (Toueille *et al.*, 2011). • Unable to compete with protein A HPLC for selectivity.

Table 1.2.3.1: Details of pseudo biospecfic ligands available. Commercially available examples are listed along with their mode of respective action and the purity achievable in comparison to protein A purification (Roque et al., 2007).

Apart from naturally occurring and pseudo specific ligands, a new generation of synthetic ligands have been produced. These have been based on a need for improved stability, reduced production costs, an increasing cycling time and allowance of cleaning in place. Most procedures have been based on increasing the stability of the ligand by the use of mini Z-domain of Protein A, an example being affibodies (Roque *et al.*, 2007). These antibody mimetics are composed of just alpha helices with no disulphide bridges. Their unique structure allows them to withstand high temperatures and acid and alkaline conditions respectively (Gebauer *et al.*, 2009). By the use of molecular modelling and protein engineering significant advances have been made in the discovery of small molecule ligands that mimic Fc-Protein A interaction. Fassina *et al* (2001) initially identified Protein A mimetic peptide (PAM) TG191318. Its inverso derivative (D-PAM), where all the amino acids are in the D configuration, has also been developed (D'Agostino

et al., 2008). Host cell protein (HCP) removal comparable to PA purification has been demonstrated. The peptide can be easily immobilised onto solid surfaces, withstand harsh cleaning procedures and does not require low pH elution.

With the use of X-ray crystallography the dipeptide motif Phe-132: Tyr 133 was seen vital in the Protein A, Fc IgG interaction. The motif was mimicked and synthesised by Li *et al*. Work by this group has culminated in the commercialization of two synthetic non-peptide Protein A mimetic ligands: Mabsorbent AIP and A2P from proMeric Bioscicences (Ghoush *et al.*, 2008). These ligands can be immobilised onto cross-linked agarose and function as normal at high pressure for column purification.

The use of tags to modify mAbs instead of the search for specific binding ligand has also been proposed (Huse *et al.*, 2002). Fusion of recombinant proteins to peptide sequence was thought to simplify purification; however clearance of tags after purification was thought to be problematic (Low *et al.*, 2007).

With respect to finding a chromatographic alterative to PA purification, another affinity ligand which has been chemically modified to deal with drawbacks of PA would be ideal. Despite synthesis of pseudo specific ligands being valuable, at present they are still unable to match Protein A in terms of specificity. The problem of ligand leaching still also persists. For large scale purification, CEX allows greatly improved titre loading at nearly 100g/l, providing a very economical alternative to PA at a fifth of the price (Chon *et al.*, 2011). As detailed previously much investigation has focussed on improving process parameters and even continuous operation modes demonstrated. As an alternative chromatographic method CEX is most suited in terms of cost and capacity, however significant optimisation to match PA purification is required (Low *et al.*, 2007).

1.3 Non chromatographic alternatives

Bioseparations using column chromatography have dominated the biopharmaceutical industry for many years. A need for change has been highlighted by the requirement for continuous processing and faster operational times. These needs however have been outweighed by the level of specificity and resolution offered by column chromatography. These factors are fundamental for biotherapeutics, which ultimately are injected or ingested by patients.

As documented by Przybycien *et al* (2004), three chromatographic alternatives exist: bulk, field based and absorptive separation techniques (Table 1.3.1).

Non chromatographic method	Examples
Bulk separations	• Aqueous two phase extraction (ATPE) • Three phase partitioning • Precipitation • Crystallization
Field based separation	• Membrane filtration • Preparative electrophoresis
Absorptive separation	• Monoliths • Membrane chromatography

Table 1.3.1: Overview of non chromatographic alternatives available, examples are categorised into bulk, field based and absorptive separations (Przybycien et al., 2004).

1.3.1 Bulk separations

Protein precipitation has been used for many years at lab scale. Historically ethanol precipitation was used; however recovery was low at 50-60%. In order to prevent protein denaturation, processing was carried out at 5˚C, which significantly increased operational cost. Ammonium sulphate precipitation is commonly used also for protein purification but suffers from low yield and purity (Wang *et al.*, 2009). In order for protein precipitation to be applied to monoclonal antibody purification, significant improvements in specificity are needed. Investigations have been with the use of charged polyelectrolytes, such as caprylic acid or poly-ether sulfone (Shukla *et al.*, 2010). Ma *et al* (2010) showed by the use of polyamine precipitation target proteins can be selected, the protein products remain in solution and impurities are removed. By the use of the polyelectrolytes these insoluble complexes can further be charged to form large clusters. It was seen by the use of this procedure, removal of host cell proteins and DNA were similar to that of Protein A purification and product quality was maintained (Ma *et al.*, 2010). The disadvantage of this technique nonetheless is lack of viral clearance data. Furthermore process integration investigation has not been sufficiently conducted to allow comparisons to be drawn.

Affinity precipitation has also been considered as a substitute to conventional column chromatography. Magnetic beads are coated with Protein A and immobilised. As demonstrated by Holschuh *et al* (2005) with the use of magprepprotein A, an IgG binding capacity of 50-100 mg per gram is possible. When compared to the column and expanded bed chromatography, adsorption time of the IgG through the matrix is greatly decreased. Column size and the volume of solution applied are limiting factors in Protein A column batch mode purification. With magnetic particles, separation is within

minutes and particulates can be tolerated hence there is no need for additional filtration and centrifugation prior to sample loading. The major disadvantage of this technique however is that only low antibody concentrations can be bound by the beads (around 50mg/L) (Holschuh *et al.*, 2005). Again other immunomagentic beads such as thiophilic magnetic polymer beads have been investigated. Despite their ease of use, efficiency and reusability, binding capacity is a major problem. Larger beads would be needed to reach required packing density to support the sample load. A higher flow rate would therefore be needed which ultimately effects antibody bioactivity (Qian *et al.*, 2009). Protein crystallization also benefits from low running costs but many factors such as protein concentration, pH, temperature and engineering issues make optimization challenging (Przybycien *et al.*, 2004)

1.3.2 Field based separations

Membrane separation has been achieved by charged ultra filtration (UF) membranes and high performance tangential flow filtration (HPTFF). Separation is reliant on pH solution and ionic strength. Separation of closely similar biomolecules in terms of size is possible. Membrane stacks have been used to further improve separation (Przybycien *et al.*, 2004). A downside of this technique is its low ability to remove aggregates or host cell proteins. It can therefore only be used as a first step bulk purification tool (Shukla *et al.*, 2010).

Preparative electrophoresis can also been used for the purification of monoclonal antibodies based on charge and size based strategies. Lim et al, 1998 used the gradiflow technology, which uses a set of polyacrylamide separating membranes, to separate molecules based on their size and charge. With the use of pH and differing pore sizes, separation their by isoelectric points is possible. The technology is both scalable and cost efficient. However the recovery of antibody activity was only 80% (Lim *et al.*, 1998), consequently affecting overall product yield.

1.3.3 Absorptive separation

Adsorptive separations have been shown by the use of monoliths. Monoliths are macroporous stationary phase with the material cast into columns as a block composed of channels. Molecule transport is by convection as opposed to diffusion (Jungbauer *et al.*, 2005). These varying channel sizes and shape can be formulated by

polymerization chemistry. With the use of monoliths differing sizes can be designed, allowing an increased flow rate and resulting throughput, with less product degradation. The major disadvantage comes with scale up and obtaining regulatory acceptance due to the non-uniform pore sizes (Przybycien *et al.*, 2004).

Membrane chromatography allows high mass transport of large molecules, thereby significantly increasing throughput. Mass transfer is improved by the elimination of pores with long diffusion pathways. Membrane binding sites are located on the surface and convection is used rather than diffusion. Knudsen *et al* (2001) demonstrated the use of ion exchange membranes that offer increased specificity and function independent of flow rate. Removal of low level impurities has also been seen. The downside of this technology however is low selectivity. Wang *et al* (2006) showed the possibility of using a hybrid technology, with the high resolution monoclonal antibody separation offered by membrane chromatography coupled with ammonium sulphate precipitation. Ammonium sulphate precipitation suffers from the inverse effect of high processing capacity but low resolution. Hybrid separation was designed based on ammonium sulphate precipitation of the mAb followed by hydrophilic interaction using membrane absorption of dissolved mAb. The retained mAb was removed from the membrane module by a single change in solution to promote mAb dissociation from the membrane (Wang *et al.*, 2006). Auxiliary improvements to this work, involving salt induced precipitation, microfiltration and membrane adsorption by the use of caprylic acid for precipitation, resulted in a purity >95%.

1.4 Aqueous two phase system (ATPS) extraction

The ability of two immiscible aqueous solutions to form two phases when mixed over a certain concentration is termed aqueous two phase system (ATPS). ATPS were discovered by Beijernick in 1886 and require structurally different polymers e.g. Polyethylene glycol (PEG) and dextran or a polymer and salt, typically PEG phosphate. The importance of ATPSs for the separation of biomolecules however was not recognised until work by Albertsson in 1950s (Ferreira *et al.*, 2008). The benefits of these systems were biocompatibility, phase systems were typically composed of 80-90% (w/w) water, providing a very mild system with low interfacial tension (Dallora *et al*., 2007; Merchuk *et al.*, 1998; Raghavarao *et al*., 1995). It was therefore considered that biological activity could thus be retained during separation (Figure 1.4.1).

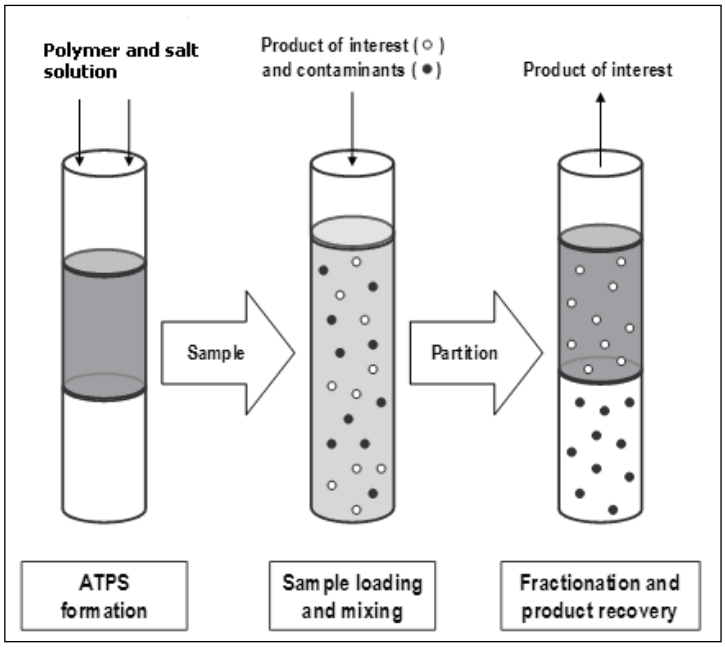

Figure 1.4.1: ATPS extraction. By the combination of a polymer polymer or polymer salt above a certain concentration an aqueous two phase system(ATPS) is formed. The product of interest is added and partitioning between the phases occurs. Ideally all containments should partition to one phase (lower phase) and target molecules to another (upper phase). (Benavides et al., 2008).

Sulk *et al*, (1992) carried out initial monoclonal antibody purification using low molecular weight PEG 1540Da and 22% phosphate. Extraction was coupled with thiophilic absorption chromatography. The antibody was targeted to the upper phase producing an overall IgG yield of 71% and 90% IgG recovery in the ATPS step. Asenjo *et al* (1996) demonstrated murine IgG purification, again using low molecular weight salt (1450Da) but a lower phosphate concentration of 14% and 12% NaCl. Initial purification was into the PEG rich phase and then back extraction into a fresh phosphate solution. (Andrews *et al.*, 1996).

Despite the promise in this work, successful protein purification using ATPS as a primary capture step required critical understanding of the partitioning process (Huddleston *et al.*, 1991). Limited predictability of the partition behaviour of proteins was a serious issue, additionally all proteins behaved differently. Classical polymer thermodynamics, such as Bronstead relationship, Flory-Huggins theory and Diamond and Hsu relationship, were based on polymer polymer systems typically PEG-Dextran (Luechau *et al.*, 2010; Maderia *et al.*, 2005). Huddleston *et al* (1996) reported that protein partition in PEG salt systems was dependent on solubility in concentrated salt solutions. The lack of a predictive model with PEG salt systems however was attributed to their

complexity (Samatou *et al.*, 2007). In order for industrial adoption this needed to be addressed, so the full economic benefits of ATPS in monoclonal antibody purification could be explored.

Partitioning of proteins in aqueous two phase systems (K) is dependent on physicochemical properties of the target protein and contaminates and the PEG-salt phase system (Andrews *et al.*, 2005; Qu *et al.*, 2009). A large array of variables is thus responsible for protein partitioning; including isoelectric point, surface hydrophobicity, protein molecular mass, polymer molecular mass, pH, salt type and respective concentration (Tubio *et al.*, 2004; Johansson *et al.*, 1998; Saravanan *et al.*, 2008). Zaslavsky *et al* (1987) also stressed the importance of water as a factor in two phase formation. Salts, especially at high concentrations, modify water structure (Farruggia *et al.*, 2004). These factors are yet to be fully understood. It is however this quantity of variables and flexibility that allows selective partitioning and targeting of proteins to be achieved by the ATPS (Selber *et al.*, 2004).

Up until 2006, the ATPS investigation focus was divided into molecular understanding of solute partitioning in ATPS and its practical implementation (Rito Palomares *et al*., 2000). Advances in ATPS implementation came with polymer recycling, as demonstrated with yeast proteins (Dembczynski *et al.*, 2010). Reduced direct costs of consumables and also waste treatment costs for the removal of salt were seen. Recycling of the top PEG-rich phase by back extraction for up to 5 cycles following ATPS extraction was possible. Furthermore the addition of fresh material compensated for any negative effects seen with the continual recycling of upper phase (Rito-Palomares *et al*., 2000). It was clear that for industrial take up a continuous mode of operation was needed with the equipment to support this. Process reproducibility and robustness was also key to allow ATPS process integration for high value products. (Rito-Palomares *et al.*, 2004)

Despite protein partitioning seen as that of a complex one, Tubio *et al* (2004) investigated the relationship of protein surface hydrophobicity to partitioning. The partition coefficient (K) was known to be dependent on hydrophobicity, charge and size.

$$K = K_{hphob} K_{el} K_{size} K_{polymer}$$

Figure 1.4.2: Equation to determine factors affecting partition coefficient K. Where K_{hphob} is hydrophobicity, K_{el} is isoelectric point, K_{size} is charge and size and $K_{polymer}$ is molecular weight of the PEG.

All factors were thought to function independently. Previous correlations using the above equation (Figure 1.4.2) were investigated with hydrophobicity. Differing hydrophobicity however resulted in differences in molecular mass, hydrophobicity and isoelectric points. A correlation was seen between partition coefficients and surface hydrophobicity when higher PEG molecular weights were used. Higher levels of hydrophobicity at these PEG molecular weights affected partitioning (Tubio *et al.*, 2004). Pico *et al* (2006) further showed the differences in partition coefficients of proteins and impurities could be exploited. Varying polymer molecular mass showed separation of model proteins with very similar isoelectric points.

A selection of example ATPS is shown in Table 1.4.3. Four main types of ATPS exist, as formed by two hydrophilic phases:

1) Polymer salt

2) Polymer-polymer

3) ATPS constructed with alternative compound e.g. varying co- polymers ethylene oxide and propylene oxide (EOPO)

4) Thermoseparating polymers e.g. EOPO and dextran, allow temperature induced phase separation, by heating of a polymer above its cloud point. These polymers have seen much potential in recycling hence making them a greener technology (Persson *et al.*, 2000)

Table 1.4.3: Selected examples of ATPSs extraction of proteins from various feed stocks. Purity achieved, analytical methods used and any noted retention of biological are shown.

Phase system	Protein	Yield (%)	Purification factor	Recovery of activity	Assay used	Biomass loaded	Reference
Ucon 50-HB-500 benzoyl-dextran	3-phosphoglycerate kinase from baker's yeast	47	2	100%	Coomassie brilliant blue G at 595nm.	Not mentioned	Lu *et a*l., 1996
PEG-phosphate ester, 16% (w/w) potassium phosphate +3% (w/w) NaCl	Intracellular human recombinant interferon	99.6	25	Not mentioned	Coomassie brilliant blue G-250 method	10% w/w	Guan *et al*., 1996
PEG 8000 phosphate system pH 9.4	Small inclusion bodies	87	1.6	Not mentioned	SDS PAGE analysis	2% w/w	Walker *et al.*, 1999
EO50PO50/HM-EOPO system (50% ethylene oxide (EO) + 50% propylene oxide (PO)	Bovine serum albumin, Lysozyme, apoloprotein A-1.	78	5.5	Not mentioned	SDS PAGE analysis	10% w/w AP-1	Persson *et al.*, 1999
PEG 1450 24.9% (w/w) phosphate 12.6% (w/w) pH 8	ß-phycoerythrin	77	2.9	Not mentioned	545-280 nm absorbance	Not mentioned	Benavides *et al.*, 2004
13.4% (w/w) PEG 3400 18% (w/w) potassium phosphate	ß-glucuronidase	74	20	Not mentioned	SDS PAGE analysis/ BCA	Not mentioned	Ross *et al.*, 2010
PEG 8000 16.1% (w/w) + 10% phosphate	Human recombinant protein	88	na	Not mentioned	SDS PAGE and Bradford assay	Not mentioned	Ibarra-Herera *et al.*, 2011

1.4.1 Monoclonal antibody purification by ATPS extration

It has been reported that the aqueous environment offered by ATPS allows the preservation of the native structure of proteins, fundamental to biological activity (Benavides *et al.*, 2008). Azevedo *et al* (2009) credited the recent re-emergence of ATPS extraction for monoclonal antibody purification with the drive to find alternatives to Protein A. The two groups working most directly within this research area are the Platis and Laubrou group in Athens and the Aires-Barros group in Lisbon. These will be detailed separately.

The Platis and Laubrou group have focussed on transgenic plants, namely tobacco plants. Tobacco plants have the same glycosylation pattern as humans; production of humanised monoclonal antibodies is thus possible. Additional benefits of these transgenic plants are low production costs and low risk of human contamination (as it is not a food product) (Balasubramaniam *et al.*, 2003). ATPS provide a benefit for a plant protein purification system that are otherwise typically based on many chromatographic steps i.e. ion exchange chromatography, gel filtration and affinity chromatography. Previously, product loss was seen at each stage. ATPS also allow larger quantities of biomass to be tolerated and can withstand particulates. Platis *et al* (2006) demonstrated the purification of mAb 2F5 using 12% (w/w) PEG 1500, 13% (w/w) phosphate buffer at pH 5. A 3-4 fold purification of the mAb was seen with 95% recovery in the bottom phase. Furthermore potentially harmful secondary metabolites of the tobacco plant were removed. Previously this was a challenge in conventional chromatographic methods, with strong binding to matrices that resulted in them exhibiting ion exchange characteristics (Platis *et al.*, 2009).

Moreover in 2008 they coupled this purification method, vital for polyphenol removal, with cation exchange chromatography and metal affinity chromatography. Purification was increased to 162 fold to 97.2% with a 65% yield (Platis *et al.*, 2008). This group have shown the ability of ATPS for bulk purification, whilst highlighting its limitations in terms of specificity. All work within this group however was carried out as a single step extraction. All preparations were also claimed to be fully active, as tested by SDS PAGE using Coomassie blue stain and ELISA with goat anti human IgG.

A significant contribution to monoclonal antibody purification by ATPS has been made by the Aires-Barros group. They have demonstrated successful single extraction through to multiple equilibrium modes (Rosa *et al.*, 2009). Recently they have

also reported the costing as a direct comparison to Protein A purification. Through the series of papers they have shown the successful use of PEG-phosphate systems for IgG purification from CHO supernatant (Azevedo *et al.*, 2007). Due to environmental reasons associated with the use of phosphate, they have further investigated alternatives, namely PEG-citrate (Rosa *et al.*, 2007; Azevedo *et al.*, 2008). An IgG yield of 99% and final purity of 96% have been demonstrated. To further improve the specificity previously seen as a problem with ATPS they investigated the use of ligands such as functionalised PEG e.g. PEG diglutaric (Rosa *et al.*, 2007; Ferreira *et al.*, 2008; Avevedo *et al.*, 2008). The use of these ligands has allowed specificity to be comparable to PA purification. Additionally thermoseparating polymers and back extraction can be employed, allowing polymer recycling (Kumar *et al.*, 2007). Finally process integration was demonstrated by aligning ATPS extraction with other purification steps e.g. hydrophobic interaction chromatography and size exclusion chromatography (Avevedo *et al.*, 2008; Azevedo *et al.*, 2009). Success achieved by this group has again been demonstrated by single batch extraction with results comparable to PA purification.

In order for ATPS extraction to be adopted as a viable downstream capture method, a scalable technique with commercial potential was required. In all papers documented by the Aires-Barros group agitated vessels were used where gravity phase separation of over 14 hours was employed. In terms of cost, production time and commercial scalability potential this would not be feasible. These papers by the Aires-Barros group have been summarised in Table 1.4.1.1. The drawbacks and the problems in their approaches have also been listed, particularly in terms of the benefits that CCC can offer.

Paper title/ Year	Aqueous two phase extraction system	Results	Assays/ techniques used to determine IgG recovery	Comparison to Protein A purification/ drawbacks of approach
Application of central composite design to the optimisation of aqueous two phase extraction of human antibodies (2007)	• PEG 3350 8% (w/w), 10% (w/w) phosphate pH6 + 15% (w/w) NaCl. • Carried out with an artificial mixture of 1mg/ml IgG, 10mg/ml serum albumin and 2mg/ml Myoglobin.	• Yield of 101±7% • Purity 99±0%.	Protein A chromatography used and a recovery of 97±4% seen.	• With back extraction into fresh phosphate phase, higher yields were possible (10% phosphate buffer pH 6), 76% yield and 100% purity. Drawback: Large amounts of NaCl needed to improve specificity. Further back extraction needed to obtain high yields and purity.
Optimisation of aqueous two-phase extraction of human antibodies (2007)	• 12% PEG, 10% phosphate, 15% NaCl pH 6. • IgG recovery from CHO cell supernatant.	• Recovery of yield 88%, • Purification factor 4.2. • Purity 100% by SEC.	• PA HPLC for IgG concentration • BCA, size exclusion chromatography, electrophoresis-SDS PAGE+ sliver stain. • No mention of the retention of biological activity	• The conditions seen to maximise extraction were high concentration of NaCl and PEG, low phosphate concentration and low pH values. • Improved yield of 88% from previous 76% with 100% purity. Drawback: Large amounts of NaCl needed to improve specificity.

Paper title/ Year	Aqueous two phase extraction system	Results	Assays/ techniques used to determine IgG recovery	Comparison to Protein A purification/ drawbacks of approach
Affinity partitioning of human antibodies in aqueous two phase systems.(2007)	• Functionalised PEG (PEG-COOH) added to PEG phosphate and PEG dextran systems. • PEG phosphate: 12% (w/w) PEG 3350 + 10% (w/w) phosphate. • PEG dextran: 8% (w/w) PEG 3350 + 8% (w/w) dextran 500.	• 60 fold increase in selectivity with functionalised PEG. Best purification in dextran systems, 93% yield, purification factor 1.9, IgG selectivity 11.	• PA HPLC for IgG concentration. • BCA, size exclusion chromatography, electrophoresis-SDS PAGE+ sliver stain. • No mention of the retention of biological activity	• Diglutaric acid was used to functionalise PEG, showed yield and specificity comparable to PA purification. Drawback: In order to make extraction by ATPS more predictable and selective (previously highlighted as a problem), a ligand with affinity for IgG was attached. The ligand however has a significant cost implication.
Purification of human immunoglobulin G by thermoseparating aqueous two phase systems (2008)	10% UCON (ethylene oxide/propylene oxide). 5% dextran + 20% TEG-COOH (Triethylene glycol-diglutaric acid)	Yield of 85% and purity 100%.	• PA HPLC for IgG concentration. • BCA, size exclusion chromatography, electrophoresis-SDS PAGE+ sliver stain. • No mention of the retention of biological activity	• By the use of thermoseparating polymers and TEG-COOH, IgG partitioning was shifted from the bottom to UCON rich phase. • Offers specificity comparable to affinity chromatography by PA purification. Drawback: The ligand to improve specificity has a significant cost implication.

Paper title/ Year	Aqueous two phase extraction system	Results	Assays/ techniques used to determine IgG recovery	Comparison to Protein A purification/ drawbacks of approach
Integrated process for the purification of antibodies combining aqueous two phase extraction, hydrophobic interaction chromatography (HIC) and size exclusion chromatography (SEC). (2008)	• 10% (w/w) PEG 3350 +12% (w/w) citrate at pH6. • Bottom phase then loaded directly onto phenyl-sepharose HIC column. • Polishing by SEC.	• After ATPS, IgG yield of 97%, 41% HPLC purity and 72% protein purity. • Following HIC: 99% antibody recovery, 86% HPLC purity and 91% protein purity. After SEC: 100% IgG and 90% yield.	• PA HPLC for IgG concentration. • BCA, size exclusion chromatography, electrophoresis-SDS PAGE+ sliver stain. • No mention of the retention of biological activity	• Showed promise for use of ATPS extraction in downstream purification which is in line with other technologies. Drawback: High level of purity obtained is dependent on SEC and HIC as oppose to ATPS extraction. No mention of end biological activity of IgG.
Partitioning of human antibodies in polyethylene glycol-sodium citrate aqueous two-phase system (2008)	• 8% (w/w) PEG 3350, 8% (w/w) citrate + 15% (w/w) NaCl at pH 6.	• 99% IgG yield, 44% HPLC purity. • Further re-extraction into citrate phase at 5% NaCl 99% yield, 76% HPLC purity.	• PA HPLC for IgG concentration. • BCA, size exclusion chromatography, electrophoresis-SDS PAGE+ sliver stain. • No mention of the retention of biological activity	• The use of citrate as opposed to phosphate avoids environmental disposal issues associated with phosphate. Drawback: Back extraction requires the use of further NaCl.

Paper title/ Year	Aqueous two phase extraction system	Results	Assays/ techniques used to determine IgG recovery	Comparison to Protein A purification/ drawbacks of approach
Affinity enhanced purification of human antibodies by aqueous two phase extraction (2008)	• PEG molecules with different molecular weight modified with different ligands and screened for their ability to bind to IgG in CHO supernatant. • 5% dextran, 8% PEG diglutaric acid, 10 mM phosphate buffer pH 7 used.	• 97% IgG yield in upper phase and 94% purity.	• PA HPLC for IgG concentration. • BCA, size exclusion chromatography, electrophoresis-SDS PAGE+ sliver stain. • No mention of the retention of biological activity	• By the use of affinity extraction, specificity was retained even at large scale. • The process can be operated continuously as opposed to PA HPLC. Drawback: Dextran used in this system is costly hence would affect scale up potential. Additionally there is the cost of the ligand.
Downstream processing of human antibodies. Integrating an extraction capture step and cation exchange chromatography. (2009)	• Functionalised PEG: PEG diglutaric acid (PEG GA). • 50%(w/w) PEG-GA, 25% (w/w) dextran and phosphate buffer pH 7.	• With the use of a cation exchange following ATPS extraction, 89% yield and 100% purity.	• PA HPLC for IgG concentration. • BCA, size exclusion chromatography, electrophoresis-SDS PAGE+ sliver stain. • No mention of the retention of biological activity.	• Again it was seen ATPS capture can be substituted for PA HPLC. • A high specificity with the definite potential for process integration was demonstrated. Drawback: The cost of the functionalised PEG would make scale up challenging.

Table 1.4.1.1: Summary of work conducted and progress made by the Aires-Barros group (Lisbon) with respect to mAb purification from CHO cell supernatant.

Rosa *et al* (2009) attempted to address the issue of a continuous system by the use of connected mixer- settler battery systems (Figure 1.4.1.2). The number of transfer stages was increased by the use of multi-stage equilibrium (maximum 6). Greater separation of IgG from impurities was possible without the need of high concentrations of NaCl to favour partition; potential manufacturing precipitation problems were therefore avoided.

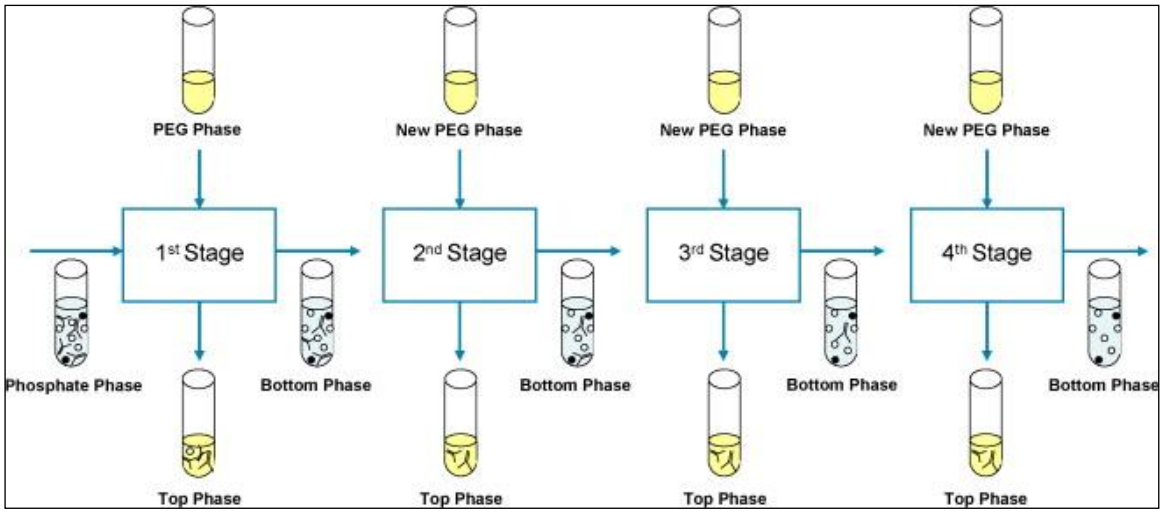

Figure 1.4.1.2: Multi-stage equilibrium ATPS extraction. By replacing the PEG phase and repeated extraction, greater concentration of purified mAb is attained. (Rosa et al., 2009).

An IgG yield of 89% and a purity of 75% was demonstrated following multiple extraction with a PEG phosphate system, as opposed to 61% recovery yield and 55% purity seen with single stage extraction. Further to this, when functionalised PEG - triethylene glycol diglutaric acid (TEG-COOH) was used in a multi-stage extraction a yield of 95% and protein purity of 95% was noted, in comparison to a single extraction of 43% purity. With the use of multiple extractions the final IgG concentration obtained due to product enrichment was 1.04mg/ml as compared to 0.21mg/ml (Rosa *et al.*, 2009). The potential of ATPS in mAb purification was previously shown by the Aires-Barros group. Furthermore the use of multi-step extraction allows greater IgG selectivity, product enrichment and increased throughput. The use of ligands also greatly helps with specificity. The attachment of actual protein A to PEG has been trialled but due to high costs of the ligands was not appropriate (Andrews, 1990). Rosa *et al* (2009) have detailed the use of alternative ligands. Glutaric acid was seen to be the most appropriate, allowing improved specificity in ATPS extraction. In addition Rosa *et al* (2011) published a direct comparison of mAb purification in ATPS extraction to that by PA. They reported by the

use of ATPS, cost can be reduced by at least 39%. This cost reduction was valid even with the use of new generation protein A binding resins with much improved dynamic binding capacities.

The protein concentration limit within ATPS is a huge issue; precipitation issues due to solubility have been seen. Asenjo *et al* (2011) in a recent review reported that partitioning behaviour which is independent of protein concentration can only occur at low concentrations. Typically around 5% w/w of the system volume of biological feedstock can be processed. Selvakumar *et al* (2010) have investigated the construction of systems in monophasic regions of phase diagram. Phase components are added directly to the feedstock, allowing intensification of loading to nearly 70%, reducing ATPS costs with the scope for further work.

The work by the Aires-Barros group has shown the potential for ATPS extraction for mAb purification. It is, however, apparent that a continuous mode of operation where greater mixing stages with improved separation efficiency is needed. By the use of Counter Current Chromatography (CCC), separation can occur continually by the use of centrifugal forces hence functionalised PEG or huge concentrations of additional salts are not required to improve selectivity. CCC is thus more efficient allowing high resolution separation in a single, shorter run time. As reported in a review by Avevedo *et al* (2009), the speed of phase separation is critical in enhancing process throughput. With CCC this is directly achievable by the use of gravitational force to aid separation and mixing, which is at a far greater rate that an ATPS extraction. Unlike ATPS extraction, CCC uses the theory of aqueous extraction but is assisted by CCC processing, ultimately achieving a considerably higher magnitude of extraction steps.

1.4.2 CCC machines for separation of proteins

The need for multi-stage extraction has long been demonstrated by Albertsson with initial work using counter-current distribution (CCD) (Albertsson *et al.*, 1970). Separation was achieved by a series of mixing, settling and transfer stages (Sutherland *et al.*, 2008). Despite high resolution separation being achieved it was both laborious and time consuming. The first high speed CCC machine using a J type centrifuge was invented by Ito in the 1980s. Unlike previous models (droplet CCC and helix CCC) it allowed improved resolution, separation time and sample loading. Continuous liquid- liquid partitioning was possible along a length of tubing, governed by either gravitational or

centrifugal forces to retain stationary phase (Ito, 2005). As both phase are liquid, the need for stationary phase retention to allow an adequate high resolution separation of target components is of paramount importance.

The CCC columns are divided into hydrostatic and hydrodynamic instruments (Conway, 1991). These modes are further divided into respective machines. Hydrodynamic machines include J type multi layer and non synchronous CCC, with two axis of rotation resulting in a variable centrifugal force (Conway, 2000). The continual tubing is wound onto a bobbin. During planetary motion the part of the coils closest to the axis of rotation undergo mixing where the g-fields are lowest, whilst settling occurs at the part of the coils furthest from the axis of rotation, hence the area of highest g-field (Sutherland, 2007). Rotation also occurs around the sun gear, which causes wave like mixing and has been applied for many successful separations with small molecules (Chen *et al.*, 2007; Wood *et al.*, 2007). A planetary rotor rotates in a synchronised motion to the main axis of rotation in a multi layer centrifuge, with a fixed 1:1 ratio. With the non synchronous machine however, this 1:1 ratio can be changed.

The hydrostatic CCC mode includes the centrifugal partitioning centrifuge (CPC) and toroidal coil (TC CCC). A constant gravitational force is produced by a single axis of rotation. The column is composed of interconnected chambers that trap stationary phase. Mobile phase is pumped through the stationary phase, cell to cell, in a cascade "waterfall-like" manner (Sticher *et al.*, 2007). Mobile phase thus penetrates the stationary phase in a more vigorous manner than that of the hydrodynamic mode. Previously the need for hydrostatic columns to allow adequate mass transfer by vigorous mixing and sufficient stationary phase retention was reported (Ito *et al.*, 2009). Previous protein separation runs were consequently focused on the CPC and Toroidal coils (Sutherland, 2010).

CCC is based on two immiscible liquid phases in a coiled column. The absence of a solid support permits separation between two phases based on partitioning differences of compounds within a sample. A continuous cycle of mixing, settling and separation occurs. Phase interchange simultaneously occurs with every turn (Ito *et al.*, 1970). Retention of the stationary phase within the coil against the flow of the mobile phase is due to the centrifugal force field applied.

The choice of solvent system is of critical importance to CCC development (Dubant *et al.*, 2008). CCC is an extension of ATPS extraction which is aided

by CCC processing. The ultimate benefit of CCC is continuous extraction along a given column length over a shorter period of time when compared to single extraction based on gravity separation. Due to multiple issues seen with solid phase chromatography, CCC is providing an exciting new opportunity, most importantly as a purification tool for biological products. The mild conditions employed are predicted to preserve protein integrity and allow total recovery of sample. There is a great need within industry to maximise column loading whilst minimizing product aggregation. CCC also shows low solvent consumption and a reduction in economic costs (Marston *et al.*, 2006). When reviewing the literature on the use of CCC, the mild conditions offered by ATPS and absence of a solid support had lead to assumptions that sample denaturation is unlikely (Sutherland, 2007; Sticher, 2008). This assumption is challenged within this project with a study of the retention of biological activity as detailed by examples.

1.4.3 CCC vs. Protein A affinity chromatography

	Protein A affinity chromatography	**CCC**
Advantages	High level of specificity	Versatile technique
	Greatly studied technique	Low levels of contamination
	Fast	Economical- lower buffer cost, reuse of coil
	High yield and throughput	Particulates and crude samples accepted
		Total sample recovery
Drawbacks	Highly expensive	Narrow polarity range
	Limited number of cycle reuse	Difficult optimisation
	Column leaching hence additional purification steps required	Labour-intensive
	Low pH elution/ aggregate production	Physical properties can be changed by sample injection.
		Lower efficiency

Table 1.4.3.1: The advantages and drawbacks of both Protein A and CCC for protein purification.

1.4.4 CCC column design for protein separation

Since the advent of CCC in the 1960s there have been many improvements to initial models. Machine performance has been improved with greater technical knowledge,

leading to many successful separations using proteins (Ito, 2005). Successful protein separation using high speed CCC (HSCCC) is dependent on stationary phase retention (Menet *et al.*, 1993). Due to the multi layer coils used in J-type centrifuges, unpredictably low stationary phase retention was seen. Stationary phase retention is dependent on the Archimedean screw force created by the planetary motion (Cao *et al.*, 2008). The Archimedean screw force ensures both phases are continuously mixed whilst one is kept within the coil. A number of factors such as viscosity, interfacial tension, spin speed, coil bore, temperature and density differences, etc, between the phases determine stationary phase retention (Ito, 2010). Despite some successful purifications being reported with the use of J-type HSCCC, extremely broad peaks are generally recorded. Most specifically Shinomiya et al (1996) reported unusual peaks following Ovalbumin separation containing both natural and denatured products. It was not mentioned whether CCC was seen to exacerbate product degradation; they merely attributed the broad peak to heterogeneity of the sample proteins.

Purification using HSCCC was also seen with alpha amylase (Zhi *et al.*, 2005) and horseradish peroxidase (Margi *et al.*, 2003). Despite purification in both demonstrated by SDS PAGE electrophoresis, a loss to biological activity was reported. Horseradish Peroxidase activity recovery was seen at ≥45% whilst 30% with alpha amylase. The use of $CaCl_2$ as a protective agent with the alpha amylase was seen to improve retention of activity.

Guan *et al* (2007) reported that, despite the need for a new coil design with improved stationary phase retention, the multi layer CCC (HSCCC) was more scalable, hence more industrially attractive. The Brunel CCC group demonstrated the importance of column design for protein separation (Guan *et al.*, 2007). They reported that the wave like mixing offered by the multi layer J type HSCCC was insufficient to allow mass transfer of high molecular weight proteins between viscous phase systems. Lysozyme and Myoglobin and a PEG 1000 12.5%/12.5% potassium phosphate system were used to demonstrate that the greater mixing vigour with hydrostatic instruments was needed to achieve the separations. Vigorous cascade like mixing could also be attained with spiral columns for J type centrifuges, as demonstrated by Ito. Ito's group, with the use of barricaded spiral disks or spiral tube assembly (Guan *et al.*, 2009); demonstrated protein separation could be enhanced from that of conventional multi layer coils. These spiral designs allowed the centrifugal force gradient to be generated along the radius of the spiral,

thus trapping and retaining stationary phase (Ito, 2010). These spiral tubes interfered with the laminar phase flow, improving phase mixing. Improvements have further been made with the addition of 1cm presses perpendicularly along the length of tubing, thus increasing spiral layer numbers and reducing dead space (Ito *et al.*, 2009). Knight *et al* (2011) have shown, by using a spiral tubing support rotor, that a range of protein separations is possible with various polymer systems (Knight *et al.*, 2007; Knight *et al.*, 1995). In addition, multiple spiral disk assemblies have been seen to produce large interface areas with mixing achieved by barricaded channels. Glass beads have been placed in mixing sections and separations occur in subsequent settling sections, providing a mixer-settler CCC in HSCCC. This was demonstrated with Myoglobin and Lysozyme using a PEG 1000 12.5%/12.5% potassium phosphate system (Knight *et al.*, 2011).

Centrifugal partition chromatography (CPC) uses a hydrostatic mode of operation (Murayama *et al.*, 2009). High resolution separation is hypothesised by increased stationary phase retention. Chen *et al* (1999) used the CPC with a PEG 6000- potassium phosphate system for the separation of bovine serum albumin (BSA) and Lysozyme. A high resolution separation was not seen however, due to the need for separation optimisation. The effect of mobile phase flow rate, rotational speed, direction of coil revolution and the pH of solvent (Shinomiya *et al*., 2004) all required consideration.

High resolution separation however was demonstrated by Ikehata *et a*l (2005) with the construction of a CPC made with toroidally wound tubing, mounted circumferentially (eccentrical) on a disk that was rotated in a centrifugal field (Sutherland, 2010). Mixing comparable to a toroidal coil was seen with a higher partition efficiency than a standard CPC model. Separation was demonstrated using a PEG 8000 4% (w/w) 5% (w/w) dextran T500 system and showed improved Myoglobin and Lysozyme separation (Shinomiya *et al.*, 2000).

To allow the further understanding of mixing, much work has been conducted by Van Buel and Marchal 2000 with stroboscopic studies. They demonstrated the importance of column efficiency, which was determined by sufficient dispersion of the mobile phase between that of the stationary phase. The flow path of the mobile phase needed to be adequately broken early in a run, which was dependent on Coriolis force. The Coriolis force was resultant from flow shape which was shown to be related to rotational speed and flow rate (Marchal *et al.*, 2000). The effect of the Coriolis force was

demonstrated by Ito *et al* (1998). Sufficient mass transfer was dependent on the Coriolis force acting parallel to the coil segment (Ikehata *et al.*, 2004). Column designs have now been created based on this knowledge e.g the Partitron 25. Cells are linked under the rotation of the rotor such that mobile phase is adequately mixed by the Coriolis force against the cell wall therefore increasing mass transfer efficiency (Margraff *et al.*, 2005). The Partitron 25 has a 25 litre capacity, thus is ready for industrial uptake. Additionally, downsizing of the model X-1.5L, (Shinomiya *et al*., 2006) allowed predictions of improved biological separations.

The linear scale up of Lysozyme and Myoglobin separations were shown by Sutherland *et al* (2008), using a CPC and PEG 1000 12.5%/12.5% potassium phosphate system. Separation was achieved with scaling from 176mg sample load using a 500ml column to 2.2g with a 6.25 litre column. The potential for industrial take up was demonstrated with a possible throughput of 40g/day. Due however to complications with the cleaning of interconnected chambers and rotary seals, which are prone to leakage, the use of toroidally wound continual tubing was preferred.

The toroidal coil CCC (TC CCC) used at Brunel is based on the use of multilayer toroidal coils wound around a drum that is rotated in a planetary motion. Unlike the CPC it doesn't contain rotating seals and has a variable force field. Vigorous cascade mixing was known due to its hydrostatic mode. Sutherland *et al* (2011) carried out a direct comparison of the CPC and TCCCC using Lysozyme and Myoglobin and a PEG 1000 12.5%/12.5% potassium phosphate system. A throughput of 0.67g/h was demonstrated with the TC CCC as opposed to 0.14g/h with the CPC. It showed the potential of the TC CCC for serial injections with no loss of stationary phase.

Initial work to observe the fundamentals of the TC CCC and the loss in the resolution of protein partitioning in comparison to small molecules, was studied by Ito. He demonstrated that mass transfer through the interface was directly correlated with molecular mass (Ito *et al*., 1998). Proteins with a larger molecular mass exhibited a lower mass transfer. The appropriate use of the Coriolis force however could prevent peak broadening. He also elucidated that possibly the protein 3D-structure, or partially denatured components, could be responsible for peak widening. In following work however, this was not reinvestigated, as sample analysis was just based on 430nm absorbance assays. He merely stated this mode of CCC, with longer or narrow toroidal

coils, would allow successful separation of biological active compounds (Matsuda *et al.*, 1998). Following this work, Shinomiya *et al* (1999) investigated the separation of Myoglobin and Lysozyme using a PEG 1000 12.5%/12.5% dibasic potassium phosphate system. Elution mode was highlighted as critical as only partially purified Myoglobin was seen by SDS-PAGE. Again there was no mention of recovery.

Within the Brunel University CCC group, toroidal coil construction was based on existing, commercially available CCC apparatus (Dynamic Extraction centrifuges). An analytical TC CCC however was investigated by Ito's group. It was reported by Guan et al in 2010 that separation of Lysozyme and Myoglobin was possible to a maximum of 7.4% sample loading of the column volume. Constraints with the TC CCC were also seen with mass transfer; however more promise of industrial scale up was seen than with the CPC. Maintenance of stationary phase retention is vital to allow the partition of molecules hence result in a separation. Various new column designs, such as Zigzag, Saw tooth and Figure 8, were suggested by Yang *et al* (2010). The potential of using longer columns to improve the resolution were suggested.

Limited work on the non synchronous CCC for protein separation has been carried out by research groups. By the separate control of bobbin to rotor rotations, mixing and settling can be independently controlled. It was seen that rotor rotations at 800rpm (Kobayashi *et al*., 2005) were sufficient for mixing of the phase system. More importantly, settling time could be increased, which was vital to allow partitioning between the viscous phase systems. Successful separations have been seen with Lysozyme and Myoglobin and also cytochrome C (Shinomiya *et al*., 2003). A PEG 8000-dextran T500 in 5mM potassium phosphate and a PEG 1000-dibasic potassium phosphate system (12.5%) was used. The PEG phosphate system was seen to be the most appropriate in terms of the separation efficiency. Again these experiments were conducted with extremely stable model proteins and there was no assay of biological activity used.

In 2010, Ignatova *et al*, published work highlighting that previous issue with mechanical complexities of the non synchronous CCC had been overcome. They suggested there was great promise for future work with biologics, predicting a step change of 30% in resolution and 90% in plate efficiency.

Liquid- Liquid extraction can also include the application of reverse micelles (Liu *et al*., 1998). Reverse micelles are formed when a surfactant is mixed in a

non-polar organic solvent. Proteins from micellar solution migrate to aqueous solutions. The partition is reliant on electrostatic interaction, manipulated by pH gradients. Work by Shen *et al* (2007) demonstrated the combination of reverse micelle enrichment and CCC processing, using Cytochrome C and Lysozyme. Further work has been demonstrated by Becker et al, 2009 with the use of additional magnetic absorbents in micellar ATPS. A Lysozyme purity of >80% was seen. The combination of techniques has great potential for protein enrichment for aqueous solutions.

In addition, the use of alternative solvents namely ionic liquids have been considered (Pei *et al*., 2009). Their low melting points (extremely close to room temperature) and 'green' characteristics along with high thermal and chemical stability for CCC separations are promising (Berthod *et al*., 2008). Previously ionic liquids were not suitable for CCC extraction due to their high viscosity. By the addition of acetonitrile to these systems these issues have been addressed. Ruiz Angel *et al* (2007) have considered the use of BM1M C1 ionic liquid (1-butyl-3-methylimidazolium chloride) which has a lower density than that of a typical upper PEG phase. The density difference allows greater stationary phase retention and Ovalbumin partitioning was investigated. Greater partitioning was reported than with a PEG salt system due to intrinsic hydrophobicity. Extensive studies however, have been limited, with loading capacity (due to phase saturation) anticipated as an issue. A need for this to be addressed before scale up is critical.

The table below (Table 21) shows a selection of protein purifications conducted using various CCC machines. In this work the retention of biological activity is critically observed.

Protein/ Feedstock	**ATPS**	**CCC conditions**	**Purity**	**Biological activity**		**Reference**
				Analytical techniques used	**Retention biological activity (%)**	
Horseradish Peroxidase (HRP) from Armoracia Rusticana	10% (w/w) PEG 1540 + 14.8% w/w phosphate	• HSCCC • 0.8ml/min • 1000rpm	Factor 6	• BCA assay + SDS page	≥45%	Magri *et al.*, 2003
Alpha amylase from supernatant of recombinant Bacillus Subtilus	• PEG 4000 + citrate 2% (w/w) sodium chloride. • 0.56 (w/w) $CaCl_2$ as protective agent	• HSCCC • 0.4ml/min • 880rpm	Not mentioned	• Alpha amylase activity measured by starch iodine method • Bradford assay • SDS PAGE + Coomassie blue stain.	From 30 to 73.1% with protective agent	Zhi *et al.*, 2005
Ovalbumin from hen egg white	16% (w/w) PEG 1000 17% (w/w) potassium phosphate pH 9.2	• HSCCC • 1.8ml/min • 850rpm	95%	Not mentioned	Not mentioned	Zhi *et al.*, 2005

Protein/ Feedstock	ATPS	CCC conditions	Purity	Biological activity		Reference
				Analytical techniques used	Retention biological activity (%)	
C-phycocyanin from Spirulina platensis	• Phase A: 0.05 mol/L sodium phosphate buffer pH 4 + 0.2mol/L KCL. • Phase B: 0.05mol/L sodium phosphate pH 8 + 0.4 mol/L KCL	• Reverse micelle HSCCC • 1.5ml/min • 850rpm	Factor 4.25	• SDS PAGE + Coomassie blue stain	Not mentioned	Yin *et al.*, 2011
Bromelain from pineapple	• Phase A: 0.05M sodium phosphate pH 9.5+ 0.2M K_cl. • Phase B: pH 7.0, 0.4M KCL	• Reverse micelle HSCCC • 1.5ml/min • 999rpm	Not mentioned	• Proteninase activity determined by Casein digestion unit. • 280nm SDS PAGE + Coomassie blue stain.	44%	Yin *et al.*, 2011

Protein/ Feedstock	**ATPS**	**CCC conditions**	**Purity**	**Biological activity**		**Reference**
				Analytical techniques used	**Retention biological activity (%)**	
Lactic acid dehydrogenase (LDH) from bovine heart crude extract	16% (w/w) PEG 1000-12.5% (w/w) potassium phosphate pH 7.3	• CPC • 1 ml/min • 500rpm	Not mentioned	• Enzymatic analysis using nicotinamide adenine dinucleotide (NAD). Colorimetric assay at 560nm. • SDS PAGE + staining with Coomassie blue	Not mentioned	Shibusawa *et al.*, 1997
Proteins from chicken egg	16% (w/w) PEG 1000 12.5% (w/w) dibasic potassium phosphate	• CPC • 1 ml/min • 500rpm	Not mentioned	• SDS PAGE + staining with Coomassie blue	Not mentioned	Shibusawa *et al.*, 1998
Glycoproteins Morchella esculenta	12.5% (w/w) PEG 8000+ 25% (w/w) potassium phosphate	• CPC • 1 ml/min • 500rpm	Not mentioned	• HPLC using methyl linoleate-sillca-based-polymer-based column	Not mentioned	Wei *et al.*, 2001

Protein/ Feedstock	ATPS	CCC conditions	Purity	Biological activity		Reference
				Analytical techniques used	Retention biological activity (%)	
Lactic acid dehydrogenase (LDH) from bovine heart crude extract	PEG 1540 ammonium sulphate + retainer (10nm) Acetic acid	• pH focussing CPC • 0.5ml/min	Not mentioned	• Enzymatic analysis using nicotinamide adenine dinucleotide (NAD). Colourmetric assay at 560nm. • SDS PAGE + staining with Coomassie blue.	Not mentioned	Shibusawa *et al.*, 2002
Single strand DNA from Escherichia cell lysate	16% (w/w) PEG 1000 + 17% (w/w) ammonium sulphate	• CPC • 0.5 ml/min • 500rpm	Not mentioned	• 280nm measurement • SDS PAGE with Coomassie blue stain	Not mentioned	Shibusawa *et al*., 2003
Alcohol dehydrogenase (LDH) from bovine liver crude extract	PEG 1000 (16%)-potassium phosphate pH 7.3 containing Procion red as affinity dye ligand	• CPC • 0.5 ml/min • 500rpm	Not mentioned	• Enzymatic analysis for ADH at 340nm. • SDS PAGE with Coomassie blue stain	Not mentioned	Shibusawa *et al.*, 2004

Protein/ Feedstock	ATPS	CCC conditions	Purity	Biological activity		Reference
				Analytical techniques used	Retention biological activity (%)	
Glucosyltransferase (GTF) from cell lysate of streptococcus mutans	4.4% (w/w PEG 8000, 6% (w/w) dextran T500 + 10mM phosphate buffer pH 9.2	• CPC • 1 ml/min • 400rpm	Increased 87%	• Bradford assay used to determine enzymatic activity • SDS PAGE with Coomassie blue stain.	79%	Yanagida *et al.*, 2004.
Glucosyltransferase (GTF) from cell lysate of streptococcus mutans	7.5% PEG 3350-10% dextran T40 +10mM potassium phosphate pH 9.	• CPC • 0.5 ml/min • 400rpm	Not mentioned	• Enzymatic assay GTF by measurement of water insoluble glucan (WIG) measured at 490nm. • SDS PAGE with Coomassie blue stain.	95%	Shibusawa *et al.*, 2006
Histone deacetylase (HDAC) from Escherichia cell lysate.	7.0% PEG 3350-10% dextran T40 + 10mM potassium phosphate pH 9.	• CPC • 0.25 ml/min • 400rpm	Not mentioned	• Analysed by HPLC to look at HDAC activity. • SDS PAGE with Coomassie blue stain.	Not mentioned	Shibusawa *et al.*, 2007

Protein/ Feedstock	ATPS	CCC conditions	Purity	Biological activity		Reference
				Analytical techniques used	Retention biological activity (%)	
Pea Albumin: PA1B	n-butanol-water-n-butanl-aqueous 20mM trifluoracetic acid (TFA)	• CPC • 5ml/min • 1200rpm	95%	• Reverse Phase HPLC, 280nm detection	Not mentioned	Berot *et al.*, 2007
Various ribonucleases	16% (w/w) PEG 1000-12.6% (w/w) potassium phosphate pH 6.6	• CPC • 0.5 ml/min • 1000rpm	88%	• RNase activity determined colour metrically. BSA as standard pH 4.25 at 37 degrees.	Not mentioned	Shinomiya *et al.*, 2009.

Table 1.4.4.1: Selected examples of protein purification from varying feed stocks with differing CCC machines. Particular attention is given to analytical techniques used and the mention of retention of biological activity.

Table 1.4.4.1 shows a large number of protein separations using CCC. Within the literature studied there seems to be neglect in the mention of biological activity following a CCC run. Protein purification seems to be attained with the assumption of full biological activity. In the few cases where biological recovery has been stated, crude absorbance assays or SDS PAGE have been used. When biologically active material is purified, there is a need to establish that material is still functional. In the case of mAbs, this is of paramount importance as the end products are injected into patients. An inactive or denatured product could potentially cause adverse immunogenic reactions.

Several successful protein purifications have been reported by CCC (Keay *et al.*, 2011). Monoclonal antibody purification however has never been demonstrated by CCC (Berthod *et al.*, 2009). It is believed that the work in this thesis is the first time that ATPS extraction with CCC purification has been combined for mAbs. Ultimately, this work investigates the feasibility of CCC as an alternative to PA HPLC purification. Usually non chromatographic purification methods lack specificity. By the use of CCC with continual mixing and settling, high resolution separation is possible. Furthermore of all the protein purifications that have been carried out by both ATPS extraction and CCC, there seems to have been a neglect for determination of biological activity preservation post purification. Throughout the project, this aspect is addressed and furthermore a solution found in providing retention of biological activity with a separation.

1.5 Aims and Objectives

The aims and objectives of this PhD project are listed below:

1) **Development of a multiprobe robotic programme**

   To allow the investigation of a range of different aqueous two phase systems (ATPS) which are fundamental to achieving a counter current chromatography (CCC) separation for biologics.

2) **Development of a Protein A HPLC quantification method**

   To allow the partitioning of the monoclonal antibody (mAb) within the varying ATPS, produced by robotic programming, to be determined analytically. Furthermore developing a method where chromatograms are not affected by the presence of the phase system.

3) **Direct comparison of centrifugal partitioning chromatography (CPC) and CCC for monoclonal antibody separation.**

   To conduct side by side comparison of the CPC and CCC with Protein A purified IgG.

4) **Investigation and further optimisation of CCC conditions using crude cell culture supernatant (CCS).**

   To carry out CCC runs with crude cell culture supernatant, with the objective of attaining high resolution separation and full retention of mAb biological activity.

5) **Characterisation of CCC purified samples with a range of Lonza quality control assays.**

   To analyse the CCC purified samples produced with the optimal CCC operating parameters to determine whether they could possible be of industry standard, ultimately, allowing comparison to be drawn to the industry gold standard of Protein A HPLC mAb purification.

CHAPTER 2: Robotic phase system selection

2) **Robotic solvent system selection**

2.1 Summary

Counter Current Chromatography (CCC) is a form of liquid chromatography, which has been developed to process scale by the Brunel Institute for Bioengineering (BIB) team. Key to this technique is phase selection, which tends to be laborious. Considerable insight is required into the effects of components on the distribution ratio of the molecule of interest. Phase systems can comprise of 2,3,4,5 or more components, hence the possibilities are endless. Previously solvent system selection was by significant trial and error. The systematic and logical approach offered by a liquid handling robot was required.

The chapter details the creation of a fully automated, robotic selection table of a range of Aqueous Two Phase Systems (ATPS). A Perkin Elmer liquid handling robot was used to prepare PEG-salt phase systems, perform partitions, and take samples for analysis. All phase systems were made from concentrated aqueous stocks. Systems included PEG 400, 1000, 3350 and 8000 with sodium, potassium and ammonium phosphate, sulphate and citrate salt. Partition coefficients (K) were subsequently calculated for each ATPS, by the ratio of mAb partitioning between upper to that of the lower phase.

The aim of this work was to allow both rapid and easy identification of the most appropriate system for mAb purification. This was based on the criteria of good

IgG recovery and a partition coefficient in the range of 0.5-2. The 0.5-2 partition coefficient range allowed IgG elution within a reasonable time, while also allowing sufficient time for the IgG to be resolved from nearby impurities. For all systems tested, IgG favoured the PEG upper phase which resulted in a very high K value. A lower K range (0.5-2) prevented excessive IgG retention within the coil, avoiding the use of significant quantities of mobile phase for elution (Garrard thesis, 2005). As the mobile phase was the lower salt phase, avoidance of the use of large amounts resulted in fewer disposal issues. The PEG 3350 11.1%/11.1% ammonium sulphate system and the PEG 1000 17.5%/17.5% sodium citrate system were seen to be the most appropriate. A range of PEG 1000 phosphate systems were also seen to fit this criteria of a K in the range of 0.5-2 and a high IgG recovery. However, due to environmental disposal issues associated with phosphates, the two systems named previously were chosen to be thoroughly investigated.

In comparison to previous work on the robot with aqueous organic systems (Garrrard, 2005), significant changes were made to robotic programming, mainly due to the nature of the aqueous two phase systems. The selection process of the most appropriate phase systems is detailed in this chapter, whilst subsequent purification in a range of CCC machines are investigated in the further chapters.

2.2 Introduction

The project objective was for the rapid, scalable purification of mAbs from crude cell culture supernatant (CCS) using countercurrent current chromatography (CCC). A robotic selection method for *aqueous-organic* two-phase systems has previously been developed and is routinely applied in the Brunel Advanced Bioprocessing Centre (ABC). The list of tables required for full robotic selection of all molecules is shown in Figure 2.2.1.

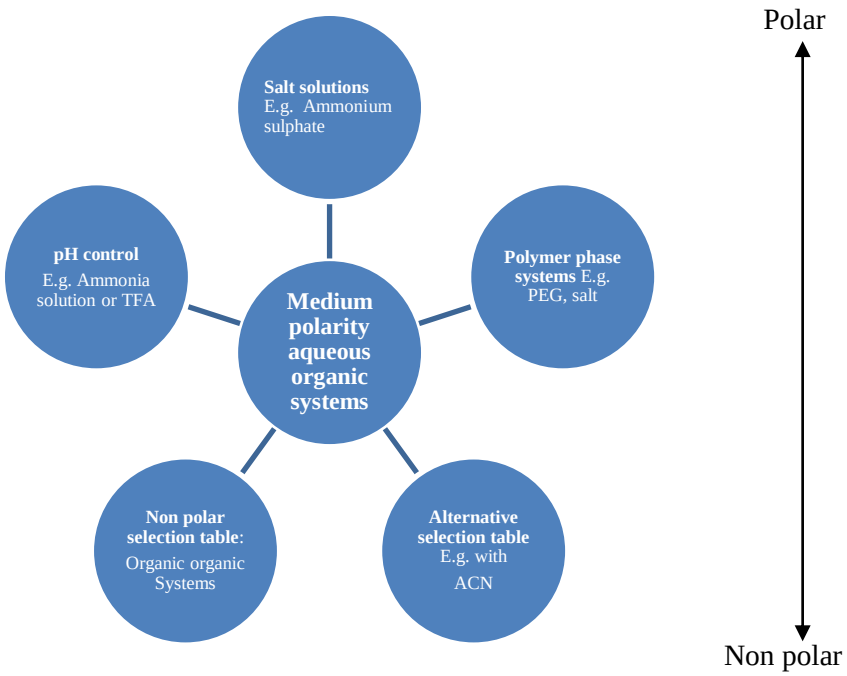

Figure 2.2.1: Overview of robot tables. Initial work completed by Dr Ian Garrard focussed on aqueous organic systems for the separation of small molecules. This chapter focuses on the creation of a polymer phase system selection table, for example, made of an aqueous PEG and aqueous salt solutions.

The studies in this chapter were conducted to provide a thorough investigation of a vast range of ATPS. Investigation was based on the robotic programming of ATPS using an automated liquid handling robot. The objective was to find the most appropriate system, to allow IgG separation from impurities, based on their respective partition coefficients. Work in this chapter details how this was achieved. Furthermore, an appropriate protein assay was developed to quantitate IgG partitioning between the phases.

2.3 Method

2.3.1 Creation of solvent system table

Initially, an ATPS table was obtained from Lukasz Grudzien (a PhD student at the Institute, investigating CCC as a possible bioreactor for enatiomer separation of an amino acid). The table comprised of 112 ATPS made of a wide range of salt and PEG concentrations, various salt types and various molecular weights of PEG (Figure 2.3.1.1).

PEG type (Da)	Salt type	Phase system Conc. %(w/w)	Strength of the stock solution (%)											Water
			55	55	35	30	40	40	40	29	29	40	40	
			PEG400	PEG1000	PEG3350	PEG8000	K citrate	KPO_4	Na citrate	$NaPO_4$	$NaSO_4$	NH_4PO_4	NH_4SO_4	
400	K citrate	16	**1064**	**0**	**0**	**0**	**1241**	**0**	**0**	**0**	**0**	**0**	**0**	**1695**
400	K citrate	18	**1197**	**0**	**0**	**0**	**1396**	**0**	**0**	**0**	**0**	**0**	**0**	**1407**
400	K citrate	20	**1330**	**0**	**0**	**0**	**1552**	**0**	**0**	**0**	**0**	**0**	**0**	**1119**
400	K citrate	22	**1463**	**0**	**0**	**0**	**1707**	**0**	**0**	**0**	**0**	**0**	**0**	**831**
400	KPO_4	16	**1064**	**0**	**0**	**0**	**0**	**1154**	**0**	**0**	**0**	**0**	**0**	**1783**
400	KPO_4	18	**1197**	**0**	**0**	**0**	**0**	**1298**	**0**	**0**	**0**	**0**	**0**	**1506**
400	KPO_4	20	**1330**	**0**	**0**	**0**	**0**	**1442**	**0**	**0**	**0**	**0**	**0**	**1228**
400	KPO_4	22	**1463**	**0**	**0**	**0**	**0**	**1586**	**0**	**0**	**0**	**0**	**0**	**951**
400	Na citrate	16	**1064**	**0**	**0**	**0**	**0**	**0**	**1252**	**0**	**0**	**0**	**0**	**1684**
400	Na citrate	18	**1197**	**0**	**0**	**0**	**0**	**0**	**1408**	**0**	**0**	**0**	**0**	**1395**
400	Na citrate	20	**1330**	**0**	**0**	**0**	**0**	**0**	**1565**	**0**	**0**	**0**	**0**	**1105**
400	Na citrate	22	**1463**	**0**	**0**	**0**	**0**	**0**	**1721**	**0**	**0**	**0**	**0**	**816**
400	$NaPO_4$	16	**1064**	**0**	**0**	**0**	**0**	**0**	**0**	**1731**	**0**	**0**	**0**	**1205**
400	$NaPO_4$	18	**1197**	**0**	**0**	**0**	**0**	**0**	**0**	**1947**	**0**	**0**	**0**	**856**
400	$NaPO_4$	20	**1330**	**0**	**0**	**0**	**0**	**0**	**0**	**2164**	**0**	**0**	**0**	**507**
400	$NaPO_4$	22	**1463**	**0**	**0**	**0**	**0**	**0**	**0**	**2380**	**0**	**0**	**0**	**157**
400	$NaSO_4$	16	**1064**	**0**	**0**	**0**	**0**	**0**	**0**	**0**	**1707**	**0**	**0**	**1230**
400	$NaSO_4$	18	**1197**	**0**	**0**	**0**	**0**	**0**	**0**	**0**	**1920**	**0**	**0**	**883**
400	$NaSO_4$	20	**1330**	**0**	**0**	**0**	**0**	**0**	**0**	**0**	**2134**	**0**	**0**	**537**
400	$NaSO_4$	22	**1463**	**0**	**0**	**0**	**0**	**0**	**0**	**0**	**2347**	**0**	**0**	**191**
400	NH4PO4	20	**1330**	**0**	**0**	**0**	**0**	**0**	**0**	**0**	**0**	**1612**	**0**	**1059**
400	NH4PO4	22	**1463**	**0**	**0**	**0**	**0**	**0**	**0**	**0**	**0**	**1773**	**0**	**765**
400	$NH4SO_4$	16	**1064**	**0**	**0**	**0**	**0**	**0**	**0**	**0**	**0**	**0**	**1301**	**1636**
400	$NH4SO_4$	18	**1197**	**0**	**0**	**0**	**0**	**0**	**0**	**0**	**0**	**0**	**1463**	**1340**
400	$NH4SO_4$	20	**1330**	**0**	**0**	**0**	**0**	**0**	**0**	**0**	**0**	**0**	**1626**	**1044**
400	$NH4SO_4$	22	**1463**	**0**	**0**	**0**	**0**	**0**	**0**	**0**	**0**	**0**	**1789**	**749**
1000	K citrate	14	**0**	**931**	**0**	**0**	**1086**	**0**	**0**	**0**	**0**	**0**	**0**	**1983**
1000	K citrate	16	**0**	**1064**	**0**	**0**	**1241**	**0**	**0**	**0**	**0**	**0**	**0**	**1695**
1000	K citrate	18	**0**	**1197**	**0**	**0**	**1396**	**0**	**0**	**0**	**0**	**0**	**0**	**1407**
1000	K citrate	20	**0**	**1330**	**0**	**0**	**1552**	**0**	**0**	**0**	**0**	**0**	**0**	**1119**
1000	K citrate	22	**0**	**1463**	**0**	**0**	**1707**	**0**	**0**	**0**	**0**	**0**	**0**	**831**
1000	KPO_4	14	**0**	**931**	**0**	**0**	**0**	**1009**	**0**	**0**	**0**	**0**	**0**	**2060**
1000	KPO_4	16	**0**	**1064**	**0**	**0**	**0**	**1154**	**0**	**0**	**0**	**0**	**0**	**1783**
1000	KPO_4	18	**0**	**1197**	**0**	**0**	**0**	**1298**	**0**	**0**	**0**	**0**	**0**	**1506**
1000	KPO_4	20	**0**	**1330**	**0**	**0**	**0**	**1442**	**0**	**0**	**0**	**0**	**0**	**1228**
1000	KPO_4	22	**0**	**1463**	**0**	**0**	**0**	**1586**	**0**	**0**	**0**	**0**	**0**	**951**
1000	Na citrate	14	**0**	**931**	**0**	**0**	**0**	**0**	**1095**	**0**	**0**	**0**	**0**	**1974**
1000	Na citrate	16	**0**	**1064**	**0**	**0**	**0**	**0**	**1252**	**0**	**0**	**0**	**0**	**1684**
1000	Na citrate	18	**0**	**1197**	**0**	**0**	**0**	**0**	**1408**	**0**	**0**	**0**	**0**	**1395**
1000	Na citrate	20	**0**	**1330**	**0**	**0**	**0**	**0**	**1565**	**0**	**0**	**0**	**0**	**1105**
1000	Na citrate	22	**0**	**1463**	**0**	**0**	**0**	**0**	**1721**	**0**	**0**	**0**	**0**	**816**
1000	$NaPO_4$	14	**0**	**931**	**0**	**0**	**0**	**0**	**0**	**1515**	**0**	**0**	**0**	**1555**
1000	$NaPO_4$	16	**0**	**1064**	**0**	**0**	**0**	**0**	**0**	**1731**	**0**	**0**	**0**	**1205**
1000	$NaPO_4$	18	**0**	**1197**	**0**	**0**	**0**	**0**	**0**	**1947**	**0**	**0**	**0**	**856**
1000	$NaPO_4$	20	**0**	**1330**	**0**	**0**	**0**	**0**	**0**	**2164**	**0**	**0**	**0**	**507**
1000	$NaPO_4$	22	**0**	**1463**	**0**	**0**	**0**	**0**	**0**	**2380**	**0**	**0**	**0**	**157**
1000	$NaSO_4$	14	**0**	**931**	**0**	**0**	**0**	**0**	**0**	**0**	**1493**	**0**	**0**	**1576**

PEG type (Da)	Salt type	Phase system Conc. %(w/w)	Strength of the stock solution (%)											Water
			55	55	35	30	40	40	40	29	29	40	40	
			PEG400	PEG1000	PEG3350	PEG8000	K citrate	KPO_4	Na citrate	$NaPO_4$	$NaSO_4$	NH_4PO_4	NH_4SO_4	
1000	$NaSO_4$	18	**0**	**1197**	**0**	**0**	**0**	**0**	**0**	**0**	**1920**	**0**	**0**	**883**
1000	$NaSO_4$	20	**0**	**1330**	**0**	**0**	**0**	**0**	**0**	**0**	**2134**	**0**	**0**	**537**
1000	$NaSO_4$	22	**0**	**1463**	**0**	**0**	**0**	**0**	**0**	**0**	**2347**	**0**	**0**	**191**
1000	NH_4PO_4	14	**0**	**931**	**0**	**0**	**0**	**0**	**0**	**0**	**0**	**1128**	**0**	**1941**
1000	NH_4PO_4	16	**0**	**1064**	**0**	**0**	**0**	**0**	**0**	**0**	**0**	**1289**	**0**	**1647**
1000	NH_4PO_4	18	**0**	**1197**	**0**	**0**	**0**	**0**	**0**	**0**	**0**	**1450**	**0**	**1353**
1000	NH_4PO_4	20	**0**	**1330**	**0**	**0**	**0**	**0**	**0**	**0**	**0**	**1612**	**0**	**1059**
1000	NH_4PO_4	22	**0**	**1463**	**0**	**0**	**0**	**0**	**0**	**0**	**0**	**1773**	**0**	**765**
1000	NH_4SO_4	14	**0**	**931**	**0**	**0**	**0**	**0**	**0**	**0**	**0**	**0**	**1138**	**1931**
1000	NH_4SO_4	16	**0**	**1064**	**0**	**0**	**0**	**0**	**0**	**0**	**0**	**0**	**1301**	**1636**
1000	NH_4SO_4	18	**0**	**1197**	**0**	**0**	**0**	**0**	**0**	**0**	**0**	**0**	**1463**	**1340**
1000	NH_4SO_4	20	**0**	**1330**	**0**	**0**	**0**	**0**	**0**	**0**	**0**	**0**	**1626**	**1044**
1000	NH_4SO_4	22	**0**	**1463**	**0**	**0**	**0**	**0**	**0**	**0**	**0**	**0**	**1789**	**749**
3350	K citrate	12	**0**	**0**	**1294**	**0**	**931**	**0**	**0**	**0**	**0**	**0**	**0**	**1775**
3350	K citrate	14	**0**	**0**	**1509**	**0**	**1086**	**0**	**0**	**0**	**0**	**0**	**0**	**1404**
3350	K citrate	16	**0**	**0**	**1725**	**0**	**1241**	**0**	**0**	**0**	**0**	**0**	**0**	**1034**
3350	K citrate	18	**0**	**0**	**1941**	**0**	**1396**	**0**	**0**	**0**	**0**	**0**	**0**	**663**
3350	KPO_4	12	**0**	**0**	**1294**	**0**	**0**	**865**	**0**	**0**	**0**	**0**	**0**	**1841**
3350	KPO_4	18	**0**	**0**	**1941**	**0**	**0**	**1298**	**0**	**0**	**0**	**0**	**0**	**762**
3350	Na citrate	12	**0**	**0**	**1294**	**0**	**0**	**0**	**939**	**0**	**0**	**0**	**0**	**1767**
3350	Na citrate	14	**0**	**0**	**1509**	**0**	**0**	**0**	**1095**	**0**	**0**	**0**	**0**	**1395**
3350	Na citrate	16	**0**	**0**	**1725**	**0**	**0**	**0**	**1252**	**0**	**0**	**0**	**0**	**1023**
3350	Na citrate	18	**0**	**0**	**1941**	**0**	**0**	**0**	**1408**	**0**	**0**	**0**	**0**	**651**
3350	$NaPO_4$	12	**0**	**0**	**1294**	**0**	**0**	**0**	**0**	**1298**	**0**	**0**	**0**	**1408**
3350	$NaPO_4$	14	**0**	**0**	**1509**	**0**	**0**	**0**	**0**	**1515**	**0**	**0**	**0**	**976**
3350	$NaPO_4$	16	**0**	**0**	**1725**	**0**	**0**	**0**	**0**	**1731**	**0**	**0**	**0**	**544**
3350	$NaPO_4$	18	**0**	**0**	**1941**	**0**	**0**	**0**	**0**	**1947**	**0**	**0**	**0**	**112**
3350	$NaSO_4$	12	**0**	**0**	**1294**	**0**	**0**	**0**	**0**	**0**	**1280**	**0**	**0**	**1426**
3350	$NaSO_4$	14	**0**	**0**	**1509**	**0**	**0**	**0**	**0**	**0**	**1493**	**0**	**0**	**997**
3350	$NaSO_4$	16	**0**	**0**	**1725**	**0**	**0**	**0**	**0**	**0**	**1707**	**0**	**0**	**568**
3350	$NaSO_4$	18	**0**	**0**	**1941**	**0**	**0**	**0**	**0**	**0**	**1920**	**0**	**0**	**139**
3350	NH_4PO_4	12	**0**	**0**	**1294**	**0**	**0**	**0**	**0**	**0**	**0**	**967**	**0**	**1739**
3350	NH_4PO_4	14	**0**	**0**	**1509**	**0**	**0**	**0**	**0**	**0**	**0**	**1128**	**0**	**1362**
3350	NH_4PO_4	16	**0**	**0**	**1725**	**0**	**0**	**0**	**0**	**0**	**0**	**1289**	**0**	**986**
3350	NH_4PO_4	18	**0**	**0**	**1941**	**0**	**0**	**0**	**0**	**0**	**0**	**1450**	**0**	**609**
3350	NH_4SO_4	12	**0**	**0**	**1294**	**0**	**0**	**0**	**0**	**0**	**0**	**0**	**976**	**1731**
3350	NH_4SO_4	14	**0**	**0**	**1509**	**0**	**0**	**0**	**0**	**0**	**0**	**0**	**1138**	**1352**
3350	NH_4SO_4	16	**0**	**0**	**1725**	**0**	**0**	**0**	**0**	**0**	**0**	**0**	**1301**	**974**
3350	NH_4SO_4	18	**0**	**0**	**1941**	**0**	**0**	**0**	**0**	**0**	**0**	**0**	**1463**	**596**
8000	K citrate	12	**0**	**0**	**0**	**1521**	**931**	**0**	**0**	**0**	**0**	**0**	**0**	**1548**
8000	K citrate	14	**0**	**0**	**0**	**1774**	**1086**	**0**	**0**	**0**	**0**	**0**	**0**	**1139**
8000	K citrate	16	**0**	**0**	**0**	**2028**	**1241**	**0**	**0**	**0**	**0**	**0**	**0**	**731**
8000	KPO_4	12	**0**	**0**	**0**	**1521**	**0**	**865**	**0**	**0**	**0**	**0**	**0**	**1614**
8000	KPO_4	14	**0**	**0**	**0**	**1774**	**0**	**1009**	**0**	**0**	**0**	**0**	**0**	**1216**
8000	KPO_4	16	**0**	**0**	**0**	**2028**	**0**	**1154**	**0**	**0**	**0**	**0**	**0**	**819**
8000	Na citrate	12	**0**	**0**	**0**	**1521**	**0**	**0**	**939**	**0**	**0**	**0**	**0**	**1540**
8000	Na citrate	14	**0**	**0**	**0**	**1774**	**0**	**0**	**1095**	**0**	**0**	**0**	**0**	**1130**

PEG type (Da)	Salt type	Phase system Conc. %(w/w)	Strength of the stock solution (%)										Water
			55	55	35	30	40	40	40	29	29	40	40	
			PEG400	PEG1000	PEG3350	PEG8000	K citrate	KPO_4	Na citrate	$NaPO_4$	$NaSO_4$	NH_4PO_4	NH_4SO_4	
8000	Na citrate	16	**0**	**0**	**0**	**2028**	**0**	**0**	**1252**	**0**	**0**	**0**	**0**	**720**
8000	$NaPO_4$	12	**0**	**0**	**0**	**1521**	**0**	**0**	**0**	**1298**	**0**	**0**	**0**	**1181**
8000	$NaPO_4$	14	**0**	**0**	**0**	**1774**	**0**	**0**	**0**	**1515**	**0**	**0**	**0**	**711**
8000	$NaPO_4$	16	**0**	**0**	**0**	**2028**	**0**	**0**	**0**	**1731**	**0**	**0**	**0**	**241**
8000	$NaSO_4$	12	**0**	**0**	**0**	**1521**	**0**	**0**	**0**	**0**	**1280**	**0**	**0**	**1199**
8000	$NaSO_4$	14	**0**	**0**	**0**	**1774**	**0**	**0**	**0**	**0**	**1493**	**0**	**0**	**732**
8000	$NaSO_4$	16	**0**	**0**	**0**	**2028**	**0**	**0**	**0**	**0**	**1707**	**0**	**0**	**265**
8000	NH_4PO_4	12	**0**	**0**	**0**	**1521**	**0**	**0**	**0**	**0**	**0**	**967**	**0**	**1512**
8000	NH_4PO_4	14	**0**	**0**	**0**	**1774**	**0**	**0**	**0**	**0**	**0**	**1128**	**0**	**1097**
8000	NH_4PO_4	16	**0**	**0**	**0**	**2028**	**0**	**0**	**0**	**0**	**0**	**1289**	**0**	**683**
8000	NH_4SO_4	12	**0**	**0**	**0**	**1521**	**0**	**0**	**0**	**0**	**0**	**0**	**976**	**1503**
8000	NH_4SO_4	14	**0**	**0**	**0**	**1774**	**0**	**0**	**0**	**0**	**0**	**0**	**1138**	**1087**
8000	NH_4SO_4	16	**0**	**0**	**0**	**2028**	**0**	**0**	**0**	**0**	**0**	**0**	**1301**	**671**

Figure 2.3.1.1: Initial solvent selection table for partitioning studies using the liquid handling robot. The salt type abbreviations used have been fully detailed in the abbreviations list on page 10. Volumes dispensed in µl from stock solutions by the robot. The total volume of each phase system was 4ml.

2.3.2 Preparation of solvents for the robot

Due to the nature of PEG and salt, stock solutions were prepared. The liquid handling robot functions based on the transfer of a known volume of liquid (Figure 2.3.2.1).

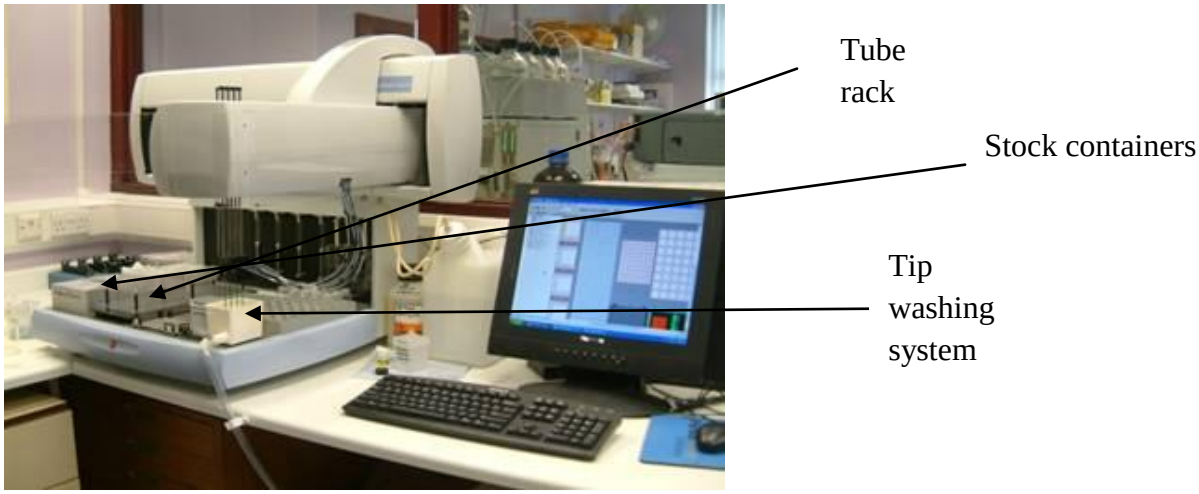

Figure 2.3.2.1: Photo of Perkin Elmer robot, based on the use of 4 probes. On the left hand side the robot platform can be seen, which includes the stock containers, tube rack and the tip washing system. The programming was conducted with the computer software shown on the right-hand side.

2.3.3 Sample used

For initial trial runs, IgG that had been purified by Protein A preparative chromatography (PA purified IgG) was used. This was provided by Lonza, batch number cB72.3 IgG4, lot number L17765/39, concentration 11.6mg/ml with storage conditions at 4ºC.

Lysozyme was also used for trial runs, purchased from Sigma Aldrich, catalogue number L6876-1G lyophilized powder, protein ≥90 %, ≥40,000 units/mg protein from chicken egg white, storage condition -20ºC.

Crude Cell culture supernatant (CCS) was provided by Lonza, and was 0.22µm filtered. Batch number IgG4 cB72.3, Lot number L16508/49

2.3.4 Stock solution preparation

A list of PEG and salts used along with their suppliers are detailed below (Figure 2.3.4.1):

Salt/PEG	Supplier	CAS number
PEG molecular weight 400	Sigma Aldrich	25322-68-3
PEG molecular weight 1000	Sigma Aldrich	25322-68-3
PEG molecular weight 3350	Sigma Aldrich	25322-68-3
PEG molecular weight 8000	Sigma Aldrich	25322-68-3
Ammonium sulphate	Fisher	7783-20-2
Potassium sulphate	Sigma Aldrich	7778-80-5
Sodium sulphate	Sigma Aldrich	7757-82-6
di-Ammonium hydrogen orthophosphate	Fisher	7783-28-0
Ammonium di-hydrogen orthophosphate	Fisher	7722-76-1
di-pottassium monohydrogen phosphate	Fisher	7758-11-4
Potassium dihydrogen phosphate	Fisher	7778-77-0
di-sodium monohydrogen phosphate	Fisher	7558-79-4
Sodium dihydrogen phosphate	Fisher	13472-35-0
Potassium citrate	Sigma Aldrich	6100-05-6
Sodium citrate	Sigma Aldrich	6132-04-03
Citric acid	Sigma Aldrich	5949-29-1

Figure 2.3.4.1: PEG/ salt product details. All products purchased were from either Fisher Scientific or Sigma Aldrich based on their corresponding CAS numbers.

Only PEG 400 was liquid at room temperature. PEG 1000 was solid and required melting prior to use. All salts, PEG 3350 and PEG 8000 were powders. Polymer

phase systems were made up weight/weight (w/w). The density of all stock solutions was measured very accurately (4 decimal places) and only anhydrous salts used. Measurement of density was performed by Lukasz Grudzien using a density equation related to water. The density difference between a glass filled with a PEG or salt solution was taken from that containing just water (Grudzien thesis, 2011). Maximum stock solution concentrations were limited due to solubility. PEG and salt stock solutions were both prepared in water, introducing a dilution effect when combined. The highest possible stock concentrations of PEG and salt were therefore required, which were extremely viscous. The salt solutions in particular were challenging to work with. They were very viscous, temperature sensitive and in some cases were seen to crystallise. Salt precipitation made aspiration and dispensing challenging. The concentrations for each stock solution are shown in Figure 2.3.4.2.

Solute	Concentration prepared for the robot (w/w)
PEG 400 & 1000	55 %
PEG 3350	35 %
PEG 8000	30 %
Most of the salts listed	40 %
Sodium sulphate/phosphate	29 %

Figure 2.3.4.2: Stock solution concentrations for the liquid handling robot. Solutions prepared in water based on maximum limits of solubility. These stocks were prepared and placed on the robot deck for subsequent dispensing using the robotic program.

2.3.5 Robot programming

Phase systems (4ml) were prepared from concentrated aqueous stocks of PEGs and salts using the Perkin Elmer multiprobe liquid handling robot. Sample was incorporated into the phase system as part of the make-up of the phases. Mixing was achieved by manual inversion of individual tubes, several times. Phases were then permitted to settle at room temperature (20-25°C) until a sharp interface was observed, typically 2 hours was required. The volume ratio was calculated by measuring the height of both phases. The robot was used to sample both the top and bottom phases. The samples were then dispensed into vials or a 96-well plate for analysis.

Solvent programming proceeded with 112 ATPS. Primarily any systems unable to form two phases were eliminated, leaving a total of 92 ATPS. Two separate robotic programs were created, allowing make up and transfer of ATPS into either HPLC vials or a 96 well micro plate (for easy readability on a plate reader).

2.3.6 Initial run with model proteins

Trial runs were carried out with Lysozyme using the ATPS detailed in Figure 2.3.1.1:

Supplementary information was obtained:

- Duplicate sample testing to establish if ATPS production was affected by protein addition.
- Phase formation timing at varying sample load (0.5 and 1mg/ml).
- Volume ratio of each phase, both with and without Lysozyme addition.

Following the trial runs it was seen that some phases were affected by protein addition. The volume ratios were changed such that they no longer formed two phases. 12 phase systems appeared to have low volume due to the high concentrations of salts used (particularly ammonium and sodium phosphate precipitation). 17 systems failed to make two phases when the Lysozyme was added. The phase appeared to be adversely affected and a single phase resulted. 63 true ATPS were left and the mAb run proceeded. The final table of 63 ATPS had three water samples (negative controls) and a 5 point dilution of the PA purified IgG added, creating a total of 71 samples. The same robotic layout was subsequently used for all the proceeding runs (Figure 2.3.6.1).

System number	% Concentration (which is the same for both PEG and salt respectively) System (w/w%)	System number	% Concentration (which is the same for both PEG and salt respectively) System (w/w%)
1	Water	36	PEG 3350 $NaPO_4$ 12.4
2	Water	37	PEG 3350 $NaPO_4$ 13.9
3	Water	38	PEG 3350 $NaPO_4$ 15.4
4	PEG 400 KPO_4 17	39	PEG 3350 $NaSO_4$ 10.7
5	PEG 400 KPO_4 18.5	40	PEG 3350 $NaSO_4$ 12.3
6	PEG 400 $NaPO_4$ 18.3	41	PEG 3350 $NaSO_4$ 13.9
7	PEG 400 $NaSO_4$ 16.8	42	PEG 3350 $NaSO_4$ 15.3
8	PEG 400 $NaSO_4$ 18.2	43	PEG 3350 NH_4PO_4 11.1
9	PEG 400 $NH4SO_4$ 19.3	44	PEG 3350 NH_4PO_4 12.8
10	PEG 1000 KPO_4 14.0	45	PEG 3350 NH_4PO_4 14.5
11	PEG 1000 KPO_4 15.5	46	PEG 3350 NH_4PO_4 16.1
12	PEG 1000 KPO_4 17.0	47	PEG 3350 NH_4SO_4 11.1
13	PEG 1000 KPO_4 18.5	48	PEG 3350 NH_4SO_4 12.8
14	PEG 1000 Na citrate 17.5	49	PEG 3350 NH_4SO_4 14.5
15	PEG 1000 Na citrate 19.0	50	PEG 3350 NH_4SO_4 16.1
16	PEG 1000 $NaPO_4$ 15.4	51	PEG 8000 K citrate 12.7
17	PEG 1000 $NaPO_4$ 16.9	52	PEG 8000 KPO_4 10.8
18	PEG 1000 $NaPO_4$ 18.3	53	PEG 8000 KPO_4 12.5
19	PEG 1000 $NaSO_4$ 13.9	54	PEG 8000 KPO_4 14.0
20	PEG 1000 $NaSO_4$ 15.3	55	PEG 8000 Na citrate 11.0
21	PEG 1000 $NaSO_4$ 16.8	56	PEG 8000 Na citrate 12.7
22	PEG 1000 $NaSO_4$ 18.2	57	PEG 8000 $NaPO_4$ 10.8
23	PEG 1000 NH_4PO_4 14.5	58	PEG 8000 $NaPO_4$ 12.4
24	PEG 1000 NH_4PO_4 16.1	59	PEG 8000 $NaPO_4$ 13.9
25	PEG 1000 NH_4PO_4 17.7	60	PEG 8000 $NaSO_4$ 10.7
26	PEG 1000 NH_4PO_4 19.2	61	PEG 8000 $NaSO_4$ 12.3
27	PEG 1000 NH_4SO_4 14.5	62	PEG 8000 $NaSO_4$ 13.9
28	PEG 1000 NH_4SO_4 16.1	63	PEG 8000 NH_4PO_4 11.1
29	PEG 1000 NH_4SO_4 17.7	64	PEG 8000 NH_4PO_4 12.8
30	PEG 1000 NH_4SO_4 19.3	65	PEG 8000 NH_4SO_4 11.1
31	PEG 3350 K Citrate 14.3	66	PEG 8000 NH_4SO_4 12.9
32	PEG 3350 KPO_4 14	67	Protein STD 1mg/ml
33	PEG 3350 KPO_4 15.5	68	Protein STD 0.8mg/ml
34	PEG 3350 Na citrate 14.3	69	Protein STD 0.6mg/ml
35	PEG 3350 Na citrate 15.9	70	Protein STD 0.4mg/ml
		71	Protein STD 0.25mg/ml

Figure 2.3.6.1: ATPS robotic programme layout. Consists of water negative controls, 63 phases system and a five point dilution of the protein A purified IgG standard. The same layout template was used for all subsequent runs.

2.3.7 Changes made to robotic handling due to the nature of ATPS

Programming changes were implemented from aqueous organic programming to aqueous two phase systems and are detailed in Figure 2.3.7.1.

Robotic step	Aqueous-Organic systems	Aqueous two phase systems (ATPS)
Probe retraction speed	Normal	• Slowed down, hence retraction time increased. • Ensured less sample was on the tip surface.
Tip submerge level	1mm depth	• Increased further to a depth of 2-3mm. • Allowed adequate aspiration, as opposed to that seen previously at liquid surface level.
Liquid level sensitivity	Ultra	• Tip sensitivity to liquid reduced to medium. • Previously, incorrect aspiration of liquids was seen due to residual liquid on the lids of stock solution containers.
Aspirating /Dispensing speed	Normal	• Speed reduced to prevent excessive pressure build up in the tips, due to viscous nature of PEGs and salts used.
Flushing	Per procedure	• Increased to per transfer group. • Allowed continual tip flushing so that no blockage occurred.
System water	Water had 10% methanol added to prevent any algae growth.	• Methanol was not added to the system water to prevent precipitation of salts; pure water was used. • Methanol was added only when the robot was inactive for an extended period of time.
Phase system settling	15 minutes	• 1 hour settling period. • ATPS took longer to form 2 phases than most aqueous organic systems.

Figure 2.3.7.1 Detailed comparison of changes made to aqueous organic programming to allow transition to aqueous two phase programming.

2.4 Results and discussion

2.4.1 Investigation into differing protein assays

Absorbance assays, as stated by Beer's Law, allows us to measure proportionally the concentration of a protein based on its absorbance of light at a particular wavelength. Absorbance is widely used to determine protein concentration due to the linear relationship that exists within a certain concentration range. Proteins absorb ultraviolet light at a maximum of 280nm allowing a direct measurement. An absorbance peak is due to the presence of structural aromatic rings. Alternatively, by the use of coloured reagents and a standard of known concentration, measurement of absorbance is possible. To determine protein concentration within ATPS and their solubility distribution, several absorbance assays were investigated. Investigations were

conducted with and without the addition of Lysozyme, to determine whether the phase system alone contributed to the absorbance. The following assays were investigated:

1) Bradford assay

2) 280nm measurement on spectrophotometer

3) Bicinchoninic acid (BCA) assay

1) Bradford assay

The Bradford assay was conducted with measurements at 630nm and 450nm (the filters available on the Brunel plate reader) to obtain a ratio. Initially all samples (Lysozyme and PA purified IgG) were diluted in water within the range of 0.4-1.4mg/ml. Absorbance readings are tabulated in Figure 2.4.1.1.

Wavelength	**Lysozyme (mg/ml)**						**PA Purified IgG (mg/ml)**					
	0.4	**0.6**	**0.8**	**1**	**1.2**	**1.4**	**0.4**	**0.6**	**0.8**	**1**	**1.2**	**1.4**
630nm	0.48	0.49	0.49	0.48	0.48	0.5	0.57	0.50	0.49	0.49	0.48	0.50
	0.49	0.49	0.49	0.48	0.48	0.49	0.49	0.50	0.49	0.50	0.48	0.50
	0.51	0.51	0.48	0.48	0.48	0.50	0.47	0.50	0.50	0.46	0.49	0.50
Average	0.49	0.50	0.49	0.48	0.48	0.49	0.51	0.50	0.49	0.48	0.49	0.50
450nm	0.91	0.92	0.93	0.92	0.91	0.94	1.09	0.90	0.88	0.91	0.90	0.90
	0.91	0.93	0.91	0.91	0.91	0.93	0.91	0.90	0.92	0.95	0.92	0.90
	0.90	0.93	0.90	0.90	0.91	0.93	0.87	0.90	0.91	0.85	0.92	0.90
Average	0.90	0.93	0.92	0.91	0.91	0.93	0.95	0.90	0.90	0.90	0.91	0.90
Ratio 630nm:450nm	0.54	0.54	0.53	0.53	0.53	0.53	0.53	0.50	0.54	0.54	0.53	0.50

Figure 2.4.1.1: Results following the Bradford assay using model protein Lysozyme and PA purified IgG. Wavelengths were measured using the Brunel plate reader at 630 and 450nm respectively. A ratio was obtained as an absorbance value and correlated to protein concentration in Figure 2.4.1.2.

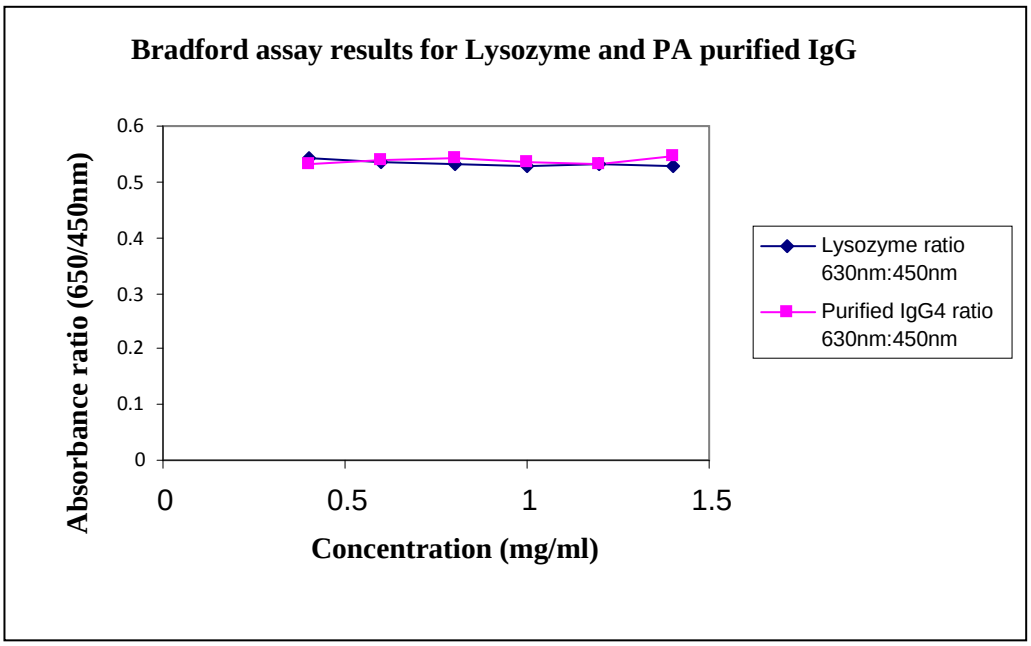

Figure 2.4.1.2: Bradford assay results, the effect of Lysozyme and purified IgG4 concentration on absorbance.

As shown in Figure 2.4.1.2, a linear trend was identified. The absorbance ratio was constant over the concentration range tested. No change in the colour of the wells were seen when the Bradford reagent was added. Saturation of the detector between 0.5-1.5mg/ml appeared to have happened. A solution would have been a dilution of samples to between 0.1-0.5mg/ml.

2) 280nm measurement on spectrophotometer

Measurement at 280nm was also investigated on a spectrophotometer. Water was used as a blank for all systems with and without protein. The robot was programmed to take 0.5ml samples from the upper and lower phase of each system respectively. The remaining samples in the tubes were mixed vigorously and 0.5ml samples quickly taken; labelled as the phase control. A control was taken to look at recovery of the protein (the sum of upper and lower phase absorbance values for a particular system should equal that of the control). All phases were broken by the addition of 0.5ml of water and subsequently read on the spectrophotometer.

No	System (% w/w)	Average upper phase	Average Lower phase	Partition coefficient	No	System (%w/w)	Average upper phase	Average Lower phase	Partition coefficient
4	PEG 400 KPO_4 17	0.064	-0.084	-0.760	36	PEG 3350 $NaPO_4$ 12.4	-0.005	0.134	-0.037
5	PEG 400 KPO_4 18.5	0.071	-0.006	-11.263	37	PEG 3350 $NaPO_4$ 13.9	0.010	0.197	0.050
6	PEG 400 $NaPO_4$ 18.3	0.022	0.277	0.078	38	PEG 3350 $NaPO_4$ 15.4	0.083	0.219	0.376
7	PEG 400 $NaSO_4$ 16.8	0.017	0.012	1.365	39	PEG 3350 $NaSO_4$ 10.7	0.024	0.045	0.539
8	PEG 400 $NaSO_4$ 18.2	0.041	0.008	5.422	40	PEG 3350 $NaSO_4$ 12.3	0.022	0.011	2.062
9	PEG 400 NH_4SO_4 19.3	0.037	-0.009	-4.111	41	PEG 3350 $NaSO_4$ 13.9	0.038	-0.020	-1.883
10	PEG 1000 KPO_4 14.0	0.040	-0.024	-1.630	42	PEG 3350 $NaSO_4$ 15.3	0.142	0.003	50.118
11	PEG 1000 KPO_4 15.5	0.018	-0.062	-0.298	43	PEG 3350 NH_4PO_4 11.1	0.070	0.020	3.446
12	PEG 1000 KPO_4 17.0	0.054	-0.042	-1.276	44	PEG 3350 NH_4PO_4 12.8	0.075	0.232	0.321
13	PEG 1000 KPO_4 18.5	-0.034	0.000	102.000	45	PEG 3350 NH_4PO_4 14.5	0.140	0.414	0.339
14	PEG 1000 Na citrate 17.5	0.023	-0.002	-10.769	46	PEG 3350 NH_4PO_4 16.1	0.094	0.157	0.597
15	PEG 1000 Na citrate 19.0	0.021	-0.002	-11.545	47	PEG 3350 NH_4SO_4 11.1	0.016	0.000	-32.000
16	PEG 1000 $NaPO_4$ 15.4	-0.042	0.154	-0.272	48	PEG 3350 NH_4SO_4 12.8	0.020	-0.006	-3.500
17	PEG 1000 $NaPO_4$ 16.9	0.001	0.204	0.004	49	PEG 3350 NH_4SO_4 14.5	0.022	-0.006	-3.686
18	PEG 1000 $NaPO_4$ 18.3	0.060	0.183	0.326	50	PEG 3350 NH_4SO_4 16.1	0.037	-0.007	-5.091
19	PEG 1000 $NaSO_4$ 13.9	0.012	0.012	0.932	51	PEG 8000 K citrate 12.7	0.037	-0.089	-0.417
20	PEG 1000 $NaSO_4$ 15.3	0.019	0.002	10.364	52	PEG 8000 KPO_4 10.8	0.058	-0.225	-0.257
21	PEG 1000 $NaSO_4$ 16.8	0.019	-0.100	-0.190	53	PEG 8000 KPO_4 12.5	0.075	-0.073	-1.032
22	PEG 1000 $NaSO_4$ 18.2	0.098	-0.002	-58.800	54	PEG 8000 KPO_4 14.0	0.210	-0.020	-10.571
23	PEG 1000 NH_4PO_4 14.5	0.092	0.698	0.132	55	PEG 8000 Na citrate 11.0	0.041	0.000	243.000
24	PEG 1000 NH_4PO_4 16.1	0.082	0.695	0.119	56	PEG 8000 Na citrate 12.7	0.035	0.011	3.059
25	PEG 1000 NH_4PO_4 17.7	0.055	0.240	0.229	57	PEG 8000 $NaPO_4$ 10.8	-0.039	0.129	-0.303
26	PEG 1000 NH_4PO_4 19.2	0.039	0.255	0.151	58	PEG 8000 $NaPO_4$ 12.4	0.125	0.168	0.743
27	PEG 1000 NH_4SO_4 14.5	0.021	-0.009	-2.296	59	PEG 8000 $NaPO_4$ 13.9	-0.011	0.255	-0.042
28	PEG 1000 NH_4SO_4 16.1	0.026	-0.008	-3.489	60	PEG 8000 $NaSO_4$ 10.7	0.021	0.010	2.016
29	PEG 1000 NH_4SO_4 17.7	0.027	-0.012	-2.203	61	PEG 8000 $NaSO_4$ 12.3	0.004	0.006	0.727
30	PEG 1000 NH_4SO_4 19.3	0.031	-0.011	-2.877	62	PEG 8000 $NaSO_4$ 13.9	0.074	0.007	10.256
31	PEG 3350 K Citrate 14.3	0.008	-0.002	-4.545	63	PEG 8000 NH_4PO_4 11.1	0.067	0.180	0.369
32	PEG 3350 KPO_4 14	-0.021	-0.021	0.961	64	PEG 8000 NH_4PO_4 12.8	0.071	0.277	0.256
33	PEG 3350 KPO_4 15.5	-0.017	0.005	-3.188	65	PEG 8000 NH_4SO_4 11.1	0.024	0.001	36.500
34	PEG 3350 Na citrate 14.3	0.025	-0.002	-15.100	66	PEG 8000 NH_4SO_4 12.9	-0.007	-0.002	4.667
35	PEG 3350 Na citrate 15.9	0.025	-0.015	-1.620					

Figure 2.4.1.3: Spectrophotometer readings at 280nm of varying phase systems with Lysozyme added, average of triplicate absorbance values taken. Partition coefficient was obtained by dividing the lower phase reading into the upper phase reading. A background correction for each system was made.

It was hypothesised that the phase system alone would contribute to the absorbance. Samples were hence prepared without protein to act as a blank. These absorbance values were subtracted from respective protein samples (Figure 2.4.1.3). Partition coefficients obtained were variable; no pattern could be seen amongst phase systems of the same salt type, thus this assay was discounted. It was thought that components within the phase system were producing considerable error. Most

considerably, the adverse effect of the phase system on linear absorbance, resulted in the 280nm absorbance readings being affected.

3) BCA assay

The BCA assay was investigated using the following conditions detailed in Figure 2.4.1.4.

PA purified IgG concentration per phase	Volume of phase sampled	Volume of water used to break phase system
1 mg/ml	50µl	200µl

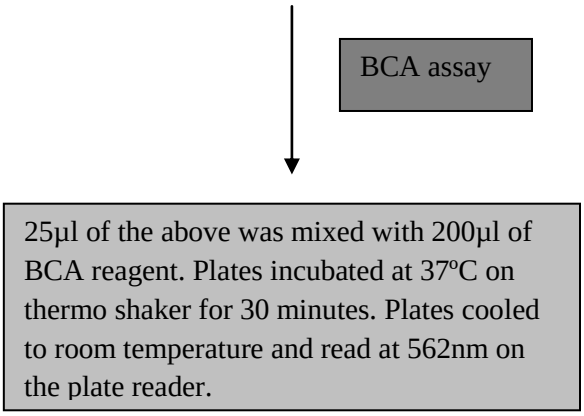

Figure 2.4.1.4: BCA assay methodology. BCA kit from Thermo Fisher Scientific, Northumberland, UK used. The samples were incubated at 37ºC and agitated. The plate was then read at 562nm using a plate reader.

Absorbance values for all systems were calculated with a background subtraction. Absorbencies obtained for the standard (PA purified IgG diluted to 1mg/ml in the phase system) were extremely low. Solubility of the IgG within the phase system due to aggregation was thought to be the issue, as low absorbance values were seen. The issue of aggregation would also make the results difficult to optimise. Optimisation was however required to increase the signal-to-noise ratio.

High background absorbency values were seen for blank samples due to phase system components. Initial conditions (Figure 2.4.1.5) caused low IgG concentrations as repeated dilutions were performed in order to minimise phase

system presence. Optimisation was investigated with respect to incubation time, incubation temperature and sample: BCA reagent ratio.

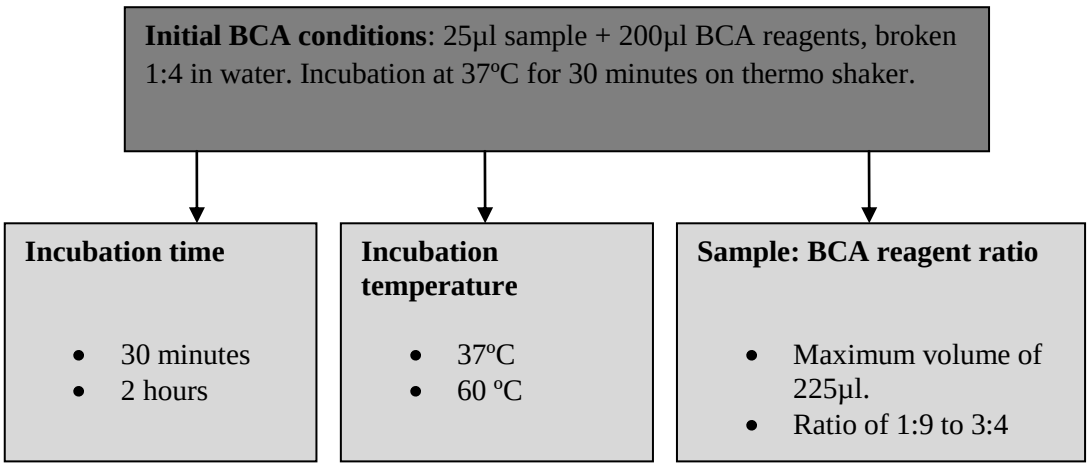

Figure 2.4.1.5: BCA assay optimisation. Initial conditions suggested by Thermo Fisher Scientific, Northumberland, UK were optimised with the aim of increasing signal to noise ratio. The three main parameters investigated were incubation time, incubation temperature and sample ratio (ratio of sample volume to BCA reagents).

Incubation time was increased from the standard 30 minutes to 2 hours. It was thought a longer incubation time would derivatise more protein, producing a larger absorbance signal. Incubation temperature was also increased from 37ºC to 60ºC. It was postulated that reaction speed would be faster as kinetics are changed by temperature, thereby creating a stronger signal. Finally sample ratio was investigated, with respect to the amount of sample added to reagent volume (to a maximum of 225µl, to fit into a multi well plate). It was hoped that a compromise between high absorbance values of the sample and a low background signal could be found. The above parameters were varied. It was discovered that by heating to 60ºC, an increased absorbance to a greater extent than 37ºC was possible. Absorbance was increased by >44 fold. As recommended by the BCA kit instructions an enhanced protocol can be used with heating to 60ºC, allowing higher absorbance values for lower protein concentrations. Due to the presence of the phase system in the sample, additional dilution was needed, affecting concentration. Higher absorbance values were obtained at 60ºC, however this was represented in the standard curve, hence calculated protein concentrations were unaffected. Any difference in absorbance was due to different kinetic behavior of the colour development at different temperatures.

The conditions that produced the most stable increase (Figure 2.4.1.7) were 125µl of sample and 100µl of BCA reagent. Absorbance values however appeared out of the linear range of the detector. The signal produced was no longer proportional to the mAb concentration. Furthermore, extremely high absorbance values were seen for the control system which did not contain any IgG. In some cases these absorbencies were higher than that of the PA purified IgG standard. It was ultimately decided to investigate HPLC analysis rather than spectroscopic absorbance. It was thought that other components within the sample were interfering with the results, producing inaccuracies and a large standard error.

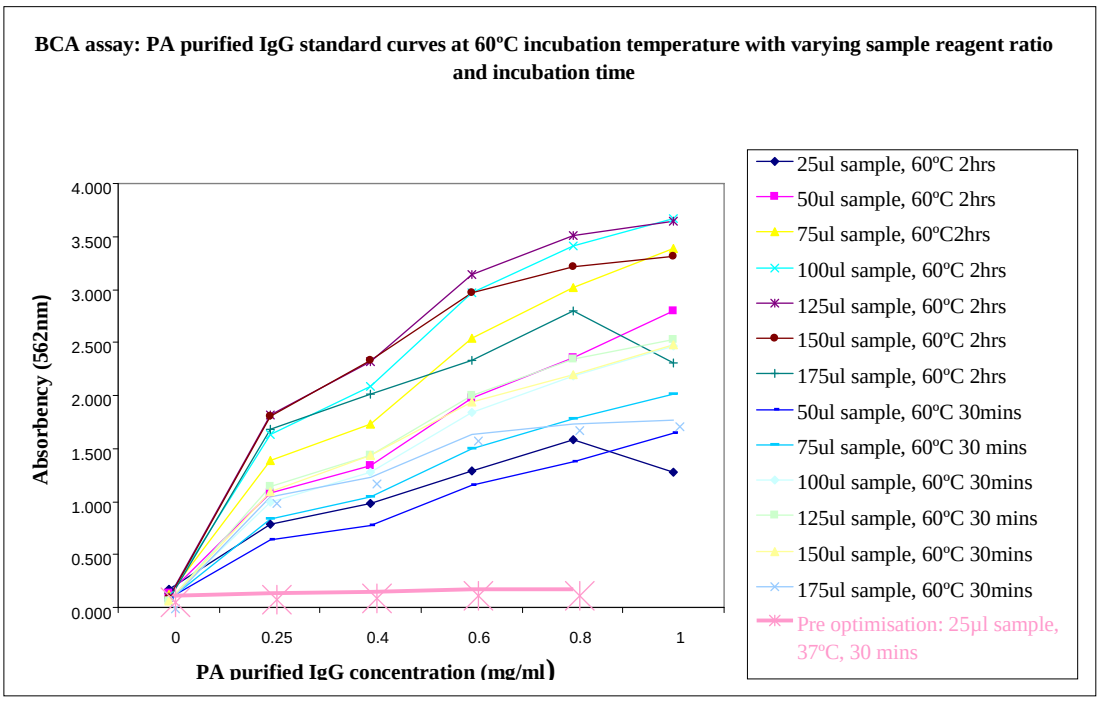

Figure 2.4.1.6: The effect of sample incubation at 60ºC. PA purified IgG sample volume listed on the legend (left hand side) was added to BCA sample reagent to a total of 225µl. Heating was increased from 30ºC degrees and seen to have a substantial increase on corresponding absorbency. Sample volume ratio (to BCA reagents) and heating time was also increased to 2 hours.

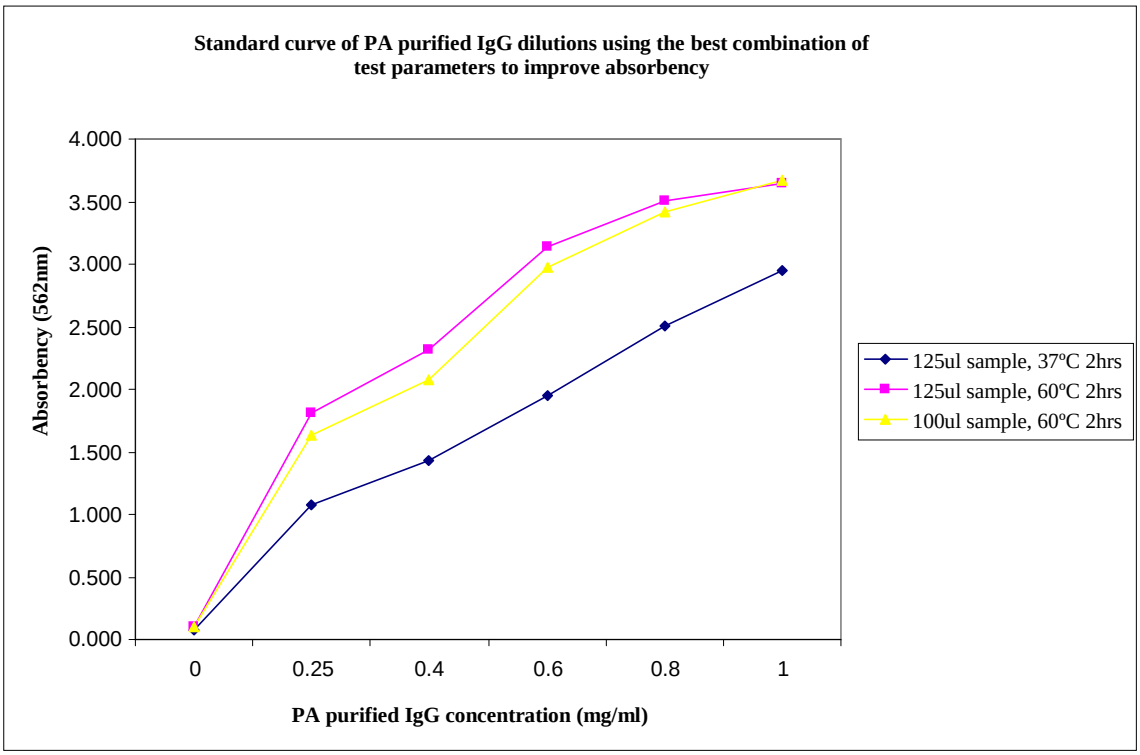

Figure 2.4.1.7: Graph following the investigation into enhancing the absorbance signal. The most appropriate conditions shown in terms of linear increase of absorbency with PA purified IgG concentration. PA immunodetection column used, Applied Biosystems,POROS, 2.1mmD x 30mmL.

2.4.2 Development of Protein A HPLC analytical method for two phase samples

All HPLC analysis was performed using a Waters 2695 Alliance system, with Waters 2996 photodiode array detector and operated using Waters EmpowerTM software (Waters Elstree, Hertfordshire, UK). A POROS Protein A 20µm column, 4.6mm x 100mm and a volume of 1.7ml was used.

At Lonza, for both preparative and analytical protein A HPLC, low pH elution is used. The following buffers are employed for HPLC analysis:

Binding buffer: 150mM sodium chloride 50mM glycine pH 8 (Buffer A)

Elution buffer: 150mM sodium chloride 50mM glycine pH 2.5 (Buffer B)

A fast run time of two minutes with an injection volume (water injection solvent) of 100µl is routinely used at Lonza. The IgG is eluted as a single sharp peak at 0.51 minutes using the HPLC program detailed in Figure 2.4.2.1.

Time (minutes)	Flow (ml/min)	Buffer A: 150mM sodium chloride, 50 mM glycine pH 8 (%)	Buffer B: 150mM sodium chloride, 50 mM glycine pH 2.5 (%)
0.00	2.0	100	0
0.50	2.0	100	0
0.51	2.0	0	100
1.26	2.0	0	100
1.30	2.0	100	0

Figure 2.4.2.1: Lonza HPLC analysis program. Protein A HPLC immunodetection column used. A total run time of 2 minutes with buffer A as the binding buffer (150mM sodium chloride, 50 mM glycine pH 8) and buffer B as the elution buffer. Elution is by a drop in pH (150mM sodium chloride, 50 mM glycine pH 2.5). IgG elution is at 0.51 minute.

All experiments within this section were conducted with a PEG 3350-sodium phosphate, (18%/18% w/w) system pH 7.2, with 1mg/ml of PA purified IgG added. Phase system within the injection solvent adversely affected the chromatograms. Peak widening was seen with the inability of the baseline to settle. Differing lines of investigation were conducted to allow HPLC programme optimisation (Figure 2.4.2.2), with the objective to improve the chromatogram.

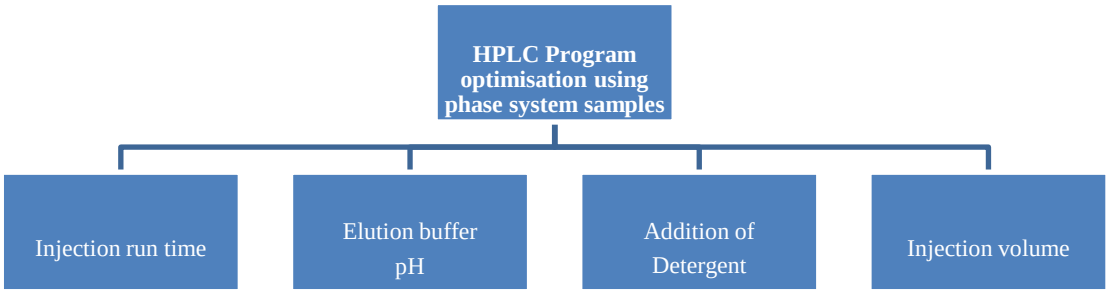

Figure 2.4.2.2: Parameters for investigation for HPLC optimisation of phase system samples. Investigation based on improving IgG elution chromatograms injected in phase system. Injection run time, elution buffer pH, detergent and injection volume were all investigated.

Injection run time

An increased HPLC run time was thought to allow all injection solvent (phase system) to be washed off the column, hence a clearer elution peak. The following HPLC program was developed (Figure 2.4.2.3) which produced clearer and improved chromatograms with a sharp IgG peak at 6 minutes (Figure 2.4.2.5). This was an improvement to chromatograms previously seen using the Lonza analytical method (Figure 2.4.2.4).

Time (minutes)	% Binding buffer (A pH8)	% Elution buffer (B pH 2.5)
0:00	100	0
5:50	100	0
5:51	0	100
6:26	0	100
6:30	100	0

Figure 2.4.2.3: Developed HPLC program. Increased run time of 6 minutes. Protein A HPLC immunodetection column used. Buffer A was used as the binding buffer (150mM sodium chloride, 50 mM glycine pH 8) and buffer B as the elution buffer. Elution by a drop in pH (150mM sodium chloride, 50 mM glycine pH 2.5). IgG elution at 6 minutes.

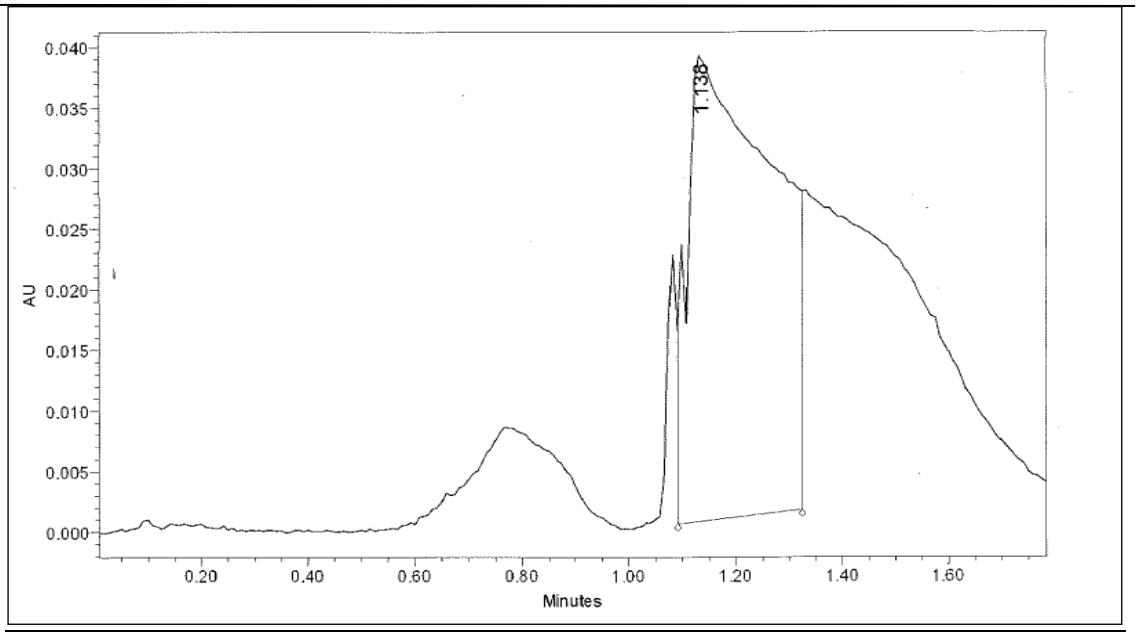

Figure 2.4.2.4: Protein A HPLC analysis of IgG in phase system using Lonza 2 minute elution program. Elution started at 1 minute. Due however to the phase system, elution was compromised. A large amount of peak tailing was seen with the inability of the baseline to settle.

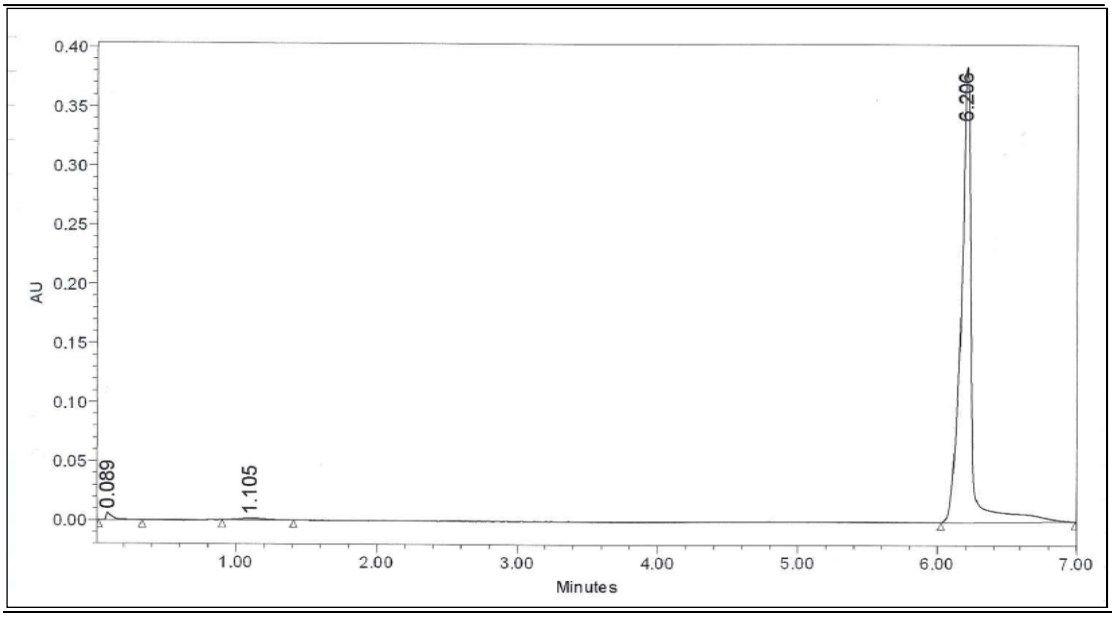

Figure 2.4.2.5: Protein A HPLC analysis of IgG in phase system using newly optimised 7 minute run time. Elution occurred at 6 minutes by the use of a low pH elution buffer. Sharp single peak elution is seen and the chromatogram was not adversely affected by the presence of the phase system.

Elution buffer pH

To further improve IgG elution peak, hence reduction of peak tailing due to the phase system, a range of lower pH elution buffers were investigated. It was hypothesised by reducing pH, the IgG would be further repelled from the protein A hence eluted. The routinely used buffer as specified by Lonza is at pH 2.5. Elution buffers at pH 1.5, 2 and 2.5 were compared.

Using the pH 1.5 elution buffer, the elution profile of the IgG was hardly affected by the phase system (a similar baseline peak width was seen as compared to the Lonza analysis method). An improvement was seen, with no IgG peak tailing using the pH 1.5 buffer. When compared to the pH 1.5 buffer, the elution profile at pH 2 was not clear. The background was very high with noisy peaks. The elution buffer at pH 1.5 was subsequently used thereafter.

Detergent

To further improve chromatograms, addition of small amounts of Triton 100 was investigated. The objective was to prevent aggregation of the antibody, allowing even clearer IgG elution from the phase system injection solvent.

Triton X-100 was added at 0.1 and 1% to the pH 1.5 elution buffer. The elution profiles produced were not clear. Extremely noisy peaks were seen even with a small addition of the detergent due to the Triton absorbing at 280nm. This line of investigation was not taken further.

Injection volume

The injection volume was also optimised to ensure maximum sensitivity without column overload. Investigations were carried out at 5, 20, 40, 60, 80 and 100µl.

A 5µl injection volume created low absorbance values with the inability of the baseline to settle. At a 100µl volume, complete saturation of the column was seen. Absorbance exceeded 1 unit and peak elution was also seen at 0.1 minutes with the solvent front (Figure 2.4.2.6). The optimum injection volume was 80µl. The best sensitivity along with the sharpest peaks was seen at this volume.

A range of different phase systems were investigated with analysis by protein A HPLC before the full robotic run was started. Low absorbance readings post HPLC analysis were seen even for the control samples (water). The pH change in the programme created an elevated background that was accounted for with each run. An average background peak area was deducted for each sample. A comparison of changes made to the Lonza HPLC program, allowing analysis unaffected by phase system in the sample injection solvents, are shown in Figure 2.4.2.7.

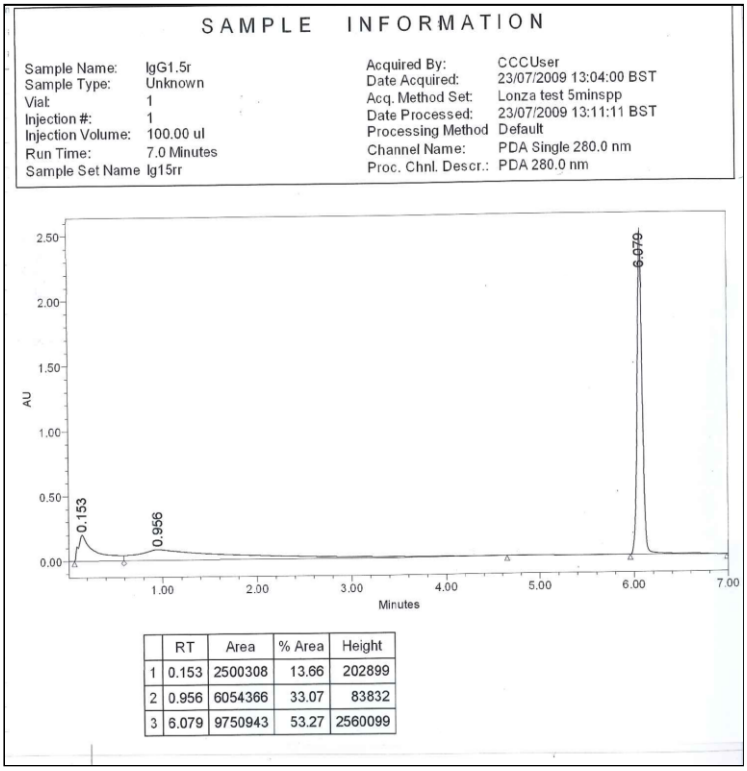

Figure 2.4.2.6: Protein A HPLC chromatogram showing column oversaturation by a sample injection volume of 100µl. PA purified IgG used, flow rate of 2ml/min and column temperature of 20ºC. Absorbance of nearly 2.50AU is reached at a single wavelength of 280nm with significant amounts also being eluted at 0.153 minutes with the solvent front.

	Lonza conditions	**HPLC conditions required to permit analysis in ATPS**
Run time (minutes)	2	7
Elution buffer (pH)	2.5	1.5
Injection volume (µl)	100	80
Binding time (minutes)	0.51	5:51
Elution time (minutes)	1:00	6:00

Figure 2.4.2.7: Comparison of HPLC conditions required to permit analysis when injection solvent is ATPS with the Lonza analytical method. 'Binding time' denotes the time given for the IgG to bind to the protein A ligand. Elution time represents when pH is lowered, such that the IgG isoelectric point is changed and released from the protein A.

2.4.3 Robotic run using crude Cell Culture Supernatant (CCS) and result analysis by developed protein A HPLC

Robotic partitioning was carried out with 63 ATPS (Figure 2.3.6.1). 1mg of CCS was incorporated into each phase system. All samples were robotically programmed to be dispensed into HPLC vials, 400µl samples were diluted with 600 µl of water to create a single phase.A five point control dilution of the Protein A purified IgG control was included at the end of the run (0.2-1mg/ml).

At the end of the robotic run samples were subject to Protein A HPLC. HPLC analysis of each sample was conducted in triplicate with an 80µl injection volume as previously defined. The 6.0 minute peak was noted as IgG. The total IgG area was calculated by the addition of the corresponding upper and lower 6 minute IgG peak areas. The partition coefficient was obtained by dividing the upper phase peak area by the lower. To determine any mass balance deviation, average total IgG area in a given phase system was defined as a percentage of the HPLC peak area of the PA purified IgG control at 1mg/ml.

The phase systems of interest were regarded as systems with a partition coefficient of 0.5-2 and a total peak area similar to that of the 1mg/ml PA purified IgG control (significant difference <85%) (Figure 2.4.3.1).

Phase system/ sample (w/w %)	HPLC injection number	Upper peak area	Lower peak area	Total area	Partition coefficient (K)	Average partition coefficient (K)
Control 1 (1mg/ml)	1			3446103		
Control 1 (1mg/ml)	2			3331455		
Control 1 (1mg/ml)	3			3294387		
Control 2 (0.8mg/ml)	1			2581755		
Control 2 (0.8mg/ml)	2			2504428		
Control 2 (0.8mg/ml)	3			2518835		
Control 3 (0.6mg/ml)	1			1927649		
Control 3 (0.6mg/ml)	2			1929415		
Control 3 (0.6mg/ml)	3			1927654		
Control 4 (0.4mg/ml)	1			1471800		
Control 4 (0.4mg/ml)	2			1469445		
Control 4 (0.4mg/ml)	3			1480765		
Control 5 (0.2mg/ml)	1			1352757		
Control 5 (0.2mg/ml)	2			1345519		
Control 5 (0.2mg/ml)	3			1328807		
Water control	1			554829		
Water control	2			537078		
Water control	3			518036		
Water control	4			527770		
Water control	5			532910		
Water control	6			514379		
PEG 400 KPO_4 17	1	1329083	1576309	2905392	0.84	
	2	1313398	1433128	2746526	0.92	
	3	1312245	1550028	2862273	0.85	0.87
PEG 400 KPO_4 18.5	1	2340075	494979	2835054	4.73	
	2	2214388	496258	2710646	4.46	
	3	2151745	495415	2647160	4.34	4.51
PEG 400 $NaPO_4$ 18.3	1	2545357	475224	3020581	5.36	
	2	2463273	461364	2924637	5.34	
	3	2413468	453616	2867084	5.32	5.34
PEG 400 $NaSO_4$ 16.8	1	2975724	403019	3378743	7.38	
	2	2958981	382935	3341916	7.73	
	3	2942245	379006	3321251	7.76	7.62

Phase system/ sample (w/w %)	HPLC injection number	Upper peak area	Lower peak area	Total area	Partition coefficient (K)	Average partition coefficient (K)
PEG 400 $NaSO_4$ 18.2	1	2514021	438528	2952549	5.73	
	2	2523741	425693	2949434	5.93	
	3	2515956	407706	2923662	6.17	5.94
PEG 400 NH_4SO_4 19.3	1	2717496	326305	3043801	8.33	
	2	2680809	324416	3005225	8.26	
	3	2663140	318377	2981517	8.36	8.32
PEG 1000 KPO_4 14.0	1	1466477	1396958	2863435	1.05	
	2	1440016	1381755	2821771	1.04	
	3	1428871	1376598	2805469	1.04	1.04
PEG 1000 KPO_4 17.0	1	1870032	1356275	3226307	1.38	
	2	1852033	1322412	3174445	1.40	
	3	1897068	1328744	3225812	1.43	1.40
PEG 1000 KPO_4 18.5	1	1848081	1924164	3772245	0.96	
	2	1829684	1933211	3762895	0.95	
	3	1826418	1926009	3752427	0.95	0.95
PEG 1000 Na citrate 17.5	1	1609361	1926009	3535370	0.84	
	2	1607102	2201470	3808572	0.73	
	3	1607928	2194160	3802088	0.73	0.77
PEG 1000 Na citrate 19.0	1	1933157	1218534	3151691	1.59	
	2	1929716	1201999	3131715	1.61	
	3	1941926	1157569	3099495	1.68	1.62
PEG 1000 $NaPO_4$ 15.4	1	1488783	174925	1663708	8.51	
	2	1490442	192527	1682969	7.74	
	3	1484273	176276	1660549	8.42	8.22
PEG 1000 $NaPO_4$ 16.9	1	1047002	178788	1225790	5.86	
	2	1043530	158672	1202202	6.58	
	3	1047067	147298	1194365	7.11	6.51
PEG 1000 $NaPO_4$ 18.3	1	974532	144737	1119269	6.73	
	2	974646	159998	1134644	6.09	
	3	977118	168556	1145674	5.80	6.21
PEG 1000 $NaSO_4$ 13.9	1	1538937	236216	1775153	6.51	
	2	1534253	194415	1728668	7.89	
	3	1528800	170489	1699289	8.97	7.79
PEG 1000 $NaSO_4$ 15.3	1	755060	209252	964312	3.61	
	2	755806	208483	964289	3.63	
	3	751283	223312	974595	3.36	3.53
PEG 1000 $NaSO_4$ 16.8	1	1158256	158650	1316906	7.30	
	2	1160466	127161	1287627	9.13	
	3	1153490	113622	1267112	10.15	8.86
PEG 1000 $NaSO_4$ 18.2	1	1144038	140862	1284900	8.12	
	2	1138371	114227	1252598	9.97	
	3	1157736	126274	1284010	9.17	9.09
PEG 1000 NH_4PO_4 14.5	1	1726906	175301	1902207	9.85	
	2	1710278	158454	1868732	10.79	
	3	1703179	149884	1853063	11.36	10.67
PEG 1000 NH_4PO_4 16.1	1	1234724	178939	1413663	6.90	
	2	1233918	187618	1421536	6.58	
	3	1237697	176929	1414626	7.00	6.82
PEG 1000 NH_4PO_4 17.7	1	1203824	171217	1375041	7.03	
	2	1200499	190834	1391333	6.29	
	3	1202377	210140	1412517	5.72	6.35
PEG 1000 NH_4PO_4 19.2	1	1419123	218649	1637772	6.49	
	2	1395298	218190	1613488	6.39	
	3	1445586	209802	1655388	6.89	6.59

Phase system/ sample (w/w %)	HPLC injection number	Upper peak area	Lower peak area	Total area	Partition coefficient (K)	Average partition coefficient (K)
PEG 1000 NH_4SO_4 14.5	1	784216	207190	991406	3.79	3.75
	2	784019	215681	999700	3.64	
	3	784740	204572	989312	3.84	
PEG 1000 NH_4SO_4 16.1	1	1116467	1142113	2258580	0.98	0.98
	2	1118026	1144690	2262716	0.98	
	3	1116142	1141370	2257512	0.98	
PEG 1000 NH_4SO_4 17.7	1	1553776	384186	1937962	4.04	4.09
	2	1512631	374476	1887107	4.04	
	3	1500071	358653	1858724	4.18	
PEG 1000 NH_4SO_4 19.3	1	1477253	324749	1802002	4.55	4.78
	2	1682449	338337	2020786	4.97	
	3	1695522	352795	2048317	4.81	
PEG 3350 K Citrate 14.3	1	1929430	345301	2274731	5.59	6.01
	2	1936831	310408	2247239	6.24	
	3	1934225	311938	2246163	6.20	
PEG 3350 KPO_4 14	1	736427	379722	1116149	1.94	1.99
	2	712772	370390	1083162	1.92	
	3	711356	339485	1050841	2.10	
PEG 3350 KPO_4 15.5	1	641619	264406	906025	2.43	2.55
	2	671167	263864	935031	2.54	
	3	657342	245619	902961	2.68	
PEG 3350 Na citrate 14.3	1	724018	261962	985980	2.76	2.75
	2	758546	269087	1027633	2.82	
	3	755182	282674	1037856	2.67	
PEG 3350 Na citrate 15.9	1	636931	309595	946526	2.06	2.34
	2	684722	286600	971322	2.39	
	3	694221	270121	964342	2.57	
PEG 3350 $NaPO_4$ 12.4	1	620912	536459	1157371	1.16	1.09
	2	605767	581535	1187302	1.04	
	3	605499	573209	1178708	1.06	
PEG 3350 $NaPO_4$ 13.9	1	268935	769992	1038927	0.35	0.32
	2	243350	772970	1016320	0.31	
	3	232301	769062	1001363	0.30	
PEG 3350 $NaPO_4$ 15.4	1	962175	1748012	2710187	0.55	0.55
	2	1000864	1826706	2827570	0.55	
	3	927947	1700206	2628153	0.55	
PEG 3350 $NaSO_4$ 10.7	1	963286	256408	1219694	3.76	3.44
	2	947514	297557	1245071	3.18	
	3	936476	277662	1214138	3.37	
PEG 3350 $NaSO_4$ 12.3	1	254698	346863	601561	0.73	0.79
	2	241220	302848	544068	0.80	
	3	255721	301162	556883	0.85	
PEG 3350 $NaSO_4$ 13.9	1	1011557	191738	1203295	5.28	5.62
	2	1010666	179271	1189937	5.64	
	3	1017495	171726	1189221	5.93	
PEG 3350 $NaSO_4$ 15.3	1	492079	223609	715688	2.20	2.08
	2	491814	243802	735616	2.02	
	3	478121	234999	713120	2.03	
PEG 3350 NH_4PO_4 11.1	1	589196	151702	740898	3.88	4.03
	2	568037	145456	713493	3.91	
	3	577802	134553	712355	4.29	
PEG 3350 NH_4PO_4 12.8	1	275041	1847982	2123023	0.15	0.14
	2	272998	1848275	2121273	0.15	
	3	230092	1848621	2078713	0.12	

Phase system/ sample (w/w %)	HPLC injection number	Upper peak area	Lower peak area	Total area	Partition coefficient (K)	Average partition coefficient (K)
PEG 3350 NH_4PO_4 14.5	1	159823	351251	511074	0.46	
	2	162891	321017	483908	0.51	
	3	176998	320898	497896	0.55	0.50
PEG 3350 NH_4PO_4 16.1	1	290261	281342	571603	1.03	
	2	271149	299914	571063	0.90	
	3	273789	301937	575726	0.91	0.95
PEG 3350 NH_4SO_4 11.1	1	1229335	183715	1413050	6.69	
	2	1229599	183944	1413543	6.68	
	3	1228534	193616	1422150	6.35	6.57
PEG 3350 NH_4SO_4 12.8	1	954722	2201328	3156050	0.43	
	2	954208	2206526	3160734	0.43	
	3	958740	2209608	3168348	0.43	0.43
PEG 3350 NH_4SO_4 14.5	1	149402	870626	1020028	0.17	
	2	159936	774499	934435	0.21	
	3	165315	731776	897091	0.23	0.20
PEG 3350 NH_4SO_4 16.1	1	141681	247081	388762	0.57	
	2	139389	275685	415074	0.51	
	3	147574	296871	444445	0.50	0.53
PEG 8000 K citrate 12.7	1	272920	228005	500925	1.20	
	2	272726	224844	497570	1.21	
	3	257017	228992	486009	1.12	1.18
PEG 8000 KPO_4 10.8	1	1214236	991919	2206155	1.22	
	2	1209248	989050	2198298	1.22	
	3	1209157	991538	2200695	1.22	1.22
PEG 8000 KPO_4 12.5	1	1067565	1123398	2190963	0.95	
	2	911128	1072995	1984123	0.85	
	3	892480	1066749	1959229	0.84	0.88
PEG 8000 KPO_4 14.0	1	326952	1059825	1386777	0.31	
	2	343962	1053821	1397783	0.33	
	3	335592	1067407	1402999	0.31	0.32
PEG 8000 Na citrate 11.0	1	1069996	437405	1507401	2.45	
	2	1045639	458799	1504438	2.28	
	3	1022284	469445	1491729	2.18	2.30
PEG 8000 Na citrate 12.7	1	355848	2647580	3003428	0.13	
	2	352749	2695476	3048225	0.13	
	3	342991	2541672	2884663	0.13	0.13
PEG 8000 $NaPO_4$ 10.8	1	253294	1087239	1340533	0.23	
	2	223436	1083486	1306922	0.21	
	3	215187	1099552	1314739	0.20	0.21
PEG 8000 $NaPO_4$ 12.4	1	266999	1396150	1663149	0.19	
	2	253552	1393063	1646615	0.18	
	3	244425	1395310	1639735	0.18	0.18
PEG 8000 $NaPO_4$ 13.9	1	511557	827242	1338799	0.62	
	2	508266	802846	1311112	0.63	
	3	512476	769193	1281669	0.67	0.64
PEG 8000 $NaSO_4$ 10.7	1	468466	445145	913611	1.05	
	2	481644	435250	916894	1.11	
	3	463279	383588	846867	1.21	1.12
PEG 8000 $NaSO_4$ 12.3	1	192877	535978	728855	0.36	
	2	189715	520222	709937	0.36	
	3	176499	513608	690107	0.34	0.36
PEG 8000 $NaSO_4$ 13.9	1	263589	393018	656607	0.67	
	2	271104	414389	685493	0.65	
	3	279631	420245	699876	0.67	0.66

Phase system/ sample (w/w %)	HPLC injection number	Upper peak area	Lower peak area	Total area	Partition coefficient (K)	Average partition coefficient (K)
PEG 8000 NH_4PO_4 11.1	1	416888	269084	685972	1.55	
	2	407126	244473	651599	1.67	
	3	381193	234594	615787	1.62	1.61
PEG 8000 NH_4PO_4 12.8	1	879445	743005	1622450	1.18	
	2	848626	743079	1591705	1.14	
	3	828363	742265	1570628	1.12	1.15
PEG 8000 NH_4SO_4 11.1	1	869232	416010	1285242	2.09	
	2	864620	429932	1294552	2.01	
	3	863153	452660	1315813	1.91	2.00
PEG 8000 NH_4SO_4 12.9	1	228629	2011564	2240193	0.11	
	2	202794	2012816	2215610	0.10	
	3	182892	2009599	2192491	0.09	0.10
Control 1 (1mg/ml)	1			3072638		
	2			3143123		
	3			3083849		
Control 2 (0.8mg/ml)	1			2603168		
	2			2597480		
	3			2602995		
Control 3 (0.6mg/ml)	1			1951974		
	2			1944271		
	3			1941796		
Control 4 (0.4mg/ml)	1			1404742		
	2			1402860		
	3			1404882		
Control 5 (0.2mg/ml)	1			760037		
	2			757628		
	3			755713		

Figure 2.4.3.1: Full robotic run results with HPLC analysis using crude CCS. HPLC analysis using optimised 7 minute HPLC program. All peak areas were measured in µV.sec. All systems highlighted in red were deemed most appropriate, based on the criteria of having a partition coefficient in the range of 0.5-2 and also an IgG HPLC peak area recovery of >85% compared to that of the PA purified IgG control.

	Partition coefficient (K)			HPLC peak area		
PEG	Average	Standard deviation	Standard error	Average	Standard deviation	Standard error
400	5.43	2.65	1.08	2967636	209924.03	85701.12
1000	4.88	2.94	0.59	1998744	798150.43	159630.09
3350	1.68	1.74	0.36	1165149	812039.31	165756.83
8000	0.74	0.69	0.16	1518003	622601.83	146748.66

Figure 2.4.3.2: Average partition coefficient and HPLC peak area of all systems tested based on PEG molecular weight. All systems were grouped based on PEG molecular weight (not salt type).

Data was collated based on the PEG molecular weight used (Figure 2.4.2.3). It appeared that as PEG molecular weight increased the resulting IgG partition coefficient decreased (Figure 2.4.3.3). The HPLC peak area of the IgG however seemed to decrease (Figure 2.4.3.4). It therefore appeared that at higher PEG

molecular weight, IgG solubility was decreasing and aggregation was occurring. A higher recovery of total peak area was seen with lower molecular weight PEGs, more specifically PEG 1000 and 400.

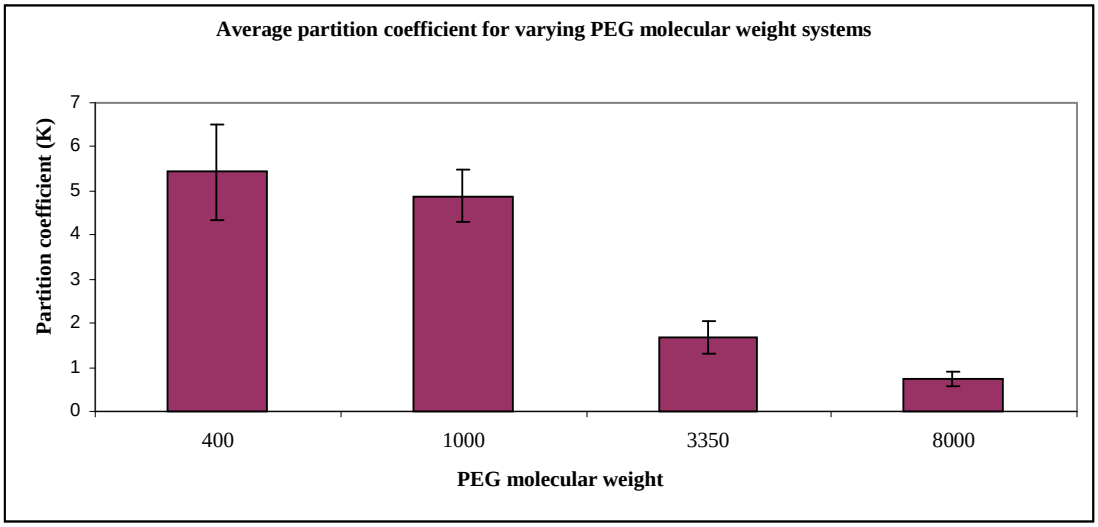

Figure 2.4.3.3: The effect of PEG molecular weight on resulting partition coefficient. Results collated from triplicate run following protein A HPLC analysis in Figure 2.4.3.1.

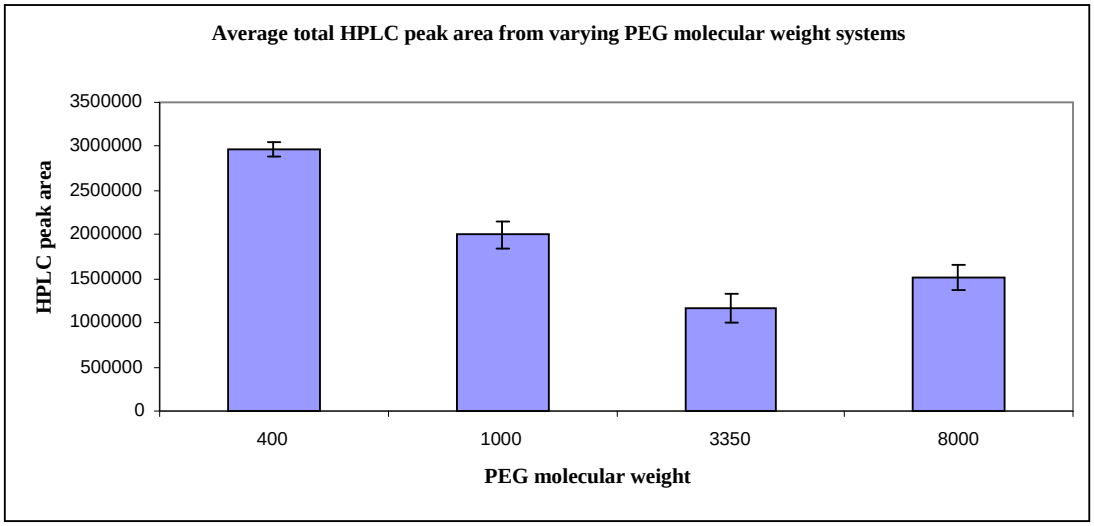

Figure 2.4.3.4: Effect of PEG molecular weight on resulting HPLC peak area. Results collated from triplicate run following protein A HPLC analysis in Figure 2.4.3.1.

The phase systems of interest are shown in Figure 2.4.3.5. These were deemed most appropriate based on a partition coefficient of 0.5-2 and a high total peak area >85% recovery in comparison to the PA purified IgG control. The PEG 3350 11.1%/11.1% ammonium sulphate system was still included despite just being out of the

specification, with a partition coefficient at 0.43, as it was extremely close to the specification of 0.5≤K≤2 and showed 100% HPLC peak area recovery. Only the 8 systems detailed in Figure 2.4.3.5 fulfilled both these criteria.

Phase system/ sample (% w/w)	HPLC injection number	Partition coefficient (K)	Average K	% IgG recovery in comparison to PA purified IgG control	Average recovery
PEG 400 KPO_4 17.0	1	0.84	0.87±0.041	93.73	91.55±2.650
	2	0.92		88.60	
	3	0.85		92.34	
PEG 1000 KPO_4 14.0	1	1.05	1.04±0.006	92.37	91.30±0.964
	2	1.04		91.03	
	3	1.04		90.50	
PEG 1000 KPO_4 15.5	1	1.38	1.40±0.025	104.08	103.52±0.961
	2	1.40		102.41	
	3	1.43		104.06	
PEG 1000 KPO_4 17.0	1	0.96	0.95±0.008	121.69	121.38±0.320
	2	0.95		121.39	
	3	0.95		121.05	
PEG 1000 KPO_4 18.5	1	0.84	0.77±0.060	114.05	119.85±5.029
	2	0.73		122.86	
	3	0.73		122.65	
PEG 3350 $NaPO_4$ 13.9	1	0.55	0.55±0.002	87.43	87.81±3.233
	2	0.55		91.22	
	3	0.55		84.78	
PEG 3350 NH_4SO_4 11.1	1	0.43	0.43±0.001	101.81	101.99±0.200
	2	0.43		101.96	
	3	0.43		102.21	
PEG 1000 Na citrate 17.5	1	1.63	1.62±0.018	101.67	100.90±0.850
	2	1.62		101.03	
	3	1.60		99.99	

Figure 2.4.3.5: Highlighted phase systems of interest following robotic run. Based on the criteria of a partition coefficient in the range of 0.5-2 and an IgG HPLC peak area recovery of >85% when compared to that of the PA purified IgG control.

Highlighted in red in Figure 2.4.3.5, are two phosphate systems. Their very high recovery was associated with experimental error and possible adverse phosphate interaction with absorbance at these high concentrations. Furthermore, of the eight phase systems considered as most the appropriate, 6 of these contained phosphate. Due to environmental disposal issues with this salt (Azevedo, 2007) the remaining 2 systems i.e. the PEG 3350 11.1%/11.1% ammonium sulphate system and the PEG 1000 17.5%/17.5% sodium citrate system were, initially investigated.

2.6 Conclusions

The robotic solvent selection for aqueous *organic* two phase systems has been very successful and is routinely applied for the separation of small molecules in the Advanced Bioprocessing Centre (ABC). For polymer phase systems however, there seems to be a greater degree of variables.

There were many challenges with the use of robotic liquid handling for the selection of polymer systems. Firstly the sheer number of ATPS produced a large selection table of 63 phase systems. Previously this table was reduced from 112 systems due to precipitation and aggregation issues. In some cases, the mAb affected the system's ability to form two phases.

The nature of the PEG, salt and the bio molecules used meant temperature and pH complications were seen. Limitations on the concentrations that can be prepared by the robot, programming issues and a slow operation time make this technique unlikely to be adopted by industry. An alternative method is required that is both quick and highly efficient, allowing bio molecules to be tested within phase systems. However, this investigation of a vast range of systems provided some very valuable data. It allowed trends to be seen, in relation to particular salts and PEG. Ultimately robotic programming allowed the identification of the PEG 1000 17.5%/17.5% sodium citrate and PEG 3350 11.1%/11.1% ammonium sulphate systems. These systems have been used for separation in the following chapters. Furthermore, this selection process, if completed manually, would have taken significantly longer.

Further work to improve the robotic selection of ATPS requires consideration of other factors such as polymer type. Only PEG has been explored in this work. Dextran and other polymers with varying hydrophobicity e.g. polypropylene glycol and hydroxypropyl dextran could be investigated. Finally, there are also affinity molecules, such as Protein A to be added, resulting in a robotic table that has the potential to be even larger. Further factors that need to be considered are pH adjustment and temperature control. These factors can greatly affect phase systems near the critical point.

CHAPTER 3: Separation of monoclonal antibody cell culture supernatant (CCS) using Centrifugal partitioning chromatography (CPC)

3) Separation of monoclonal antibody from cell culture supernatant (CCS) using Centrifugal partitioning chromatography (CPC).

3.1 Summary

The experiments in this chapter explore mAb separation by centrifugal partitioning chromatography (CPC). Previous work by Guan *et al* (2008) showed the importance of column design, hence mode of column mixing, allowing both high stationary phase retention and adequate mass transfer between the phases. CPC studies in this chapter have shown experimental predictability and separation from impurities. A loss, however, has been demonstrated with the ability of IgG to bind to Protein A. IgG that was purified was unable to bind Protein A (PA) and was given the term "Protein A non binding IgG". Furthermore, attempts at reversing the production of this non functional form by temperature, pH and sonication were not successful. The PEG 3350 11.1%/11.1% ammonium sulphate system previously highlighted from the robotic run in chapter 2 was seen to cause a precipitation effect on the IgG. This effect had not been seen previously, however this became evident following prolonged incubation time and CCC processing. It was thought that this effect added to the reduction of biological activity found in the IgG once it had been through the CCC

instrument. The PEG 1000 17.5%/17.5% sodium citrate, also previously highlighted from the robotic run, was deemed more suitable and used thereafter. The experiments within this chapter ultimately show the necessity for high resolution separation by thorough cascade mixing, affect the resulting IgG functionality.

3.2 Introduction

CCC instruments types can be divided into two forms: hydrostatic and hydrodynamic. Both utilize a liquid mobile and stationary phase and require rotation, to allow stationary phase retention (Sutherland, 2007). The resulting mixing vigour is the main difference between these modes. Hydrodynamic mixing utilises gentler wave-like mixing as compared to hydrostatic cascade mixing.

Hydrodynamic mixing, as seen in all J-type centrifuges, allows separation along a continuous length of tubing (Figure 3.2.1). Stationary phase is held within the column by centrifugal forces created by continual planetary rotation. Mobile phase is pumped into the column, creating zones of mixing and settling. The continual length of tubing is wound around a bobbin which rotates in a planetary motion i.e. rotating around its own axis whilst simultaneously rotating around the sun gear. These two axes of rotation create the gentler wave like mixing.

A hydrostatic mode of mixing is seen with the CPC. Stationary phase is trapped by a series of interconnected chambers mounted circumferentially on a disk. Rotation is around a single axis (Figure 3.2.1). Pressure is used to push the mobile phase through the chambers. The mixing that ensues is much more vigorous when compared to the hydrodynamic mode. The mobile phase penetrates the stationary phase by rapid jets or droplets, causing waterfall cascade like mixing.

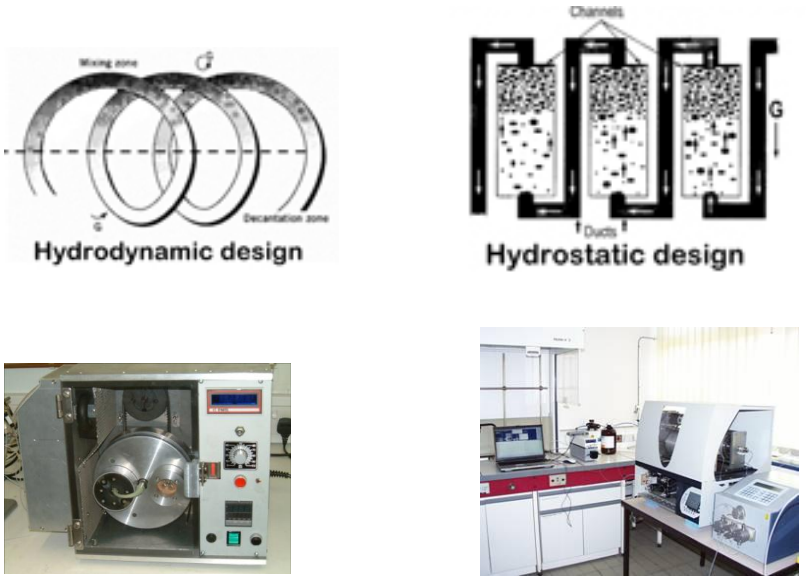

Figure 3.2.1: Hydrostatic and hydrodynamic column designs. Hydrodynamic design is shown on the left hand side, seen with J type centrifuges. The hydrostatic design is shown on the right hand side as seen with the CPC.

As shown by Guan *et al* (2008), column design is of paramount importance for the separation of biological molecules. Poor protein separation of a model mixture of Lysozyme and Myoglobin was previously seen using a J type centrifuge (Bourton *et al.,* 2007). Numerous successful high scale separations of small molecules however have been seen with aqueous organic systems (Wood *et al*., 2007; Chen *et al*., 2007; Garrard, 2007). Protein separations using ATPS and hydrodynamic mixing have been seen as inefficient (Sutherland *et al.*, 2008; Guan *et al*., 2008). Adequate mass transfer of high molecular weight proteins was considered to be insufficient. The viscous nature of the ATPS, due to the high concentrations in each phase, was also to blame. Resulting mixing vigour was inadequate (depicted by peak broadening), resolution was hence lost and separation from impurities not seen.

Earlier work by Bourton (2007) had showed the thorough mixing, as achieved by the CPC, was vital. Consequently, having highlighted the possible phase systems for separation within this project by robotic selection, these were subject to separation by CPC. These studies will be discussed within this chapter.

3.3 Method and materials

3.3.1 Preparation of phase system

Polyethylene glycol of average molecular weight 3350 Daltons and ammonium sulphate salts were obtained from Sigma-Aldrich. 4 litres of phase system were prepared (Figure 3.3.1.1).

Component	Molecular weight (g/mol)	Weight added to make 11.1%/11.1% system (g)	CAS number
PEG 3350	3350	444	25322-68-5
Water	18.02	2600	
Ammonium sulphate	132.14	444	7783-20-2

Figure 3.3.1.1: Phase system preparation: PEG 3350 11.1%/11.1% ammonium sulphate system. System prepared weight for weight (w/w %) producing a total volume of 4 litres.

The thoroughly mixed phase system was placed in a separating funnel and left to equilibrate. Following the formation of a sharp, clean interface (minimum 1hr), upper and lower phase were decanted into individual bottles.

3.3.2 Sample preparation

The need for sample conditioning prior to injection on the CPC was found to be of great importance. Previously, a dilution of the CCS in lower phase alone (11g lower phase in 39ml CCS) was sufficient to cause the two phase system within the CPC to be broken. In this sample excess water in the CCS was injected onto the column flooding CPC chambers, and creating one phase. As a result all material loaded eluted at the K=1 point without separation.

Thus, all samples for injection were prepared as a two phase system, allowing the composition within the machine to be unaffected. To do this, 11% PEG and the salt were added directly to the CCS (5.5g salt, 5.5g PEG in 39ml CCS). To ensure the antibody did not aggregate or become damaged, PEG was added first to the CCS in a slow, step wise manner, whilst the sample was gently mixed using a magnetic stirrer. The salt was then sprinkled slowly and the sample left to stir until the solution was fully dissolved. The mAb was confirmed as 100% viable at the start of each CPC run by protein A HPLC analysis.

3.3.3 CCC processing

The CPC unit used was from Armen instruments (Vannes, France). It was composed of two 500ml rotating coils. In this work, only one of the two coils were used. Each coil consisted of 1008 chambers, giving a total active volume of 429ml. When the volume of the small bore interconnected tubes was accounted for at 71ml, a combined volume of 500ml was attained.

The CPC was designed with inbuilt pumps; one was used to pump upper phase and the other the lower phase respectively. The sample loop was attached to the pump, allowing direct injection onto the column, following equilibration. The CPC unit was operated in both the ascending and descending mode as described further in the chapter.

Prior to all runs, the coil was flushed with at least 1000ml of water, to remove all air bubbles and residual contaminants. The column was then spun in ascending mode and filled with stationary phase, then operated in descending mode or vice versa. When equilibration was reached with the elution of mobile phase, injection of sample proceeded.

Example experimental conditions are outlined below (Figure 3.3.3.1).

CPC - separation
ATPS…11.1%/ 11.1 %(w/w)……PEG/Salt, pH…6.40
PEG…3350……Salt …Ammonium sulphate
Coil volume……..429ml
Sample loop……..18.7ml
Operating mode.…Descending
Injected mAb:
1) IgG4 CCS……..… (Batch number L16508/49)
Volume….....39mls diluted with:
5.5g…. Ammonium sulphate
5.5g….. PEG
Concentration of the antibody injected into the column……..4mg/ml
Spin speed…2000rpm, temperature…22.4°C, flow rate…..….5ml/min
Equilibrated at……5ml/min, extra coil volume……..76ml
Stationary phase displaced……200ml, pressure…4Bar

Figure 3.3.3.1: Typical CPC experimental conditions using a PEG 3350 11.1%/11.1% ammonium sulphate system. Operated in descending mode using a 18.7ml sample loop at a flow rate of 5ml/min.

The sample (mAb made up in a two phase system) was subject to 0.45µm filtration (Millipore, Watford, UK) prior to loading onto the sample loop. The PVDF filters

were used due to their low protein binding properties (MILLEX-HV PVDF 33mm diameter). During the CPC run, fractions were collected every 10 minutes (50ml) and subject to protein A HPLC analysis (Figure 3.3.3.2)

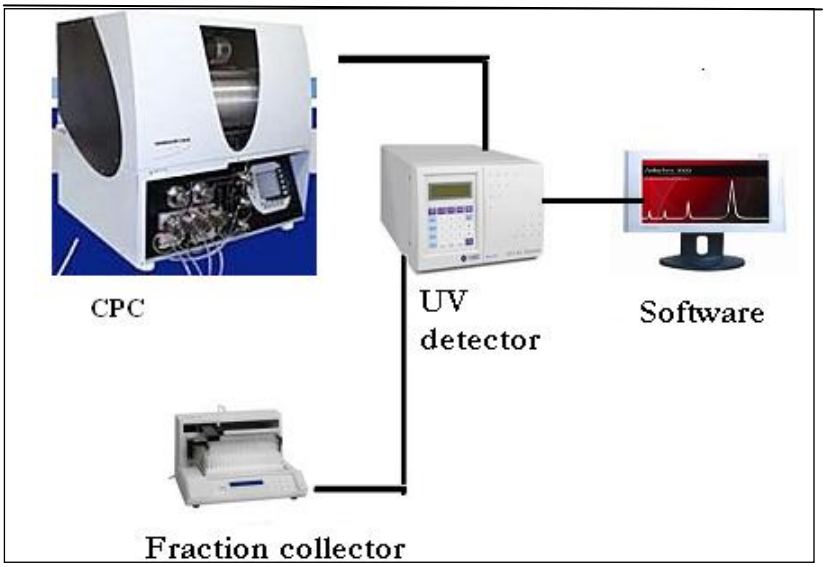

Figure 3.3.3.2: Schematic diagram of CPC processing is collected using a 280nm UV detector. A fraction collector was used for further analysis by protein A HPLC.

3.4 Results and discussion

3.4.1 mAb separation from crude Cell Culture Supernatant (CCS) using CPC: CPC run 3-1

A CPC run was performed with the conditions outlined in Figure 3.3.3.1. The results following Protein A HPLC analysis are shown in Figure 3.4.1.1. The partition coefficient (K) obtained from the robot run was 0.43; elution was therefore as theoretically predicted, around 4000 seconds (67 minutes). The crude CCS can be seen eluting as several different peaks, as expected due to its heterogeneous nature

.

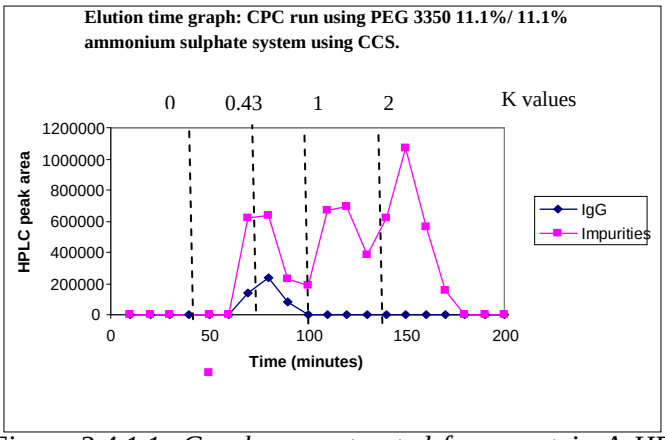

Figure 3.4.1.1: Graph reconstructed from protein A HPLC chromatograms. CCS separated using a PEG 3350 11.1%/11.1% ammonium sulphate system, 500ml coil volume, 5ml/minute flow rate, 18.7ml injection volume. CPC run at 20ºC.

Although there is no separation of the IgG in Figure 3.4.1.1 from the impurities, the main positive was that the compounds showed some retention in the column, and a number of impurities were separated from the product of interest (mAb).

A background value was calculated due to the presence of phase system contributing to absorbency values in Protein A HPLC analysis; this background was subtracted from all fractions. In addition, using a calibration curve created from the Protein A purified IgG, the recovery in each fraction was calculated (Figure 3.4.1.2).

Total mg of functional IgG recovered from fractions	52.4
Total mg of functional IgG in control sample	75.2
% Recovery of functional IgG	69.8

Figure 3.4.1.2: IgG recovery, calculated following a CPC run for the purification of CCS. A PEG 3350 11.1%/11.1% ammonium sulphate system used, 500ml coil volume, 5ml/min flow rate, 18.7ml injection volume at 20ºC and analysis by protein A HPLC.

The HPLC analysis chromatogram from the crude CCS injection can be seen in Figure 3.4.1.3. Any material eluted at 0.1 minutes was termed impurities, as it was unable to bind to the protein A column. Material bound to protein A with elution at 6 minutes was assumed to be IgG (protein A binding).

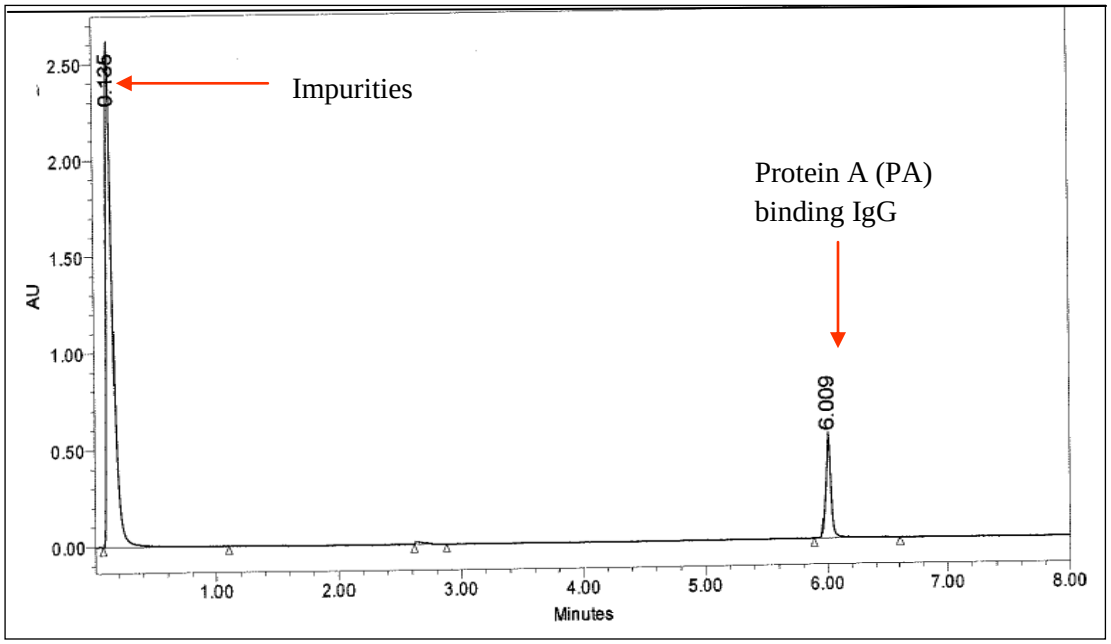

Figure 3.4.1.3:HPLC analysis of the Crude CCS using a protein A column. Material obtained from Lonza at 4mg/ml IgG. Analysis using optimised 8 minute protein A HPLC analysis. Elution buffer at pH 2 employed at 6 minutes, 80µl injection volume, and detection at 280nm.

Fraction 7, collected at 70 minutes (Figure 3.4.1.4), contained the highest concentration of purified IgG although there was also elution of impurities (0.1 minutes). The CCS (Figure 3.4.1.3) and the Fraction 7 (Figure 3.4.1.4) chromatograms appeared similar. Purity was defined as the ratio of IgG to the sum of the masses of IgG and impurities.

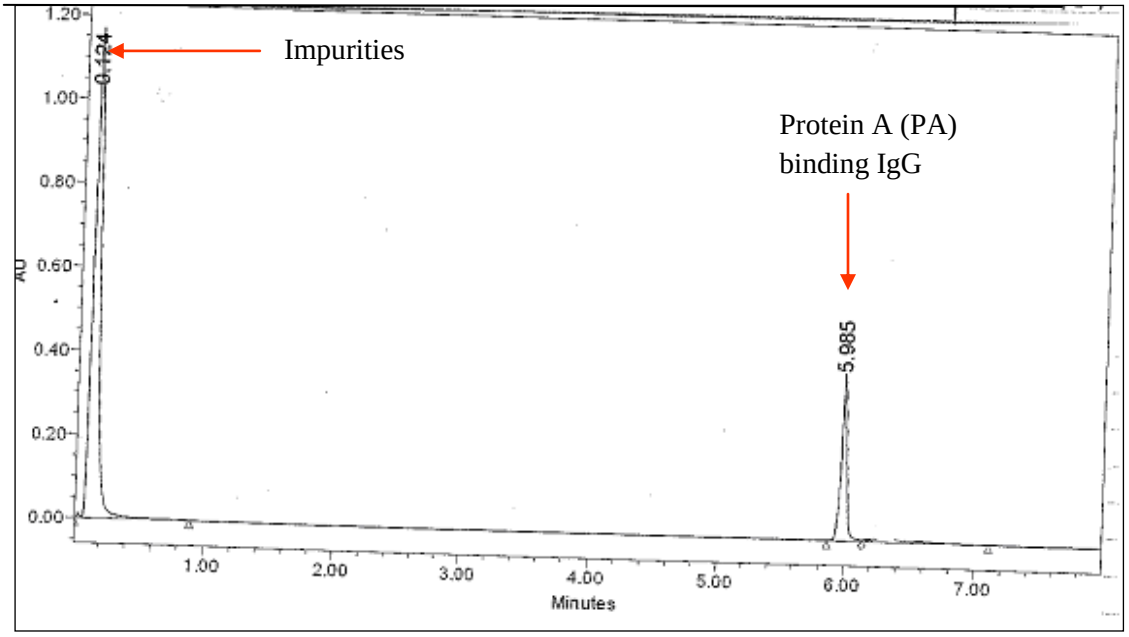

Figure 3.4.1.4: Fraction 7 collected at 70 minutes. Protein A HPLC chromatogram, following CPC purification of crude CCS. Analysis using optimised 8 minute protein A HPLC analysis, pH 1.5 elution buffer employed at 6 minutes. 80µl injection volume.

3.4.2 SDS PAGE results

SDS is a negatively charged detergent that causes protein denaturation on association producing an SDS-protein complex. Under the influence of an electric field, proteins migrate towards the positive anode, due to the negative charge of the detergent. The resulting size of the SDS-protein complex corresponds directly to the protein molecular weight. When the electric field is applied over a polyacylamide gel, separation is based on varying rates of migration through the gel matrix, corresponding to molecular weight.

Both reduced and non-reduced gels can be carried out. Reduced gels involve the inclusion of reducing agents e.g Mercaptoethanol in the sample buffer. Reducing conditions hydrolyse disulphide bonds present between heavy and light chains. A Novex X Surelock minicell from Invitrogen (Paisley, UK) was used with pre cast Novex 4-20% tris glycine gradient gels (EC6025BOX). All samples were diluted to 2mg/ml using equal volumes of water and reducing buffer. 0.5ml 2-mercocaptoethanol (Sigma m-7154) was added to 9.5ml of Novex tris glycine SDS sample buffer and adjusted to pH8. Samples were then placed in a water bath set at 70ºC for 2 minutes. 10µl of sample were loaded into each appropriate well.

Running buffer was prepared by 1:10 dilution in water (Invitrogen LC2675). The gel was run using the Novex X cell Surelock minicell apparatus and a power pack of high voltage (Biorad), at 140V, until the dye had run to approximately 1cm from the slit in the bottom of the gel cassette. The gel was subsequently stained with Commassie blue stain for 2 hours, replaced with de-stain and left over night. Repeated washing of the gel in deionised water was used to improve the gel background and then analysed.

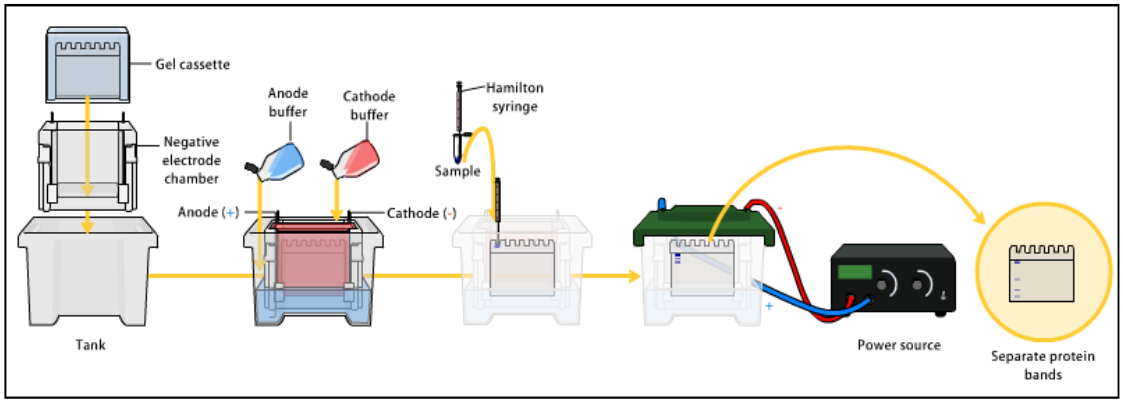

Figure 3.4.2.1 Electrophoresis overview. Schematic of protein separation based on molecular weight. Gel loading and gel running conditions allow the preparation of gel for staining.

To further observe purification in a qualitative manner, SDS PAGE gel electrophoresis was used in a complimentary manner with HPLC analysis. SDS PAGE allows purification to be monitored such that any major changes in protein structure can be determined. HPLC analysis however is more specific, allowing quantification of specific proteins. Following HPLC analysis Fraction 7 was shown to still be impure (as predicted in Figure 3.4.1.2). Several fractions from CPC run 3-1 were investigated using SDS PAGE; Fractions 7, 8, 9,10,14,15 and 16. These were comparable with the PA purified IgG and the crude CCS starting material.

Initially it was noted (Figure 3.4.1.2) that other contaminants co eluted with the IgG. As shown in Figure 3.4.2.2, all IgG fractions (7-10) appear more similar to the PA purified IgG control (lane 2) than would be expected from the HPLC chromatogram presented in Figure 3.4.1.4. The PA purified IgG control had 3 bands representing heavy chain, light chain and free light chain. The electrophoresis results showed just the IgG proteins. It was therefore hypothesised, that previously labelled

'impurities' in these fractions, were actually denatured IgG that was unable to bind to protein A. This was subsequently termed protein A non-binding IgG (Figure 3.4.2.3).

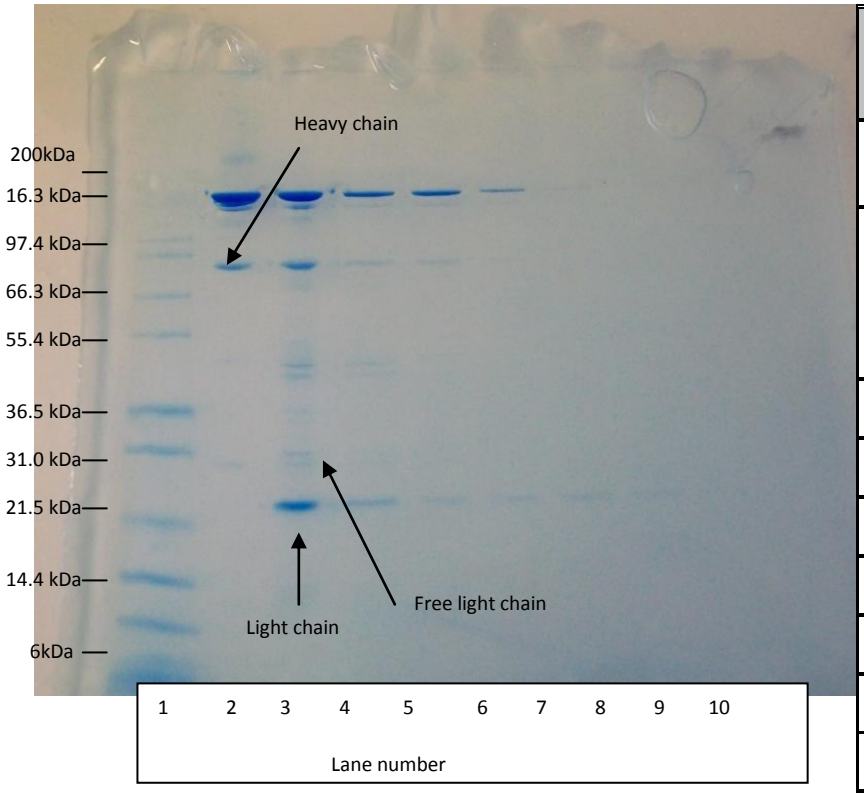

Lane number	Sample
1	Molecular weight marker (MWM)
2	Protein A IgG (Previously purified by Lonza using preparative protein A HPLC)
3	CCS
4	Fraction 7
5	Fraction 8
6	Fraction 9
7	Fraction 10
8	Fraction 14
9	Fraction 15
10	Fraction 16

Figure 3.4.2.2: Reduced SDS PAGE gel. Samples analysed post CPC run, CCS separated using a PEG 3350 11.1%/11.1% ammonium sulphate system, 500ml coil volume, 5ml/min flow rate, 18.7ml injection volume . CPC run at 20ºC.

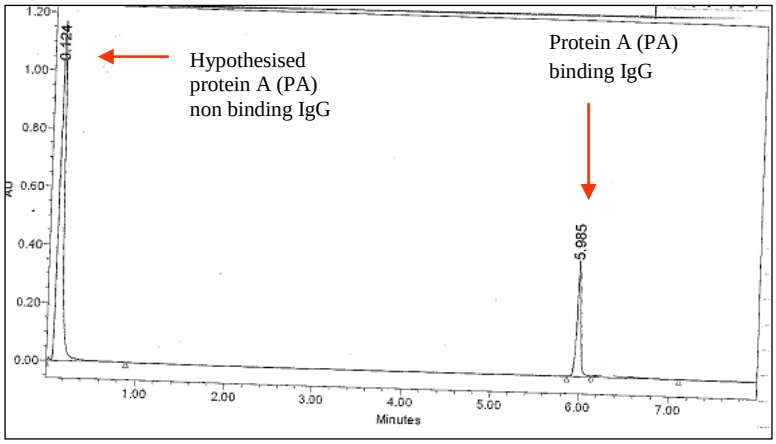

Figure 3.4.2.3: Hypothesis of creation of protein A non-binding IgG post CPC processing as opposed to previously thought impurities.

3.4.3 Investigation of the formation of protein A non-binding IgG

The Protein A HPLC program was developed to tolerate the phase system, and was based entirely on two peak elution. The first peak eluted at 0.1 minutes and accounted for anything non-binding to protein A. The second peak at 6 minutes was assumed to be IgG that bound to protein A. Elution followed a drop in pH to change the protein's isoelectric point (PI) away from that of the protein A.

The following observations were noted when CPC Fraction 7 (with the highest concentration of IgG) was analysed by protein A HPLC. Fractions were seen by protein A HPLC to have elution at both 0.1 minutes and 6 minutes. When these fractions were run on a SDS PAGE gel they appeared as just one species, indicating purification as no impurities bands were present (Figure 3.4.3.2). They also appeared as one species by 280nm trace and as shown by the spectra (Figure 3.4.3.1). They resembled that of the PA purified IgG control.

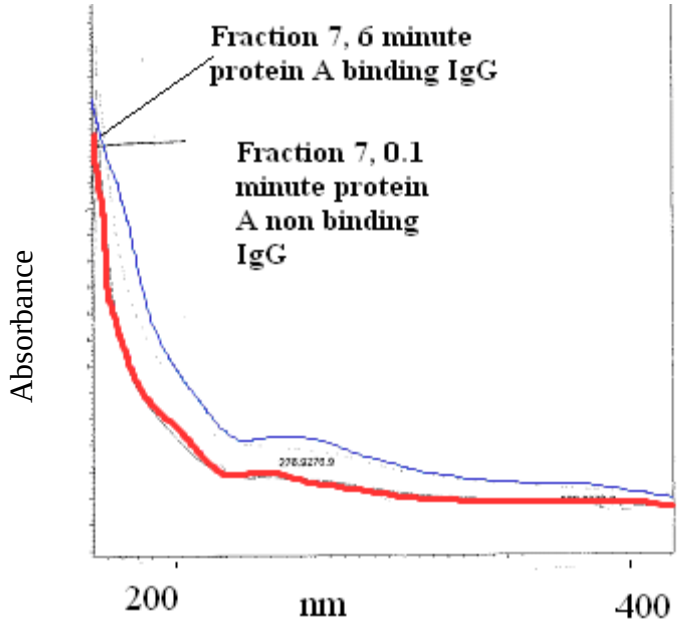

Figure 3.4.3.1: Spectra for the 2 peaks in Fraction 7 post CPC. Two spectra obtained using the Waters HPLC programme at 200-400nm. Spectra at 0.1 minute (Protein A non-binding IgG) and at 6 minutes (protein A binding IgG) from Protein A HPLC chromatogram.

The 0.1 minute HPLC peak seen in Fraction 7 CPC run 3-1 was previously regarded as 'impurities', thus was assumed an impure sample. However analysis by SDS PAGE and the UV spectra results suggested that these samples were actually predominately IgG. It was hypothesised that non-functional IgG was being produced by the CPC run, and this was termed "PA non-binding IgG". The 0.1 minute peak in other samples could contain impurities, non-functional IgG, host cell proteins, detergents, media components etc. However, in the case of Fraction 7 from CPC run 3-1, as shown by SDS PAGE, only IgG existed. Protein A non-binding IgG was seen in some Fractions (7, 8 and 9 from CPC run 3-1) but in the other fractions, this 0.1 minute peak was actually impurities.

Consequently, it was suggested that CPC processing or the phase system itself was causing an IgG species change. The protein A binding capacity of the IgG appeared to have changed, rendering functional IgG non-functional (PA non-binding IgG). Moreover it was postulated, having identified these two forms, they could possibly be inter convertible. IgG incubation in the phase system alone could possibly cause aggregation, resulting in the production of two IgG forms. The binding and non-binding IgG were detected only by PA HPLC.

3.4.4 Study into species interconversion

A component of CPC processing (phase system or machine) was seen to cause an IgG species change. Functionality of some of the IgG was altered creating a protein A binding and non-binding form. It was postulated these species were possibly interconvertible. Conversion between the PA binding to non-protein A binding was investigated by heating to 50ºC, sonciation and pH.

These studies were conducted with CCS and Fraction 7 from CPC run 3-1 (Figure 3.4.1.3) which had previously been subject to protein A HPLC analysis and SDS PAGE. Aliquots were taken and subject to incubation at 50ºC and sonication for 250 minutes, samples were taken at 50 minute intervals. With the samples for pH adjustment, drops of acid or alkaline (either concentrated NaOH or HCl) were added to each aliquot until the required pH was attained. The samples were then diluted 1 in 4 in water to prevent turbidity and analysed by protein A HPLC.

Initially the CCS sample and the Fraction 7 sample were subject to incubation at 50ºC, as shown in Figure 3.4.4.1, The graphs show a plot of HPLC peak area of the respective PA binding peak (6 minutes) and the PA non binding peak (0.1 minutes) over time. For both samples the graphs of the data at differing conditions for the 0.1 minute and the 6 minute peak appeared to be mirror image of each other. There was a possibility of species being interconvertible, however the spread of the data was large with fluctuation. With the CCS at 50ºC incubation, the amount of binding to non binding PA material remained completely stable (Figure 3.4.4.1). Fraction 7 however was not stable due to having a >10 times lower HPLC peak area, this was thought to be due to HPLC variation as opposed to a species change. Experiments were carried out only one.

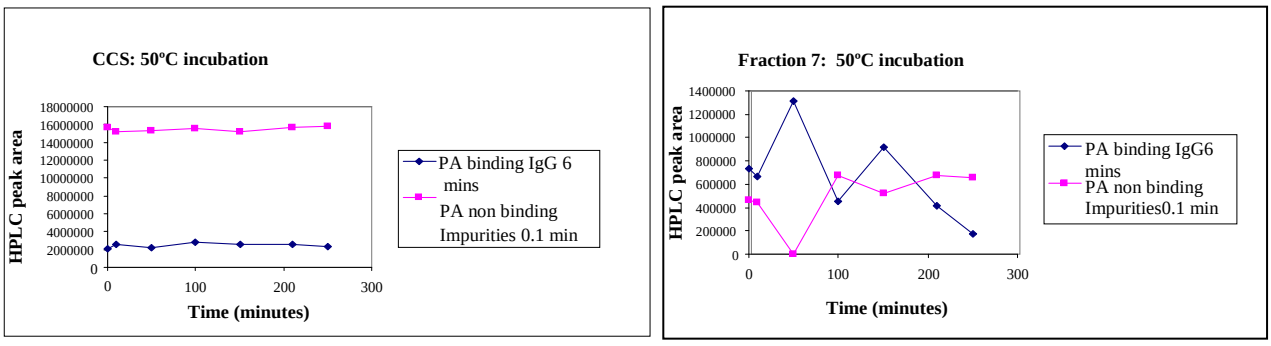

Figure 3.4.4.1: CCS and Fraction 7 (post CPC processing) results at 50ºC incubation. Incubation over 250 minute, samples taken every fifty minutes and plotted against

corresponding HPLC peak area (obtained using protein A HPLC developed analytical method).

CCS sample and the Fraction 7 sample were subject to sonication over 200 minutes, results are shown in Figure 3.4.4.2. The graphs show a plot of HPLC peak area of the respective PA binding peak (6 minutes) and the PA non-binding peak (0.1 minutes) over time. With both samples a decline in protein A binding IgG was seen, this degradation was seen almost immediately in Fraction 7 and also the CCS. (Figure 3.4.4.2)

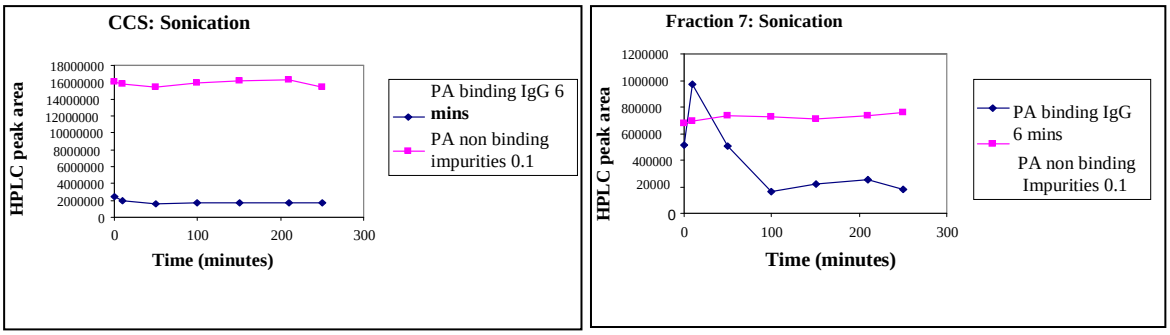

Figure 3.4.4.2: Effect of sonication: CCS and Fraction 7 (post CPC processing). Sonication over 250 minute, samples taken every fifty minutes and plotted against corresponding HPLC peak area (obtained using protein A HPLC developed analytical method).

CCS sample and the Fraction 7 sample were also subject to pH change, the respective change in HPLC peak area is shown in Figure 3.4.4.3. The graphs show a plot of HPLC peak area of the respective PA binding peak (6 minutes) and the PA non-binding peak (0.1 minutes). With both samples, as the pH increased so did the amount of PA binding IgG, to decline in PA non-binding IgG. This increase was more evident with Fraction 7, as compared to the CCS sample. An optimum pH in both samples allowing the maintenance of higher levels of PA binding IgG was between 8-9.

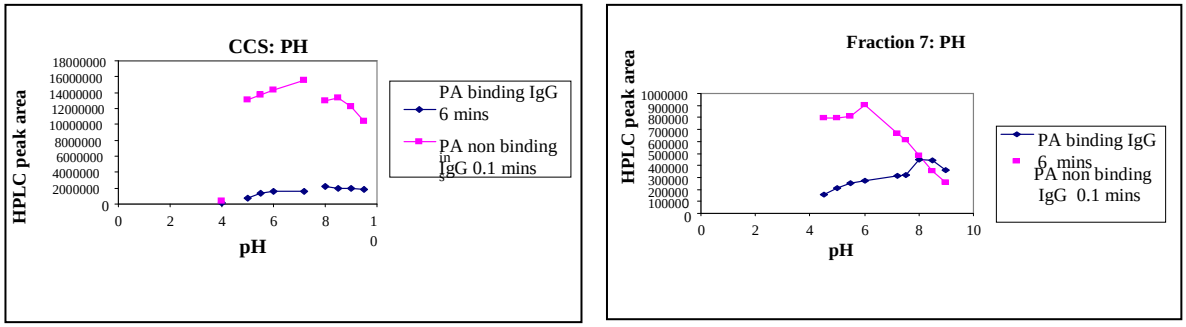

Figure 3.4.4.3: Effect of pH on CCS and Fraction 7 (post CPC processing), pH changed with drops of concentrated NaOH or HCl. Samples subject to protein A HPLC developed analytical method and plotted against corresponding HPLC peak area.

A criterion of 20% significant difference in HPLC peak area was set, as samples were subject to change in the parameters (50ºC incubation, sonciation and pH). When the significant difference was calculated, using a >20% change in HPLC peak area, the only condition that caused a significant degradation was sonication. It appeared to actually further degrade the IgG, rather than, as hoped to return the non-viable form of IgG back to its viable form. Temperate had no effect; however increasing pH slightly increased the creation of functional IgG but not greatly. These results showed that, under these conditions the only possibility of conversion was from the functional protein A binding IgG to non binding PA IgG. With the processes tested, there seemed to be no possibility of converting back to the functional form. A large spread of data and no trends towards protein A binding IgG conversion were seen.

3.4.5 Sample loading capacity: CPC run 3-2

To improve resolution, a second CPC run (Run 3-2) was performed using CCS at 1mg/ml (previous run was at 4mg/ml) using the same 18.7ml sample loop. The reconstructed protein A HPLC chromatogram graph is shown in Figure 3.4.5.1, with the IgG elution confirmed at around 57 minutes (Fraction 6).

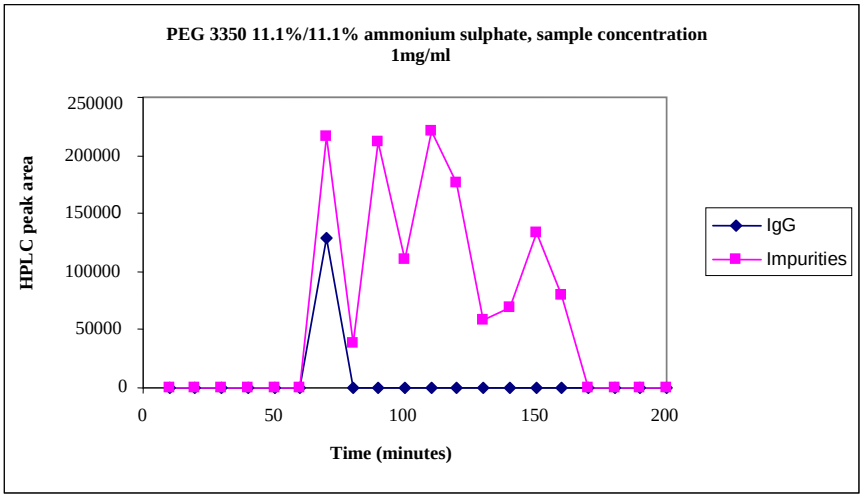

Figure 3.4.5.1: Protein A HPLC analysis of CPC runs using crude CCS starting material. 500ml coil volume, 18.7ml sample loop, operation was in descending mode and a flow rate of 5ml/min. CCS separated using a PEG 3350 11.1%/11.1% ammonium sulphate system, 500ml coil volume, 5ml/min flow rate, 18.7ml injection volume at 20ºC.

The elution time graph was very similar to that seen at 4mg/ml (Figure 3.4.1.2). Elution of protein A binding IgG and the remaining non protein A binding IgG was with the elution of several impurities.

A reduced SDS PAGE was conducted to assess purity as described previously in section 3.4.2 (Figure 3.4.5.2). It was seen that Fraction 6 had a banding pattern that resembled that of the protein A control. However, no other bands, which would have been expected in fractions containing the impurities, were seen (Lane 7-10). When rechecking the data it was seen that an error was made in the preparation of samples. Samples were prepared identically and not adjusted for their respective concentrations. Despite the differences in concentration due to a calculation error, there appeared to be a reduction in impurities in Fraction 7, similar to that of the PA purified IgG. Furthermore some impurities had been removed when compared to the CCS control in Lane 3.

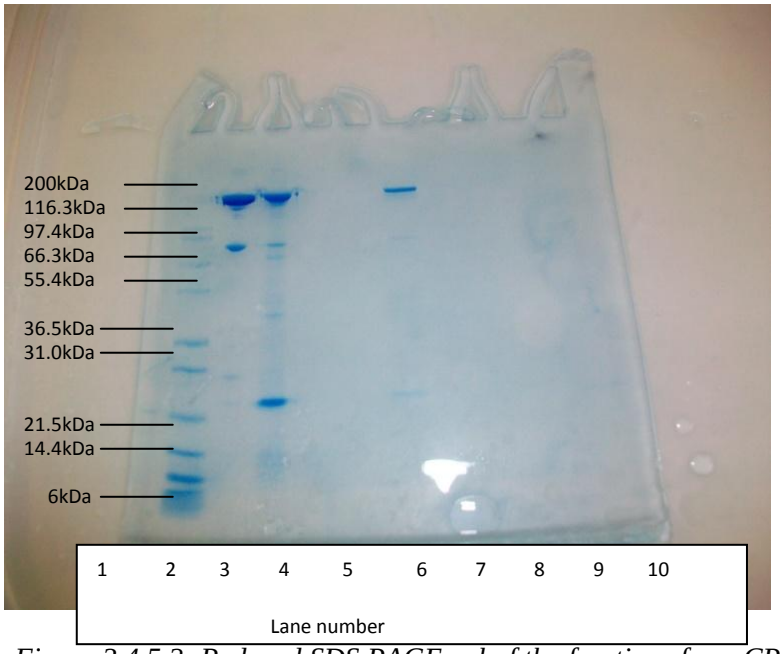

Lane number	Sample
1	MWM
2	Protein A IgG
3	CCS control
4	Fraction 5
5	Fraction 6
6	Fraction 7
7	Fraction 8
8	Fraction 9
9	Fraction 10
10	Fraction 16

Figure 3.4.5.2: Reduced SDS PAGE gel of the fractions from CPC run 3-2. Samples analysed post CPC run. Gel run at 140 V for 2 hours and stained with Coomassie blue.

3.4.6 Stationary phase retention and stripping

With all CPC runs, the equilibration method was used. Firstly the coil was filled with stationary phase while spinning at 2000rpm in ascending mode. One litre of phase was pumped (two column volumes), allowing the column to be completely flushed clean with stationary phase. The column spin direction was then changed to descending mode and the mobile phase pumped. Displacement of stationary phase was followed

by ‘breakthrough’ of mobile phase, represented by the attainment of full equilibration. Once full equilibration was reached, sample injection proceeded.

Following breakthrough, there should ideally be no more displacement of the stationary phase, termed stripping. If displacement continues, to the extent that all stationary phase is stripped from the column, then only mobile phase is left. All material will hence be eluted un-separated at the K=1 point. The continued stable retention of stationary phase is important for a separation to occur.

To measure stripping, samples post a CPC run (CPC run 3-2) were observed. CPC fractions were collected in 50ml graduated tubes. Stripping was calculated by observing the percentage of upper stationary phase in graduated 50ml collection tubes to lower phase. With the PEG 3350 11.1%/11.1% ammonium sulphate system, very little stripping was seen (Figure 3.4.6.1) and by 50 minutes this had stopped.

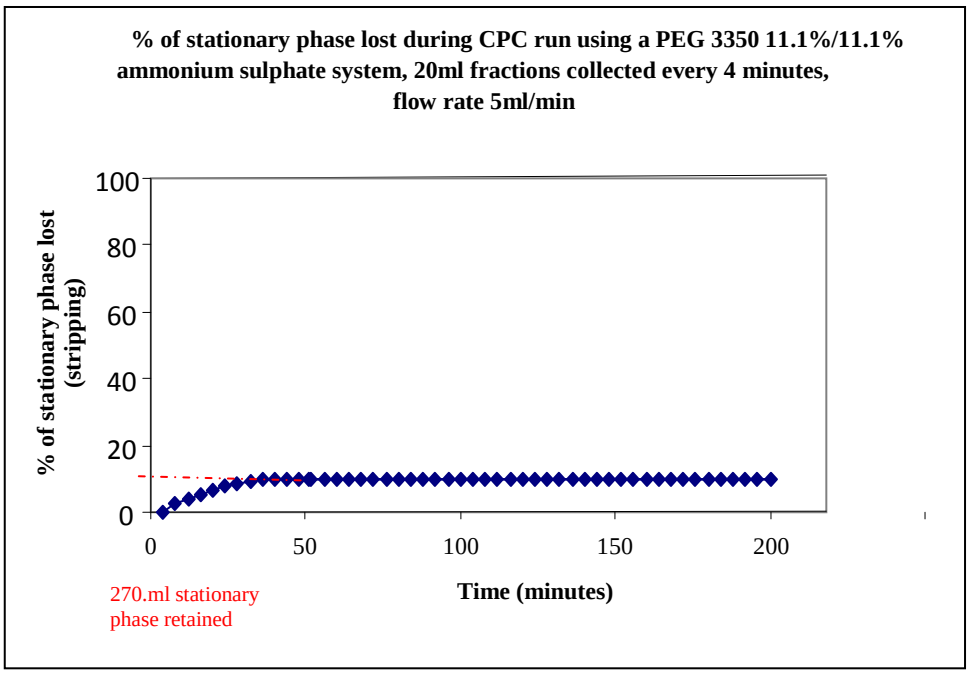

Figure 3.4.6.l: Stripping data during a CPC run. 200ml of stationary phase was initially lost during equilibration. Of the 300ml left at the start of the CPC run, a final 90.2% of stationary phase was retained in the coil, which equalled 270ml. CCS starting material used. 500ml coil volume, 18.7ml sample loop, 4 bars of pressure. Operation in descending mode and a flow rate of 5ml/min. Stripping calculated by observing percentage of upper stationary phase in graduated 50ml collection tubes.

3.4.7 Prediction of retention time

Prediction of retention time was obtained using the elution time equation applied to CCC peak elution. Berthod's group (2004) used the following equation: $V_{RI} = V_M + K_{DI}V_S$.

This where the following applies:

V_M = Volume of mobile phase

V_S = Volume of stationary phase

V_{RI} = Retention volume of molecule of interest

K_{DI} = Partition coefficient

Figure 3.4.7.1: Elution time equation used by Berthod's group (Berthod et al., 2004) where retention volume is calculated (V_{RI}). Mobile phase and stationary phase retention are used with the partition coefficient of the determinant of interest.

The equation in Figure 3.4.7.2 was used to determine predicted elution time of IgG from a CPC run. The volume of mobile phase was calculated by subtracting the amount of stationary phase eluted by that of the extra coil volume ($V_{ec)}$. Total V_{ec} was calculated by considering all dead volume (76ml) seen within the CPC, including all interconnecting tubing between the chambers and tubing to feed the exterior fraction collector. The partition coefficient (K) was 0.43 as obtained from the robot runs (Figure 2.4.3.5). Stationary phase volume was calculated by subtracting the coil volume of 500ml by the amount of stationary phase eluted prior to breakthrough (200ml). The predicted elution time was 65.8 minutes, which was very close to the actual IgG elution of 67 minutes seen in Figure 3.4.5.1 and 3.4.1.2.

$$\text{Elution time} = \frac{V_M + (K * Vs)}{F} + \frac{V_{ec}}{F}$$

V_M = Volume of mobile phase = 200-76= 124ml

K = Partition coefficient = 0.43

Vs = Volume of stationary phase = 500-200=300ml

F = Flow rate = 5ml/min

V_{ec} = Extra coil volume = 71ml (estimated value, including 5ml tubing volume)

Figure 3.4.7.2: Elution equation based on time. Flow rate is additionally used to determine elution time of molecule of interest (de Folter et al., 2008).Figures obtained from CPC run 3-2.

3.4.8 Comparison of work with that of Aires-Barros group (Lisbon, Portugal): PEG 1000 14%/14% potassium phosphate system

Due to the low levels of functional IgG (PA binding) seen post CPC purification, the possibility that ammonium sulphate could be having a precipitation effect was investigated. Ammonium sulphate precipitation is used as a first step for many protein purifications (Ahlstedt, 1973; Arend *et al.*, 1974). Due to the large concentration of salt used along with PEG, it was hypothesised that the ammonium sulphate system was actually rendering the IgG inactive, or causing IgG precipitation on contact with the phase system. Previously during the robotic run (Chapter 2), no IgG aggregation was seen with a total peak area of >85%, where many system were rejected. It was thought that due to the vigorous mixing with a CPC run as opposed to just bench incubation with the robotic run, increased aggregation would result. Furthermore during CPC processing the mAb was incubated in the phase system for much longer when compared to the robotic run, when the mAb sample was added last following phase make up. These were thought to result in the effect ammonium sulphate had on the mAb not being seen previously.

Comparative studies were carried out with the BIB phase system (PEG 3350 11.1%/11.1% ammonium sulphate system) and that of the Aires Barros group (PEG 1000, 14%/14% potassium phosphate). The BIB and the Aire-Barros group phase system were prepared and CCS was incorapted in the sample make up. The phase system was mixed thoroughly and triplicates were taken immediately (0

hours), 250µl sample were diluted 1 in 4 in water. These samples were subject to protein A HPLC analysis. The two phase systems with the CCS incorporated were then incubated for 3 hours on the bench. Following three hours samples were again taken in triplicate as described previously and subject to protein A HPLC analysis.

As shown in Figure 3.4.8.1, a decrease in viable IgG HPLC peak area was seen following three hour incubation in the ammonium sulphate system. This highlighted the issue of IgG precipitation with the ammonium sulphate. Instability was seen in the ammonium sulphate system, relative to the potassium phosphate system used by the Aires-Barros group.

The potassium phosphate phase system used by the Aires Barros group (Azevedo *et al.*, 2009) (PEG 1000, 14% potassium phosphate) has been used for many successful separations and resulting published papers. To confirm that the issues seen with the loss in IgG functionality were due to CCC processing, a CPC run was carried out with this phase system. Loss in IgG functionality had not been noted by this group, as they were just using batch extraction (Azevedo *et al.*, 2009). ATPS extraction was carried out without the CCC processing.

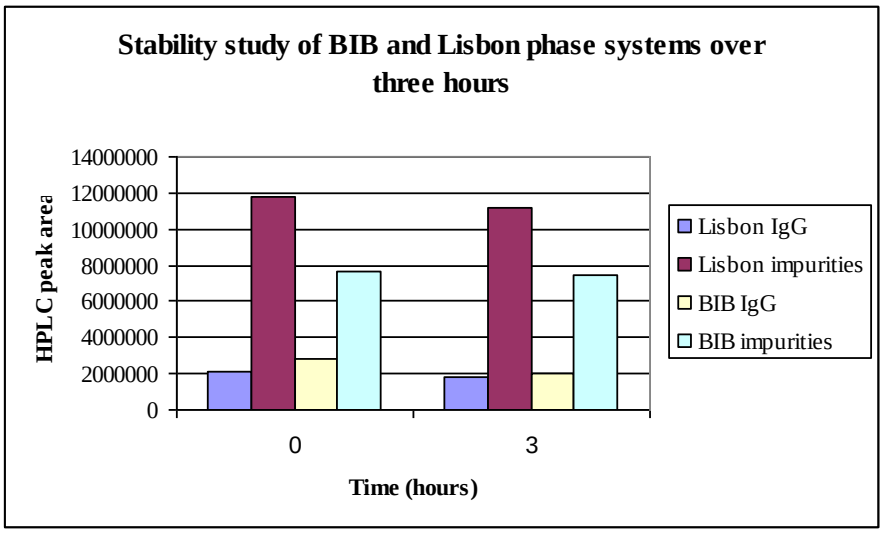

Figure 3.4.8.1: Comparison of phase system stability. PEG 3350 11.1%/11.1% ammonium sulphate system (BIB) compared to that of the Aires-Barros group (PEG 1000, 14%/14% potassium phosphate system. Individual phase systems incubated for 3 hours with CCS and then samples subject to protein A HPLC analysis.

A CPC run was carried out with the PEG 14%/14% potassium phosphate system with the same conditions outlined in Figure 3.3.3.1. A control sample was taken pre and

post CCC processing and subject to protein A HPLC analysis. To determine the exact cause of instability, controls (CCS) were taken in both the phase system and water following a 5 hour incubation period. In parallel phase system and water incubation samples were prepared. The CCS was prepared in both the PEG 1000 14/14% potassium phosphate system and water and subject to bench top incubation for 5 hours. All samples were mixed thoroughly and diluted 1 in 4 in water before analysis by protein A HPLC.

The CCS sample was typically composed of 16-20% PA binding IgG. This was calculated from the percentage of PA binding IgG (6 minutes), obtained from a protein A HPLC chromatogram in comparison to the PA non-binding HPLC peak area. Samples were also taken before and after the actual CPC run and the percentage of PA binding IgG calculated (results shown in Figure 3.4.8.2). Experiments were carried out singly. As shown in Figure 3.4.8.2, CCC processing itself was causing instability and a species change. A drop in PA binding IgG from 20.55% to 7.63% was reported. Purification was seen by SDS PAGE; however the majority of IgG produced was non-functional.

CCC	**Pre**	**Post**
IgG HPLC peak area	2357114	194280
PA binding IgG (%)	20.55	7.63
Phase 5 hour incubation	**Pre**	**Post**
IgG HPLC peak area: In phase	2255679	2312576
PA binding IgG (%)	19.23	18.63
Water 5 hour incubation	**Pre**	**Post**
IgG HPLC peak area: In water	2190504	2212626
PA binding IgG (%)	16.19	16.25

Figure 3.4.8.2: Overview of stability of IgG through whole CCC process (phase system incubation and CCC processing) using the PEG 1000 14/14% potassium phosphate system. All samples subject to protein A HPLC analysis, 6 minute PA binding peak used. Percent of PA binding IgG calculated from that of the starting CCS sample.

The potassium phosphate phase system was not responsible for any instability, HPLC peak area in the phase system and water post 5 hours incubation were unaffected. The results were highlighted by the use of a phase system used

routinely by the Aires-Barros group for aqueous extraction (no CCC processing). Many successful separations of IgG from impurities had been demonstrated by this group. No losses were seen with aqueous extraction alone, highlighting mixing and/or other mechanical aspects of the CCC operation were responsible for loss in IgG functionality. A reasonable degree of purification was being achieved, but at the cost of damaged and consequently non-functional IgG, which greatly affected yield

Despite these results suggesting that CPC processing was resulting in the production of inactive IgG, incubation experiments suggested the ammonium sulphate system was exacerbating this effect (Figure 3.4.8.1). A decrease in viable IgG was seen when incubation was just carried out on the bench for 3 hours. Even without CPC processing, precipitation and reduction in viable IgG was seen with the ammonium sulphate system. Investigation into how close this phase system was to the critical point and its robustness in comparison to another system was required.

3.4.9 PEG 1000 17.5%/17.5% sodium citrate system vs. PEG 3350 11.1%/11.1% ammonium sulphate system

To determine how close the PEG 3350 11.1/11.1% ammonium sulphate system was to the critical point a phase diagram was required. If too close to the boundary of a single phase the system would be sensitive to a number of parameters, for example temperature, pH and any small changes in polymer or salt concentrations. The phase diagram was constructed to show the potential working area for this phase system.

Stock solutions of PEG and ammonium sulphate were made and the turbidometric (Zaslavsky, 2005) titration method used. PEG and ammonium stock solutions were made to 28% by dissolving each separate component (20g) in 50g water respectively. Drops of each stock solution (PEG and ammonium sulphate respectively) were added to one another in a step wise manner until turbidity was seen. The weight was noted, and water added to clear the solution. This was repeated over a range. The total weight of the test tube and the weight of the diluents added were used to calculate the percentage of PEG and salt at particular points.

As shown in Figure 3.4.9.1 ammonium sulphate (%w/w) was plotted against PEG (%w/w) for the PEG 3350 system. These results were then plotted against those using PEG 1000 and 6000 from Boris Zaslavsky's aqueous two-phase

partitioning book (Aqueous two-phase partitioning, 2005). The phase diagram for PEG 3350 was seen to fit the trend shown for PEG 1000 and 6000. A high ammonium sulphate concentration was needed, lower than that of the PEG to produce a two phase system (Figure 3.4.9.1).

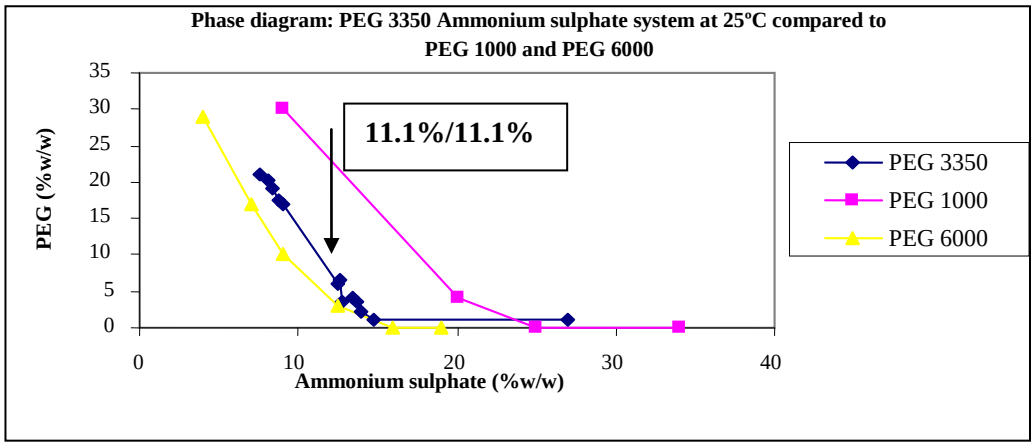

Figure 3.4.9.1 Phase diagram: PEG ammonium sulphate system. Phase diagram constructed using stock solutions of PEG 3350 and ammonium sulphate. Turdoimetric titration method was employed. PEG 1000 and PEG 6000 phase diagrams (carried out at 25ºC) obtained from Zaslavsky's book (1995) for comparison. The closeness of PEG 3350 11.1%/11.1% system to the critical point is highlighted.

As Figure 3.4.9.1 shows, the PEG 3350 11.1%/11.1% system was very close to the critical point, hence possibly sensitive to temperature. Due to seasonal fluctuation in the laboratory, a constant temperature was hard to maintain. It was thought that the mobile phase needed to be maintained at 20ºC or less to prevent the possible denaturation of the mAb during CPC processing.

Temperature as a variable to phase system composition was then investigated using the PEG 3350 11.1%/11.1% ammonium sulphate system. A range of temperatures were used. The PEG 1000 17.5%/17.5% sodium citrate system (as highlighted in Chapter 2 as appropriate following the robotic run) was compared to the PEG 3350 11.1%/11.1% ammonium sulphate system. The two phase systems were prepared in graduated measuring cylinders (10g in a 50ml tube) and incubated or placed in the fridge (4ºC). After temperature equilibration, the tubes were mixed and allowed to phase separate. The volumes of top and bottom phase were measured. The tube was then placed at another temperature, thermally equilibrated and then mixed

and phase volumes measured. A range of temperatures from 4ºC to 67°C were studied. The volume ratio was obtained by dividing the upper volume by the lower volume (Figure 3.4.9.2).

Temperature (ºC)	Volume ratio (Upper/lower)	
	PEG 1000 17.5%/17.5% sodium citrate	PEG 3350 11.1%/11.1% ammonium sulphate
4	0.80	0.88
12	0.80	0.77
20	0.80	0.75
26	0.80	0.70
28	0.80	0.70
35	0.80	0.55
37	0.80	0.51
44	0.80	0.47
48	0.80	0.42
52	0.54	0.37
67	0.54	0.30

Figure 3.4.9.2: Effect of temperature on volume ratio in PEG 1000 17.5%/17.5% sodium citrate system and PEG 3350 11.1%/11.1% ammonium sulphate system.

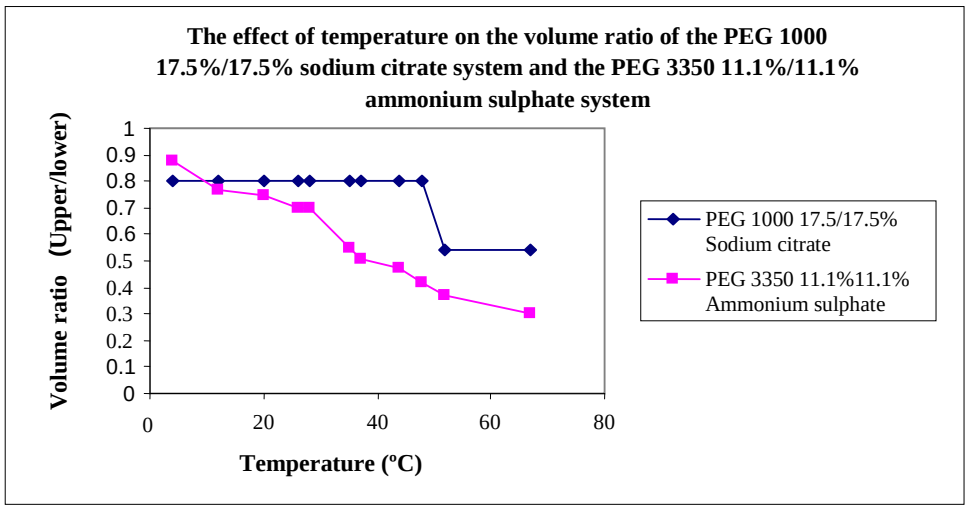

Figure 3.4.9.3: Graph to show the effect of temperature on the volume ratio for two different PEG-salt two phase systems.

Figure 3.4.9.3 demonstrates increasing temperature plotted against volume ratio for the two phase systems. With the PEG 3350 11.1%/11.1% ammonium sulphate system a clear linear decrease in volume ratio is seen as temperature increases. By comparison, the PEG 17.5%/17.5% sodium citrate system had a stable volume ratio to around 50 ºC. The range of phase volume ratios seen with the PEG 3330 11.1%/11.1% ammonium sulphate system varied from 0.88 at 4ºC to 0.3 at 67ºC. The typical

working range in the lab was from 20°C to 33ºC; the upper temperature range arose from heat produced by the machines (CCC). Within this temperature range, a volume ratio range from 0.7 to 0.51 with the PEG 3350 11.1%/11.1% ammonium sulphate system was seen. The PEG 1000 sodium citrate 17.5%/17.5% system by comparison appeared greatly more consistent over the temperature range tested. A change in the extremely stable volume ratio can only be seen at temperatures greater than 48ºC.

Finally the respective calibration curves of the PEG 11.1%/11.1% ammonium sulphate and the PEG 1000 17.5%/17.5% sodium citrate system were compared. This to confirm that the PEG 1000 17.5%/17.5% sodium citrate system was more suitable. PEG 1000 17.5%/17.5% sodium citrate and PEG 3350 11.1/11.1% ammonium sulphate systems were prepared with CCS incorporated. Calibration curves for each phase system were produced using protein A HPLC with a CCS concentration from 0-1mg/ml (Figure 3.4.9.4). On preparation of the ammonium sulphate system, precipitation of the IgG in the HPLC vial was noticed.

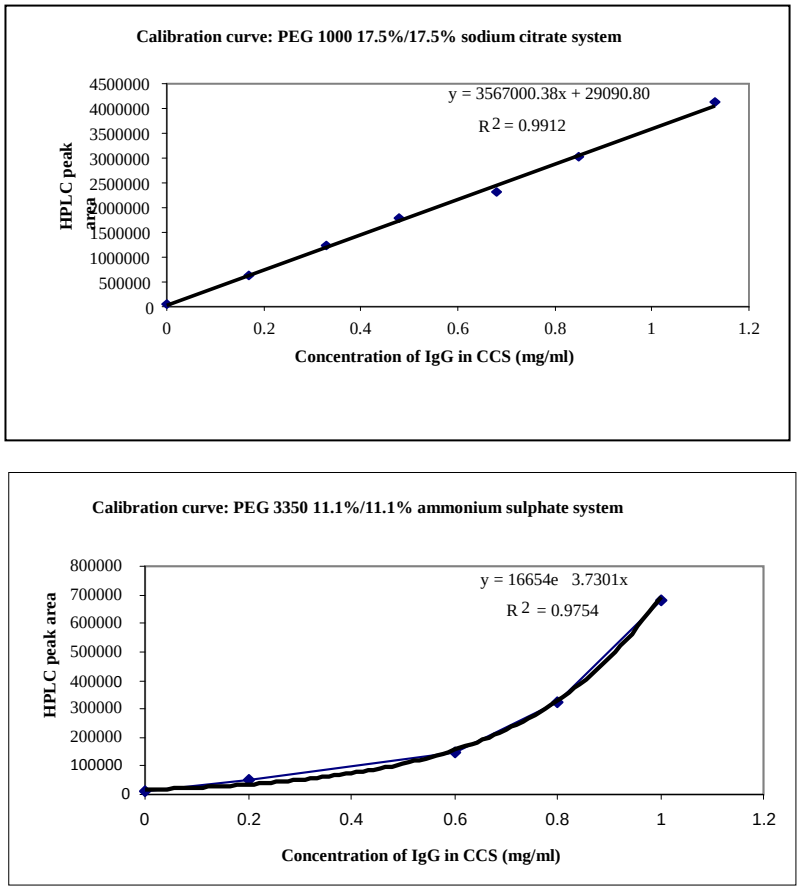

Figure 3.4.9.4: Calibration curves for PEG 3350 11.1%/11.1% ammonium sulphate system and PEG 1000 17.5%/17.5% sodium citrate system. All based on CCS with an injection volume of 80µl using protein A HPLC analysis, 8 minute run time injection in phase system.

As shown in Figure 3.4.9.4 IgG concentration in the CCS was plotted against HPLC peak area. With the PEG 1000 17.5%/17.5% sodium citrate system a typical linear calibration curve was seen. With the PEG 3350 11.1%/11.1% ammonium sulphate system however an exponential curve was demonstrated. With the PEG 3350 11.1%/11.1% ammonium sulphate system, a maximum peak area at 1mg/ml of IgG was 700,000 µV.sec. With the PEG 1000 17.5%/17.5% sodium citrate system however, this was 400,0000 µV.sec (Figure 3.4.9.4). The calibration curve for the ammonium sulphate system did not follow a linear trend. An exponential curve was seen. It was hypothesised a precipitation effect was seen on the IgG with the use of ammonium sulphate. It was thought at a low CCS concentration the ammonium sulphate precipitation was reducing IgG solubility and thus the resulting absorbance signal was lower (around 100,000 in comparison to 500,000 seen with the sodium citrate system). At a higher CCS concentration, aggregation of the insoluble IgG was suspected, resulting in the increased exponential absorbance signal seen (Figure 3.4.9.4).

The robustness of the PEG 1000 17.5%/17.5% sodium citrate system was demonstrated as opposed to that of the PEG 3350 11.1%/11.1% ammonium sulphate system. As the ammonium sulphate system was so close to the critical point, it was greatly affected by temperature and prone to aggregation. The PEG 1000 17.5%/17.5% sodium citrate system was selected for all future separations. When compared to the ammonium sulphate system, it had both a higher pH (7.39 as opposed to around 6) therefore reducing the possibility of aggregation (Pan *et al*., 2009; Wang, 2005). When the ammonium sulphate phase system was prepared the pH was not adjusted. This as adding sulphuric acid to the high salt concentration would have resulted in a pH that was challenging to measure. However for the phosphate and citrate salt finding the appropriate combination of salts to get a system within the physiological range of pH range of 7.5-9 was relatively easier and hence conducted.

3.4.10 CPC runs with PEG 1000 17.5%/17.5% sodium citrate system

The phase system was prepared as shown below (Figure 3.4.10.1).

Component		Mol weight	Weight added to make 17.5%/17.5% system (g)	CAS
PEG 1000		1000	700	25322-68-3
Water		18.02	2600	
Sodium citrate	Acid	294.1	5.75	5942-29-1
	Base	210.14	694.25	6132-04-3

Figure 3.4.10.1 Phase system preparation: PEG 1000 17.5%/17.5% sodium citrate system. Sodium citrate dihydrate (base) and citric acid monohydrate (acid) added in the weights shown above. Both were anhydrous salt, prepared in this particular proportion to obtain a pH of >7.4.All components were dissolved in water (g) as noted above to a final volume of 4000g. The phase system was left to equilibrate for over two hours and upper and lower phase decanted separately.

Initial CPC runs were conducted to investigate if a separation was possible using the PEG 1000 17.5/17.5% sodium citrate system. Typical run conditions are outlined below (Figure 3.4.10.2).

CPC - separation
ATPS…17.5/17.5% w/w……PEG/Salt, pH…7.41
PEG…1000……Salt …Sodium citrate
Coil volume……..429ml
Sample loop……..18.7 ml
Operating mode.…Descending
Injected mAb:
1) IgG4 CCS……..… (Batch number L16508/49)
Volume….....32.5ml diluted with:
8.75g…. Sodium citrate
8.75g….. PEG
Spin speed…2000rpm, temperature…20.4°C, flow rate…..……10ml/min
Equilibrated at……10ml/min, extra coil volume……..76ml
Stationary phase displaced……400ml, pressure…4Bar

Figure 3.4.10.2: Typical CPC run conditions used.

The CPC was operated in descending mode at a flow rate of both 5 and 10ml/min. The stationary phase retention using the CPC at both flow rates was typically low at 20%. 400ml of stationary phase was displaced leaving 100ml within a 500ml coil volume. The PEG and salt phases in turn were used as upper phase, and the results can be seen in Figure 3.4.10.4. Time in minutes for each run is plotted against HPLC peak area. Results at both flow rates were similar. Impurities were seen to elute within the run time (100 or 200 minutes) as shown by protein A HPLC analysis. The IgG however appeared to be retained in the column. The IgG was eluted when the column content was blown out with nitrogen gas at 4 bars.

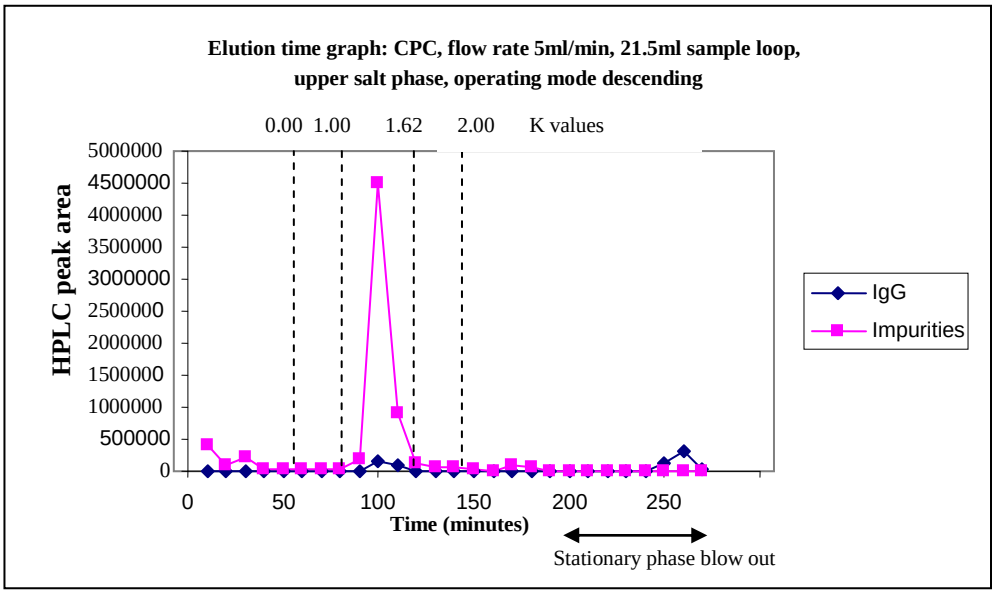

Figure 3.4.10.3: CPC run at a 5ml/min. CCS starting material used with the PEG 1000 17.5%/17.5% sodium citrate system. Samples analysed by protein A HPLC.

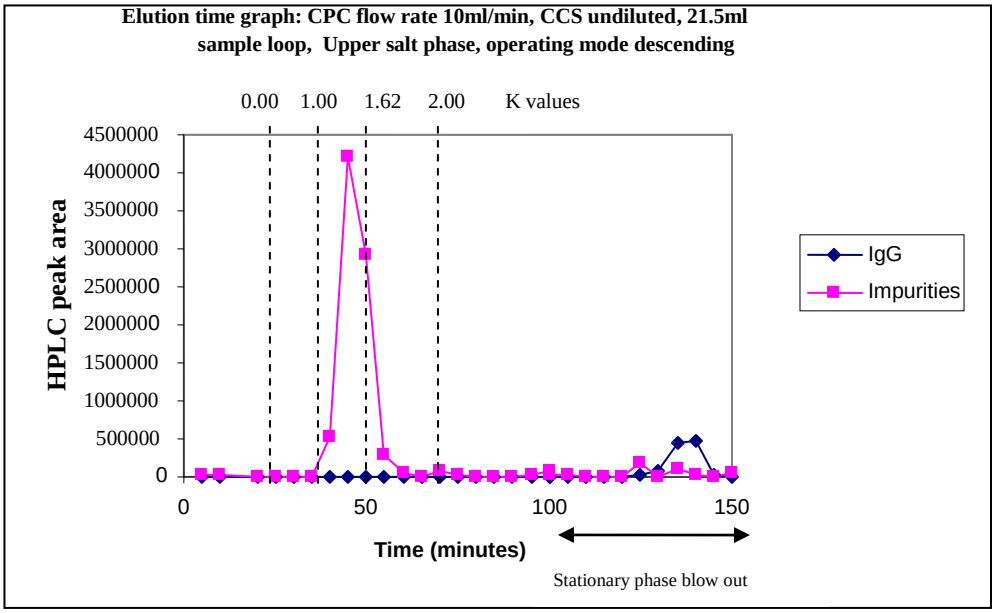

Figure 3.4.10.4: CPC data 10ml/min. CCS starting material used with the PEG 1000 17.5%/17.5% sodium citrate system. Samples were analysed by protein A HPLC.

Subsequent HPLC analysis showed the IgG was reasonably pure, with 89.2% purity from the 10ml/min run and 98.7% purity from the 5ml/min run. By comparison, >99% IgG Purity was seen in the protein A purified IgG control sample. (Figure 3.4.10.3 and 3.4.10.4). The IgG did not elute at the predicted K=1.62 at a flow rate of 10ml/min (Figure 3.4.10.4). When a flow rate of 5ml/min was used, a very small

amount of IgG eluted at the predicted K=1.62. With both flow rates, the IgG seemed to remain in the column and was only eluted when the column content was blown out.

Increased flow rate was furthermore investigated (Figure 3.4.10.4) with the aim to reduce the residence time of the IgG within the machine. It was considered that a reduction in the number of mixing and settling steps would retain IgG activity. CPC runs as described in Figure 3.4.10.2 were conducted where both the PEG and salt phases were used alternatively as stationary phase, at a flow rate of 5 and 10 ml/min. Results can be seen in the bar chart in Figure 3.4.10.5. Flow rate is plotted against the recovery of IgG functionality following analysis by protein A HPLC. IgG functionality was calculated by dividing the total IgG HPLC peak area in the fractions of interest by that of the amount present in the injection sample. At a flow rate of 10ml/min regardless of whether salt or PEG was used as an upper phase a considerably higher retention of activity was seen when compared to those runs conducted at 5ml/min.

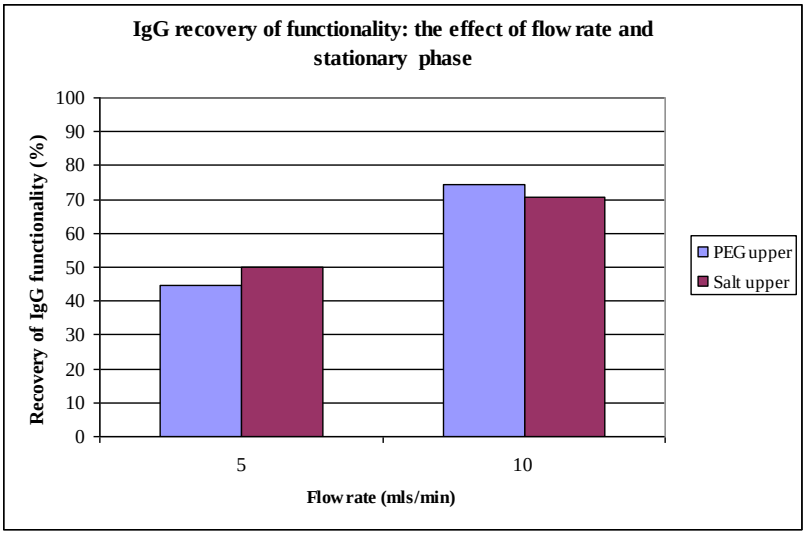

Flow rate (ml/min)	Recovery of IgG functionality (%)	
	PEG upper	Salt upper
5	44.6	49.83
10	71.41	70.75

Figure 3.4.10.5: Effect of flow rate on retention of IgG functionality, using both PEG and salt in separate CPC runs as the upper phase. Experiments performed at a flow rate of both 5 and 10 ml/min. PEG 1000 17.5%/17.5% sodium citrate system, 500ml coil volume with PA purified IgG.

As shown in Figure 3.4.10.5, despite the use of either PEG or salt as the stationary phase, flow rate significantly affected recovery of IgG functionality. A higher IgG recovery was seen at 10ml/min (71%) compared to the run at 5ml/min (50%). Mass recovery of the IgG post CPC was always >95%, however loss in the recovery of active hence viable IgG was seen. Thus, when a recovery of 71% viable IgG recovery was seen following a run at 10ml/min, it was assumed the remaining 29% of IgG was unfunctional. This unfunctional IgG was further assumed to be showing up as 'impurities' on the HPLC chromatogram.

Despite an increase in the retention of functional IgG at an increased flow rate, there was still a loss in the functionality. As it was considered earlier that the ammonium sulphate system was having a negative effect on recovery, the PEG 1000 17.17.5% sodium citrate system was used for these experiments. Losses however were still seen. It was thought a mechanical process within the CPC instrument was causing an alteration in the ability of some of the IgG to bind to Protein A.

3.5 Conclusions

High vigour mixing, previously seen fundamental to high resolution separation in ATPS (Bourton *et al*., 2007), appears to have a detrimental effect on IgG functionality. Work in this chapter has concluded that either the phase system itself or some mechanical procedure during CPC processing has altered the Protein A binding capacity of some of the IgG.

Protein A HPLC analysis has been optimised, allowing chromatograms to be unaffected by the presence of phase system in the injection sample. The HPLC method produces 2 peaks, one at 6 minutes, the other at 0.1 minutes. The 0.1 minute peak was found to consist of both impurities (if present) and non-functional IgG. Previously this peak was regarded as just impurities but, as shown by SDS PAGE, this was not the case and non-functional IgG eluted at the same time of 0.1 minutes.

The phase system and the need for high resolution separation based on vigorous cascade mixing has been concluded to not be as benign as previously considered (Guan *et al*., 2008; Sutherland, 2007; Sutherland,2008). Furthermore any changes to the non-functional IgG species appeared to be non-reversible. The chemical properties of the PEG 3350 11.1%/11.1% ammonium sulphate system have been seen to negatively affect the IgG. A precipitation effect, was seen that would possibly exacerbate the effect on IgG functionality has been seen. All future runs were therefore conducted with the PEG 1000 17.5%/17.5% sodium citrate system.

This chapter has shown the trade-off between the need for vigorous mixing to allow separation from impurities and the resulting detriment to IgG functionality. The possibility of adequate mixing in a system which combines features of both hydrostatic and hydrodynamic mixing will be studied next. The toroidal coil allows scalability, with no rotating seals, hence is easier to clean.

CHAPTER 4: Separation of monoclonal antibody from cell culture supernatant (CCS) using toroidal coil CCC (TC CCC) centrifuge

4) **Separation of monoclonal antibody from cell culture supernatant (CCS) using Toroidal coil CCC (TC CCC) centrifuge.**

4.4 Summary

4.5 Introduction

4.6 Method and materials

4.3.1 Preparation of phase system

4.3.2 TC CCC operation

4.4 Results and discussion

4.4.1 PEG 1000 17.5%/17.5% sodium citrate run on the TC CCC: Run 4-1.

4.4.2 SDS PAGE results: silver stain

4.4.3 Determination of purity: host cell ELISA and concentration by stirred cell.

4.4.4 Effect of flow rate, peak width and spin speed.

4.4.5 Theoretical predictability: CCC2 modelling programme

4.4.6 Overview

4.5 Conclusions

4.1 Summary

Toroidal coil (TC CCC) mAb separation and its resulting effect on IgG functionality are investigated within this chapter. The primary aim was to minimise the production of non-reversible non-functional IgG. A milder form of cascade hydrostatic mixing than described previously in Chapter 3 was investigated. Retention of IgG biological activity with the separation from impurities post TC CCC processing was the objective of this chapter.

Unfortunately a loss in IgG functionality was again seen following TC CCC processing. The loss was relatively smaller when compared to that of the CPC, however still evident. Such a loss in biological activity cannot gain regulatory acceptance or be used to demonstrate the potential of this process for industrial uptake. The studies within this chapter look at various experimental parameters and their resulting effect on the retention of IgG biological activity. An increased flow rate reduced the transit time of the IgG within the machine and significantly increased the retention of IgG functionality. A reduction in rotational speed also improved retention of activity, but at the detriment to IgG peak width. Peak broadening was seen, it was assumed that would ultimately lead to a poor resolution separation.

This chapter demonstrates IgG separation from impurities, as confirmed by SDS PAGE gel and the removal of host cell proteins as shown by

ELISA. However, as highlighted in Chapter 3, following CPC processing a loss in IgG functionality was also seen with the TC CCC.

4.2 Introduction

Chapter 3 highlighted the clear separation of the mAb from crude CCS, using the CPC hydrostatic column; a detrimental effect on IgG functionality was however seen (based on the inability of the IgG to bind to the protein A, that is used as an indicator of functionality, in the absence of a true bioassay). Initially, precipitation seen with the ammonium sulphate system was thought to cause the IgG degradation. However, after changing to the sodium citrate system, IgG degradation post CPC was still seen. It was hypothesized that a mechanical process within the CPC process was causing a species change. The result was a reduction in the ability of the IgG to bind to PA. An alternative CCC machine was sought after that had the benefits of the CPC with high resolution separation and good stationary phase retention but did not reduce Protein A binding activity. Hypothesized benefits of the hydrodynamic mode were also needed; e.g. gentler mixing that was less detrimental to the IgG. However it was anticipated a reduced level of mixing would result in the loss of IgG resolution from impurities.

The TC-CCC bears similarities to the CPC in that it also uses a hydrostatic mixing motion. The CPC uses a uniform, high g-force field created by high spinning revolution. Pressure is used to drive material through mixing chambers and small bore interconnected tubes (Sutherland, 2011). The wide bore, continuous tubing of the TC CCC results in a lower pressure inside the tubing. Additionally, unlike the CPC there are no small interconnected chambers and high pressure is not applied.

The toroidal column CCC is composed of multilayer toroidal coils wound around a drum. Cascade mixing occurs in its continuous tubing with a variable g force field. The coil design allows vigorous mixing, hence good mass transfer and a high resolution separation. The stable retention of stationary phase is also seen with minimal stripping. Another advantage is the lack of rotating seals, making TC CCC less prone to leakage and contamination (Matsuda *et al.*, 1998; Ito, 2005). Moreover the TC CCC has more potential for scale up, with no corresponding issues involved in the cleaning of small tubing and interconnected chambers. It was predicted the TC CCC would allow high stationary phase retention and separation from impurities by

high mass transfer across the phase system. As cascade mixing was still employed but at a reduced vigor to the CPC, it was postulated that the resulting g force field associated with processing would be lower.

4.3 Method and materials

4.3.1 Preparation of phase system

The PEG 1000 17.5%/17.5% sodium citrate system was prepared. The phase system was prepared as detailed in Chapter 3 (Section 3.4.9).

4.3.2 TC CCC operation

The toroidal coil CCC (TC CCC) machine had a column volume of 333ml. Due to the way the column is wound (Figure 4.3.2.1) a maximum of 50% stationary retention is possible. A lower level of stationary phase retention is seen with the TC CCC as each helical turn is entirely occupied by the mobile phase (Zhang *et al*., 2010). Centrifugal forces are used to retain the stationary phase. Mobile phase however, passes recurrently through the stationary phase, resulting in stationary phase retention that is typically less than 50% of the 333ml column volume (Ito *et al*., 2009)

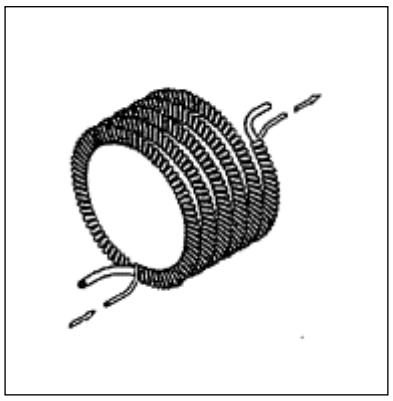

Figure 4.3.2.1: Schematic of TC CCC bobbin (Sutherland et al, 2010). TC CCC employs the use of tubing that is wound toroidally around the drum. Cascade mixing is achieved within the spinning coil.

Typical TC CCC conditions used are outlined in Figure 4.3.2.2.

TC-CCC separation
ATPS…17.5/17.5% w/w..…PEG/Salt, pH…7.39
PEG……1000…Salt …Sodium citrate
Coil volume……333ml
Sample loop……16.8ml
Operating mode…Forward
Column filled at ……30ml/min
Injected mAb:
1) CCS…… (Batch number …L156568/47)
Volume…….....32.5ml diluted with:
…..8.75g sodium citrate
…..8.75g PEG
Concentration of the antibody injected into the column……2.2mg/ml
Spin speed…2000rpm, temperature….20°C, flow rate…..…5ml/min
Equilibrated at……5ml/min,
Stationary phase displaced.….240ml

Figure 4.3.2.2: Typical TC CCC run conditions, using a PEG 1000 17.5%/17.5% sodium citrate system. Operated from centre to periphery using a 16.8ml sample loop at a flow rate of 5ml/min.

4.4 Results and discussion

4.4.1 PEG 1000 17.5%/17.5% sodium citrate run on the TC CCC: Run 4-1

A purification run was completed using CCS on the TC CCC using the conditions outlined in Figure 4.3.2.2. Fractions were collected every 5 minutes for 200 minutes and subject to Protein A HPLC analysis. Figure 4.4.1.1 shows a reconstructed chromatogram following HPLC analysis. Elution time of the IgG and impurities is plotted against HPLC peak area. Again, impurities were regarded as anything that did not bind to the Protein A column, these were eluted along with the solvent front at 0.1 minutes. The IgG eluted as theoretically predicted at K=1.62.

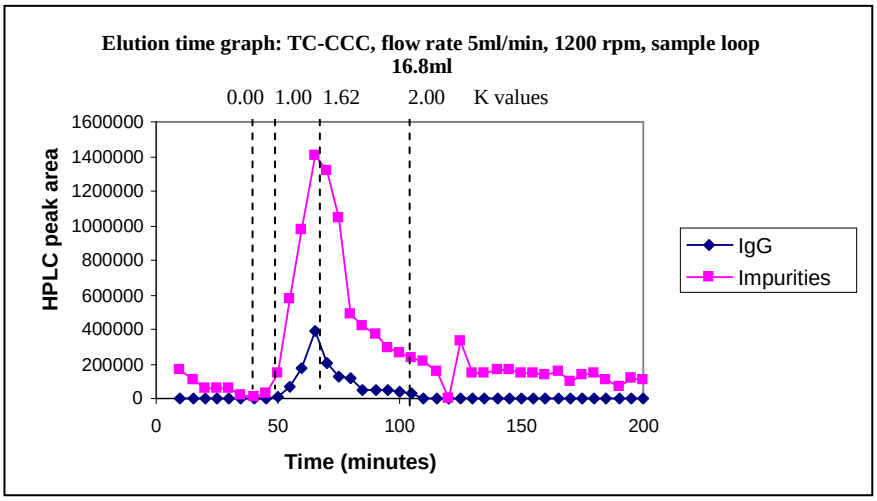

Figure 4.4.1.1: Elution time graph following protein A HPLC analysis of TC CCC run. PEG 1000 17.5%/17.5% sodium citrate system. Operated from centre to periphery using a 16.8ml sample loop at a flow rate of 5ml/min.

As shown in Figure 4.4.1.1, elution of the IgG was seen with assumed protein A non-binding IgG and impurities. Recovery of the IgG functionality however, (calculated using the appropriate calibration curve in Figure 3.4.7.1) was seen to only be 58.21% (Figure 4.4.1.2). Loss in IgG functionality following the TC CCC processing could possibly be explained by HPLC variation causing large experimental error and/or the Protein A binding capacity of the IgG being altered, creating a non-functional form.

Total mg of viable IgG recovered from fractions	6.81
Total mg of viable IgG in injection sample	11.70
% recovery of functional IgG	**58.21**

Figure 4.4.1.2: Functional IgG recovery, calculated following a TC CCC run for the purification of CCS. A PEG 1000 17.5%/17.5% sodium citrate system was used. 333ml coil volume, 5ml/min flow rate, 16.8ml injection volume. Analysis by protein A HPLC.

4.4.2 SDS PAGE results: silver stain

The SDS PAGE protocol as described in Section 3.4.2 was used for fractions from TC CCC run 4-1. The gels were initially stained with Coomassie blue (Figure 4.4.2.1). All the tested fractions (10-16) appeared to contain the IgG with fewer contaminant bands, when compared to the CCS control. As no impurities band were visible with the Coomassie blue stain, the more sensitive silver stain was employed.

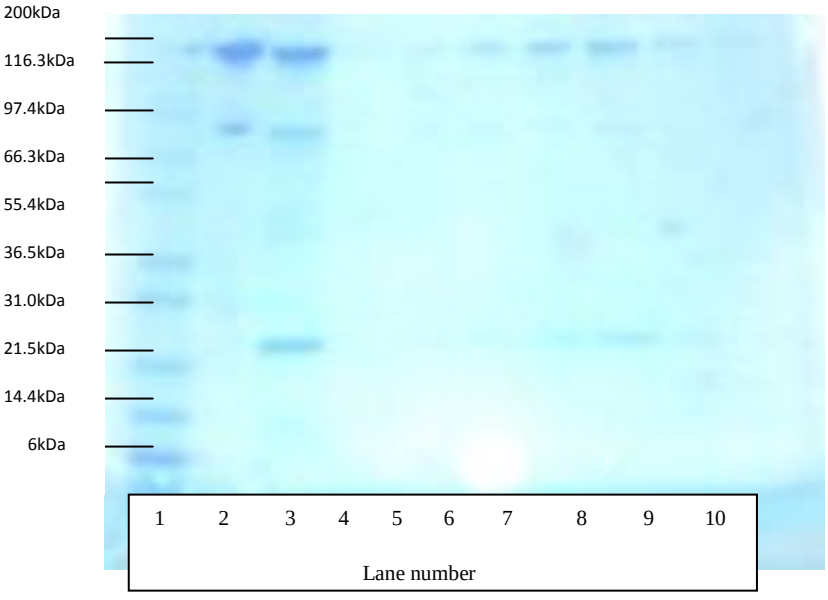

Lane number	Sample/ Fraction time
1	MWM
2	Protein A purified IgG
3	CCS control
4	Fraction 10 (50 minutes)
5	Fraction 11 (55 minutes)
6	Fraction 12 (60 minutes)
7	Fraction 13 (65 minutes)
8	Fraction 14 (70 minutes)
9	Fraction 15 (75 minutes)
10	Fraction 16 (80 minutes)

Figure 4.4.2.1: SDS PAGE gel with Coomassie blue staining. Reduced SDS PAGE gel. Samples analysed post TC CCC run 4-1. CCS purified using a PEG 1000 17.5%/17.5% sodium citrate system, 333ml coil volume, 5ml/min flow rate, 16.8ml injection volume, TC CCC run at 20ºC. 10µl sample injected per well.

A silver staining kit was purchased from Invitrogen and results can be seen in Figure 4.4.2.2. A marked difference was seen not only in sensitivity but gel quality. Interestingly, despite dilution differences, Fractions 12, 13 and 14 have fewer bands than the CCS control. However as the CCS is so concentrated, it was thought if this sample was diluted many bands apart from those that are very darkly stained would disappear. Sliver stain is much more sensitive but not quantitative, hence allowing all bands to be detected, however giving no conclusions regarding amount. It appeared as shown in Figure 4.4.1.1 very little purification was being achieved. The species change suggested by protein A HPLC does not appear by the SDS PAGE. The molecular weights of the fractions post TC CCC purification were not altered. It was thought a structural change had occurred or a subtle chemical modification of residues at the IgG: Protein A binding interface. As shown in Figure 4.4.2.1 by SDS PAGE gel, it was not a molecular weight change.

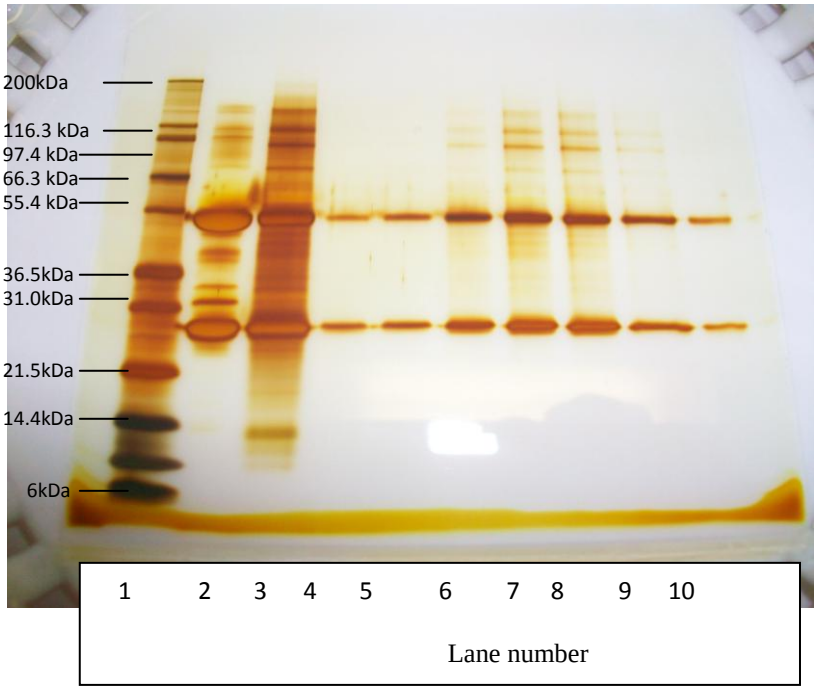

Lane number	Sample/ Fraction time
1	MWM
2	Protein A purified IgG
3	CCS control
4	Fraction 10 (50 minutes)
5	Fraction 11 (55 minutes)
6	Fraction 12 (60 minutes)
7	Fraction 13 (65 minutes)
8	Fraction 14 (70 minutes)
9	Fraction 15 (75 minutes)
10	Fraction 16 (80 minutes)

Figure 4.4.2.2: SDS PAGE results using silver stain. Reduced SDS PAGE gel. Samples analysed post TC CCC run 4-1. CCS separated using a PEG 1000 17.5%/17.5% sodium citrate system, 333ml coil volume, 5ml/minute flow rate, 16.8ml injection volume, TC CCC run at 20ºC. 10µl sample injected per well.

Purification was shown by SDS PAGE and silver stain (Figure 4.4.2.2). Further concentration of samples however was required to validate the SDS PAGE results seen at differing dilutions. Without concentration, the SDS PAGE showed no impurities. As

the HPLC 280nm detector (Figure 4.4.1.1) measured non protein components not detected by both the Commassie and sliver stain a large impurities peak is seen. It was thought that low level impurities could be present in fractions, perhaps below the level of detection. 4 pooled samples were prepared from the TC CCC run (Run 4-1) fractions: pre IgG elution (fraction 2-10), IgG elution peak (fraction 11-16), post IgG elution (fraction 17-40) and stationary phase blow out.

An Amicon (Watford, UK) stirred cell was used and attached to a pressure line. The pressure maintained the flow of the liquid through the membrane, allowing concentration. The use of a magnetic stirrer allowed controlled concentration without the build-up of molecules on the membrane surface; filter blockage was thus prevented. An ultrafiltration membrane (10,000 NMWL and diameter 63.5nm) was placed in the bottom of the cell and individual pooled samples loaded and nitrogen pressure attached.

Both the pooled, pre IgG elution fractions and that of the stationary phase were subject to a ten-fold concentration. The pooled post IgG elution fractions were concentrated five-fold. Only a five-fold concentration of the pooled post IgG elution fraction was conducted due to time constraints. Following the two days of concentration, no further concentration was achieved. It was noted during this concentration that precipitation of the salts occurred; this would not be desirable during manufacturing.

The SDS PAGE gel following concentration showed all impurities were in the pooled samples of both the pre and post IgG elution peak. The IgG elution peak was not contaminated with impurities, demonstrating purification had not been compromised and that all impurities were accounted for.

4.4.3 Determination of purity: Host Cell Protein (HCP) ELISA

Despite the production of two IgG species, purification with the removal of all host proteins was demonstrated by ELISA assay. The host cell protein assay was performed at Lonza. A range of fractions were used (Fraction 11, 12, 13, 14, 15, 16) from the TC CCC run 4-1 (Figure 4.4.1.1).

The basic principle of an ELISA is the detection of binding between a specific antigen and an antibody by the use of an enzyme (Ma *et al.*, 2006). The

immunoreactivity between the capture and detection antibody is key. The capture antibody recognises the target antigen and the detection antibody subsequently recognises the bound target (Thompson, 2010). By the use of a blocking buffer any non-specific binding is kept to a minimum. Ultimately, the enzyme allows the conversion of the substrate into a coloured product, which allows quantification of the target antigen, based on the antigen antibody binding affinity.

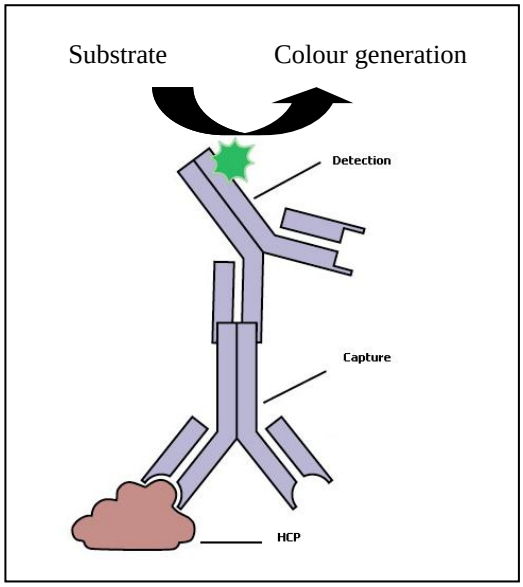

Figure 4.4.3.1: Schematic to show the generation of colour that is measured by a HCP ELISA. The colour generation is a result of the binding interaction between the antibody and host cell proteins present, which by the use of a substrate generates a change in assay solution.

The HCP ELISA used allowed the determination of purity. Moreover it highlights all the potential HCPs that could potentially contaminate a product during a manufacturing/ purification step have been removed. It is a regulator requirement to obtain the lowest level of HCP possible during mAb production (<100ng HCP/mg IgG) for human use, following complete purification including polishing steps).

To perform the assay, a 96 well plate was coated with pooled sheep and donkey IgG anti-Chinese Hamster Ovary (CHO) HCP and left overnight. Blocking buffer was applied the following day, to prevent any non-specific binding. The blocking buffer was subsequently washed off and a serial dilution of the standard was loaded into the initial wells. All fractions were diluted 1:200 in sample buffer and placed in appropriate wells. The plate was then incubated at 37ºC for 1.5hrs.

Biotinylated anti-HCP was added followed by extravidin. Finally the ABTS (2,2'-Azinobis [3-ethylbenzothiazoline-6-sulfonic acid]-diammonium salt) substrate was added and the plate incubated until a suitable colour development was seen (20-50 minutes). The plate was read at 490nm on the plate reader.

The following calculations were used:

HCP (ng/ml)= Measure HCP in unspike (mg/ml) x Sample dilution factor (200)

$$\text{HCP (pg/ml)} = \frac{\text{Measure HCP in unspike (mg/ml) x Sample dilution factor (200)}}{\text{Sample protein concentration (mg/ml) From HPLC}}$$

Recovery of HCP spike:

$$\text{Recovery (\%)} = \frac{\text{HCP in spiked (ng/ml)} - \text{HCP in unspiked (ng)} \times 100}{\text{HCP in control sample (ng/ml)}}$$

Acceptability of recovery was ±25% of 100%.

To calculate HCP removal, the sample (unspiked) was subtracted from a spiked control. The PA purified IgG was also tested in the phase system as a comparison. Results are tabulated in Figure 4.4.3.2, HPLC concentration for each respective sample is used to determine HCP concentration that remains in ng/ml. It was seen that CCC fractions showed a decrease in HCP when compared to the CCS starting material. However, this loss of HCP was not comparable to the removal shown in the PA purified IgG sample. Nevertheless there was a tenfold reduction in HCP in the fractions from that of the CCS control, demonstrating a degree of purification.

Sample name	HPLC value (mg/ml)	HCP (ng/ml)	HCP (ng/ml)
PA purified IgG in phase system	2.45	<10000.0	<4081.6
CCS in phase system	0.85	138620.0	163082.3
Fraction 11	0.45	11218.1	24933.3
Fraction 12	1.52	27580.0	18144.7
Fraction 13	3.67	50160.0	13667.6
Fraction 14	1.81	34380.0	18994.5
Fraction 15	1.05	24280.0	23123.8
Fraction 16	0.93	15980.0	17182.8

Figure 4.4.3.2: HCP ELISA removal results. Conducted at Lonza using fractions post TC CCC. PEG 1000 17.5%/17.5% sodium citrate system, 333ml coil volume, 5ml/min flow rate, 16.8ml injection. TC CCC run at 20ºC.

4.4.4 Effect of flow rate, peak width and spin speed

To determine whether adjusting the experimental parameters could improve the retention of IgG functionality, several parameters were investigated. These parameters included flow rate, stationary phase retention and rotational speed.

TC-CCC runs were carried out at varying flow rates to observe the direct effect of transit time of the IgG within the machine. Figure 4.4.4.1 shows that the effect of flow rate plotted against resulting IgG functionality and stationary phase retention. IgG functionality was calculated by Protein A HPLC analysis. As flow rate increased, so did the corresponding IgG recovery considerably. However a slight decrease in stationary phase retention as flow rate increased was observed. All experiments were carried out only once.

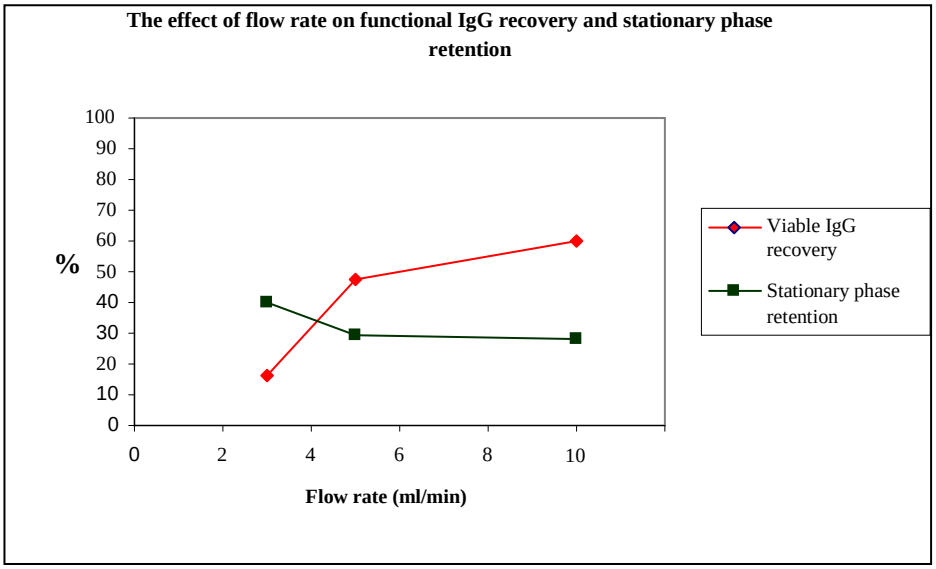

Figure 4.4.4.1: The effect of flow rate on recovery of IgG functionality. Flow rate investigated at 3,5 and 10ml/min using the TC CCC, PEG 1000 17.5%/17.5% sodium citrate system, 333ml coil volume, 5ml/min flow rate, 16.8ml injection volume, TC CCC run at 20ºC.

Elution profiles were compared at the differing flow rate. As shown in Figure 4.4.4.2 elution time was plotted against IgG concentration. At a higher flow rate a much sharper peak was observed when compared to a lower flow rate at 5ml/min. With the flow rate at 3ml/min, the IgG did not elute and was found in the stationary phase pump out (after a 400 minute run time). Recovery was extremely poor at 16.33% and was thought to be due to excessive time in the machine, causing degradation to the mAb. These results appeared to be similar to that of the CPC where a loss in IgG

functionality was seen.

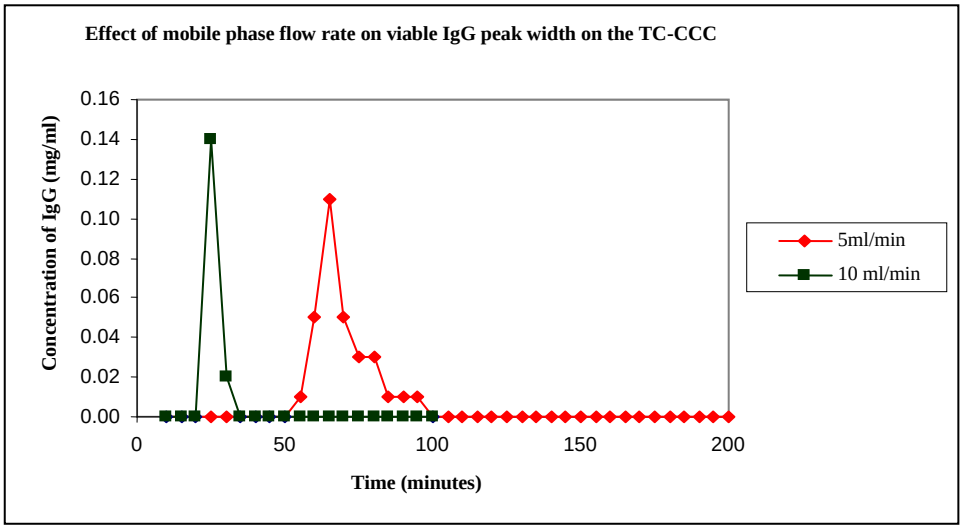

Figure 4.4.4.2: Effect of flow rate on viable IgG peak width, Investigated at 5 and 10ml/min using TC CCC, PEG 1000 17.5%/17.5% sodium citrate system, 333ml coil volume, 5ml/minute flow rate, 16.8ml injection volume. T`C CCC run at 20ºC.

The effect of rotational speed was also investigated, with the aim of reducing the 'g-force' and thus the potential damage to the functionality of the IgG. As seen in Figure 4.4.4.3, elution times are plotted against IgG concentration at rotational speeds of 900 and 1200 rpm. At a higher rotational speed of 1200rpm the resulting peak sharpness was much greater than that seen at 900 rpm.

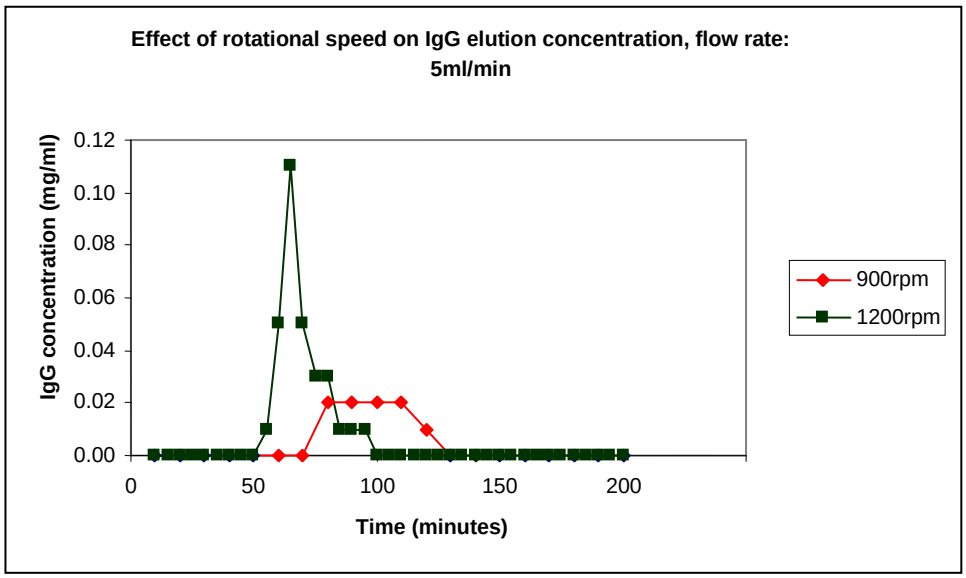

Figure 4.4.4.3: Effect of rotational speed of IgG peak broadening. Investigated at 900 and 1200rpm at a flow rate of 5ml/min on TC CCC using PEG 1000 17.5%/17.5% sodium citrate system, 333ml coil volume, 5ml/min flow rate, 16.8ml injection volume. TC CCC run at 20˚C.

When the spin speed was decreased to 900rpm at a lower flow rate of 5ml/min as opposed to 10ml/min, IgG recovery actually decreased (from 60.54% at 47.56% at 900rpm). Additionally IgG peak sharpness was lost, resulting in the likelihood of elution with impurities being much greater.

4.4.5 Theoretical predictability: CCC2 modelling programme

Experimental predictability was investigated using a CCC programme design by Joost de Folter (a PhD student working on CCC modelling within the Institute). The programme allowed the determination of experimental predictability and reproducibility using a theoretical model. As seen in Figure 4.4.5.1 all parameters were detailed, most importantly the partition coefficient of the IgG and the volume ratio of the phase system.

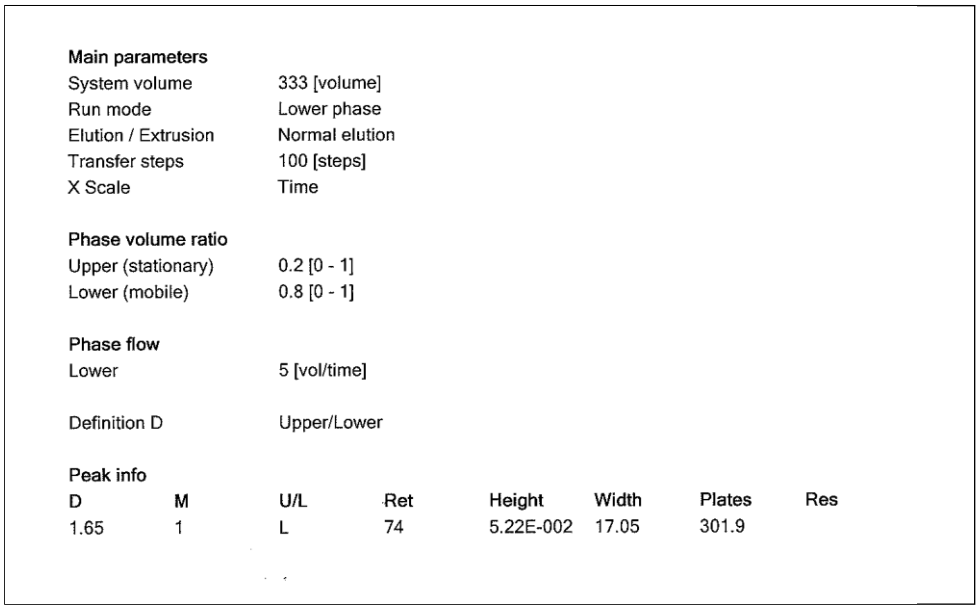

Main parameters

System volume	333 [volume]
Run mode	Lower phase
Elution / Extrusion	Normal elution
Transfer steps	100 [steps]
X Scale	Time

Phase volume ratio

Upper (stationary)	0.2 [0 - 1]
Lower (mobile)	0.8 [0 - 1]

Phase flow

Lower	5 [vol/time]

Definition D	Upper/Lower

Peak info

D	M	U/L	Ret	Height	Width	Plates	Res
1.65	1	L	74	5.22E-002	17.05	301.9	

Figure 4.4.5.1: Parameters entered into the CCC2 programme designed by Joost de Folter, 2008. Parameters were included to allow the calculation of predicted elution time and peak width. System volume was 333ml the coil volume of the CPC, phase volume ratio 0.2:0.8 and a flow rate of 5ml/min. D is the partition coefficient of the mAb,

Figure 4.4.5.2 shows the model results based on TC CCC run 4-1 (Figure 4.4.1.1), that were replicated for direct comparison with the model prediction. A broad peak elution is seen starting at 60 minutes and tailing off around 90 minutes. When directly compared to the actual experimental results obtained seen in Figure 4.4.5.3 (TC CCC run 4-1), a similar elution time and peak broadness can be seen.

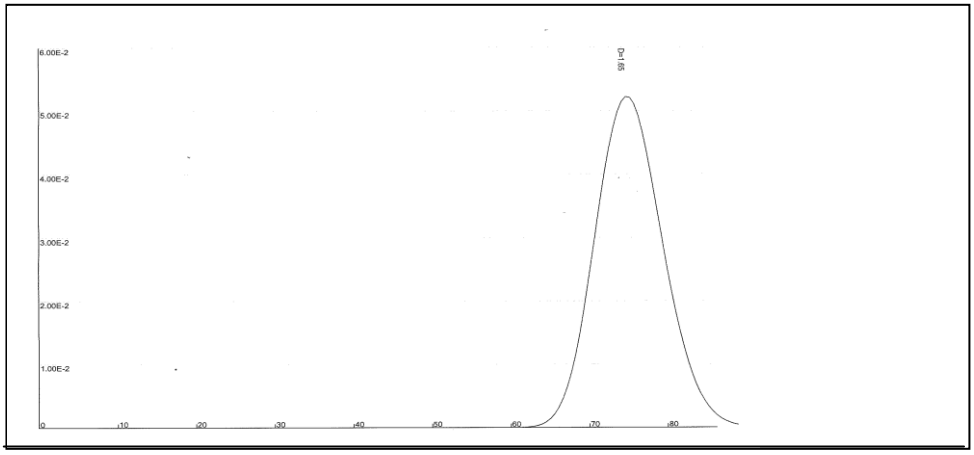

Figure 4.4.5.2: Predicted elution peak of IgG using CCC2 programme. Parameters included in the program are seen in Figure 4.4.5.1.

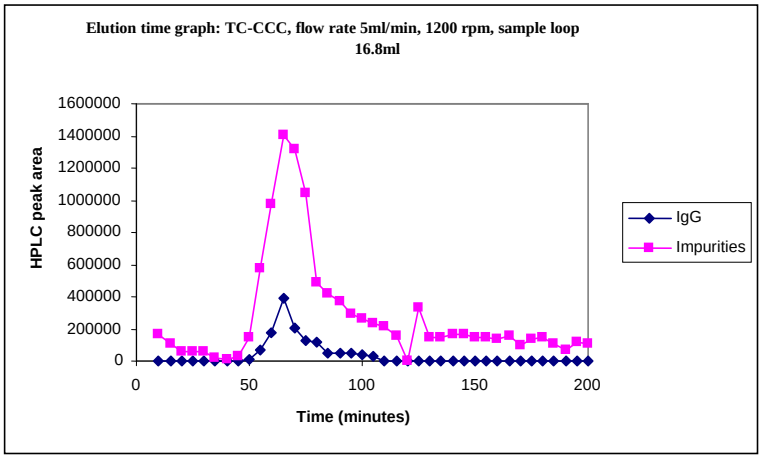

Figure 4.4.5.3: Actual experimental TC CCC results using PEG 1000 17.5%/17.5% sodium citrate system, 333ml coil volume, 5ml/min flow rate, 16.8ml injection volume. TC CCC run at 20ºC.

4.4.6 Overview

An overview of TC CCC run results can be seen in Figure 4.4.6.1. Despite stationary phase retention being improved by a lower flow rate, improved IgG retention of activity was seen at a higher flow rates. The best conditions with regards to retaining IgG activity were seen at an increased flow rate of 10ml/min due to a reduced transit time of the IgG within the CCC machine. A maximum functional IgG recovery was seen of 68.35% (Figure 4.4.4.2). When speed spin was decreased from 1200 to 900rpm, at a flow rate of 5ml/min, the recovery of IgG activity was virtually the same (58.21% and 60.54%). However, at a higher spin speed stationary phase retention was improved.

Recovery of viable IgG (%)	Rotational speed (rpm)	Flow rate (ml/min)	S*f* retention	Comments	Figure number
16.33	1200	3	39.9	Recovery extremely poor	n/a (mAb retained in column)
58.21	1200	5	29.5		4.4.1.1
68.35	1200	10	27.9	High resolution, sharp peak	4.4.4.2
60.54	900	5	26.4	Lower spin speed of 900rpm	4.4.4.3

Figure 4.4.6.1: Overview of TC CCC results. All conducted with, PEG 1000 17.5%/17.5% sodium citrate system, 333ml coil volume, 16.8ml injection volume. TC CCC runs conducted at 20ºC and sample subsequently analysed by protein A HPLC.

4.5 Conclusions

The TC CCC, following on from results obtained in Chapter 3, was used to investigate mAb separation from CCS. It was considered that the loss in functionality seen with the CPC would be reduced with the TC CCC. There was a need for vigorous hydrostatic mixing, to allow sufficient mass transfer of the large weight protein (150 kDa), however to a reduced degree, to prevent the creation of non functional IgG. It was thought that the TC CCC with its continuous wide bore tubing would allow gentler mixing when compared to the pressure driven mixing chambers of the CPC connected by thin tubing.

Runs performed on the TC CCC were comparable to those using the CPC in terms of separation from impurities. At lower flow rates however, and with most operating conditions, better retention of biological activity was seen with the TC CCC. Despite an increase to a maximum of 68.35% IgG recovery, this was still insufficient to be adopted for biological purification in industry. 100% bioactivity is always the aim.

Purification was demonstrated by SDS page and silver stain and HCP ELISA, illustrating no change to the molecular weight of the protein had occurred. Future investigations into the exact cause of loss to IgG functionality are needed within the whole CCC process (phase system and processing).

Studies in this chapter have shown high resolution separation using the TC CCC is possible. Again however it has been seen, as shown in Chapter 3 with the CPC, this level of mixing vigour has a detrimental effect on IgG recovery. The effect, whether presented in terms of phase system or design of the column, needed to be addressed. The studies in the next chapter (Chapter 5) were designed to thoroughly investigate this.

CHAPTER 5: Critical look at IgG functionality

5) Critical look at IgG functionality

5.1 Summary

Both the hydrostatic CCC columns (CPC and TC CCC) with different degrees of mixing vigour (as described in Chapters 3 and 4) have been noted to cause IgG degradation. Further investigation into the actual cause of loss in IgG functionality was conducted. The studies within this chapter were designed to look at a number of CCC processing aspects, including the stability of the IgG within the phase system and multiple factors associated with mixing in the CCC machine itself.

Biacore analysis, based on affinity technology was used to confirm results previously seen by Protein A HPLC analysis. Auxiliary proof was obtained that purified IgG, following CCC, had a reduction in binding affinity (expressed in resonance units) to Protein A. It was generally considered (within pharmaceutical companies particularly at Lonza) and within the scope of this project that if IgG was able to bind to Protein A, it was still fully functional in vivo. However the results within this chapter show this binding association after CCC was reduced. Therefore it was hypothesised this IgG could not long bind to the PA due to a structural change and hence was non or partially functional. The loss in biological activity was investigated by incubation in the phase system (to maximum of 50ºC) and spinning the samples at a constant g (de Belval *et al*., 1998; Wu *et al*., 2006). Neither of these factors however was seen to be detrimental to IgG functionality.

By the use of a custom built shaker, some of the relationships between the phase system, the shearing effect, mixing vigour and the sample itself (PA purified IgG material and CCS) were demonstrated. Loss in IgG functionality was seen to involve a combination of factors rather than a single underlying cause. Moreover, the effects of other proteins components (e.g. anti-foaming agents, host cell proteins) in the CCS, thus increasing total protein concentration were seen to affect the retention of IgG functionality. The interface of the phase system was also highlighted as an issue in the loss of IgG functionality. Losses were still seen when the IgG was processed in a single phase, however not to the same level of degradation as in the phase system. The series of experiments within this chapter were designed to understand the complexity of mixing within the CCC machines. The causes of loss in functionality were highlighted and suitable operating parameters and machine type suggested. Ultimately, a balance between separation of the IgG from impurities and the retention of biological activity was crucial.

5.2 Introduction

Hydrostatic CCC columns have been used in previous chapters for the separation of the mAb from cell culture supernatant (CCS). Purification has been achieved by CCC in Aqueous Two Phase Systems (ATPS) using the PEG 1000 17.5%/17.5% sodium citrate system. Protein A HPLC was used to detect the mAb as it eluted post CCC. A protein A binding peak was detected (6 minutes), and this was confirmed by SDS PAGE. Also detected was an IgG peak, confirmed by SDS PAGE, which did not bind to protein A (0.1 minutes). Previously this form was regarded as impurities but as shown by SDS PAGE was not the case, and some purification had been achieved. It was considered, therefore that possibly the ATPS or another factor in CCC processing was altering the protein A binding capacity of part of the IgG sample (Asenjo *et al*., 2011; Zhi *et al.*, 2005; Shibusawa *et al*., 2006). Since the ATPS had both a high polymer and salt concentration, its effect on the specific protein A-IgG interaction needed to be considered.

The following observations were noted when individual TC CCC fractions were analysed by Protein A HPLC:

1) Purified fractions as seen by Protein A HPLC had elution peaks at both 0.1 minutes and 6 minutes.

2) When these fractions were run on a SDS PAGE gel they appeared as just one species, with the same mobility as the IgG. Thus fractions eluted from CCC contained two IgG species; one binding Protein A and one non-binding protein A. The single IgG band demonstrated purification had occurred and that other protein bands present in the loaded CCS sample were absent.

3) The IgG HPLC peak in the CCC fractions and the PA purified IgG control had a similar spectra, that was different from that of the CCS

In order to determine the exact cause of loss in IgG functionality, the studies in this chapter were designed to investigate a number of potentially relevant aspects of the CCC technique. Biacore analysis was initially used to confirm the species change and is detailed first.

5.3 Method and materials

5.3.1 Aim of using Biacore for this work

The Biacore work was completed as a collaboration with Dr Ian Boulton from the Biosciences department of the University. The objective was to use the BiaCore instrumentation to measure the interaction between Protein A and the monoclonal antibody (mAb), in the presence of the PEG 1000 17.5%/17.5% sodium citrate system.

5.3.2 Biacore theory: Surface Plasmon resonance

Biacore is an affinity technology, which is used to determine quantitatively how proteins interact. The technology relies on Surface Plasmon resonance (SPR) and measuring the small change in total internal reflection of light produced by binding (Thongborisute *et al*., 2008).

The SPR phenomenon allows the measurement of adsorption of a particular analyte onto a metal surface (Huang *et al*., 2007).With the Biacore instrumentation a gold layer is attached to the chip sensor surface (Papalia *et al*., 2006; Gopinath *et al.*, 2010). The ligand of interest (in this case Protein A) is immobilised on the chip surface. When the analyte is injected through the flow channel, binding between the analyte and the ligand is possible (Figure 5.3.2.1). Binding causes an accumulation of protein on the chip surface which consequently increases the refractive index (Van der Merwe *et al*., 1996). The change in SPR signal is dependent

on the solute concentration at the chip surface, when in contact with the analyte. The change in refractive index is thus measured in real time as shown in Figure 5.3.2.1, with the production of a sensorgram where resonance units is plotted against time.

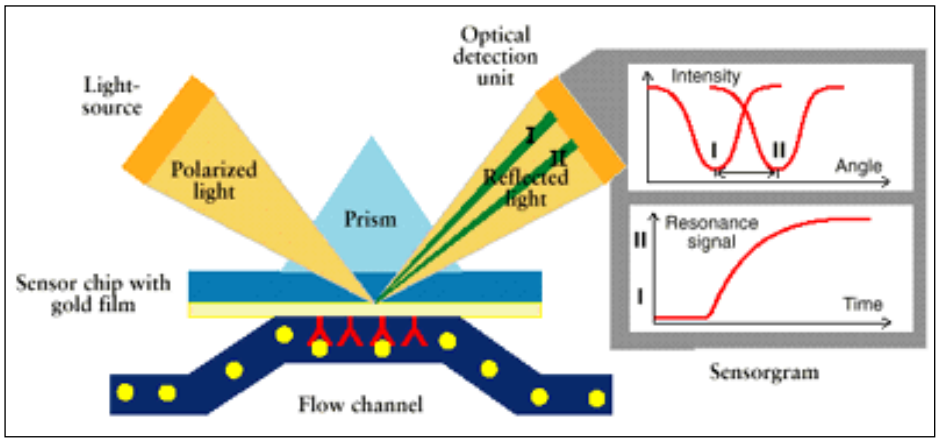

Figure 5.3.2.1 Surface Plasmon Resonance (SPR) theory. Protein A was immobilised on to the chip surface. The IgG species was flowed over the protein A chip and a sensorgram generated. A detector was used to determine quantitatively binding between the IgG species and the PA. The analysis was measured in real time, allowing the production of an association dissociation curve (Homoll, 2003).

Solutions containing the sample (the two different species of IgG following CCC) were flowed over the chip surface. Four channels were used to measure the increase in SPR both independently and in real time. The technology allowed the investigation of the unique binding interactions and affinity. It was hoped the Biacore instrumentation would demonstrate whether or not the two different species IgG species were functional.

5.4 Results and discussion

5.4.1 Effect of phase system incubation on IgG functionality

It was commonly noted in the literature (Albertsson, 1970; Zaslavsky *et al*., 2000) that due to the high water content and low interfacial tension of aqueous two phase systems (ATPS), a mild environment for separation was created. It has been predicted in the literature that these phase systems are used due to their negligible effect on biological material. However, in the experiments conducted thus far using CCC processing, a loss to the IgG biological activity was always seen. The effect of phase system incubation on activity was investigated.

Both CCS and PA purified IgG were used. The 7 phase systems of interest (from the full robotic run Figure 2.4.3.5) along with a PEG dextran system were investigated. The PEG dextran system was included as it has been well documented in the literature for being a mild system, which has been used successfully for many cell separations (Albertsson, 1958). Furthermore these systems do not contain any salts and the resulting interfacial tension is very low (Kumar *et al*., 2007). This particular system (PEG 8000 5% Dextran 500K 7%) was included as it had previously been used within the Brunel CCC group and no adverse effect on enzyme stability was noted (Grudzien thesis, 2011).

Phase systems were prepared with the addition of CCS and PA purified IgG respectively. Samples were taken pre and post a 5 hour bench top incubation. Samples were diluted 1 in 4 and subject to Protein A HPLC analysis. The tested systems, resulting HPLC area pre and post incubation and percentage change in mass recovery of functional IgG are listed in Figure 5.4.1.1. Experiments were carried out only once.

	HPLC peak area (µV.sec)					
	PA purified IgG			**CCS**		
	Incubation time (hr)		**Mass recovery of functional IgG (%)**	**Incubation time (hr)**		**Mass recovery of functional IgG (%)**
Phase systems	**0**	**5**		**0**	**5**	
Control: PA purified IgG in water	7130597	7234222	101.45	2118839	2077332	98.04
PEG 400 17%/17% KPO_4	5325071	5415075	101.69	1612834	1628464	100.97
PEG 1000 14%/14% KPO_4	6372758	6669763	104.66	1600437	1634015	102.10
PEG 1000 17%/17% KPO_4	5194963	5643470	108.63	1517696	1364418	89.90
PEG 1000 15.5%/15.5% KPO_4	5801476	5298336	91.33	1130312	1137342	100.62
PEG 1000 18.5%/18.5% KPO_4	4772497	4152171	87.00	1639800	1596064	97.33
PEG 3350 11%/11% NH_4SO_4	4535435	2418408	53.33	1872937	1323365	70.66
PEG 1000 17.%5/17.5% Na Citrate	5141081	4458171	86.72	1565084	1482723	94.74
PEG 8000 5% Dextran 500k 7%	6641923	3128767	47.11	1923421	1097162	57.04

Figure 5.4.1.1: Functional IgG mass recovery data following incubation at 25ºC in various phase systems. The potassium phosphate system (KPO4) was prepared with di potassium hydrogen phosphate and mono potassium phosphate at a ratio of 3.78:1, to achieve an end pH of 8. Recovery of functional IgG post incubation in phase systems was determined by measurement of the 6 minute HPLC peak following protein A HPLC analysis.

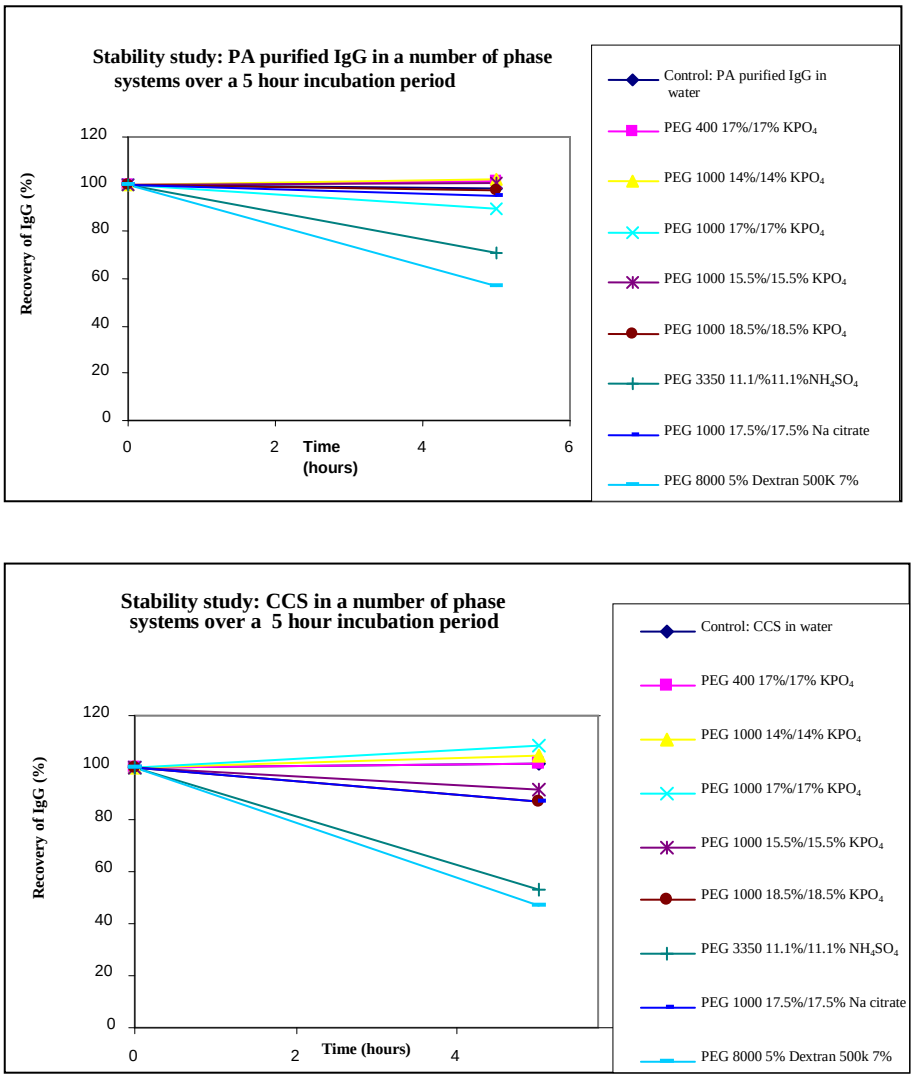

Figure 5.4.1.2: Graphical representation of Figure 5.4.1.1. Functional IgG recovery in a number of phase systems using both Protein A purified IgG (top graph) and CCS (bottom graph). Recovery determined as change in HPLC peak area, as a percent of initial conditions to those post 5 hour incubation.

Figure 5.4.1.1 shows the various phase systems and the % change in HPLC peak area, firstly with the PA purified IgG and secondly with the CCS. Generally most systems appeared to have a mass recovery of functional IgG that was greater than 85%, as seen with both the CCS and PA purified IgG material. Figure 5.4.1.2 is a graphical representation of the data in Figure 5.4.1.1, time in hours is plotted against the recovery of functional IgG. As highlighted from Figure 5.4.1.1 all systems apart from two (the PEG dextran and PEG ammonium sulphate system) had a straight line between the pre and post 5 hour incubation, denoting no significant change (<85% HPLC peak area). These results were as opposed to the decreasing IgG recovery seen

with the PEG dextran and PEG ammonium sulphate systems. Furthermore, it showed that the change to the Protein A binding IgG capacity that had previously been seen was not primarily due to the phase system. Therefore, some mechanical mechanism in the CCC machine was at fault.

The phase systems that appeared to affect the IgG stability was the PEG 3350 11.1%/11.1% ammonium sulphate system (where previous issues with precipitation and aggregation were seen) and the PEG 8000 5% dextran 500k 7% system. The result for the PEG dextran systems was contradictory to that seen in the literature (Karakatsanis *et al*., 2007; Mattiasson *et al.*, 1982; Mattiasson *et al*., 1998). PEG-dextran systems had been typically been used as an alternative to PEG/salt systems for milder, lower interfacial tension separation of biologics such as cells (Walter *et al*., 1994; Azevedo *et al*, 2008). It was considered that a detection issue by Protein A HPLC had occurred or in the phase system make up.

The PEG dextran results were hence retested. A typical 1:4 dilution (250µl sample + 750 µl water) had previously been used for all the samples, this was increased 10 fold (25 µl sample+ 975 µl water). Additional samples were made at 50µl (50µl sample + 950 µl water) and 100µl (100µl sample + 900 µl water). Samples were taken on the hour, for a 5 hour time period and subject to protein A HPLC analysis. Experiments were carried out only once.

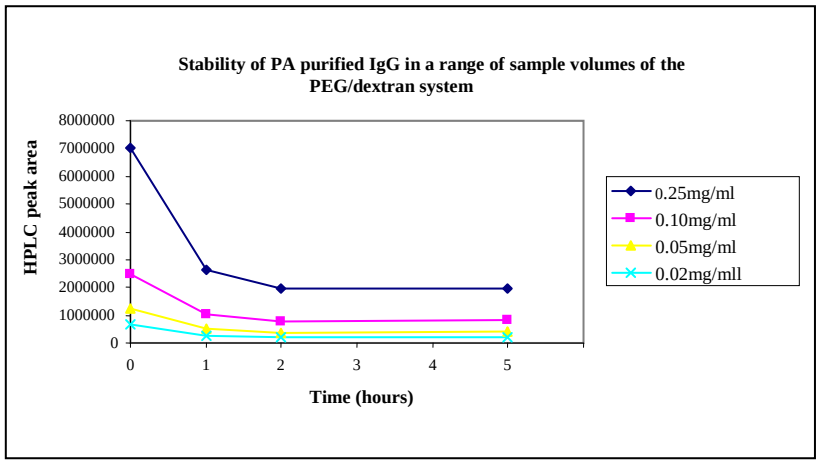

Figure 5.4.1.3: Investigation of PEG/dextran systems on IgG stability at 25ºC. Dextran was from Sigma Aldrich lot number 1387318V. Various concentration of IgG were loaded and subject to analysis by the 8 minute protein A HPLC programme. The incubation period was over 5 hours.

The results of the experiment can be found in Figure 5.4.1.3, HPLC peak area has (μV.sec) been plotted against the incubation time, for 4 different concentrations of IgG in the PEG dextran system. It can be seen that HPLC peak area declines over time for all the concentrations tested. IgG stability was affected by the PEG dextran system, even following a tenfold dilution of the usually loaded sample volume. A sharp decline in the HPLC peak area was seen following 1 hour of incubation at 25ºC, a further decrease was sustained at a slower rate to 5hours.

Further checks were carried out with a new batch of dextran (lot number 0001382453) to ensure the loss in activity was genuine. It was thought the dextran may have expired and was degraded, causing changes to the IgG or the way in which it was detected by Protein A HPLC. The results are shown in Figure 5.4.1.4 where results are listed at incubation times (0-4 hours in triplicate) and % change in HPLC area. It was seen that as incubation time increased the % change in the HPLC peak area appeared to decrease, then increase again. Figure 5.4.1.5 is a graphical representation of Figure 5.4.1.4, where incubation time is plotted against average HPLC peak area. Again the instability in HPLC peak area data can be seen with a decrease followed by the line plateauing off. It was hypothesised that possibly the high concentration combination of PEG and dextran were causing the IgG to aggregate. Following a 4 hour incubation period, 80.97% recovery of the original IgG peak area was seen. Despite a loss in HPLC peak area being seen (Figure 5.4.1.4) the data appeared unstable and was seen to decrease, then increase again after a 4 hour incubation period. It was hence suggested, loss in HPLC peak area was due to experimental analysis detector error, rather than instability caused by the presence of dextran to the IgG.

Incubation time (hours)	HPLC peak area	Average HPLC peak area	STD error	% of the original peak area
0	616479	663205	23966	100.00
	677319			
	695818			
1	469224	483819	7530	72.95
	487902			
	494330			
2	373955	390385	31249	58.86
	450821			
	346380			
3	518514	494686	13954	74.59
	495353			
	470190			
4	462645	537028	38197	80.97
	589297			
	559143			

Figure 5.4.1.4: Repeat investigation of PEG/dextran systems on IgG stability. Individual samples taken in triplicate over a 4 hour period and subject to protein A HPLC analysis. Initially samples diluted 10 fold with a new batch of dextran (lot number 0001382453).

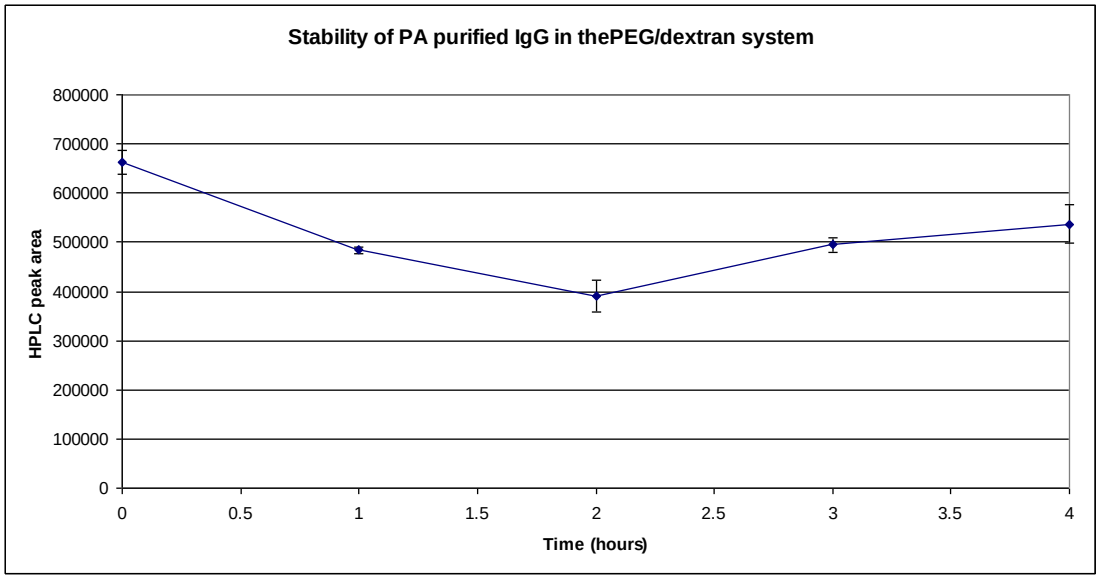

Figure 5.4.1.5: Graphical representation of Figure 5.1.1.4. Effect of PEG/dextran system on IgG HPLC peak area stability over a 4 hour period. Points used are an average of readings shown in Figure 5.4.1.4 following protein A HPLC.

5.4.2 Investigation of HPLC column saturation

The protein A HPLC column only had a 1cm column volume, with a column dimension of 0.7x2.5cm and a dynamic binding capacity of at least 30mg. It was hypothesised that overloading and column saturation could possibly be an issue, resulting in the production of the two IgG species.

PA purified IgG was diluted in 5ml of upper and 5ml of lower phase (of the PEG 17.5%/17.5% sodium citrate system). Injection volumes from 5µl up to 80µl were run using the previously developed protein A HPLC programme.

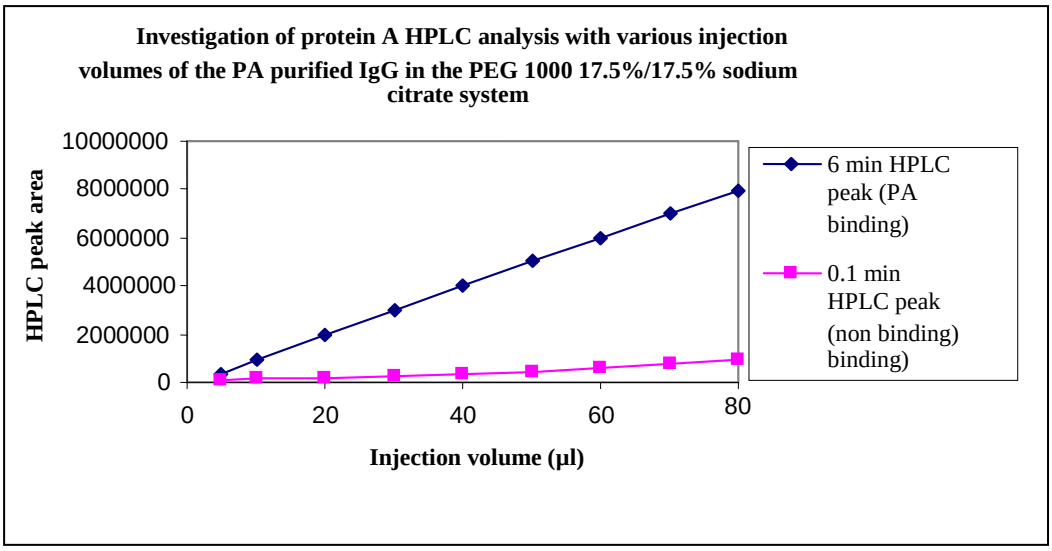

Figure 5.4.2.1: Investigation of protein A HPLC column saturation. Various injection volumes of PA purified IgG were diluted in equal volumes of the PEG 1000 17.5%/17.5% sodium citrate phase system. Results analysed by protein A HPLC, peak area of the 0.1 and 6 minute peak plotted.

Results can be seen in Figure 5.4.2.1 where HPLC peak area is plotted against increasing injection volume (µl). For both the 6 minute and the 0.1 minute peak there was a linear increase in HPLC peak area as injection volume increased. These results showed that column saturation was not an issue.

5.4.3 Biacore analysis

Biacore analysis was conducted with Fractions 13 and 14 which following TC CCC run 4-1 had the highest concentration of IgG. In order to assess the two supposed 'species' of IgG, these were collected separately following HPLC injection. The peak at 0.1 minutes (non binding IgG) and 6 minutes (PA binding IgG) were collected (Figure 5.3.3.1). The fraction itself, which was mixed, therefore containing both forms was also tested.

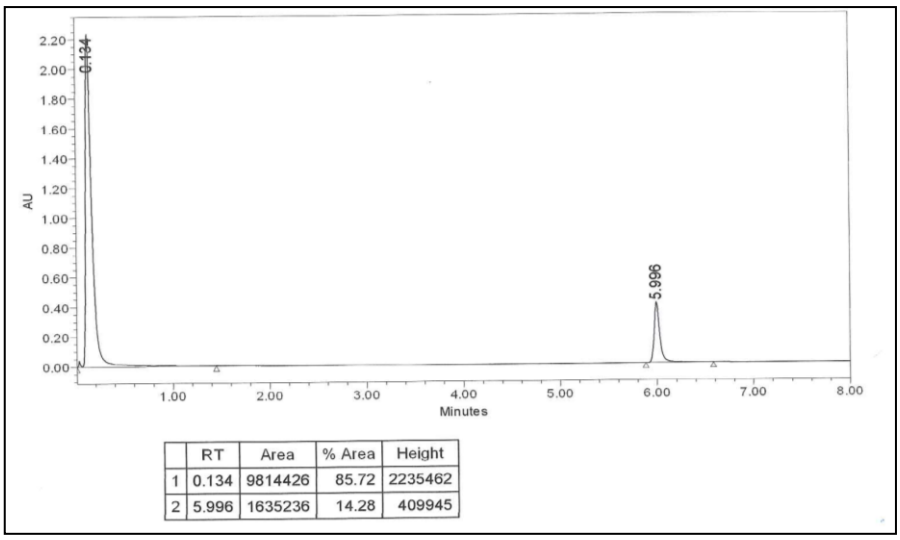

	RT	Area	% Area	Height
1	0.134	9814426	85.72	2235462
2	5.996	1635236	14.28	409945

Figure 5.4.3.1: Protein A HPLC chromatogram of the CCS starting material used in the Biacore analysis. 8 minute adapted HPLC programme used with 80µl injection volume. The 0.1 minute and the 6.0 minute fraction were collected separately for Biacore analysis.

Initially a chip was coated with protein A. Activation of the chip surface was by lysine and a mixture of activation solution. The PA was flowed onto the chip surface and immobilised (Figure 5.4.3.2). The refractive index was measured and the level of PA attachment determined. To improve PA suspension to the chip surface, a pH 8.6 buffer was used. A negative control was primarily used to assess that no background binding was seen. This was demonstrated by injection with water, as no background readings was seen, no correction for background binding was required. Glycine injections were used alternatively between each injection to regenerate the column. 10mM glycine of low pH (1.5-2.5) was used, this low pH caused the proteins to unfold, and additionally they were positively charged thus repelled from the ligand. Importantly, glycine allowed regeneration whilst keeping the ligand active (Drescher *et al*., 2009). All the other samples were tested undiluted.

The Biacore instrumentation measured a change in total internal reflection, denoted by resonance units (R). Results were analysed in terms of the change in resonance units between association and dissociation. A higher dissociation value i.e. maximum resonance unit as compared to the initial association value was indicative of greater binding. Ultimately the greatest difference between dissociation and association was required to show specific binding.

Results following Biacore analysis can be seen in Figure 5.4.3.3 for Fraction 13 and Figure 5.4.3.4 for Fraction 14. These association dissociation graphs show the change in resonance units against time. It was noted the CCC fractions containing the IgG did not have the classical association dissociation curve, typically seen in the literature (Gopinath *et al*., 2010). A typical association dissociation curve is shown in Figure 5.4.3.2, where there is a steady baseline, followed by sample injection and association between the analyte of interest and the ligand, a steady state is then reached and the analyte is dissociated from the ligand. With the CCC samples the shapes of the curves were very much random and hence the difference between association and the dissociation resonance values were used to calculate association.

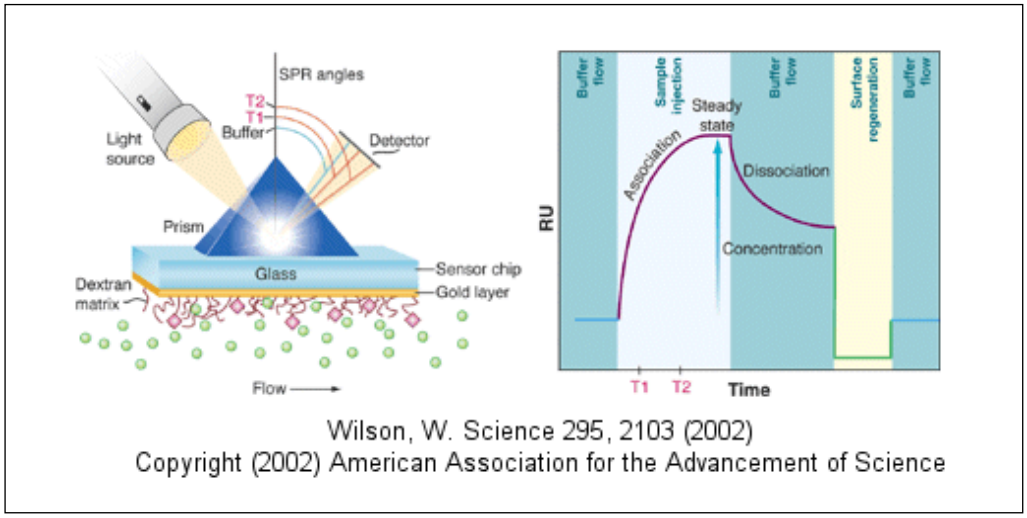

Figure 5.4.3.2: Typical association/dissociation curve following Biacore analysis. Changes in refractive index, thus resonance units are shown at injection, association, sample end and finally dissociation (Gopinath et al., 2010). Binding affinity is calculated by change in baseline association curve from that of baseline dissociation curve.

Control 180R

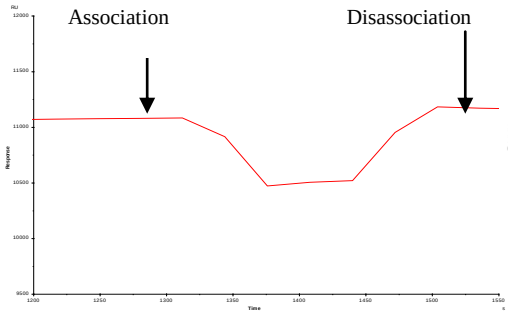

Fraction 13, 6 minute, 2266R

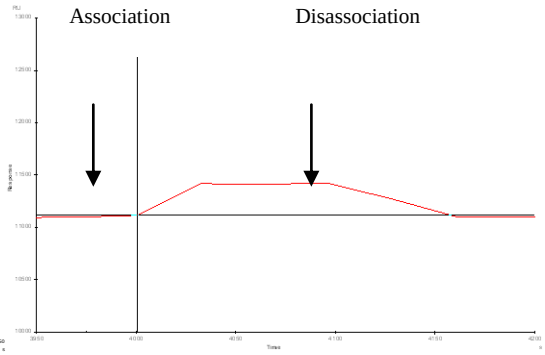

Fraction 13, 0.1 minute, 0R

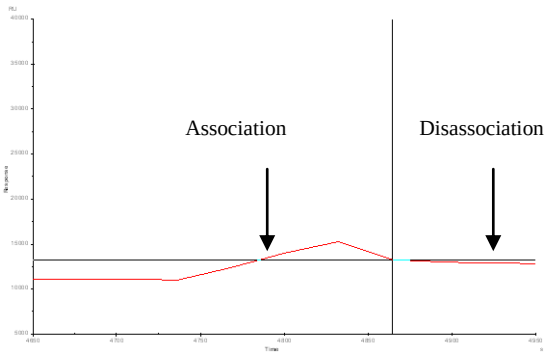

Fraction 13, Mixed, 269R

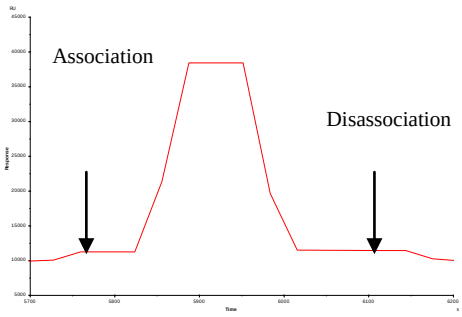

Figure 5.4.3.3: Individual Biacore association/dissociation curves for Fraction 13. Individual fractions obtained by using the HPLC in a preparative mode with the protein A HPLC programme. Samples used include CCS (containing both PA binding and non PA binding IgG), 6 minute sample (PA binding IgG), 0.1 minute sample (PA non binding IgG) and a mixed sample CCS (containing both PA binding and non PA binding IgG). The resulting resonance units (R) were obtained by subtracting the respective dissociation resonance value from that of the initial association curve baseline.

Fraction 14, 6.0 minute, 1758R

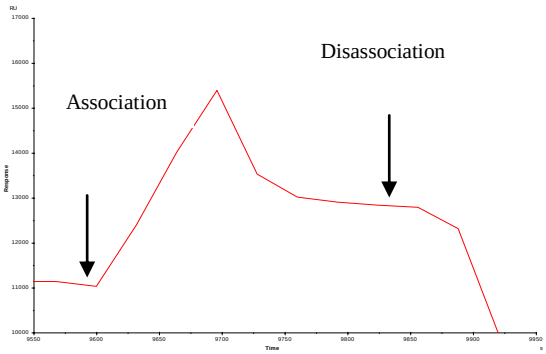

Fraction 14, 0.5 minute, 0R

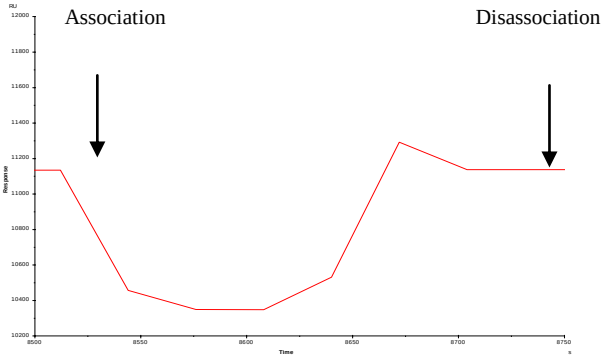

Fraction 14, mixed, 192R

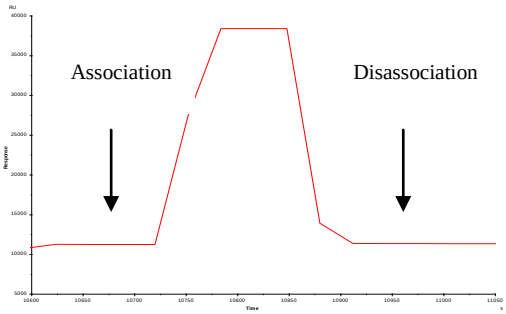

Figure 5.4.3.4: Individual Biacore association/dissociation curves for Fraction 14. Individual fractions obtained by using the HPLC in a preparative mode with the protein A HPLC programme. Samples used include CCS (containing both PA binding and non-binding IgG), 6 minute sample (PA binding IgG), 0.1 minute sample (PA non-binding IgG) and a mixed sample CCS (containing both PA binding and non-binding IgG. The resulting resonance units (R) were obtained by subtracting the respective dissociation resonance value from that of the initial association curve baseline.

The interpretation of the results in Figure 5.4.3.3 and 5.4.3.4 can be seen in Figure 5.4.3.5. Results from the tested fractions are tabulated in terms of degree of binding (R) and respective interpretation about the binding association that exists between the IgG and the PA ligand. It was seen that in both fractions the association between the PA and IgG in the 6 minute (PA binding IgG) peak was high. This degree of binding was > 10 fold that of the CCS control, the sample containing just the 0.1 minute peak (PA non-binding IgG) and the CCC 'mixed' sample (with both the 0.1 and 6 minute peak).

Sample	Description	Degree of binding (R)	Observations
Control: CCS diluted in water	CCS mixed sample containing both PA binding and non-binding peak	180	Weak Association
Fraction 13: 0.1 minute	Fraction 13 PA non-binding peak	0	No association
Fraction 13: 6.0 minute	Fraction 13 PA binding peak	2266	Association
Fraction 13: Mixed	Fraction 13 containing both PA binding and non-binding peak	269	Weak association
Fraction 14: 0.1 minute	Fraction 14 PA non-binding peak	0	No association.
Fraction 14: 6.0 minute	Fraction 14 PA binding peak	1758	Association.
Fraction 14: Mixed	Fraction 14 containing both PA binding and non-binding peak	192	Weak association.

Figure 5.4.3.5: Results following Biacore analysis. Fraction 13 and 14 used from TC CCC run 4-1 as they had the highest concentration of purified IgG. Samples were prepared by using the HPLC in a preparative mode and collecting the 0.1 minute peak and the 6 minute peak of TC CCC fractions separately. The initial TC CCC fraction was also included and contained both the 0.1 minute and the 6 minute peak, termed 'mixed'. Samples were subject to Biacore analysis and compared to that of the CCS control.

The Biacore results confirmed the previous hypothesis: after CCC processing in the phase system, there was an increase in the proportion of the IgG that did not bind to PA. These samples had no resonance units (0.1 min samples), indicative of no binding. When the 6 minutes HPLC peak for both Fractions 13 and 14 were subject to Biacore analysis, there was significant binding of >1758R. This was as expected as the 6 minute peak from the TC CCC run 4-1 fractions was previously shown to be the purified binding form. When the 0.1 minute (non-binding) and 6 minute (binding) forms were tested combined the resonance units decreased to around 200, similar to the CCS starting control. This highlighted the binding capacity of the IgG had been altered, and therefore resulting functional IgG yield was greatly affected. A species change was thus evident due to the CCC processing.

5.4.4 Investigation of shaking vigour using a bench top centrifuge.

The implication of g force damage on IgG alone was investigated. Samples (PA purified IgG) were spun in a bench top centrifuge in varying solutions (upper, lower, mixed phase and water) for 200 minutes.

Four tubes were prepared (tubes from Eppendorf, Cambridge, UK) and PA purified IgG added to each. Samples were taken in triplicate pre and post centrifugation. The results can be seen in Figure 5.4.7.1 where percent change in IgG HPLC peak area is listed in varying medium. It was seen in the medium tested that following shaking at 200rpm for 200 minutes HPLC peak area of the PA binding IgG peak was unaffected (< 10% change in HPLC area). The constant 'g force' alone created by samples spun using a bench top centrifuge was not responsible for the degradation. It was concluded that degradation was due to the mechanism of mixing of the two phases within the CCC machines.

2000 rpm/200 minutes	HPLC peak area			
	Upper	**Lower**	**Mixed**	**Water**
	3113873	3053085	3106122	3083437
	3226236	3027522	2969299	2904844
Pre centrifuge	3252350	3167076	2974464	3062486
STD error	42481	42897	44772	56365
	3208517	3005143	2956845	3073054
	3267784	2704655	3152545	3199816
Post centrifuge	3211865	2986457	3142173	2872096
STD error	19222	97198	63575	95409
Change in HPLC peak area (%)	**1.00**	**6.00**	**2.20**	**1.00**

Figure 5.4.4.1: Effect of g force in a bench top centrifuge on IgG stability. IgG incubated in varying buffers and spun in a bench top centrifuge at 2000rpm for 200 minutes (typical CCC run time). Samples then analysed by protein A HPLC. The change in HPLC area pre and post centrifugation was calculated.

5.4.5 Investigation of shaking vigour at one 'g' using a custom built shaker

To further emulate the forces occurring within the CCC machines in terms of mechanism of mixing, shearing and interfacial tension, a shaker was built. The shaker allowed experiments to be conducted without the impact of additional parameters such as flow rate and stationary phase retention.

Mr Tony Bunce, an engineer at Brunel University, designed the shaker based on the design specification of a two sample clamp position that would allow extremely vigorous shaking. Complete phase system mixing (resulting in one phase) was seen during run times. A photo of the shaker can be seen in Figure 5.4.5.1. The shaker itself was connected to a laboratory regulated power supply, which allowed the mixing vigour of samples in the clamp to be controlled.

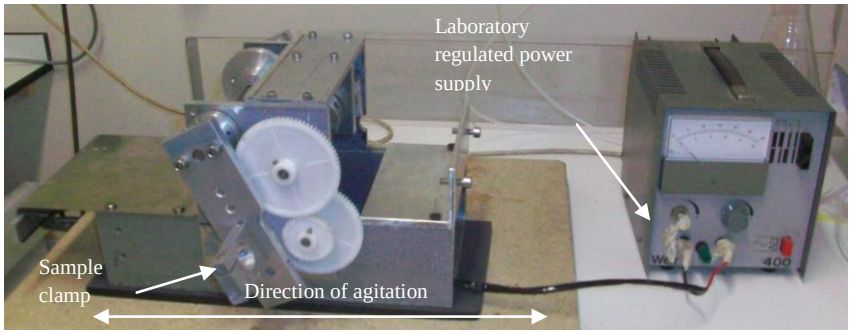

Figure 5.4.5.1: Photo of custom built shaker. The two clamp positions allowed the sample of interest to be tested alongside that of a control. Mixing vigour could also be controlled separately by the use of a laboratory regulated power supply.

The direct effect of mixing vigour on IgG degradation in the phase system was investigated. A control sample of water was used. Samples were prepared as shown in Figure 5.4.4.2 and no air gap was left at the top of the vials. Samples were taken at 30 minutes then 1, 2 and 3 hours. 50µl samples were taken to minimise any air bubble production in the shaker vials. These were then broken with 950µl of water and analysed by protein A HPLC. Experiments were carried put only once but repeated at a shaking vigour of 5, 7.5 and 10 Volts (V) with corresponding vibrations per minute listed in Figure 5.4.4.3.

	Sample	
	PA purified IgG in phase system (ml)	**PA purified IgG in water (ml)**
Upper phase	11	
Lower phase	11	
Water		22
PA purified IgG	1	1

Figure 5.4.5.2: Sample preparation for shaker investigation. Samples were always prepared in parallel; one in the PEG 17.5%/17.5% sodium citrate system and the other in water as a control.

Shaking vigour (V)	**Vibrations per minute**
5	175
7.5	245
10	315

Figure 5.4.5.3: Vibrations per minute for the individual shaker vigour, measured in volts (V).

The results are tabulated in Figure 5.4.5.4 and show the effect of increasing shaker speed over time on PA purified IgG (HPLC peak area) in both water and the phase system. With the PA purified IgG in the phase system, as shaking speed increased the

percentage change in HPLC peak area decreased. The percentage retention of bioactivity went from 94.1% at 5V to 78.4% at 10V. However with the PA purified IgG in water, bioactivity remained relatively unchanged at > 98%. Figure 5.4.5.5 is a diagrammatic representation of the results in Figure 5.4.5.4. PA binding IgG HPLC area is plotted against time at various shaker speeds. With the IgG in the phase system a clear decrease in HPLC peak can be seen at all vigours tested, which consequently further increased with vigour. This was as opposed to the PA purified IgG incubated in water, the graph remained stable over the incubation time and various shaker speeds. Furthermore in Figure 5.4.4.6 (data obtained from Figure 5.4.5.4) percent recovery of PA binding IgG following shaking at various vigour in water and phase system is plotted. IgG in water was stable over increasing shaker speed. However in the phase system a decrease in functional IgG recovery was again evident, with increased degradation as shaker speed was increased.

PA purified IgG in phase system (HPLC peak area)				**Control: PA purified IgG in water (HPLC peak area)**			
	Shaker speed				**Shaker speed**		
Time (hr)	**5**	**7.5**	**10**	**Time (hr)**	**5**	**7.5**	**10**
0	85302	84350	85888	0	86266	84221	84569
0.50	83599	82331	78310	0.5	89050	82240	82352
1	83381	80021	68969	1	88567	81285	86723
2	82331	75263	70997	2	88789	81004	84407
3	80304	71420	67348	3	86528	82687	86082
% retention of bioactivity	**94.1**	**84.7**	**78.4**	**% retention of bioactivity**	**100.3**	**98.2**	**101.8**

Figure 5.4.5.4: IgG shaker results in both water and PEG 1000 17.5%/17.5% sodium citrate phase. Samples shaken at differing mixing vigour over three hours. Samples were taken following shaking and subject to PA HPLC analysis. % change in HPLC peak area as a percentage of initial starting IgG peak area was calculated, following three hours.

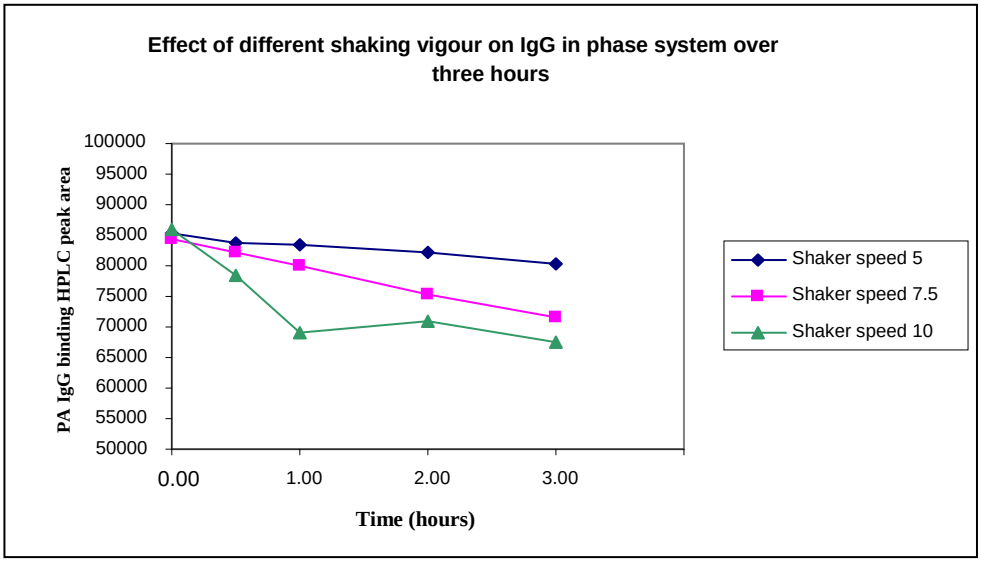

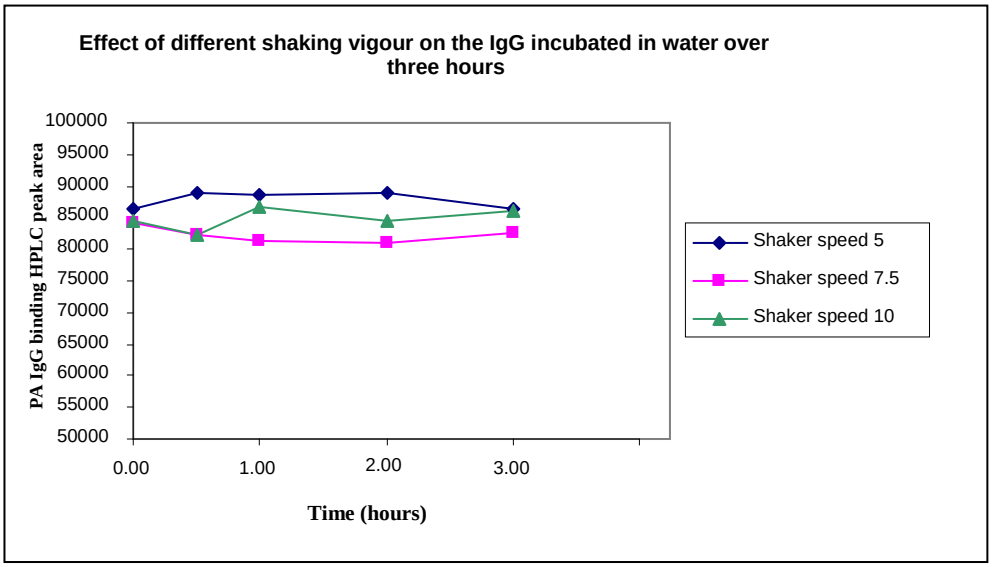

Figure 5.4.5.5: Diagrammatic representation of Figure 5.4.5.4. Graphs comparing IgG stability in phase system and water over three hours. Following respective shaking runs, samples were subject to protein A HPLC analysis.

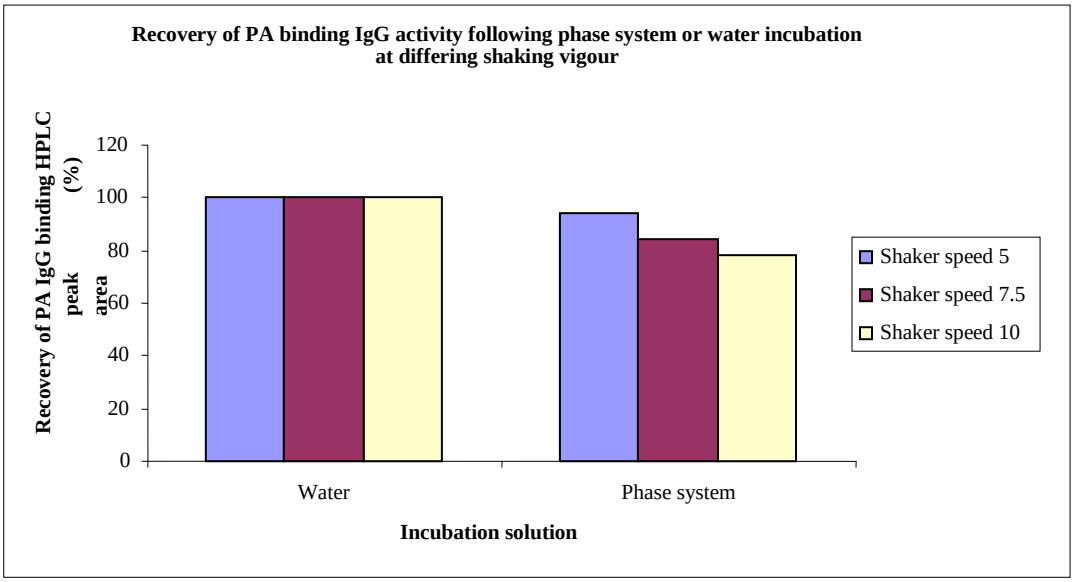

Figure 5.4.5.6: Diagrammatic representation of Figure 5.4.5.4. IgG expressed in terms of biological recovery at different shaking vigour in water and the phase system. 8 minute protein A HPLC analysis program used. PA IgG binding peak following three hour incubation shown.

The IgG within the water control system remained constant and unaffected by both shaking vigour and respective time. A loss in PA IgG binding peak area however in the phase system was seen at all the shaking vigour tested (5, 7.5 and 10V). Loss in activity was further dependent on increased incubation time and resulting shaker speed. The longer the run time, the greater the damage seen. Previously this had been highlighted with the CCC runs, resulting in higher flow rates being used in CCC runs to reduce IgG transit time in the machines (Section 4.4.4). The interface of the phase system or mechanical effects of shearing of the two phases on the IgG were clearly thought to accelerate degradation.

CCS, when run on a CCC machine, had lower IgG recovery when compared to the PA purified IgG. It was hypothesised that additional components within the CCS e.g. anti-foaming agents or surfactants were exacerbating the detrimental effect of CCC. This was investigated using both IgG samples (CCS and PA purified IgG) and various solutions of the PEG 1000 17.5%/17.5% sodium citrate system (upper, lower, mixed phase and water). Firstly the two different IgG samples were made up in the phase system (PEG 1000 17.5%/17.5% sodium citrate) and incorporated at a 1ml volume, hence had different IgG and total protein concentrations. Then also at a 2mg/ml IgG concentration in the CCS and PA material. These samples therefore had

the same IgG concentration but differing total protein concentration. Secondly the CCS and PA purified IgG was made up in just lower phase, then just upper phase (of the PEG 1000 17.5%/17.5% sodium citrate system) and water. All the prepared samples were placed on the shaker for 3 hours at a shaking vigour of 7.5V.

The results are shown in Figure 5.4.5.7, CCS and PA purified IgG results are listed in varying volume, concentration and medium in respect to their effect on IgG recovery. For all the conditions tested stability with the PA purified IgG was always higher to that of the CCS. Figure 5.4.5.8 is a diagrammatic representation of Figure 5.4.5.7 where IgG recovery of bioactivity was plotted against incubation in various solutions. It showed that incubation in all buffers even in a single phase (upper or lower) or water also had a negative effect on recovery. This was seen in both samples but degradation was to a greater degree with the CCS. However when both samples (CCS and PA purified IgG) were at a similar concentration (2mg/ml), the IgG recovery was higher for the PA material, but not considerably.

	1 ml volume		**2mg/ml**		**Lower phase**		**Upper phase**		**Water**	
HPLC peak area	**CCS**	**PA purified IgG**	**CCS**	**PA purified IgG**	**CCS**	**PA purified IgG**	**CCS**	**PA purified IgG**	**CCS**	**PA purified IgG**
	40087	86997	26797	26631	16109	16494	17148	18315	17583	16552
	49958	83126	28586	29675	18748	17197	16897	18175	16544	15869
Pre	46047	90461	27260	20912	20151	15977	15496	17212	16756	17251
Average	45364	86861	27548	25739	18336	16556	16514	17901	16961	16557
Standard error	2870	2119	536	2569	1185	354	514	347	317	399
	33014	79237	22741	23075	13019	12691	13622	15008	14245	15231
	32287	83335	19587	20095	14411	16172	10507	15033	14736	14995
Post	34997	78388	26583	24448	13688	12093	12758	15630	14323	15213
Average	33433	80320	22970	22539	13706	13652	12296	15224	14435	15146
Standard error	810	1527	2023	1285	402	1272	928	203	152	76
% change in recovery	**73.7**	**92.47**	**83.38**	**87.57**	**74.75**	**82.46**	**74.46**	**85.05**	**85.11**	**91.48**
% Standard error	2.71	0.49	5.61	3.41	2.48	5.80	3.20	0.51	0.68	1.71

Figure 5.4.5.7: Stability of IgG in various buffer mediums and phase system pre and post shaking at 7.5V. CCS and protein A purified IgG used. Each sample was taken in triplicate. Following shaking experiments samples were subject to Protein A HPLC analysis. The 6 minute IgG peak was used; change in recovery was calculated by change in peak area following shaking at 7.5V for three hours.

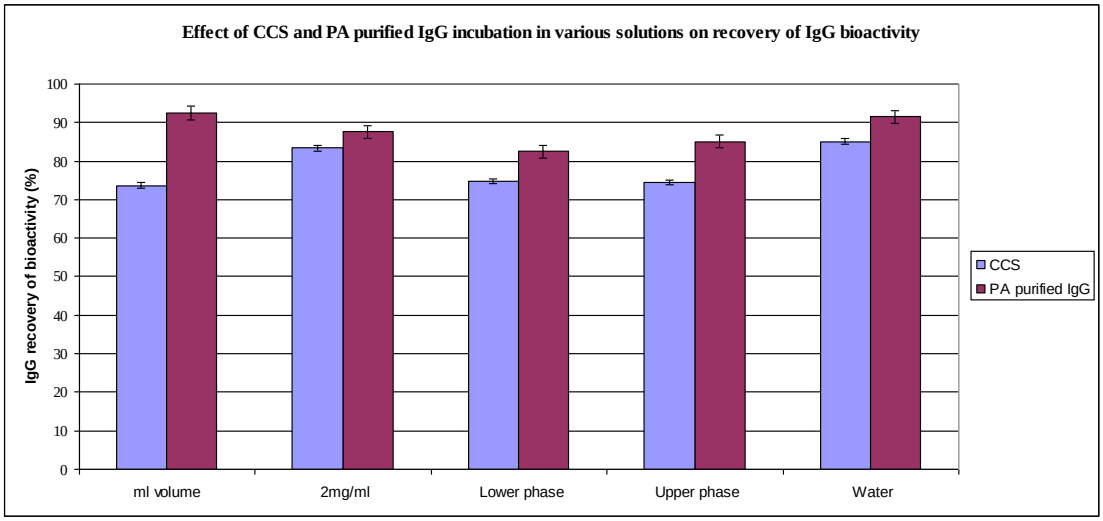

Figure 5.4.5.8: Diagrammatic representation of Figure 5.4.5.7. Expression in terms of different IgG recovery in various buffering medium and phase system. Samples were subject to protein A HPLC analysis. The 6 minute IgG peak was used; change in recovery was determined by calculating change in HPLC peak area following shaking at 7.5V for three hours.

The hypothesis of total protein concentration further exacerbating degradation was supported. This as additional components would add to shearing and possibly aggregation when shaken at such vigours. When the 1ml sample volumes were used, CCS recovery was 73.70% as compared to 92.47% when PA purified IgG was used. When CCS was diluted to a specific IgG concentration that didn't account for total protein concentration, a very considerable effect on acceleration of degradation was seen. This was due to the presence of additional proteins and components within the CCS. Degradation was not due to the interface alone. It appeared a single phase and water were also having a contributory negative effect when shaken at such vigour. The possibility of IgG degradation in the single phases and water was thought to be due to the amplitude and frequency of the mixing occurring. IgG shearing at the interface of the two phase systems was also suggested.

5.5 Conclusions

A critical investigation of IgG functionality was conducted. Previously it was observed that hydrostatic CCC (CPC and TC CCC) was responsible for the degradation of Protein A binding capacity of the IgG. It was hypothesised and experimentally supported in this chapter that this degradation was not due to incubation in the phase system, despite the previous concerns about high salt and polymer concentrations in phase systems. The only phase system exceptions were the PEG 3350 11.1%/11.1% ammonium sulphate, seen to cause a precipitation effect to the IgG, and a PEG dextran system which affected the HPLC analysis.

Degradation was also quantitatively confirmed by Biacore affinity technology. IgG post CCC was shown to have an extremely poor affinity to the PA. Purification was demonstrated, but the IgG left was rendered unfunctional.

The loss in IgG functionality was shown to be caused by some mechanism of mixing within the CCC machine. The effect however was that of a complex one dependent on a number of inter-connected factors. Shearing of the two phases, interfacial tension and the CCS sample content itself with a number of other components e.g. anti-foaming agents and surfactants, have all been implicated. A reduction in these combined effects was required to retain IgG functionality during CCC processing. It was thought by gentler wave like mixing, as offered by that of the hydrodynamic Mini CCC, a separation would be possible without the loss in IgG functionality.

CHAPTER 6: Separation of monoclonal antibodies using J-type CCC centrifuges: the need for gentler mixing

6) Separation of monoclonal antibodies using J-type CCC centrifuges: the need for gentler mixing

6.1 Summary

In the previous chapters, the need for gentle mixing was highlighted due to the detrimental effect mixing vigour had on IgG functionality. The studies within this chapter explore the use of the Mini CCC centrifuge, with its milder, wave like mixing. Flow rate was seen to be critical to the retention of IgG activity. A faster flow rate, hence shorter CCC run time, was needed to reduce the corresponding number of mixing and settling steps the IgG was exposed to. The resulting damage to the IgG was consequently reduced. Rotational speed was also seen to be key. At an increased flow rate of 1ml/min and a rotational speed of 1200rpm, a recovery of 81.97% viable IgG, was achieved when using PA purified IgG. This was the first time such high recovery of the functional IgG (>80%) had been seen using any CCC instrument. When this run was repeated with CCS however, the resolution of the IgG from the impurities was poor. The IgG was seen to elute over 60 minutes, which inevitably meant it co-eluted with the impurities. Resolution of the IgG was improved by increasing rotational speed; this conversely negatively affected viable IgG recovery.

IgG degradation within the CCC machine was seen even when processed in a single phase. Greater detriment to recovery was seen with the salt phase as opposed to that of the PEG phase. This IgG degradation effect, even in single phase, was observed to be exacerbated when both phases were together.

The chapter finally looks at degradation with model proteins, also confirming the damage to more robust, smaller molecules. An in-depth look at the literature also suggested biological recovery post CCC was frequently just assumed, and even those that did investigate it suffered losses.

6.2 Introduction

The harsh mechanical effect seen with cascade mixing using both the CPC and TC-CCC caused an irreversible loss in the Protein A binding capacity of the antibody. An alternative milder form of mixing was sought.

The Mini CCC utilises hydrodynamic, wave like mixing, which is less vigorous when compared to the hydrostatic instrument, used in the CPC and TC CCC. Hydrodynamic CCC occurs along a continuous length of tubing which is wound around a drum. The coil planet centrifuge has two axis of rotation (planetary and solar) allowing the creation of mixing and settling zones. Where mixing occurs closest to the centre of the planetary coil, g force is lowest. At the farthest side of the planetary coil the force field is highest and settling occurs (Sutherland, 2007).

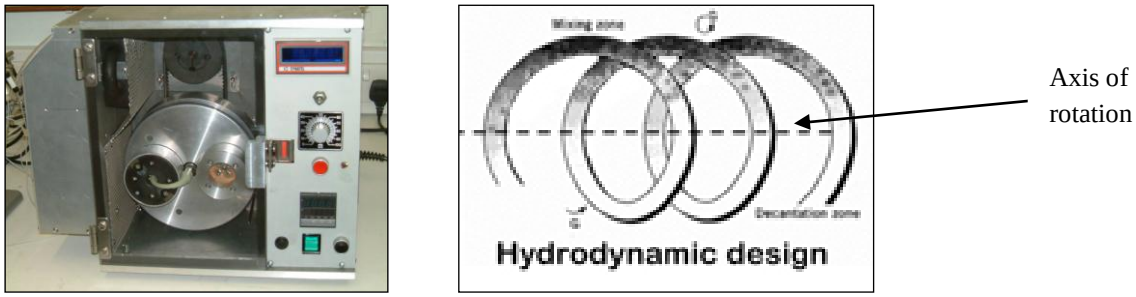

Figure 6.2.1: On the left is a photo of the prototype Mini CCC used for all experiments in this chapter. It had a 45.1ml column volume and 2.7mm bore size. On the right-hand side is a diagram showing functioning in the hydrodynamic mode CCC. Mixing and settling occurs along the continuous length of tubing.

It was postulated that by using this different mechanism of mixing as opposed to the previously used cascade mixing, the retention of biological activity would be possible. The mechanism of mixing was thought to be gentler on solutes, presumably due to the lower shear forces being present. It was hoped that IgG damage could therefore be reduced with sufficient separation of IgG from impurities, without resolution being compromised.

6.3 Method and materials

6.3.1 Sample preparation

Initially to investigate degradation, PA purified IgG was used. Latter runs were conducted with CCS as the loading sample, allowing investigation of the separation of the IgG from the impurities.

6.3.2 CCC processing

The Mini prototype (Brunel Mini CCC) was used. The tubing was composed of wide bore polytetrafluoroethylene (PTFE) and the specification is detailed in Figure 6.3.2.1. The typical Mini CCC run conditions are listed in Figure 6.3.2.2.

Bore size (mm)	2.7
Column volume (ml)	45.1
Column length (m)	7.9
Rotor radius (mm)	5
β value	0.53-0.73

Figure 6.3.2.1: Overview of Mini CCC machine parameters including beta (β) value; the ratio of the tube coil radius over the rotor radius.

Mini CCC separation
ATPS…17.5/17.5% w/w..…PEG/Salt, pH…7.41
PEG……1000…Salt …Sodium citrate
Coil volume……45.1ml
Sample loop……1.72ml
Operating mode…Run flowed from head to tail
Stationary phase…..Lower phase
Column filled at ……5ml/min
Injected mAb:
1) CCS…… (Batch number …L156568/47)
Amount…….....6.4 mls diluted with:
…..0.44g sodium citrate
…..0.44g PEG
Spin speed…1200 rpm, temperature….20°C, flow rate…..…0.5ml/min
Equilibrated at……0.5ml/min,
Stationary phase displaced….22ml % stationary phase retained……..51.2%

Figure 6.3.2.2: The typically used Mini CCC operating parameters.

6.4 Results and discussion

6.4.1 Effect of rotational speed on IgG functionality

Rotational speed was investigated with the hypothesis that reduction of g-force by lowering rotational speed would allow increased IgG recovery. A Mini CCC run was carried out with Protein A purified IgG and a PEG 1000 17.5%/17.5% sodium citrate system. A 1.72ml injection volume was used with a flow rate of 0.5ml/min (flowing from head to tail). Repeat runs were carried out at a rotational speed of 800, 1000 and 1200 rpm. Samples were subsequently analysed by Protein A HPLC and recovery of functional IgG was obtained by totalling functional IgG in fractions as a percentage of the amount in the starting injection. Experiments were carried out only once.

The results are shown in Figure 6.4.1.1, increasing rotational speed is listed against resulting recovery of functional IgG. It can be seen as rotational speed increases the recovery of functional IgG decrease. Furthermore the graph in Figure 6.4.1.2 shows the relationship between recovery of viable IgG, stationary phase retention and IgG total elution time at various rotational speeds. It can be seen as rotational speed is increased, stationary phase retention is also increased however viable IgG recovery decreases. However the time taken for the IgG to elute from the column is extended as rotational speed increases.

Rotational speed (rpm)	**800**	**1000**	**1200**
Recovery of functional IgG (%)	60.77	46.35	41.05

Figure 6.4.1.1: Effect of rotational speed on recovery of viable IgG (PA binding IgG). All experiments carried out with protein A purified IgG, flow rate of 0.5ml/min. Samples analysed by protein A HPLC, 8 minute injection time and 80µl injection volume.

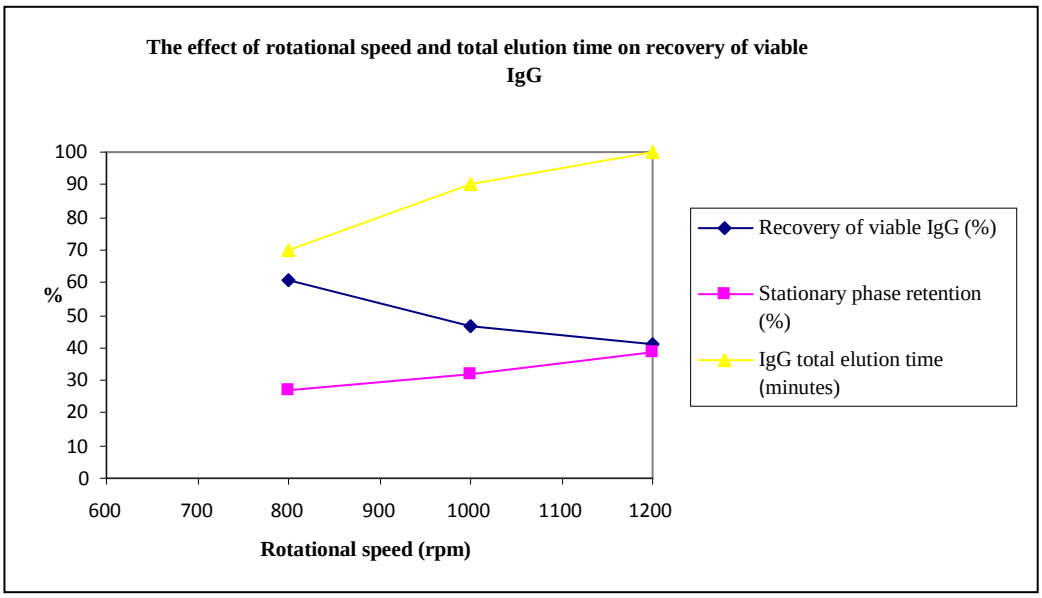

Figure 6.4.1.2: Effect of rotational speed on recovery of viable IgG. All experiments carried out with protein A purified IgG, flow rate of 0.5ml/min.

The observations were as predicted. As rotational speed increased, IgG recovery decreased (Figure 6.4.1.2). A higher rotational speed however allowed greater mixing, which achieved the peak sharpness needed for a successful separation. The detrimental effect of increased rotational speed on resulting IgG recovery was seen. As rotational speed increased, higher stationary phase retention was attained, thus increasing the total time taken for IgG to elute from the coil. Consequently, the IgG was retained in the coil for longer at a high rpm, resulting in the corresponding loss in recovery of viable IgG.

6.4.2 Investigation of CCC transit time on IgG functionality

As seen in Chapter 4 (Section 4.4.6), an increased flow rate resulted in shorter run times and allowed a significant improvement in retention of IgG activity. A higher flow rate was investigated on the Mini CCC. A typical run at 0.5ml/min was 200 minutes long; the flow rate was doubled to 1ml/min. The same run condition as detailed in Section 6.4.1 were used with an increased flow rate (1ml/min) and a rotational speed of 1200rpm. Retention of viable IgG was again calculated following Protein A HPLC analysis. An IgG recovery of 81.97% was seen at 1ml/min as opposed to the previously demonstrated 41.05% at 0.5ml/min. A substantial improvement was made and no previous results with this level of IgG recovery had been achieved on any other CCC machine.

6.4.3 Investigation into sample loading capacity

The sample loading capacity was investigated; previously a 1.72ml (3.82% coil volume) sample loop was used on a 45.1ml column. Sample load was increased to a 4.95ml sample loop (10.98% coil volume).

Operating conditions as detailed in Figure 6.3.2.2 were used for both runs at different sample sizes. The results are shown in Figure 6.4.3.1 where as sample size is increased from 1.72ml to 4.95ml recovery of functional IgG remains very similar at > 80%. The higher recovery of 84.37% functional IgG showed great promise for throughput as column saturation had not been reached at 10.98% of the coil volume (Figure 6.4.3.1). This as the recovery of functional IgG appeared to be unaffected by the increased load, as opposed to resulting in further IgG degradation.

Sample size (ml)	**Recovery of functional IgG (%)**
1.72	81.97
4.95	84.37

Figure 6.4.3.1: Effect of sample size on the recovery of viable IgG (PA purified IgG). Experiments carried out with protein A purified IgG and an increased flow rate of 1ml/min. Samples analysed by protein A HPLC, 8 minute injection time and 80µl injection volume.

The reconstructed elution time profile for both sample volumes followed the same distinct pattern but at different concentrations, showing reproducibility (Figure 6.4.3.2).

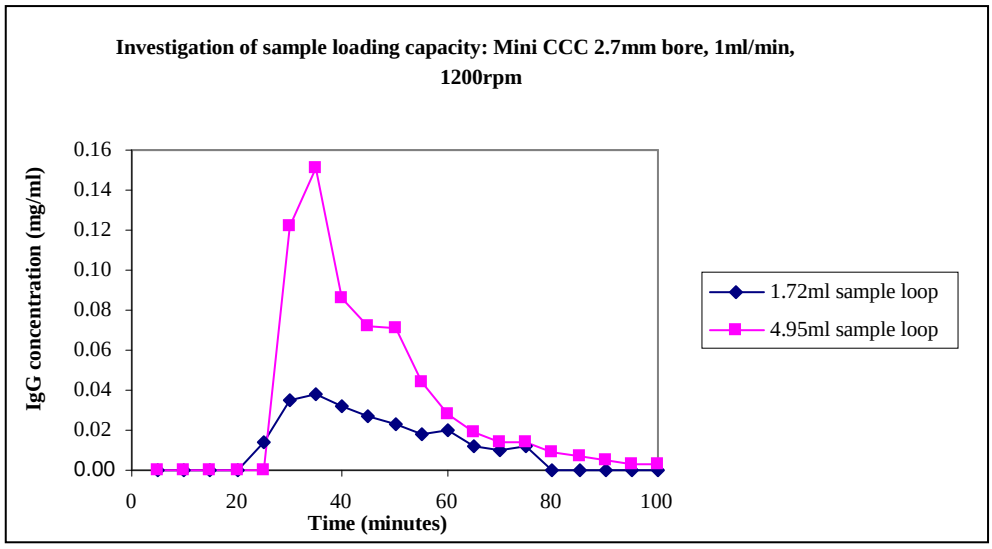

Figure 6.4.3.2: Reconstructed CCC chromatogram. Protein A HPLC used to make reconstructions. IgG concentration calculated using calibration curve and plotted against time of elution. Similar elution patterns are seen at 2 concentrations, showing reproducibility.

6.4.4 Mini CCC separation using CCS

Significantly higher IgG recovery was seen with the Mini CCC in comparison to previously used hydrostatic columns. Results were attained with an increased flow rate of 1ml/min. Previous runs were conducted with the PA purified IgG to look specifically at IgG functionality. Further investigations were with crude CCS, to observe the separation from impurities and any resulting effect on functionality. The results seen in Figure 6.4.4.1 show HPLC peak area plotted against elution time (minutes). The IgG can be seen to be eluted over 55 minutes (25-80 minutes). The elution of the IgG is also with that of the impurities, which can be seen to co elute at a higher HPLC peak area. Furthermore the elution profile of the IgG when in the impure CCS (Figure 6.4.4.1) is very similar to that in the pure material (Figure 6.4.3.2), with the elution peak starting and ending at the same times. Although a high recovery of 77.12% IgG functionality (calculated following protein A HPLC analysis) was demonstrated, resolution and final purification were completely compromised. The IgG eluted over a very large/wide peak (around 60 minutes) which would inevitably include the impurities.

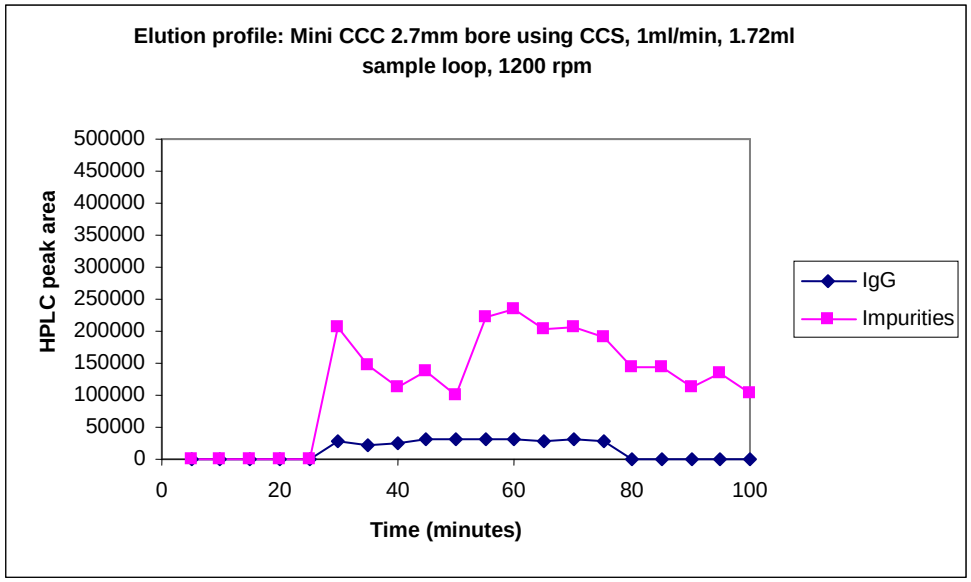

Figure 6.4.4.1: Reconstructed CCC chromatogram. Protein A HPLC used to make reconstructions. Carried out with CCS (crude sample), CCC run at a flow rate of 1ml/min. Samples analysed by protein A HPLC, 8 minute injection time and 80µl injection volume. IgG HPLC peak area (6 minute peak) and impurities (0.1 minute peak) plotted against time of elution from the CCC coil.

When the separation shown in Figure 6.4.1.1 was compared with the TC CCC results in Figure 4.4.5.3, it could be seen that resolution had been completely lost. The sharp peak elution of the IgG by the TC CCC is not seen, with the impurities also eluting over an extended period. When the separation in Figure 6.4.4.1 is compared with other Mini CCC results however, similar IgG elution within the same time scale is seen (Figure 6.4.3.2). Again, as detailed in Chapter 5 (section 5.4.4.7) IgG recoveries from CCC processing using PA purified IgG had higher recoveries than CCS, despite the same experimental conditions being used.

IgG recovery at the expense of purification was seen as shown in Figure 6.4.4.1. It was predicted that higher resolution could be attained by an increased rotational speed (1200rpm was previously used). An increased rotational speed was needed that would allow adequate mixing but be gentle enough to minimise any damage to the IgG. Mini CCC runs were carried out with crude CCS and a PEG 1000 17.5%/17.5% sodium citrate system. A 1.72ml injection volume was used with a flow rate of 1ml/min (flowing from head to tail). Runs were carried out at a rotational speed of 1500 and 1800 rpm and samples analysed by protein A HPLC. A very similar stationary phase retention of around 30% was seen with both runs.

Results are tabulated in Figure 6.4.4.2 and show the relationship between rotational speed, stationary phase retention, IgG elution peak time and viable IgG recovery. When CCS was loaded in similar concentration (around 0.80 mg of IgG) as rotational speed increased so did corresponding stationary phase retention and IgG elution time. Viable IgG recovery however decreased as rotational speed increased over the speeds tested. Moreover as shown in Figure 6.4.4.3 (a diagrammatic representation of Figure 6.4.4.2), recovery of functional IgG is plotted against increasing rotational speed. The very clear trend of loss in functional IgG can be seen as rotational speed is increased. The CCC chromatograms reconstructed from protein A HPLC analysis at 1500 and 1800rpm are shown in Figure 6.4.4.4. The results showed HPLC peak area plotted against time in minutes. The IgG at both speeds (1500 and 1800rpm) eluted from 30 to 65 minutes. Also co elution with impurities was seen. At a rotational speed of 1500rpm a higher HPLC peak area was seen for the impurities as compared to a rotational speed of 1800rpm.

Rotational speed (rpm)	Amount of IgG loaded (mg)	Stationary phase retention (%)	Elution time of IgG peak (minute)	Viable IgG Recovery (%)
1200	0.84	29.5	35	77.12
1500	0.79	31.8	40	56.88
1800	0.79	36.4	45	44.24

Figure 6.4.4.2: Effect of rotational speed on recovery of viable IgG on the Mini CCC, at an increased flow rate of 1m/min using CCS (crude.) PEG 1000 17.5%/17.5% sodium citrate system used and 4.95ml sample load. Samples analysed by protein A HPLC, 8 minute injection time and 80µl injection volume.

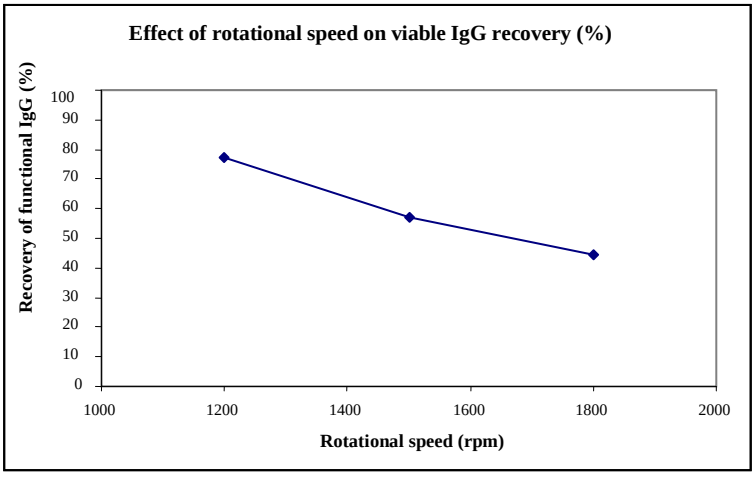

Figure 6.4.4.3: Diagrammatic representation of Figure 6.4.4.2. Effect of rotational speed on recovery of viable IgG on the Mini CCC, at an increased flow rate of 1ml/min using CCS (crude). The detrimental effect of increased rotational speed on the resulting IgG recovery can be seen. The PEG 1000 17.5%/17.5% sodium citrate system used and 4.95ml sample load

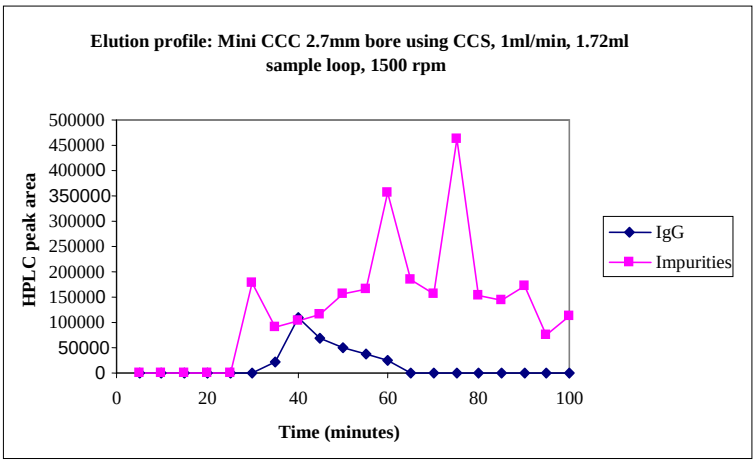

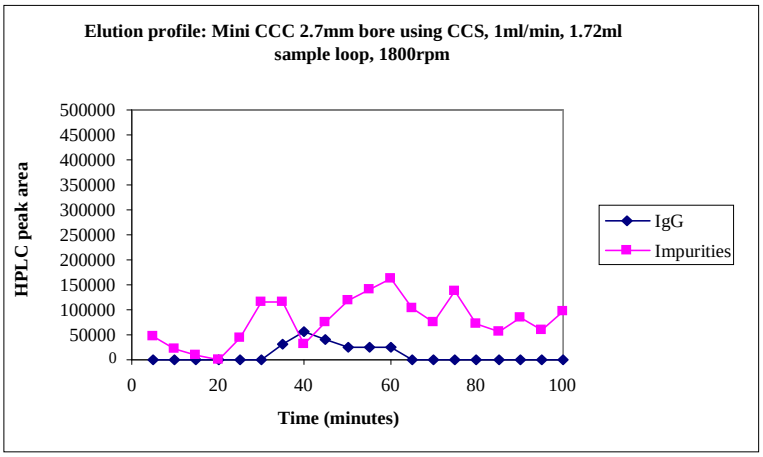

Figure 6.4.4.4: Reconstructed CCC chromatogram. Protein A HPLC used to make reconstructions. Carried out on the Mini CCC, at varying rotational speed, with CCS (crude sample), flow rate of 1ml/min. Samples analysed by protein A HPLC, 8 minute injection time and 80µl injection volume. IgG HPLC peak area (6 minute peak) and impurities (0.1 minute peak) plotted against time of elution.

Figure 6.4.4.2 and 6.4.4.3 confirmed that, as rotational speed increased even at a higher flow rate, a decrease in functional IgG recovery was seen. Surprisingly, even at higher rotational speeds (1500 and 1800pm) IgG peak sharpness was still lost (Figure 6.4.4.4). It was thought at such an extreme spin speed, emulsification could possibly be occurring inside the machine. Emulsification would result in the broadening of the IgG peak, such that the distinction between the stationary phase and mobile phase was lost. The transition therefore between the two would be blurred and peak broadening would mean that the separation from impurities was not achieved (Figure 6.4.4.4).

The results showed, even with the Mini CCC at a higher rotational speeds, which typically results in higher stationary phase retention hence improves resolution, a high resolution separation could not be demonstrated. Rotational speed

was detrimental to the IgG functionality even at a higher flow rate. Under the conditions employed, an acceptable balance between recovery of IgG activity and the separation from other contaminants was not achieved.

6.4.5 Investigation of model proteins

Following on from the effect CCC had on the monoclonal antibody functionality, a review was prompted of previous work using model proteins. Dr Emma Bourton has previously investigated the separation of model proteins Lysozyme and Myoglobin with CCC using a PEG 1000 12.5%/12.5% dipottassium phosphate system. (PhD thesis 2008). Altered Myoglobin was seen post CCC known as Apomyoglobin. This was Myoglobin that had lost its haem group. The Myoglobin sample itself initially contained 63.4% of this Apomyoglobin form. It was thought when drawing on conclusions from previous work with the IgG that CCC processing would further accelerate the formation of this non-functional Myoglobin.

To observe the recovery of these model proteins and the effect of CCC processing on the retention of their functionality, a Mini CCC run was conducted. The HPLC analysis program previously designed by Dr Bouton was used for the quantification of Lysozyme, Myoglobin and Apomyoglobin. A C_{18} column with an extra-large pore size (20nm) (Figure 6.4.6.1.) was used and the calibration curve for each respective protein component was created as seen in Figure 6.4.5.2. Following the CCC separation of model proteins, samples were subject to HPLC analysis, the HPLC method is described in Figure 6.4.5.1.

Column details	YMC, ODS-AQ, particle size 5µm, pore size 20nm, length 150mm and internal diameter 4.6mm
Injection volume	10µl
Run time	15 minutes
Flow rate	1 ml/min
Column temperature	40ºC ± 5ºC
Gradient	30% Acetonitrile to 55% Acetonitrile over 10 minutes Solvent A: 0.05% TFA + ultrapure water Solvent B: 0.05% TFA + acetonitrile Held at final conditions for 1 minute.
Detector wavelength range	210-600nm.

Figure 6.4.5.1: HPLC analysis method used, as designed by Dr Bourton for the separation of model proteins Lysozyme and Myoglobin.

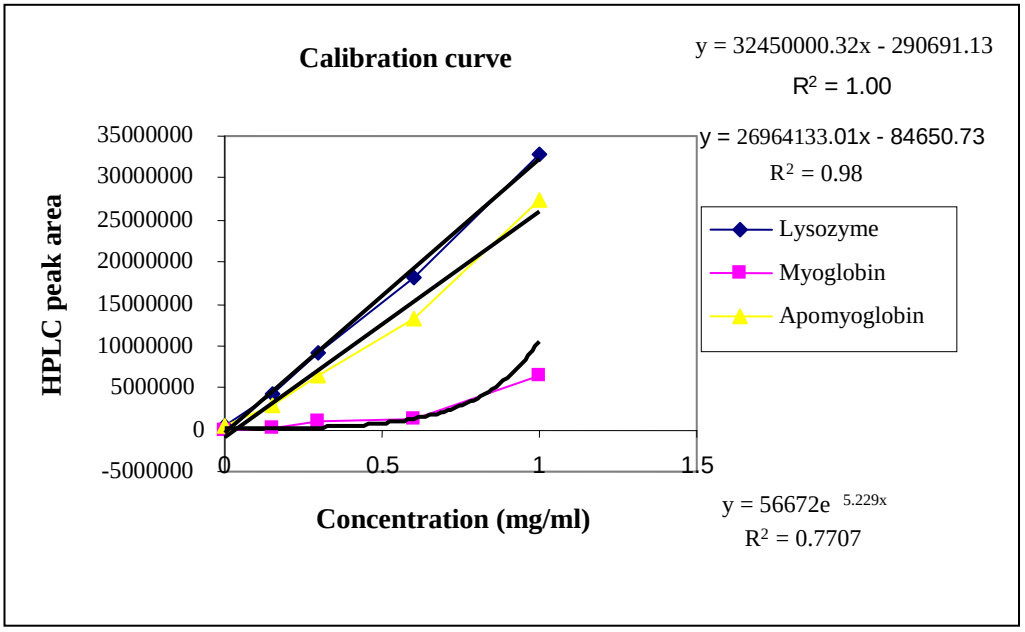

Figure 6.4.5.2: HPLC calibration curve for Lysozyme, Myoglobin and Apomyoglobin. C18 column with extra large pore size used. Respective concentrations of proteins plotted against HPLC peak area.

A Mini CCC run was conducted with the run conditions outlined in Figure 6.4.5.3.

Mini-CCC separation
ATPS…12.5%/12.5% PEG/Salt
PEG……1000 Salt …Dipotassium phosphate
Coil volume……45.1 ml
Sample loop……...1.72ml
Operating mode…run flowing from head to tail
Column filled at …5ml/min
Stationary phase…..Lower phase
Injected sample:
1) Lysozyme and Myoglobin
Amount…..0.03mg of both mixed with 3ml upper phase + 3ml lower phase:
…..…3g sodium citrate
…..…3g PEG
Spin speed…1800rpm, temperature….20°C, flow rate…..0.5ml/min
Equilibrated at……0.5ml/min,
Stationary phase displaced……28ml

Figure 6.4.5.3: Typical Mini CCC conditions used in previous work by Dr Bourton when preparing the PEG 1000 12.5%/12.5% dipotassium phosphate system for the separation of model proteins Lysozyme and Myoglobin.

Results can be seen in Figure 6.4.5.4 where the amount of protein is plotted against elution time (minutes). The separate elution of Lysozyme and Myoglobin is seen. Furthermore, the co-elution of Myoglobin with the Apomyoglobin is evident. In Figure 6.4.5.5 the amount of Myoglobin and Apomyoglobin is plotted against time in minutes. It shows that following CCC a clear increase in Apomyoglobin can be seen to

a decrease in the Myoglobin. The Apomyoglobin rose from 0.70 to 0.90mg from the start of the CCC run, at the expense of a decrease in functional Myoglobin from 0.42 to 0.12mg.

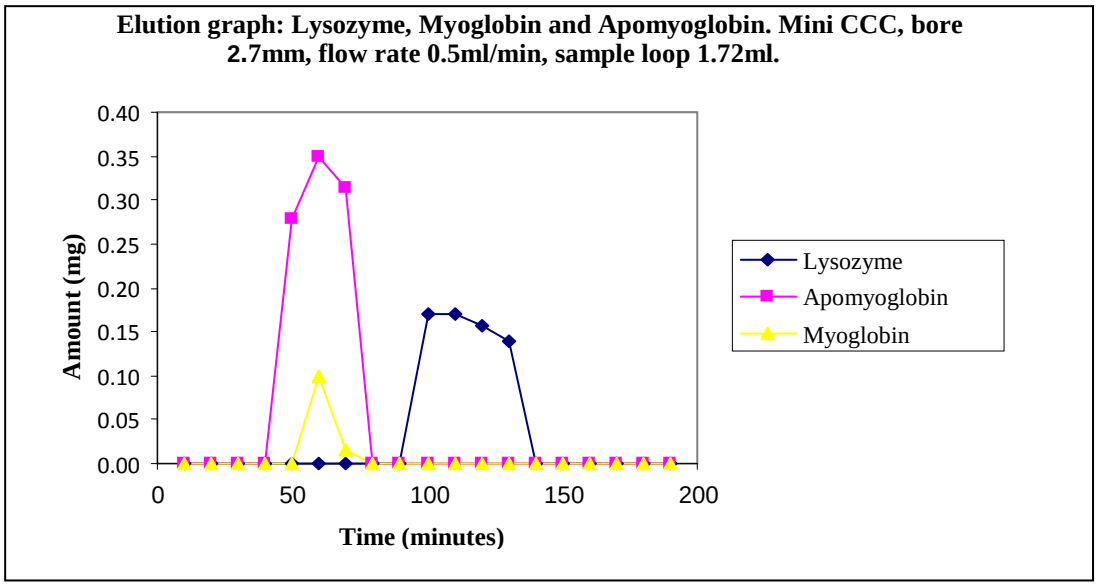

Figure 6.4.5.4: Elution time graph following HPLC analysis (using conditions as described in Figure 6.4.5.1) C18 column with extra large pores used (20nm), model protein mixture of Lysozyme, Myoglobin and non functional Myoglobin named Apomyoglobin prepared and loaded as a single injection. Respective concentrations of proteins plotted against elution times.

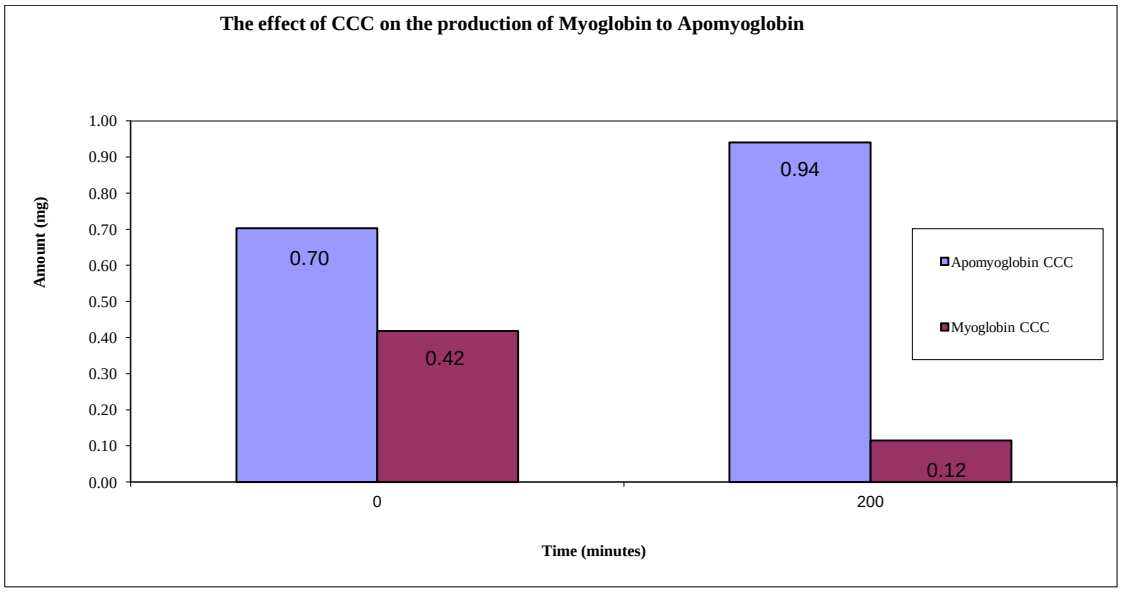

Figure 6.4.5.5: The effect of Mini CCC processing on the production of Apomyoglobin from the decline of functional Myoglobin. Results following a 200 minute Mini CCC separation using a flow rate of 0.5ml/min and a PEG 1000 12.5%/12.5% di potassium phosphate system.

In addition to the Mini CCC run with the model proteins, incubation studies were also performed. The mixture of model proteins was incubated in water and the potassium phosphate phase system for three hours on the bench at 25ºC. The overview results table is shown in Figure 6.4.5.6. It showed that water and the phase systems alone were not detrimental to the Lysozyme, Myoglobin and Apomyoglobin stability, all proteins had a recovery of ≥92%. The total recovery of Apomyoglobin and Myoglobin pre and post CCC were almost identical (94.64%), showing mass balance. After the CCC runs however, the ratio between them changed. Apomyoglobin increased by 133.78% whilst Myoglobin fell to 27.48% of the original starting amount. The damaging effect CCC was having on functionality was highlighted in this study and furthermore in small robust model proteins (Thielges *et al*., 2011; Jory *et al*., 2008). The IgG was a larger, more fragile protein and would therefore be more prone to damage. The measurement of Apomyoglobin production against loss in functional Myoglobin allowed direct comparisons to be made.

Total mg	Apo	Lysozyme	Myoglobin	Recovery of Apomyoglobin and Myoglobin (%)	
Water control start	0.56	0.48	0.27		
Water control end	0.55	0.46	0.27		
Recovery (%)	**99.58**	**95.52**	**101.23**	98.8	Water control
Control phase start	0.41	0.42	0.24		
Control phase end	0.40	0.39	0.24		
Recovery (%)	**97.83**	**92.83**	**97.26**	98.46	Phase system control
CCC Start	0.70	0.73	0.42		
CCC end	0.94	0.64	0.12		
Recovery (%)	**133.78**	**87.18**	**27.48**	94.64	CCC

Figure 6.4.5.6: Overview of production and decline of Apomyoglobin, Lysozyme and Myoglobin following water incubation, phase system incubation and CCC processing. Recovery of Apomyoglobin and Myoglobin calculated by determining any % change in Apomyoglobin and Myoglobin at the start to end of each condition. Recovery of each protein for various conditions was determined by calculation of the amount of individual proteins at the end of incubation in comparison to that at the start. Concentrations of proteins were calculated using individual HPLC calibration curves (Figure 6.4.6.2).

6.4.6 Conclusions drawn from the literature

A critical review of protein separation by CCC was carried out to see if other groups had experienced similar issues with a lack of retention of activity post CCC. As documented in section 4.4 a thorough literature review was conducted from 1960 to present. Papers were collected from Scopus, science direct and pubmed and over 100 papers studies. From the review of papers carried out, there seemed to be a frequent

neglect in the mention of recovery of activity. Purification was reached with no mention of recovery. Most papers used either enzyme assays, 280nm absorbance or protein assays for quantification. Only two papers found within the search mentioned recovery of biological activity using the multi-layer J-type CCC and they too both suffered losses.

Paper 1: Performance of an aqueous two phase based countercurrent chromatographic system for horseradish peroxidase purification. Magri *et al*, 2003, Argentina

This group used a multilayer CCC (1.6mm diameter), at 1000rpm, with a 4 hour run time. A system of 10% w/w PEG 1540 14.8% w/w di-phosphate was used with 2mol/kg of sodium chloride added. A recovery of 45% activity with a purification factor of 6 was noted. Peroxidase activity was measured according to an enzymatic assay were guaiacol was used as the substrate. They attributed the loss of activity to overloaded stationary phase, other species, and thermal inactivation. Previously this group had mentioned recoveries as low as 15%.

Paper 2: Purification of glucosyltransferase from cell-lysate of streptococcus mutants by counter-current chromatography using aqueous polymer two phase system. Journal chromatography B (2004). Ito *et al* .

The researchers used a 4.4% (w/w) PEG 8000, 6% (w/w) dextran T500 pH 9.2 and a flow rate of 1ml/min. The Streptococcus mutant was retained in the dextran rich lower stationery phase. Samples were analysed for enzymatic activity and by SDS PAGE. Purity was seen to have increased 87 times. Recovery of 79% bioactivity was stated as ‘good’ by this research group.

6.4.7 Overview of results

As documented in previous chapters varying results were obtained with the use of the CPC, TC-CCC and multilayer CCC (Mini). Results are presented in Figure 6.4.8.1 in terms of resolution, separation and resulting retention of IgG recovery with differing machines.

Machine	Sample	Rotational speed (rpm)	Flow rate (ml/min)	S*f* Retention (%)	Functional IgG Recovery (%)	Comments	Section of thesis
CPC	CCS	2000	5	20	**44.60**	• When rotational speed was high, recovery was low. • An increased flow rate greatly improved functional IgG recovery.	3.4.10
CPC	CCS	2000	10	14.2	**71.41**		3.4.10
TC-CCC	PA Purified IgG	900	5	26.4	**60.54**	• Resolution highest at a high flow rate. • Best separation results were seen at maximum spin speed and a high flow rate; however functional IgG recovery was adversely affected.	4.4.4.
TC-CCC	PA Purified IgG	1200	10	27.9	**68.35**		4.4.4
TC-CCC	PA Purified IgG	1200	3	39.9	**16.33**		4.4.4
TC-CCC	CCS	1200	5	29.5	**58.21**		4.4.1
Mini CCC	PA Purified IgG	800	0.5	27.4	**60.77**	• With increased rotational speed (800-1200rpm) at a flow rate of 0.5ml/min, IgG recovery decreased.	6.4.1
Mini CCC	PA Purified IgG	1000	0.5	31.8	**46.35**		6.4.1
Mini CCC	PA Purified IgG	1200	0.5	38.6	**41.05**		6.4.1
Mini CCC	PA Purified IgG	1200	1	29.5	**81.97**	• Recovery at 1200rpm is greatly improved by increasing flow rate to 1 ml/min. • As rotational speed increased (1200-1800rpm) at 1ml/min, functional IgG recovery decreased. However, separation was much improved at expense of recovery.	6.4.2
Mini CCC	CCS	1200	1	29.5	**77.12**		6.4.4
Mini CCC	CCS	1500	1	31.8	**56.88**		6.4.4
Mini CCC	CCS	1800	1	36.4	**44.24**		6.4.4

Figure 6.4.7.1: Overview of experimental runs on various CCC machines. Results tabulated in terms of machine type, functional IgG recovery, sample used, rotational speed, flow rate and resulting stationary phase retention.

The results showing the effect of flow rate on functional IgG recovery, in varying machines is shown in Figure 6.4.7.2. In both the CPC and the Mini CCC, doubling of the flow rate allowed a very significant increase in the retention of IgG activity. In the CPC using crude CCS retention of activity went from 44.60 to 71.34%. Whilst also with the Mini CCC an increase in IgG functionality from 44.72% to 77.12% was seen. In the TC CCC however this increase was not as significant going from 60.54 to 68.35%.

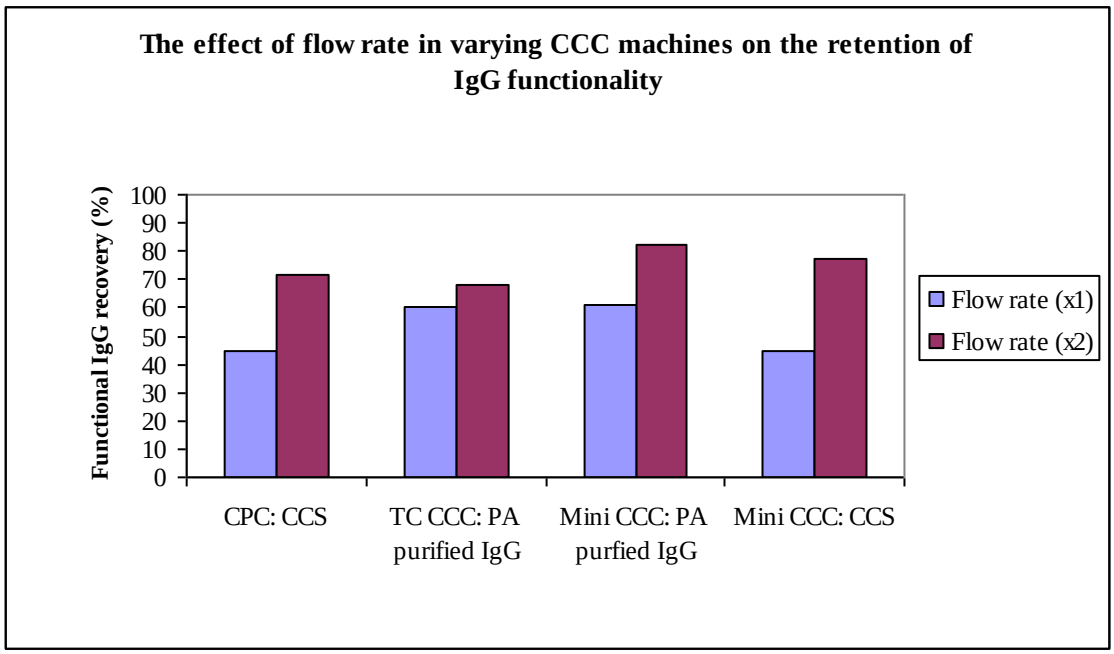

Figure 6.4.7.2: The effect of flow rate on functional IgG recovery in various CCC machines. Recoveries calculated following sample analysis by protein A HPLC, 8 minute injection time and 80µl injection volume. The IgG recovery was plotted against flow rate used.

A lower retention of functional IgG activity (around 70% as shown in Figure 6.4.8.3), even at increased flow rate was seen with the hydrostatic machines when compared to the Mini CCC. The CPC allowed high speed spin and pressure driven, successful IgG separation. Functional IgG recovery however was badly affected at 44.60% at 5ml/min and 71.40% at 10ml/min. With the TC CCC, separation was also seen but at the expense of IgG functionality. Again high flow rate and speed spin was needed, giving a functional IgG recovery of 58.21% at 5ml/min and 68.35% at 10ml/min. It was suggested that an increased flow rate with the CPC, resulted in such a difference in initial recoveries when compared to the TC CCC, as the IgG was less exposed to high

g forces associated with using this hydrostatic machine. As doubling the flow rate, halved CCC run times and respective mixing and settling steps.

With the Mini CCC, as flow rate was doubled with a rotational speed of 1200 rpm using PA purified IgG, the functional IgG recovery rose from 41.05% to 81.97%. With a trial run using the CCS at this doubled flow rate, IgG recovery was comparable with the PA purified IgG at 77.12%, showing a higher IgG recovery than had been seen with any other CCC machine. The multilayer CCC (Mini) using a hydrodynamic design allowed greater retention of biological activity than had been seen in any hydrostatic machine. Conversely this mechanism of mixing was not adequate to allow the separation of IgG from impurities, IgG elution was over an extended time period, thus resolution was lost.

6.5 Conclusions

The studies in this chapter showed that hydrodynamic, wave like mixing, as offered by the Mini CCC allowed the significant retention of biological activity up to 81.97%. Retention of activity however, was only possible at extremely low rotational speeds thus IgG resolution was affected, with broad IgG elution peaks. At these lower rotational speeds, resulting stationary phase retention is lower hence separation is affected. The Mini CCC allowed for relatively increased retention of IgG activity but separation from impurities was not achieved.

The retention of activity is critical with biological molecules. When reviewing the literature there appeared, in the vast majority of cases, no mention of recovery. For those groups who did analytically determine recovery, it was with crude absorbance assay and losses were still encountered.

Despite an IgG activity of 81.97% being retained with the use of the Mini CCC, no separation was possible. Moreover despite this being an improvement to the TC CCC and the CPC, it is still not industrial acceptable, as particularly expressed by the purification scientists at Lonza.

A compromise between hydrostatic and hydrodynamic mixing was needed. A mode was required where mixing was gentle enough to retain the IgG biological activity. However this needed also to be sufficient to allow mass transfer and adequate stationary phase retention, such that separation from impurities could be achieved. Previously CCC machines were designed based on high throughput, high g separation of small molecules, which are robust. Work in this project thus far has shown this level of mixing is not suitable for large, fragile biologics. An alternative mode of CCC is detailed and discussed in the next chapter.

CHAPTER 7: Successful monoclonal antibody separation: Solution as provided by the non synchronous CCC

7) Successful monoclonal antibody separation: Solution as provided by the non synchronous CCC

7.1 Summary

7.2 Introduction

7.3 Method and materials

7.4 Results and discussion

7.4.1 Investigation of differing Pr ratios using PA purified IgG: effect on recovery

7.4.2 Investigation of differing Pr ratios using CCS

7.4.3 Investigation of sample loading capacity using CCS

7.4.4 Increased fraction collection: effect on purity

7.4.5 Throughput: Studies into sample loading capacity

7.4.6 Effect of mass balance, purity and IgG recovery on throughput.

7.4.7 Investigation of associated g force with non synchronous processing

7.5 Conclusions

7.1 Summary

The need for a change in CCC design for protein separation has been highlighted in previous chapters. Loss in IgG functionality was seen with hydrostatic machines and also hydrodynamic CCC machine, using a gentler wave like mixing. The studies in this chapter investigate a non-synchronous CCC machine operated in a hydrodynamic mode. The benefit of this non synchronous (non-synch) CCC machine is that the rotor to bobbin speed ratio (Pr ratio) can be altered. Independent control of mixing and settling is thus possible. Reduction of the Pr ratio from a normal 1, in J type centrifuges (Mini) to 0.33 was investigated; giving reduced mixing and increased settling time. The retention of IgG biological activity with a sharp, high resolution separation of the IgG from impurities was seen. This chapter details how this was achieved with optimisation of loading capacity and the maintenance of purity (>85%). The low level g force associated with these machines was also investigated and compared to other CCC machines, using the g force program created by Dr Van den Heuvel (Van den Heuvel *et al*., 2011).

The resulting verdict from the studies in this chapter showed promise for the non-synchronous CCC instrument in monoclonal antibody separation from fermentation cell culture supernatant.

7.2 Introduction

The vigour of mixing or the shear created by the two phases appeared detrimental to IgG functionality in all the CCC machines tested thus far (CPC, TC CCC and Mini CCC). There was a need for gentler mixing with increased settling time. Mixing needed to be just sufficient such that the stationary phase could be retained inside the column and allow mass transfer.

The loss to IgG activity was experienced in both hydrostatic and hydrodynamic mode (as shown in Figure 7.2.1 depicted by the red colour). There was the situation of either:

1) Higher recovery of biological activity but the loss of IgG resolution, resulting in no separation from impurities e.g. in the Mini multilayer CCC.

Or

2) Separation of IgG from the impurities but loss of IgG biological activity e.g. as seen in the CPC and toroidal coil CCC

A compromise between the two modes was needed. It was thought that the non synchronous CCC could provide a solution.

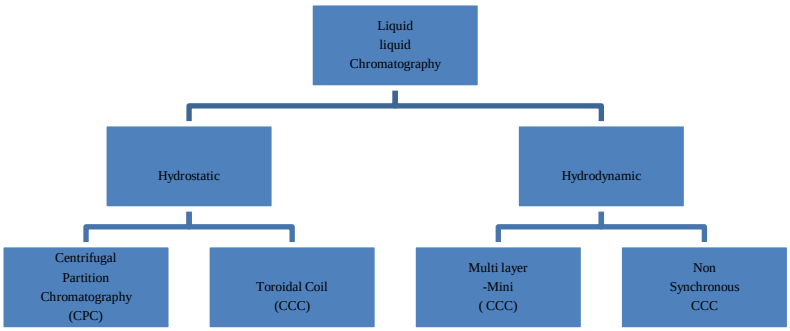

Figure 7.2.1: A diagram to show the varying modes of CCC operation; hydrostatic and hydrodynamic and the respective machines they encompass. The red colouring is used to illustrate the machines that have been investigated and have been found unsuitable. The green colour is used for the non synchronous CCC machine, representing a possible solution.

The non-synchronous CCC, when first introduced, was investigated using biologics (Shinomiya *et al*., 2003). Its non-synchronous nature allowed the combination of the rotor rotation (about its own axis and the sun gear) and revolution of the bobbin around the coil holder (Kobayashi *et al.*, 2005). The non-synchronous machine uses a hydrodynamic mode which is governed by the selected planetary drive ratio (Pr ratio). The planetary drive ratio (Pr ratio) is defined as the speed of the bobbin over the speed of the rotor (ratio of bobbin to rotor speed) (Wood, 2010). Hence the with the non-synchronous CCC machines the bobbin and rotor speed can be controlled separately, ultimately allowing independent control of mixing and settling.

As highlighted by Ito, normal J type centrifuges have a 1:1 ratio (Ito, 2000). The bobbin rotates once for every rotor rotation, hence termed synchronous. Non synchronous CCC has recently been developed with the use of non-twist 'flying leads', permitting the machine design without the use of rotary seals. A 1:1 ratio, as seen in previous chapters, has some constraints when attaining separations using ATPS. ATPS require greater settling time with reduced bobbin to rotor speed. The small density differences between the phases and resulting interfacial tension means mixing vigour is not as critical as previously thought (Ito *et al*., 1983). The adjustable coil rotation offered by the non-synchronous CCC, allows the theoretical separation and also the retention of stationary phase. A low bobbin rotation rate, increases phase system settling time which is needed by ATPS under a strong centrifugal force field (Shinomiya *et al*., 2003).

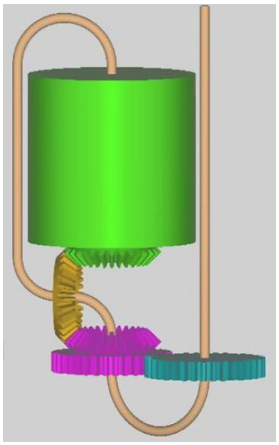

Figure 7.2.2: Diagram to show non twist flying leads. The use of flying leads in synchronous CCC has allowed the connection of the bobbin to that of the rotor, without the use of rotary seals. Previously this 1:1 ratio was needed to prevent the flying leads from twisting. Non twist flying leads have now been developed which allows the CCC machine to be operated in a non synchronous mode.

A normal J-type centrifuge has a Pr ratio of 1 (Figure 7.2.3). As the Pr ratio decreases e.g. 0.33 or 0.67 the bobbin rotates once for increased rotor rotations. More settling and gentler mixing is thus achieved when compared to that of the J-type centrifuge. It was considered that, by fixing the rotor speed at 800 rpm and investigating a Pr ratio of 0.33 and 0.67, IgG recoveries would be sustained. Previously high vigour mixing was seen to be detrimental to the IgG. By a reduction in mixing time but an increase settling time, greater mass transfer was predicted, allowing high resolution separation of mAb from the impurities.

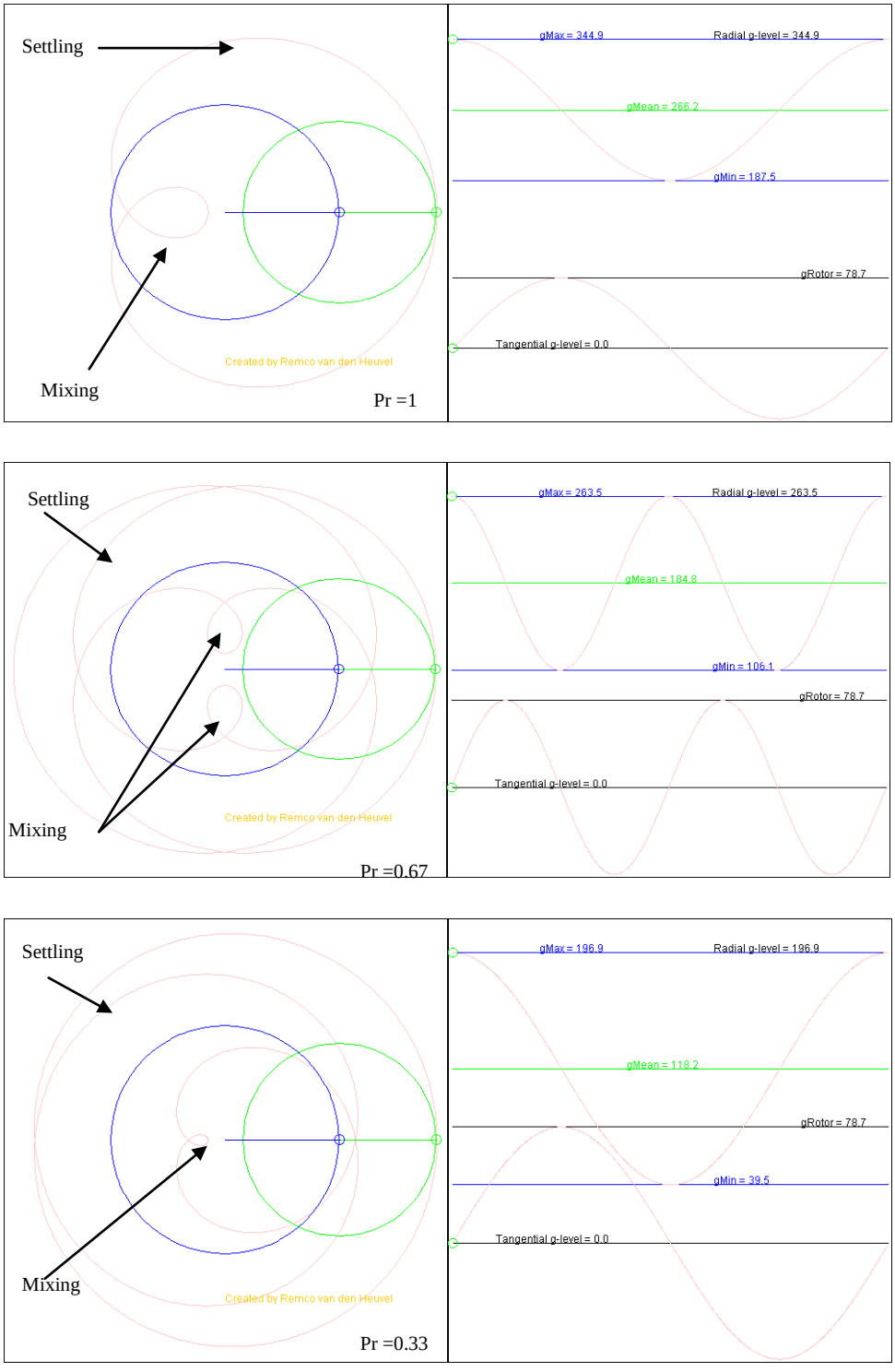

Figure 7.2.3: Diagrammatic representation using the g force program (Van den Heuvel et al., 2011) at various Pr ratios. Pr of 1 (top) seen in J type synchronous centrifuges. The bobbin rotates once for one rotor rotation. Pr ratio of 0.67(middle) seen using a non-synchronous centrifuge. The bobbin rotates twice for three revolutions of rotor rotation. Pr ratio of 0.33(bottom,) seen using non synchronous centrifuge. The bobbin rotates once for three revolutions of rotor rotation. Maximum, minimum and mean g forces for each Pr ratio are noted. Below this, also on the right hand side, tangential g-force is shown. Within this work the g force range is predominately used.

7.3 Method and materials

The non-synchronous coil planet centrifuge was used for separations, initially with PA purified IgG and subsequently when the crude CCS. Rotor and bobbin parts were supplied by Dynamic Extractions, Slough, UK. The column volume was 475mL.

The machine (Figure 7.3.1) used a spider, which allowed the speed of the rotor to be changed relative to that of the bobbin. The spider allowed motion to continue and ensured the flying leads were not twisted during operation, thus no rotator seals were required. With a J type centrifuge, bobbin and rotor speed are identical. They have a Pr ratio of 1 and no spider is used. The spider allows a range of Pr ratios to be investigated from the normal J type centrifuge (Pr=1) through to Pr=0 (a toroidal coil centrifuge) and -1 (I type centrifuge).

Figure 7.3.1: A photo of the interior of the non synchronous CCC machine. Typically the rotor speed would be kept constant at 800rpm. The spider speed control is changed to attain the appropriate Pr ratio for the run.

7.4 Results and discussion

7.4.1 Investigation of differing Pr ratios using PA purified IgG: effect on the recovery of biological activity

To determine optimum operating parameters in terms of the retention of IgG functionality in the non-synchronous CCC, protein A purified IgG was initially used.

The operating conditions as detailed in Figure 7.4.1.1 were used, where material was flowed from periphery to centre, the upper phase being PEG.

Non synchronous CCC separation
ATPS…17.5%/17.5% w/w.…PEG/Salt, pH…7.43
PEG……1000…Salt …Sodium citrate
Coil volume……475ml
Sample loop……16.8ml
Operating mode…Forward
Column filled at ……50ml/min
Injected mAb:
1) CCS…… (Batch number …L156568/47)
Volume…….....32.5ml diluted with:
…..8.75g sodium citrate
…..8.75g PEG
Spin speed…800rpm, temperature….20°C, flow rate…..…10ml/min
Equilibrated at……10ml/min,
Stationary phase displaced.….425ml % stationary phase displace 10.5%

Figure 7.4.1.1: Typical non synchronous CCC operation parameters.

IgG however did not elute, it remained in the column Water was used to flush the column contents out, 10x 50ml fractions were taken and analysed by protein A HPLC. The IgG was seen to be in the stationary phase pump out.

In order to allow the IgG to be eluted within a column volume the direction of flow and flow rate were changed. Material was pumped from centre to periphery at a flow rate of 10ml/min and the upper phase was changed to salt. Stationary phase retention was around 20%, but the elution of the IgG within the coil volume was seen. Triplicate non synchronous CCC runs were conducted at a Pr ratio of 0.33 and 0.67.

Results are shown in Figure 7.3.1.2 where the IgG concentration recovered from the fractions is compared to that of the starting control, at a Pr ratio of 0.33 and 0.67. For both Pr ratios a recovery of around 80% functional IgG was seen. Furthermore reproducibility between the runs was seen.

Pr=0.33						
Run	IgG concentration (mg) Fractions	Control	Functional IgG recovery (%)	Mean	st dev	st error
1	2.00	2.52	79.37			
2	1.99	2.48	80.24			
3	2.00	2.55	78.43	**79.35**	0.91	0.30
Pr=0.67						
Run	IgG concentration (mg) Fractions	Control	Functional IgG recovery (%)	Mean	st dev	st error
1	1.93	2.48	77.53			
2	2.14	2.55	83.98			
3	2.00	2.55	78.47	**79.99**	3.48	1.16

Figure 7.4.1.2: Tabulation of triplicate non synchronous runs at a Pr ratio of 0.33 and 0.67. The 'fractions' column in the table refers to total functional IgG in all fractions collected for each individual run. This is as compared to IgG in the starting 'control'. Carried out with PA purified IgG. Fractions were analysed by protein A HPLC, 80µl injection and 8 minute run time.

7.4.2 Investigation of differing Pr ratios using CCS

IgG recovery of nearly 80% was attained with both Pr ratios using protein A purified IgG. Investigations with crude CCS followed, to observe if separation from impurities was possible. Previous experimental conditions as outlined above were used. Concerning the analysis of the fractions, a HPLC calibration curve (Figure 7.4.2.1) as previously used (Figure 3.4.7.1) for other CCC runs was applied to obtain the IgG concentrations.

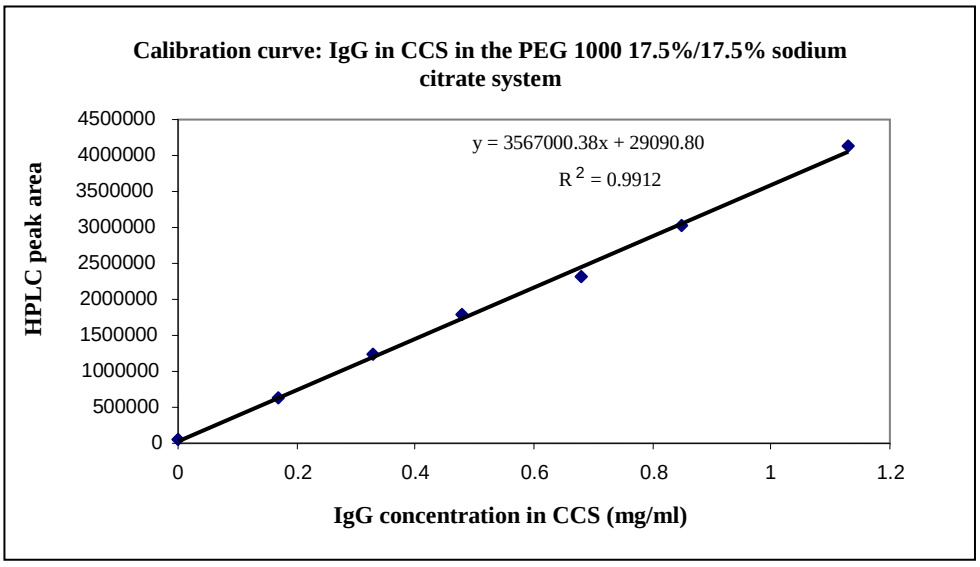

Figure 7.4.2.1: Calibration curve used to calculate the concentration of IgG in CCS sample. Calibration curve prepared by samples diluted in the PEG 1000 17.5%/17.5% sodium citrate system and then subject to protein A HPLC, 80µl injection and 8 minute run time.

Initial runs using conditions outlined in Figure 7.3.1.1 were employed. Material was pumped from centre to periphery at a flow rate of 10ml/min and salt was used as the upper phase. Results are shown in Figure 7.4.2.2 and detail the recovery of viable IgG at a similar concentration, at a Pr ratio of 0.33 and 0.67. At a Pr ratio of 0.33 the retention of viable IgG was seen at 73.07%. At a Pr ratio of 0.67, viable IgG recovery fell to 60.39%.

IgG concentration in CCS loaded (mg/ml)	Pr ratio	Viable IgG recovery (%)
0.67	0.33	73.07
0.66	0.67	60.39

Figure 7.4.2.2: Overview of resulting functional IgG recovery using differing Pr ratios and crude CCS. Samples subject to non-synchronous CCC and protein A HPLC was used to determine IgG recovery, 80µl injection and 8 minute run time. Viable IgG recovery was calculated by comparing initial IgG concentration to that remaining after the CCC run.

Again, a lower recovery was seen following the non-synchronous CCC processing with the crude CCS material, as opposed to PA purified IgG (Chapter 5.7.4 and 6.4.4). The possibility of column overloading was thought to be the cause. As seen previously, the CCS contained a whole host of additional proteins, anti-foaming agents, cell culture components etc which exacerbated the IgG degradation (Figure 6.3.2.2). When the CCS samples was loaded to the same concentration of the PA purified IgG, total protein concentration was many times greater and therefore needed to be taken into consideration.

With relatively more mixing to settling at a Pr ratio of 0.67 when compared to a Pr ratio of 0.33, increased damage to the IgG functionality was seen (Figure 7.4.2.2). Even at this mixing vigour compared to a Pr ratio of 1 used for all other CCC machines, loss of functional IgG recovery was seen.

The CCC reconstructed chromatogram following protein A HPLC analysis can be seen in Figure 7.4.2.3. HPLC peak area is plotted against elution time in minutes, at both a Pr ratio of 0.33 and 0.67. At a Pr ratio of 0.33 the IgG elutes as a single sharp peak at 55 minutes. At a Pr ratio of 0.67 the IgG had a broader peak eluting over 20 minutes between 30 to 50 minutes.

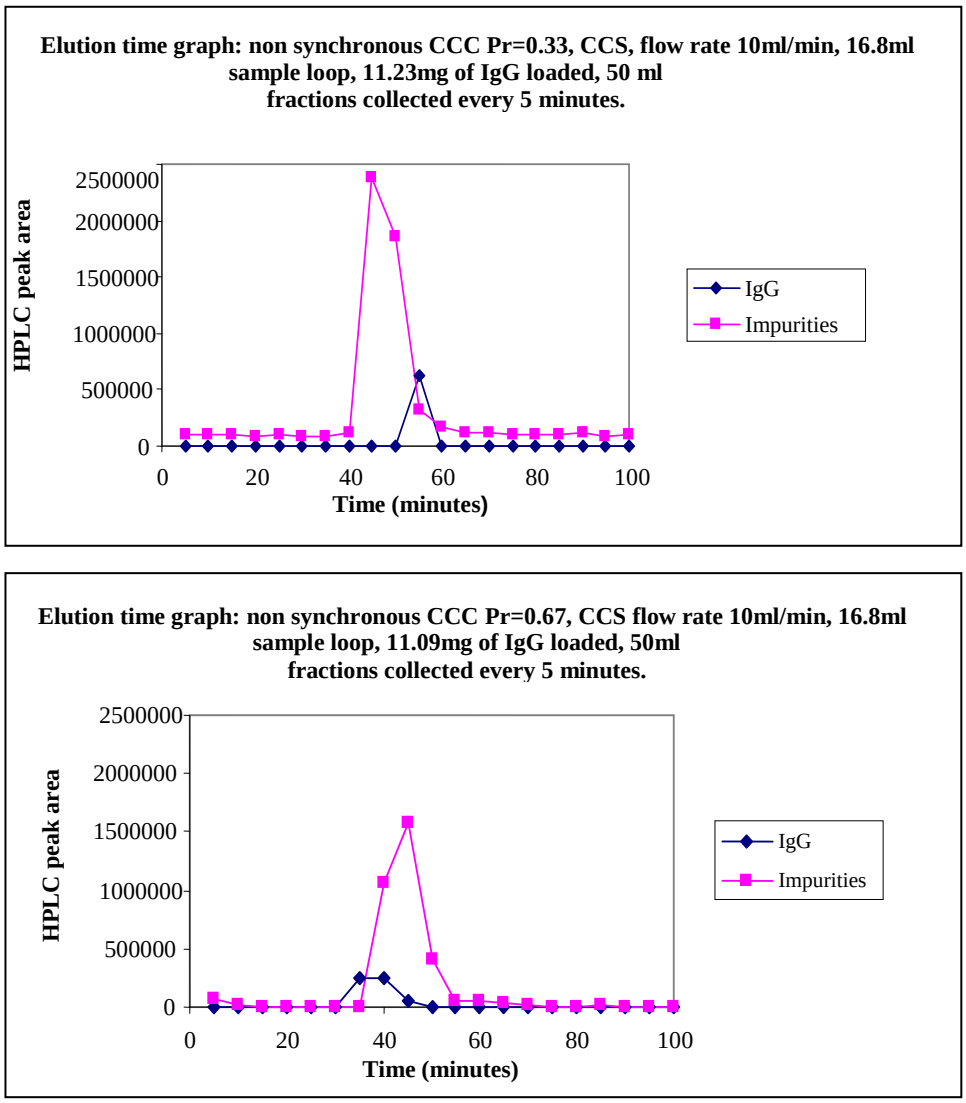

Figure 7.4.2.3: Elution time graph at a Pr ratio of 0.33(top) and 0.67 (bottom). Reconstructed protein A HPLC chromatograms following non-synchronous CCC runs. Carried out with CCS (crude sample), flow rate of 10ml/min. Samples analysed by protein A HPLC, 8 minute injection time and 80µl injection volume. IgG HPLC peak area (6 minute peak) and impurities (0.1 minute peak) plotted against time of elution. IgG elutes just before the impurities at Pr=0.67 but just after the impurities at a Pr=0.33.

At a Pr ratio of 0.67 as opposed to 0.33, a broader IgG elution peak was seen. It suggested that these systems did not require a great extent of mixing due to the low interfacial tension of the phase system, but sufficient settling time was critical. With a lower Pr ratio of 0.33 adequate settling time was given, allowing mass transfer of the high molecular weight IgG between the phases. All proceeding runs were subsequently conducted at a Pr of 0.33.

7.4.3 Investigation of sample loading capacity using crude CCS

When 11.23mg of the IgG was injected onto the non-synchronous CCC at a Pr of 0.33, a recovery of 73.07% viable IgG was seen. As previously mentioned it was thought the total protein concentration in the CCS load was having a detrimental effect. The IgG load was hence lowered and the effect on functionality investigated.

A CCC run was conducted using the conditions outlined in Figure 7.3.1.1. Material was pumped from centre to periphery at a flow rate of 10ml/min and salt was used as the upper phase. 1.34mg of IgG was loaded onto the non-synchronous CCC at a Pr ratio of 0.33. Following the CCC run, the column contents were flushed out with 500ml of water. 10 x50ml fractions were taken termed 'pump out 1-10'. These were then subject to Protein A HPLC analysis with the other samples. These additional samples were taken to ensure that all IgG had been accounted for and that no IgG had been trapped in the column.

The results table can be seen in Figure 7.4.3.1 where the concentration of IgG in fractions is noted. The table lists HPLC peak area, concentration of IgG in mg (obtained using the calibration curve in Figure 7.4.2.1) and mg per fraction (obtained by multiplying the IgG concentration by the sample volume). The HPLC peak area of the impurities (from the 0.1 minute peak following Protein A HPLC analysis) is also noted and background correction noted. The IgG was seen to elute in Fractions 11 and 12 between 60-65 minutes. A total recovery of 93.28% functional IgG was seen. Figure 7.4.3.2 is a representation of the data in Figure 7.4.3.1 which shows a reconstructed CCC chromatogram following protein A HPLC analysis. HPLC peak area is plotted against time in minutes. The relatively smaller IgG peak can be seen to be co eluting with that of the larger impurities peak (overlap between 55-60 minutes).

Fraction	Time (minutes)	PA binding IgG			Volume of sample (ml)	Impurities	Corrected impurities peak area
		Peak area	conc./ mg/ml	Mg per fraction			
Control: load		353219			16.8	2792620	2617769
Control: load		307722			16.8	2552060	2377209
Control: load		325336	0.08	1.34	16.8	2682043	2507192
1	5	6037			50	193020	18169
2	10	6371			50	176975	2124
3	15	5688			50	186487	11636
4	20	9400			50	202138	27287
5	25	7212			50	192317	17466
6	30	6019			50	217365	42514
7	35	4154			50	186520	11669
8	40	6097			50	137818	0
9	45	7675			50	547850	372999
10	50	3422			50	531068	356217
11	55	11593	0.005	0.25	50	254689	79838
12	60	94106	0.02	1.00	50	198640	0
13	65	6736			50	181493	6642
14	70	7400			50	171644	0
15	75	5803			50	197527	22676
16	80	6170			50	174573	0
17	85	6089			50	187167	12316
18	90	6689			50	163963	0
19	95	7254			50	182121	7270
20	100	3322			50	172576	0
Pump out 1		6082			50	183334	
Pump out 2		4991			50	192877	
Pump out 3		6339			50	202171	
Pump out 4		6017			50	183688	
Pump out 5		9574			50	159774	
Pump out 6		7038			50	152630	
Pump out 7		6582			50	199688	
Pump out 8		5387			50	183268	
Pump out 9		5891			50	162319	
Pump out 10		6578			50	89944	
Total mg in fraction			1.25				
Total mg in control			1.34				
% recovery of functional IgG			**93.28**				

Figure 7.4.3.1: IgG (6 minute peak) and impurities (0.1 minute peak) HPLC peak area and respective concentration following protein A HPLC analysis. 50ml pump out fractions were taken to a total of 500ml to ensure that all possible IgG had been accounted for. These results were following a non synchronous run using a Pr of 0.33 using crude CCS at a flow rate of 10 ml/min.

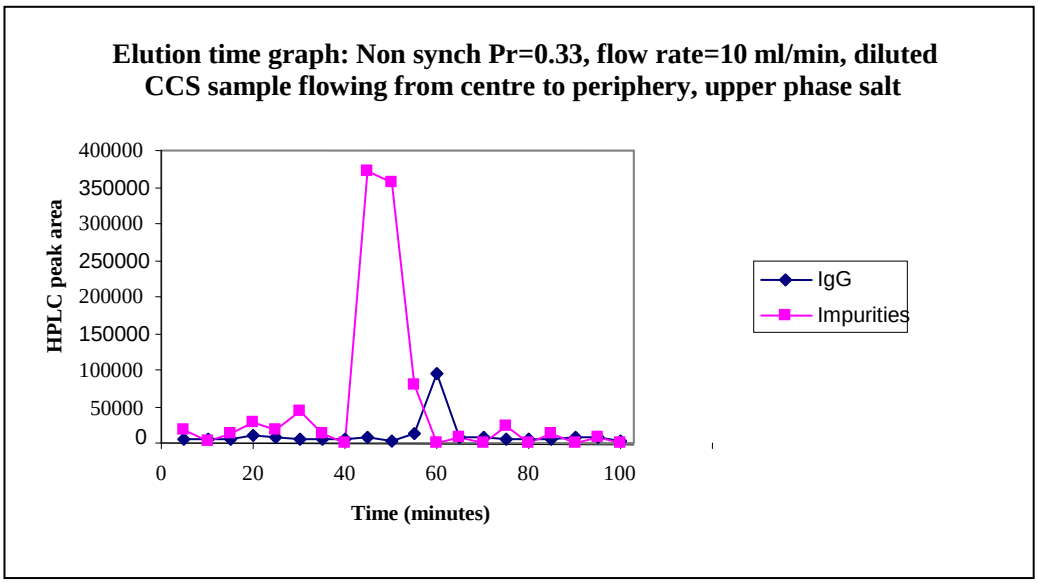

Figure 7.4.3.2: Elution time graph. Reconstructed protein A HPLC chromatogram following a non-synchronous CCC run at a Pr ratio of 0.33. Carried out with CCS (crude sample), flow rate of 10ml/min. Samples analysed by protein A HPLC, 8 minute injection time and 80µl injection volume. IgG HPLC peak area (6 minute peak) and impurities (0.1 minute peak) plotted against time of elution.

Despite the overlap of IgG and impurities (Figure 7.4.3.2) these results were promising. The HPLC program detected anything that absorbed at 280nm. Absorbance could thus not necessarily be proteins and could for example include medium components and foaming agents. These results showed the best retention of IgG biological activity seen thus far, with any CCC instrument.

7.4.4 Increased fraction collection: effect on purity

Previously fractions were collected every 5 minutes, with a corresponding volume of 50ml, it was thought this fraction size was too large and needed to be reduced. It was considered that by increasing collection to every minute during the period of overlap (Figure 7.4.3.2) separate elution would be possible.

A CCC run was conducted using the conditions outlined in Figure 7.3.1.1. Material was pumped from centre to periphery at a flow rate of 10ml/min and salt was used as the upper phase. Fractions were taken every 5 minutes up to 50 minutes, then from 50-65 minutes fractions were collected every minute. The CCS was diluted 6 times (to 0.09mg/ml) and used as the injection load. Following the CCC run samples were subject to Protein A HPLC analysis.

The results are shown in Figure 7.4.4.1 where HPLC peak area is plotted against time in minutes. The IgG and impurities can be seen to elute separately. Furthermore the IgG elutes as a sharp peak, whilst the impurities peak is larger and broader and can be explained by its heterogeneous nature.

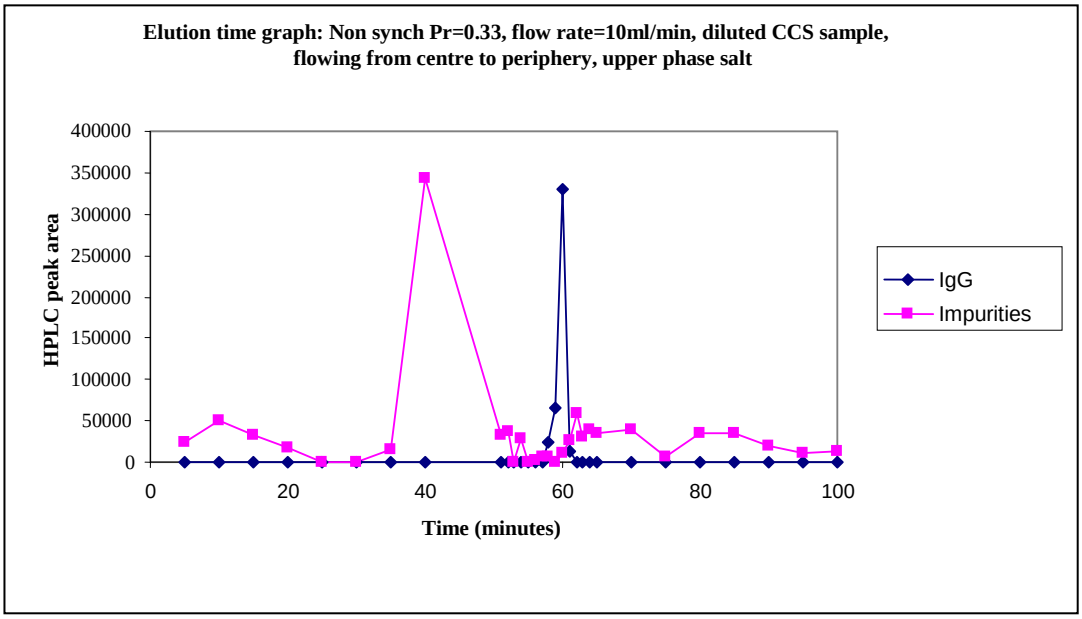

Figure 7.4.4.1: Elution time graph with increased fraction collection between 50-65 minutes as compared to Figure 7.4.3.2. Non synchronous CCC run at a Pr ratio 0.33. Carried out with CCS (crude sample), flow rate of 10ml/min. Samples analysed by protein A HPLC, 8 minute injection time and 80µl injection volume. IgG HPLC peak area (6 minute peak) and impurities (0.1 minute peak) plotted against time of elution.

A clear separate elution of the IgG from impurities with recovery of 89.29% of viable IgG was seen (Figure 7.4.4.1). When Figure 7.4.4.1 was compared with Figure 7.4.3.2, the results looked reasonably similar showing a degree of reproducibility. The same experimental conditions were used but with increased fraction collection.

7.4.5 Throughput: Studies into sample loading capacity

Previous results in Section 7.4.4 indicated both separation and the retention of IgG activity. Throughput however needed to be improved by increasing the sample load. A constraint was seen with loading capacity due to the need for CCS preparation in the phase system, such to not affect the running of the CCC machine. As detailed in Section 3.3.2, if the injected sample was not prepared appropriately as part of a two phase system prior to injection onto the CCC, this could perturb the two phase system

within the machine. The result could mean the two phase system being broken, creating a single phase where all material is eluted at the K=1 point, unseparated.

Experiments were conducted with increased CCS load to observe both separation and the resulting effect on IgG recovery. The experimental outline as shown in Figure 7.3.1.1 was followed for all runs in this section, but adjustments in sample preparation were made based on the starting IgG concentration required.

Non synchronous CCC run 1

A sample loading of 10.81mg of IgG was used and a non-synchronous CCC separation conducted. Results can be seen in Figure 7.4.5.1, where HPLC peak area is plotted against elution time in minutes. The IgG was clearly seen to elute separately from that of the impurities. A recovery of >100% viable IgG was demonstrated by protein A HPLC.

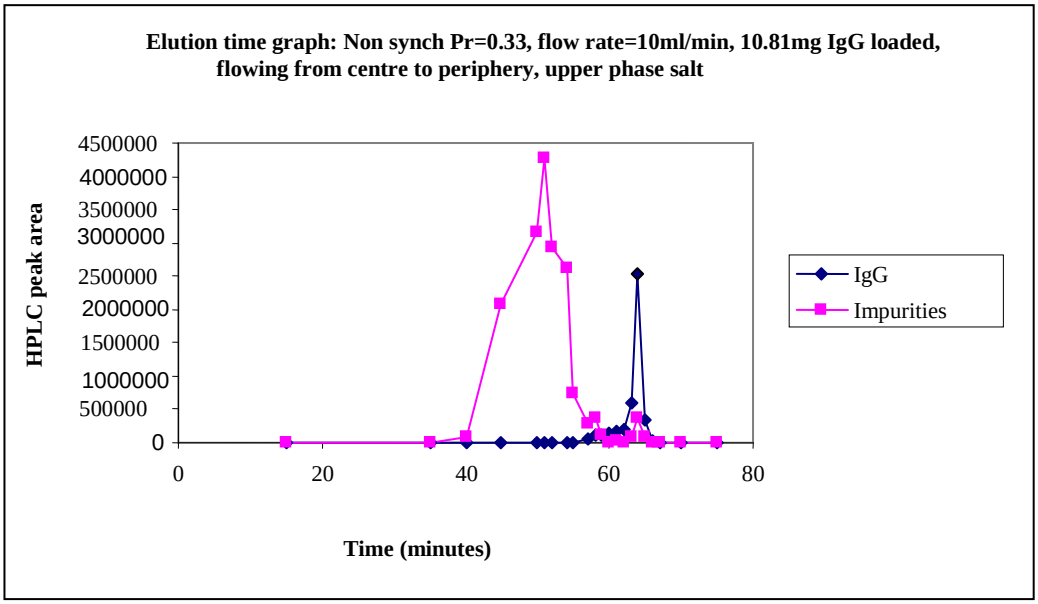

Figure 7.4.5.1: Elution time graph with increased fraction collection between 50-65 minutes and 10.81mg sample load. Non synchronous CCC run at a Pr of 0.33. Carried out with CCS (crude sample), flow rate of 10ml/min. Samples analysed by protein A HPLC, 8 minute injection time and 80µl injection volume. IgG HPLC peak area (6 minute peak) and impurities (0.1 minute peak) plotted against time of elution.

Non synchronous CCC run 2

All runs previously mentioned were conducted with a 16.8ml sample loop. To further increase sample load a 29.8ml sample loop was used and 20.56mg of IgG injected.

Results following protein A HPLC analysis are shown in Figure 7.4.5.2. The table lists HPLC peak area, concentration of IgG in mg (obtained using the calibration curve in Figure 7.4.2.1) and mg per fraction (obtained by multiplying the IgG concentration by the sample volume). The HPLC peak area of the impurities (from the 0.1 minute peak following protein A HPLC analysis) is also noted and background correction noted. IgG purity is further calculated by determining the percentage of PA binding IgG HPLC area to that of the impurities. The IgG appeared to elute over 7 minutes; however the greatest amount was at 55 and 56 minutes. The purity in the other fractions was lower due to low concentrations of IgG. When all the fractions were taken into consideration a 96.72% recovery of functional IgG was demonstrated. The results in Figure 7.4.5.3 are a diagrammatic representation of Figure 7.4.5.2, where HPLC peak area is plotted against elution time. Some co elution of the impurities was seen at the beginning of the IgG elution peak, however the majority of impurities had eluted at 50 minutes.

Fraction	Time (minutes)	PA binding IgG			Volume of sample (ml)	Impurities	Corrected impurities peak area	IgG purity (%)
		HPLC peak area	conc/ mg/ml	Mg per fraction				
Control: load		2456033			29.8	13788669	13229547	15.66
Control: load		2420758			29.8	15152485	14593363	14.23
Control: load		2496434	0.68	20.26	29.8	15531071	14971949	14.29
1	**5**	0	0.00	0.00	50	799255	240133	
2	**10**	0	0.00	0.00	50	800389	241267	
3	**15**	0	0.00	0.00	50	466755	0	
4	**20**	0	0.00	0.00	50	598995	39873	
5	**25**	0	0.00	0.00	50	355831	0	
6	**30**	0	0.00	0.00	50	377364	0	
7	**35**	0	0.00	0.00	50	424401	0	
8	**40**	0	0.00	0.00	50	543596	0	
9	**45**	0	0.00	0.00	50	4151064	3591942	
10	**50**	0	0.00	0.00	50	5196734	4637612	
	51	64185	0.01	0.10	10	2007388	1448266	4.24
	52	352865	0.09	0.90	10	1246024	686902	33.94
	53	374361	0.10	1.00	10	1473160	914038	29.06
	54	403523	0.10	1.10	10	772603	213481	65.40
	55	2695153	0.75	7.50	10	1285837	726715	78.76
	56	3036294	0.84	8.40	10	784369	225247	93.09
	57	238681	0.06	0.60	10	1148293	589171	28.83
	58	0	0	0	10	725609	166487	
	59	0	0	0	10	691321	132199	
	60	0	0	0	10	608949	49827	
	61	0	0	0	10	648330	89208	
	62	0	0	0	10	602019	42897	
	63	0	0	0	10	523744	0	
	64	0	0	0	10	550598	0	
	65	0	0	0	10	484991	0	
14	**70**	0	0	0	50	460411	0	
15	**75**	0	0	0	50	486534	0	
16	**80**	0	0	0	50	524129	0	
17	**85**	0	0	0	50	509214	0	
Total mg in fraction		19.60						
Total mg in control		20.26						
% recovery of functional IgG		**96.72**						

Figure 7.4.5.2: Results following a non-synchronous CCC run using a Pr of 0.33, crude CCS and a flow rate of 10 ml/min (Figure 7.4.5.1). IgG (6 minute peak) and impurities (0.1 minute peak) at increased sample load of 20.56mg. HPLC peak area and respective concentration following protein A HPLC analysis are shown.

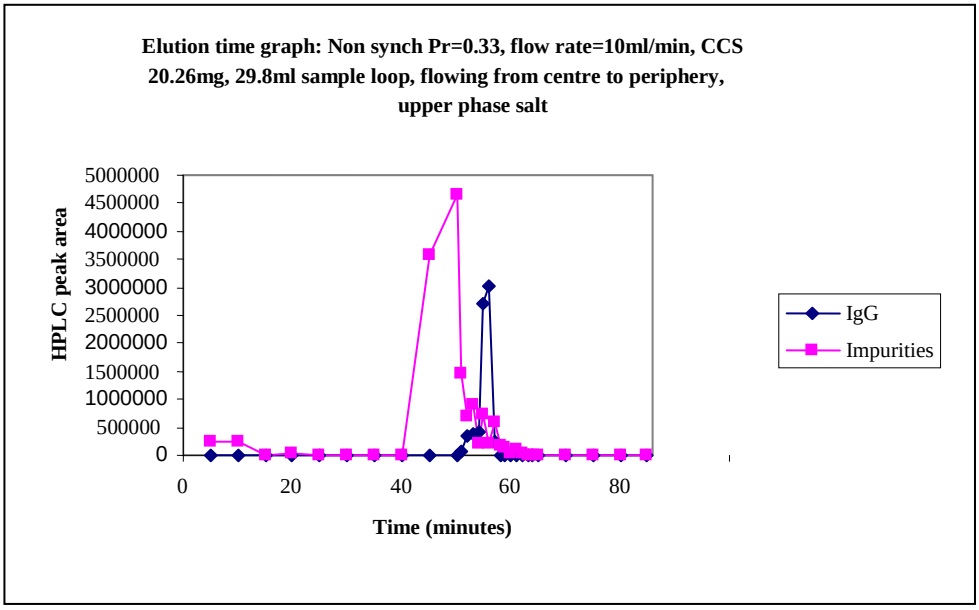

Figure 7.4.5.3: Elution time graph with increased fraction collection between 50-65 minutes and 20.56mg sample load. Non synchronous CCC run at a Pr of 0.33. Carried out with CCS (crude sample), flow rate of 10ml/min. Samples analysed by protein A HPLC, 8 minute injection time and 80µl injection volume. IgG HPLC peak area (6 minute peak) and impurities (0.1 minute peak) plotted against time of elution.

Purification of non-synchronous CCC run 2 fractions was observed by an SDS PAGE gel and silver stain. The method as described in Section 3.42 was used for the running of the SDS PAGE gel and sliver staining was carried out as described in Section 4.4.2. The use of silver stain ensured not only the separation of IgG from impurities but that all impurity where accounted for.

The results are shown in Figure 7.4.5.4, a molecular weight marker is used for indication, along with control samples of PA purified IgG and crude CCS which are compared to the eluted impurities and purified fractions following non synchronous CCC. Firstly the eluted impurities as shown in Fraction 9 and 10 had a very similar banding to that of the CCS. Furthermore the purified IgG fractions (54-56) had much fewer bands than compared to the crude starting CCS material. The CCC purified fractions resemble that of the PA purified control, all unwanted protein bands from the CCS appear to have been removed and are captured in the eluted impurities fractions.

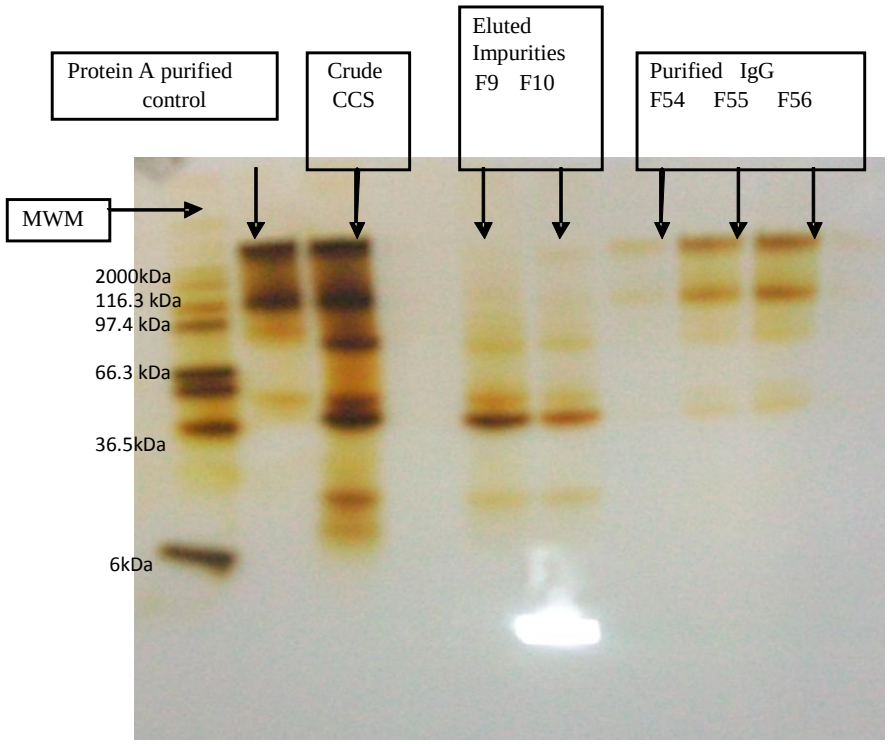

Figure 7.4.5.4: Reduced SDS PAGE gel, samples from Figure 7.4.5.3 used. Gel run at 150V using a pre cast tris-glycine gradient gel. 10µl sample injected into each respective well along with the molecular weight marker, PA purified IgG control and crude starting CCS sample. Gel then subject to silver stain.

Purification by the non-synchronous CCC which was comparable to that of the protein A control was shown by SDS PAGE in Figure 7.4.5.4. When the purity of time point Fractions 55 and 56 (Figure 7.4.5.2) are just considered an IgG purity of 85.93% can be attained following Protein A HPLC analysis. The majority of impurities were accounted for and the gel highlighted the removal of bands, (hence proteins) following non synchronous CCC purification.

7.4.6 Effect of mass balance, purity and viable IgG recovery on throughput.

The results in Figure 7.4.6.1 show the effect of increasing sample load on mass recovery, biological activity recovery and purity. IgG amount in mgs in the CCS starting material is initially listed, this was calculated using protein A HPLC analysis and the calibration curve in Figure 7.4.2.1. Mass recovery was calculated by summing all fractions used that contributed to purity, as a percentage of that initially loaded in the CCS. Biological activity was calculated by determining the percentage of

functional PA binding IgG post a CCC run in comparison to that of the starting control. Purity was calculated as a percentage of the PA binding IgG HPLC peak area to that of the peak area of the corresponding impurities within the fractions.

IgG in CCS (mg)	%		
	Mass recovery	Biological activity recovery	Purity
1.34	74.60	89.29	98.48
1.51	86.09	86.64	93.87
4.53	88.37	88.37	99.13
10.81	90.66	104.53	92.38
11.32	80.39	93.61	89.91
20.26	78.48	96.72	85.93

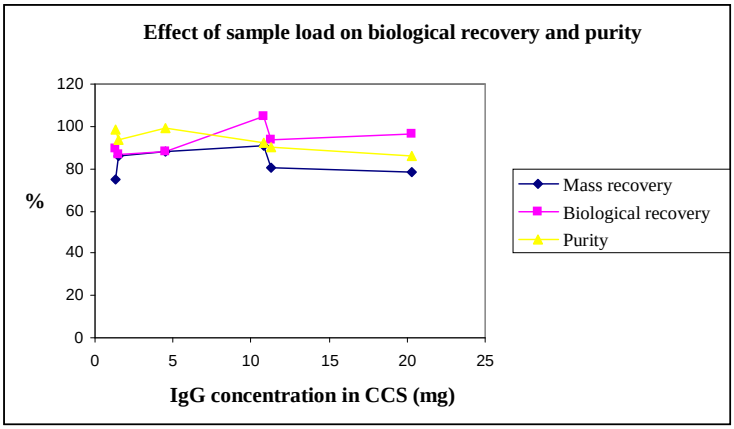

Figure 7.4.6.1: The effect of increasing sample load on mass recovery, biological recovery and corresponding purity. Increased CCS starting concentrations. Samples subject to protein A HPLC analysis. Recovery calculated by the change in IgG amount at the start of the run to that at the end of CCC processing.

In order to improve the purity only fractions of ≥10% of the starting amount were considered. Figure 7.4.6.1 showed biological recovery was always high (>88%). Purity however seemed to decrease slightly as concentration increased. The results showed that even when sample load was pushed to 20.26mg (10 fold that of the starting concentration), purity and biological recovery was not greatly affected, showing promise for future runs.

7.4.7 Investigation of associated g force with non-synchronous CCC processing

A variable and high g-force was previously implicated in contributing to the IgG degradation. High g-force however was needed to allow the stationary phase retention required for resolution. As seen in chapter 5, a continual g force, when material was spun down in a bench top centrifuge, was not detrimental. The varying g force created within the CCC machines, along with the sheer created by the two phases, was investigated using the g force program (as introduced in Figure 7.2.3). With the use of the Pr ratio, beta values and radius, as listed in Figure 7.4.7.1, g force ranges were calculated.

Machine	Pr ratio	Beta values (mm)	Radius (mm)
CPC	0	1	70
TC CCC	1	0.85	110
Mini CCC	1	0.85	50
Non synch	0.33 or 0.67	0.85	110

Figure 7.4.7.1: Overview of Pr ratios used for differing CCC machine types and respective beta values with radius. Figures were used to calculate g-force ranges using Dr Van den Heuvel's program.

Using the above figures and corresponding rotational speed, the g force program was used to determine the minimum, maximum and mean predicted g force (Figure 7.4.7.2). Highlighted in red were the best conditions for each machine in terms of retention of the biological activity of the IgG. The g force program had the ability to calculate both tangential and radial g force, for this work radial g force was observed.

Pr ratio	Machine	Recovery of viable IgG (%)	Concentration IgG loaded (mg)	Sample	Rotational speed (rpm)	Minimum 'g'	Maximum 'g'	Mean predicted 'g'
0	CPC	56.00	18.06	PA Purified IgG	2000	577.00	577.00	577.00
0	CPC	71.41	18.22	PA Purified IgG	2000	577.00	577.00	577.00
0.33	Non synch	79.35	18.15	PA Purified IgG	800	39.00	196.50	117.70
0.67	Non synch	79.99	18.01	PA Purified IgG	800	106.90	264.30	185.60
0.33	Non synch	89.29	1.34	CCS	800	39.00	196.50	117.70
0.33	Non synch	86.64	1.51	CCS	800	39.00	196.50	117.70
0.33	Non synch	88.37	4.53	CCS	800	39.00	196.50	117.70
0.33	Non synch	>100	10.81	CCS	800	39.00	196.50	117.70
0.33	Non synch	96.72	20.26	CCS	800	39.00	196.50	117.70
1	Mini	60.77	2.18	PA Purified IgG	800	84.40	156.00	120.20
1	Mini	46.35	2.22	PA Purified IgG	1000	131.90	243.80	187.90
1	Mini	41.05	2.13	PA Purified IgG	1200	190.00	351.00	270.50
1	Mini	81.97	1.46	PA Purified IgG	1200	190.00	351.00	270.50
1	Mini	44.72	0.82	CCS	1200	190.00	351.00	270.50
1	Mini	77.12	0.84	CCS	1200	190.00	351.00	270.50
1	Mini	56.88	0.79	CCS	1500	296.90	548.50	422.70
1	Mini	44.24	0.79	CCS	1800	427.50	789.80	608.70
1	Mini	57.49	0.35	PA Purified IgG	1800	427.50	789.80	608.70
1	TC-CCC	60.54	13.95	PA Purified IgG	900	237.30	436.60	336.90
1	TC-CCC	68.35	14.15	PA Purified IgG	1200	421.90	776.10	599.00
1	TC-CCC	16.33	11.15	PA Purified IgG	1200	421.90	776.10	599.00
1	TC-CCC	58.21	14.09	CCS	1200	421.90	776.10	599.00

Figure 7.4.7.2: Varying machine types and modes of CCC operation. Figures grouped by machine type, Pr ratio, IgG recovery, sample type, rotational speed and respective g-force range (minimum, maximum and mean) using Dr Van Den Heuvel's g force program

The g force created by the non-synchronous CCC at both Pr ratios (0.33 and 0.67) was much lower when compared to the multilayer CCC (Mini), TC-CCC and CPC (Figure 7.4.7.2). From an engineering stance, as rotational speed increased, so did the associated g force. In the Mini CCC and the TC-CCC the higher the g force, the greater the difference (Δg) between maximum (g_{max}) and minimum (g_{min}) values. When using the highest rotational speed as an example, a Δg= 362.3 for the Mini CCC and Δg =354.2 for the TC CCC was seen. With the non-synchronous CCC however, this Δg =< 157.

When CCC machines are ordered in terms of increasing g force a very clear pattern can be seen. Results are shown in Figure 7.4.7.3, the hydrodynamic machines with the lowest g force (non-synchronous and Mini CCC) are plotted first then the hydrostatic (CPC and TC CCC) machines. It can be seen that as g force increases, recovery of functional IgG decreases. G force appears detrimental to IgG functionality. Consequently a pattern was seen in terms of the machines that provided

the greatest IgG recovery. A trend appeared which highlighted the most detrimental machines to IgG functionality to be equally the CPC and TC-CCC. This was followed by the Mini CCC and then the non-synchronous CCC, which provided the best recoveries with the lowest g force.

Even when the non-synchronous CCC was used at a Pr of 0.67, the g force fields created were similar to that of the Mini CCC. Similar recovery was seen with 79.99% of IgG activity retention with the non-synchronous CCC at a Pr of 0.67 and 81.97% IgG recovery with the Mini CCC. It further highlighted the ability of the non-synchronous CCC to provide a low g force separation, not detrimental to IgG recovery with a Pr ratio of 0.33.

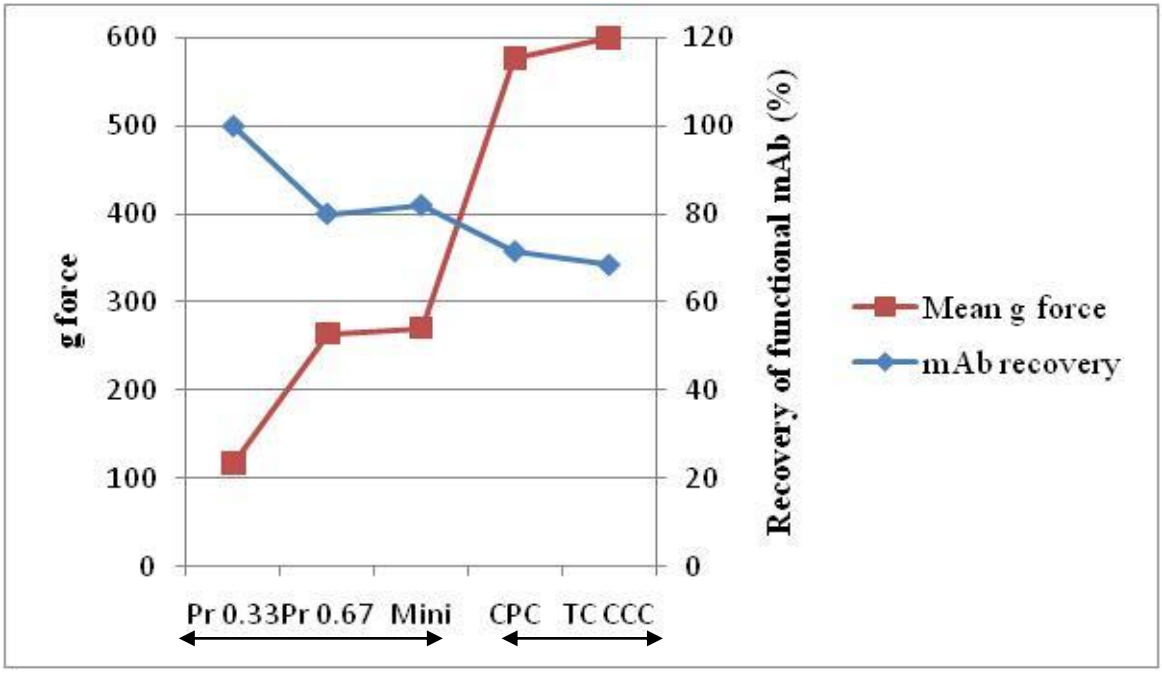

Figure 7.4.7.3: Representation of the effect of varying machine types on viable IgG recovery and corresponding mean g force value. g force mean calculated using the g force program. Recovery was calculated using protein A HPLC, where change in IgG concentration post CCC to initial starting concentration was calculated as a percentage.

7.5 Conclusions

A thorough investigation of the non-synchronous CCC has been conducted. The novel machine allows the independent control of mixing and settling, which was exploited to allow increased rotor to bobbin rotations (Pr ratio). With a J type Mini CCC the Pr ratio is always 1, with non-synchronous CCC this Pr ratio can be changed. Investigations were carried at by reducing the Pr ratio to 0.67 and 0.33, to allow increased settling time with decreased mixing.

In previous chapters, mixing at a Pr ratio of 1 on the Mini CCC with wave like mixing was sufficient to cause loss to IgG functionality. With the non-synchronous CCC, investigations at a Pr ratio of 0.33 and 0.67 with crude material showed clear high resolution separation of IgG from impurities. It was seen however, even at reduced Pr ratio of 0.67, this was still sufficient to cause IgG damage when compared to a ratio of 0.33. Additionally, at this Pr 0.67 ratio, IgG resolution was decreased due to reduced settling times.

One of the most critical parameters noted in the study of this mAb separation using CCC has been settling time. Vigorous mixing which was previously highlighted (both in the literature and by the Brunel CCC group) as key has been seen as secondary to settling. Low interfacial tension and density differences between the phases meant vigorous mixing was not critical. However, adequate settling time, where IgG could experience mass transfer, was vital. Even at a Pr ratio of 0.67, this level of settling for the amount of mixing offered was not sufficient.

By optimisation of the sample fraction collection in a non-synchronous CCC run at a Pr ratio of 0.33, clear separate elution of the IgG from impurities was seen and furthermore confirmed by SDS PAGE and silver stain. Loading capacity was pushed to 20.26mg of IgG with a 29.6ml sample loop and a separation was demonstrated.

With the use of the g force program, the clear relationship of increased g force ranges created by various machines (both hydrostatic and hydrodynamic) and degradation to IgG functionality were seen. A significantly lower g force was created with the non-synchronous CCC machine, especially at a Pr ratio of 0.33. As mentioned in other chapters, degradation was not resultant on a single

parameter. However g force created within the machine itself was clearly a major factor.

Work within this chapter has showed the separation of IgG from impurities with the retention of biological activity by the non-synchronous CCC at a Pr of 0.33. Clearly sample loading and throughput could be improved, as the sample must be prepared in a two phase system. The work that is detailed in the next chapter investigates non-synchronous CCC fractions undergoing rigorous quality control testing at Lonza. A direct comparison of this technology in terms of purification with Protein A HPLC can hence be drawn. These results will be indicative of whether this technology could possibly, with optimisation, be an economical alternative to Protein A HPLC purification.

CHAPTER 8: Characterization of non synchronous CCC purified samples using Lonza quality control assays

8) Characterization of non-synchronous CCC purified samples using Lonza quality control assays

8.1 Summary

A CCC operational mode with a non-synchronous machine at a Pr ratio of 0.33 has been found. At a Pr ratio of 0.33, rotor rotations are increased relative to those of bobbin rotations, allowing greater phase settling time with reduced mixing. A correspondingly lower g force range results, that was sufficient to allow high resolution separation but retain IgG functionality. This was the first time such results had been achieved with any CCC instrument used and these fundamental studies showed promise for the separation of biologics.

Following the work on the non-synchronous CCC, an investigation to characterise the purified proteins at Lonza was carried out by their purification scientists. A range of QC assays were conducted that demonstrated not only the removal of product contaminates such as free DNA and host cell proteins but also highlighted any evidence of structural changes. It was seen that the removal of impurities by the non-synchronous CCC processing is possible, but a significant amount of optimisation work is essential. Due to the mixing and setting that occurs as part of the CCC technique, compounded also by the high concentration of PEG and salt used, aggregation of the IgG was not surprising. Isoelectric focussing results showed that some structural changes had occurred post non synchronous CCC that were not evident with the PA purified IgG control.

The fundamental work that has been carried out within this project has given a positive indication. With significant process optimisation, the non-synchronous CCC may possibly be adopted in the future as an industrially used purification protocol. The consideration of other purification steps that can be aligned

with CCC must be investigated. The removal of all product related contaminates should be observed following three separate purification steps, as opposed to just one protocol. The production of aggregates or any structural changes however that have been implicated following QC testing by CCC processing, requires considerable further investigation.

8.2 Introduction

As detailed in Chapter 7, the best CCC instrument for mAb separation was found to be the non-synchronous machine. Furthermore, a rotor to bobbin rotational speed ratio of 0.33 was identified as the most appropriate. At this Pr ratio both the retention of mAb biological activity and also high resolution separation from impurities was possible. As shown with the work in other chapters (judged using PA binding as an indicator), this was the only machine tested thus far that was able to fulfil the criteria of separation and retention of biological activity.

Non synchronous CCC sample were investigated with a range of quality control assays. These assays were conducted at Lonza by their purification scientist. Non synchronous runs were carried out in triplicate and the preparation of samples and reproducibility is documented. The studies within this chapter described the reasoning for why particular assays were conducted and what the results showed. Ultimately this chapter will debate whether optimisation of the fundamental CCC conditions found within this work would be sufficient to interest future industrial use of this technology.

8.3 Method and materials

8.3.1 Investigation of sample up clean using PD-10 size exclusion columns

All quality control assays were performed at Lonza by their purification scientists. To allow these assays to be conducted without interference from the presence of the phase system, most specifically the PEG mobile phase, sample clean-up was required. A form of buffer exchange was necessary to exchange the IgG from the PEG phase to a low salt formulation buffer used at Lonza (10mM sodium phosphate/40mM sodium chloride pH 7.0). Initially this was investigated with the non-synchronous CCC samples. PD-10 columns were purchased from GE healthcare, which were designed for the clean-up of biological molecules of >5kDa. As the PEG was 1kDa this column was thought to retain the IgG within the pores, allowing other impurities and

contaminants to flow straight through the column (termed flowthrough). The elution of the IgG from the column was by the use of an elution buffer.

PA purified IgG was made up in both water and upper phase respectively and applied to a fresh PD-10 column (2ml of PA purified IgG and 18ml of water or phase). A sample was taken prior to PD-10 column loading (named pre PD-10) and 25ml of Lonza formulation buffer (10mM sodium phosphate/40mM sodium chloride pH 7.0) was used to equilibrate the column. 2.5ml of PA purified IgG sample in either upper phase or water was applied to the column. The flow though that eluted was collected. Anything that eluted in the flowthrough was assumed to be PEG or salt, as the IgG was thought to be retained inside the column pores The PD-10 column was then washed once with 3.5ml of formulation buffer (Eluate 1) and then subsequently with another 3.5ml of formulation buffer (Eluate 2), these samples were collected separately. Formulation buffer was applied to the column to prompt the elution of IgG retained in the column pores.

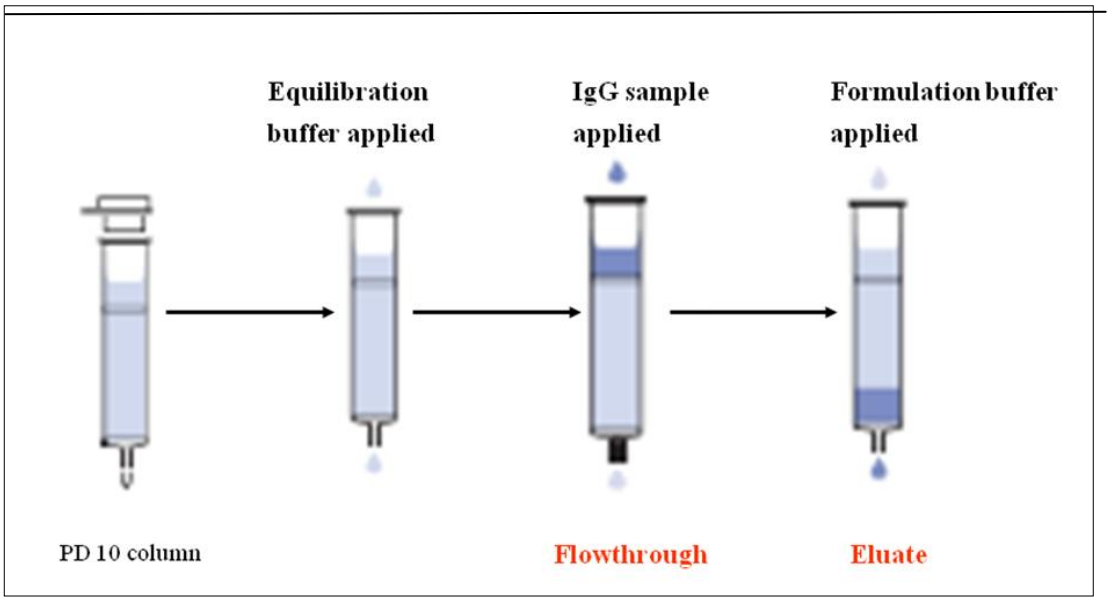

Figure 8.3.1.1: Schematic overview of the PD-10 column sample cleanup process. Buffer exchange was used to swap the phase system non synchronous CCC IgG samples into Lonza formulation buffer. Sample clean up was conducted to avoid any interference to QC assays.

All collected samples were subject to protein A HPLC and the HPLC peak areas can be seen in Figure 8.3.1.2. The results shown list changes in HPLC peak area following PD-10 treatment of IgG in water and the upper phase. It was seen in both samples when IgG peak area for flow through and eluate fractions were compared to

that of the pre PD-10 column, a considerable loss in IgG was seen. For the water control this was less than 2% and the upper phase sample <6%.

	HPLC peak area					
	Water control			Phase sample (upper)		
	Non-binding	IgG	% IgG of initial sample	Non-binding	IgG	% IgG of initial sample
Pre PD-10	4768	1852955		360246	1904686	
Flow through	32629	31423	1.70	24201	102518	5.38
Eluate 1	133166	27094	1.46	165986	113562	5.96
Eluate 2	164579	25286	1.36	397144	27788	1.46

Figure 8.3.1.2: Triplicate HPLC peak area of PA binding IgG and PA non-binding IgG at varying stages of PD-10 column sample clean up. PA purified IgG was applied to the column in upper phase and water as a control. The % IgG of initial sample was calculated with flow through and eluate samples as a percentage of the pre PD-10 HPLC peak area.

It was thought with the water control that the IgG had not eluted and was subsequently stuck within the column. Several further rounds of washing steps were thought to be required to allow elution, however the resulting peak would be diluted over several fractions. It was also noted that the non-binding peak appeared to be increasing and perhaps this was due to denaturing within the PD-10 column. This was thought unlikely however, as was not seen previously by gel electrophoresis.

With respect to the upper phase sample, it was seen that nearly 60% of the IgG came straight out in the flow through and wasn't retained in the pores of the column. It was considered that when the IgG was loaded onto the PD-10 column in PEG, the PEG was displacing the IgG.

Ultimately this work showed that the PD-10 columns were not suitable for buffer exchange of these samples due to the adverse effect of the presence of PEG. Possibly these filters were more suitable for globular proteins rather than the more complex IgG structure.

8.3.2 Investigation of ultrafiltration columns for sample clean up

The PD-10 columns based on size exclusion chromatography were seen inappropriate for IgG sample clean up post non synchronous CCC processing. A differing mode of sample clean-up was thus investigated with ultrafiltration columns from Sartorius known as Vivaspin columns. The Vivaspin columns were investigated over a range of

sample cut off values, ranging from 5-100 kDa. Samples were prepared as previously described (section 8.3.1.2) with PA purified IgG in water and upper phase. The residue was termed as the material retained by the filter and was re-suspended with formulation buffer to a final volume of 500µl. These samples were then subject to Protein A HPLC analysis. All experiments were carried out once at each filter size.

The results are shown in Figure 8.3.2.1 where IgG in water and upper phase is subject to ultrafiltration using varying cut off size filters. Results are tabulated for filtrate and residue samples. The filtrate was termed as all material eluted from the column, which would be predicted to contain the PEG. A control sample was prepared of PA purified IgG in either water or the phase system that had not been subject to ultrafiltration. Mass recovery of the IgG was calculated by determining the HPLC peak area of the IgG in upper phase post ultrafiltration as a percentage of the control IgG. It can be seen in Figure 8.3.2.1 that as ultrafiltration cut off size increases the amount of IgG retained in the residue decreases. Hence the mass recovery of IgG decreases as cut off value kDa increases. Figure 8.3.2.2 is a diagrammatic representation of Figure 8.3.2.2 and the results show percentage IgG plotted against ultrafiltration filter size. A downward slop of IgG recovery in residue samples is shown when filter size increases. An increase in IgG recovery in filtrate sample can only be seen at 100 kDa.

Sample	Cut off value (KDa)	HPLC peak area				Mass IgG recovery (%)
		Water control		Upper phase		
		Non-binding	IgG	Non-binding	IgG	
	5			40025	1207180	110.00
	10			564498	783657	71.41
	30	4446	2048461	709815	403967	36.81
	50	1203089	23904	542124	324988	29.61
residue	100	788430	71524	243350	64321	5.86
	5			611937	30169	2.75
	10			636263	29448	2.68
	30	10775	75979	617652	17344	1.58
	50	11147	50316	660826	26060	2.37
Filtrate	100	25414	39262	584091	398046	36.27
Control		5978	2104346	711248	1097420	

Figure 8.3.2.1: Investigation of a number of ultrafiltration cut off sizes. HPLC peak areas of PA binding IgG and PA non-binding IgG with the differing filters are listed. PA purified IgG was applied to the column in upper phase and just in water as a control and the mass recovery determined.

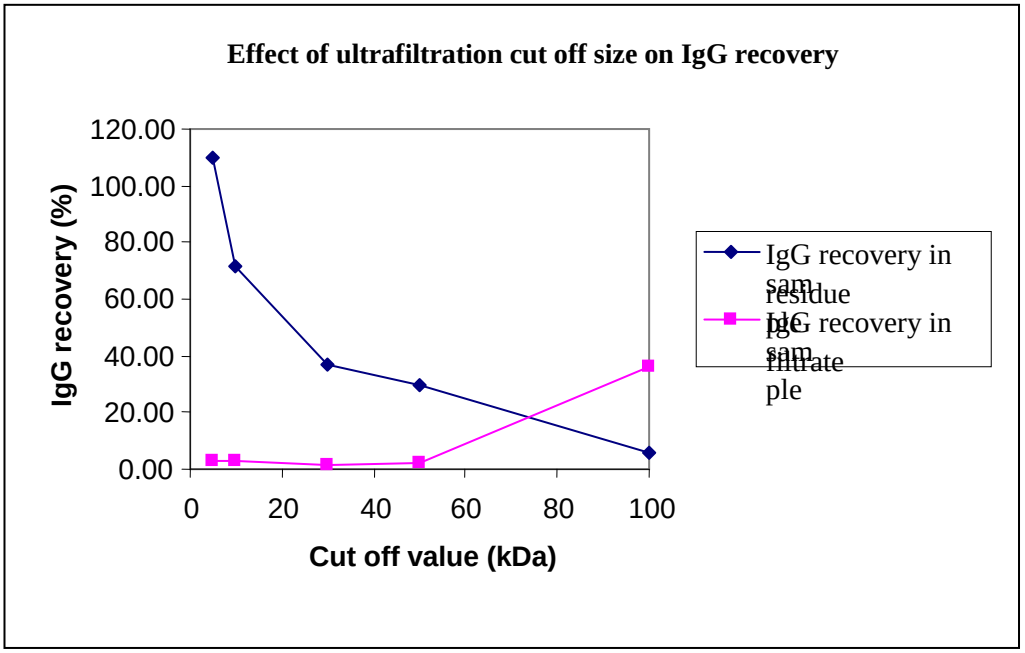

Figure 8.3.2.2: Diagrammatic representation of Figure 8.3.2.1. Effect of increasing ultrafiltration cut off size on IgG mass recovery in both residue and filtration samples. Starting sample of PA purified IgG in upper phase used.

As shown in Figure 8.3.2.2, as the ultrafiltration cut off size increased (kDa) the IgG mass recovery (calculated in relation to the control) decreased. Interestingly, using the 5kDa filter, greater than 100% IgG recovery was seen. Further to this, the non-binding peak was greatly reduced when compared to the control by around 94%, which was assumed to be the removal of the PEG. These results showed ultrafiltration with a 5 kDa filter had some potential and was therefore used for sample clean up post non synchronous CCC processing.

8.3.3: Triplicate non synchronous CCC run with sample clean up using a 5kd ultrafiltration column.

A triplicate non synchronous CCC run at a Pr ratio of 0.33 was conducted, with samples subject to 5kDa clean, prior to delivery to Lonza for a range of QC assays. As the previously used batch of CCS had finished, an older batch that was still available was used (465668/47). As this IgG4 batch produced at Lonza was used for research purposes only, no more was available in their storage. The CCC processing conditions as detailed in Figure 8.3.3.1 were used and repeated in triplicate.

Non synchronous CCC separation
ATPS…17.5/17.5% w/w..…PEG/Salt, pH…7.42
PEG……1000…Salt …Sodium citrate
Coil volume……475ml
Sample loop……29.8ml
Operating mode…Forward flowing from head to tail
Stationary phase……Lower phase
Column filled at ……50ml/min
Injected mAb:
1) CCS…… (Batch number …465668/47/47)
Volume…….....32.5ml diluted with:
…..8.75g sodium citrate
…..8.75g PEG
Spin speed…800rpm, temperature….20°C, flow rate…..…10ml/min
Equilibrated at……10ml/min,
Stationary phase displaced.….425…..ml % stationary phase retention……..10.5%

Figure 8.3.3.1: Non synchronous CCC conditions used for the production of triplicate samples for QC testing.

Results from each separate run and the samples chosen for QC testing are highlighted in Figure 8.3.3.2. The table lists HPLC peak area, concentration of IgG in mg (obtained using the calibration curve in Figure 7.4.2.1) and mg per fraction (obtained by multiplying the IgG concentration by the sample volume). The HPLC peak area of the impurities (from the 0.1 minute peak following protein A HPLC analysis) is also noted with background corrections made. It can be seen for all runs that the majority of the IgG eluted at 54 minutes. Furthermore the recovery of functional IgG in all runs was > 95%. The peak area of the impurities that is also listed showed the majority of elution was around 40-52 minutes, which was before the elution of the IgG. Figure 8.3.3.3 is a diagrammatic representation of Figure 8.3.3.2 where HPLC peak area is plotted against elution time in minutes. The clear separate elution of IgG from impurities in all three runs can be seen. The impurities elute as a large heterogeneous peak in comparison to the smaller sharper elution of the IgG peak. Moreover the elution profiles of the three runs showed reproducibility.

Fraction	Time (minutes)	Volume of sample (ml)	Run 1				Run 2				Run 3			
			PA binding IgG HPLC peak area	PA binding IgG conc/ mg/ml	PA binding IgG mg per fraction	Impurities HPLC peak area	PA binding IgG HPLC peak area	PA binding IgG conc/ mg/ml	PA binding IgG mg per fraction	Impurities HPLC peak area	PA binding IgG HPLC peak area	PA binding IgG conc/ mg/ml	PA binding IgG mg per fraction	Impurities HPLC peak area
Control		29.8	755793	0.20	5.96	8233613	731598	0.20	5.87	8278239	342884	0.19	5.71	8015167
Control		29.8	758330	0.20	5.96	8555857	766446	0.21	6.16	8211093	322611	0.19	5.71	8423940
Control		29.8	726270	0.20	5.96	8895632	696503	0.19	5.58	8108793	333196	0.19	5.72	8321759
1	**5**	50	0			0	0		0.00	0	0			0
2	**10**	50	0			0	0		0.00	0	0			0
3	**15**	50	0			0	0		0.00	0	0			0
4	**20**	50	0			0	0		0.00	0	0			0
5	**25**	50	0			0	0		0.00	0	0			31421
6	**30**	50	0			0	0		0.00	0	0			55017
7	**35**	50	0			0	0		0.00	0	0			67381
8	**40**	50	0			139500	0		0.00	158926	0			162380
9	**45**	50	0			1266601	0		0.00	1470564	0			1334060
10	**50**	50	0			2449688	0		0.00	2620642	0			2823823
	51	10	0			1229256	0		0.00	1300349	0			1481684
	52	10	0			630054	0		0.00	500462	74609	0.01	0.13	624007
	53	10	0			23978	98611	0.02	0.19	0	137229	0.03	0.30	62384
	54	10	1529092	0.42	4.21	0	1367580	0.38	3.75	29249	1369268	0.42	4.18	19889
	55	10	576438	0.15	1.53	0	525643	0.14	1.39	49522	462282	0.12	1.21	0
	56	10	133620	0.03	0.29	0	316663	0.02	0.25	11567	0			0
	57	10	0			0	0		0.00	117213	0			0
	58	10	0			0	0		0.00	97238	0			0
	59	10	0			0	0		0.00	66126	0			0
	60	10	0			0	0		0.00	36122	0			0
Total mg of functional IgG in			6.03				5.58				5.82			
Total mg in functional IgG in			5.96				5.87				5.71			
% recovery of functional IgG			101.22				95.17				101.93			

Figure 8.3.3.2: Triplicate non synchronous CCC data for preparation of sample for Lonza quality assurance assay. PEG 1000 17.5%/17.5% sodium citrate system used. Fractions highlighted in red were selected and subject to samples clean-up to remove PEG by use of 5kDa ultrafiltration column.

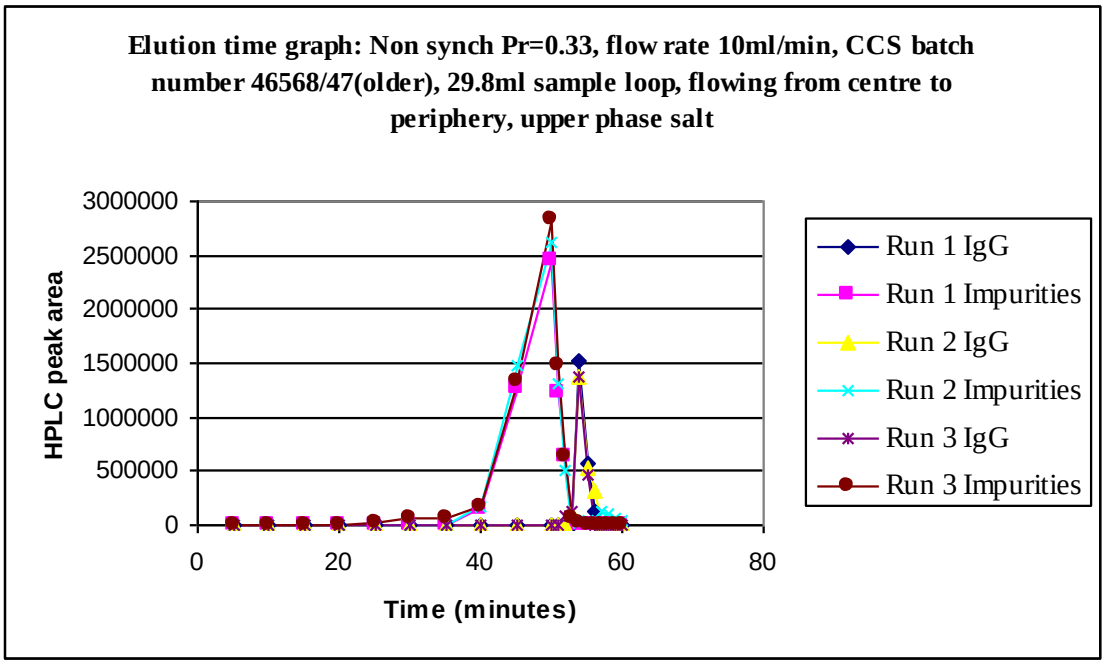

Figure 8.3.3.3: Non synchronous CCC separation at a Pr ratio of 0.33 reconstructed from protein A HPLC analysis chromatograms. 6mg IgG sample load used, 29.8ml sample loop at a flow rate of 10ml/min. The elution profiles of the IgG and impurities from different runs showed similarities.

8.3.4 Child's assay for the removal of PEG from samples post ultrafiltration

As PEG did not have absorbency at 280nm, it was hard to prove that it had been removed from samples post ultrafiltration by protein A HPLC. It had been seen previously that the presence of PEG caused interference to assays with band smearing. To observe that PEG had been removed in samples post ultrafiltration, before they were sent to Lonza for QC testing, the Child's assay was conducted. The Child assay developed in 1975 allows the determination of PEG removal in gamma globulin solution. Proteins are treated with barium and iodine producing a barium-iodide complex with the glycol allowing detection at 535nm (Child, 1975).

The Child's assay was used to quantitate the amount of PEG present in sample. 0.5ml samples of the IgG post ultrafiltration was mixed with 1.5ml of water. 2ml of 10m trichloroacetic acid (TFA prepared in water) was added to the IgG solution and allowed to stand for 15 minutes. A standard solution was then prepared with 0.5ml of $BaCl_2$ solution and 0.25ml of 0.1 N iodine solution added to the IgG. Standard dilution of the PEG was made equalling samples of 10, 20, 30 and 40µg PEG (i.e. 0.5, 1, 1.5 and 2ml of standard solution to 1.5, 1, 0.5 and 0 ml of water). The sample preparation was repeated for ultrafiltration samples and 0.5ml of $BaCl_2$ solution and 0.5ml iodine was added to each

sample. The samples were then subject to a 100 times dilution and 250µl were then added to a multiwall plate and read at 562nm. The results can be seen in Figure 8.3.8.1 and the calibration curve in Figure 8.3.8.2. It was determined that the starting PEG control had 210µ/g of PEG present, following ultrafiltration Fraction 1 had 10.91µ/g of PEG, Fraction 2 had 4.38µ/g of PEG, Fraction 3 4.99µ/g of PEG and Fraction 4 4.59µ/g of PEG present. Overall it was demonstrated that 97.82% of the PEG had been removed by ultrafiltration.

	x100 dilution			Average
Control: PEG	0.497	0.626	0.549	0.557
STD 1	0.155	0.149	0.161	0.155
STD 2	0.221	0.286	0.241	0.249
STD 3	0.302	0.311	0.308	0.307
STD 4	0.332	0.327	0.341	0.333
UF1	0.046	0.039	0.42	0.168
UF2	0.054	0.049	0.041	0.048
UF3	0.071	0.064	0.059	0.065
UF4	0.061	0.052	0.048	0.054

Figure 8.3.4.1: Absorbency values using Child's assay obtained with readings at 562nm with standard and ultrafiltration samples. The 'STD' sample was prepared following the heating of PEG to 60ºC and mixing with the appropriate amounts of barium and iodine. The same protocol was followed for the ultrafiltration samples labelled UF1-UF4 where the same standard dilutions were carried out. All samples were diluted 1 in 100 in water and read on the spectrophotometer.

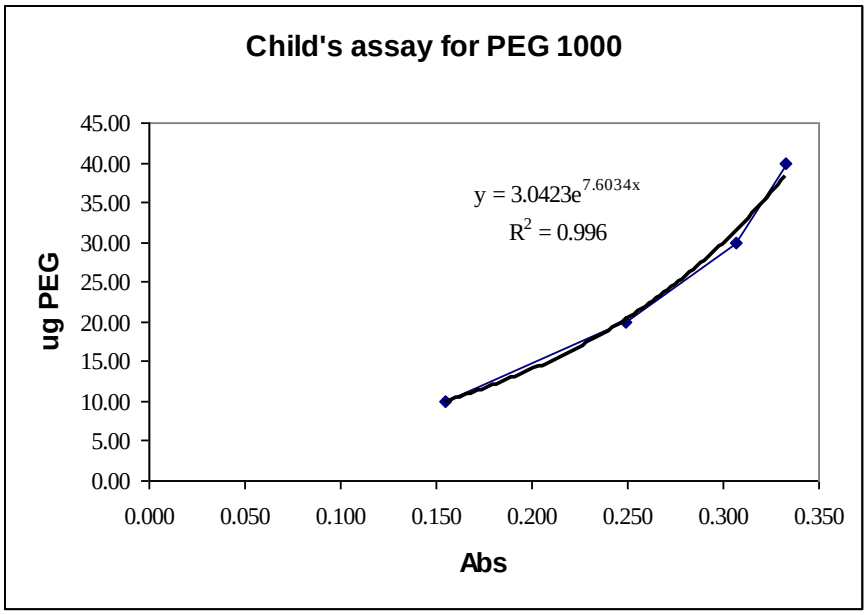

Figure 8.3.4.2: Calibration curve used to quantitate PEG following Child's assay with the measurement of absorbance at 562nm.

8.3.5 QC assays conducted at Lonza by purification scientist Samit Patel

A range of QC assays were conducted with the non-synchronous CCC fractions highlighted in Figure 8.3.3.2. The samples were subject to buffer exchange by the use of a 5kDa ultrafiltration column. The concentration of the samples as determined by Protein A HPLC was 0.4mg/ml. The results for each assay are separately listed below.

1) Removal of Host cell protein: ELISA and dual stain Western blot

The CHO cell line used to produce the mAb is derived from mammalian species than contain thousands of host cell proteins. During fermentation, additional proteins can also be produced that have the potential to contaminate the end product. Host cell protein removal assays are used to observe the clearance of HCPs present in the CCS starting material, that can ultimately affect the overall quality of the end product. It is a regulatory requirement to obtain the lowest level of HCP possible as they have the potential to cause adverse immune responses in patients or reduced drug efficacy.

A HCP ELISA and a dual stain Western blot were carried out. Each assay despite providing the same indication with an anti HCP antibody is very different. The ELISA for HCP removal is more sensitive when compared to the Western blot and quantitative. It measures the whole HCP and does not require any denaturation. The Western blot however is a very powerful tool to qualitatively determine HCP protein removal. Furthermore the Western blot can show the presence of product related band and confirm that no major structural changes have occurred. With the Western blot method however, denaturation with the use of a detergent is needed during electrophoresis, which can potentially destroy some antigenic determinants. Additionally some variants can be lost during the blotting protocol e.g. not transferred onto the membrane. Nonetheless the Western blot does allow the detection of multiple components with their relative molecular weight (Hoffman, 2000). As results are subject to individual user interpretation however a combination of both techniques (ELISA and Western blot) with the ELISA providing quantitative end point results is necessary.

An initial Western blot was carried out to show the removal of host cell proteins, seen in blue in Figure 8.3.5.2. A dual stain Western blot can subsequently be seen in Figure 8.3.5.3 with the retention of product specific functional IgG bands shown in red.

Sample ID	Product Concentration (mg/ml)	HCP Concentration (ng/ml)	HCP Concentration (ng/mg)	HCP removal (%)
CCS	2.29	114004	261069	
CCS Post UF	0.38	89022	33828	
CCC Post UF Run 1	0.36	27944	10060	96.11
CCC Post UF Run 2	0.32	25305	8098	
CCC Post UF Run 3	0.41	30064	12326	
Protein A IgG Std	15.12	<88.2	1323	99.49

Figure 8.3.5.1: HCP ELISA removal results using samples post non synchronous CCC with sample clean up using 5 kDa ultra filtration columns.

HCP removal by 96.11% post non synchcronous CCC and ultrafiltration was seen compared to a 99.49% HCP removal with the protein A purfied IgG control.

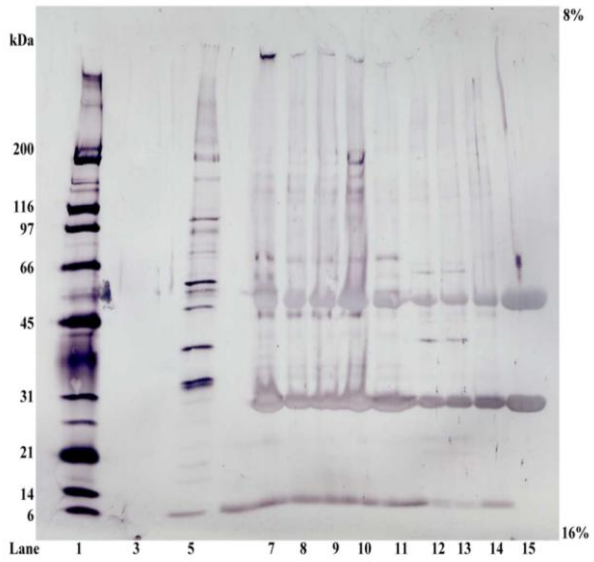

Lane	Sample ID
Lane 1	Molecular weight markers
Lane 3	BSA / IgG IAC
Lane 5	CHO HCP IAC
Lane 7	Cell culture supernatant
Lane 8	CCC Run 1
Lane 9	CCC Run 2
Lane 10	CCC Run 3
Lane 11	Cell culture supernatant (post UF)
Lane 12	CCC Run 1 (post UF)
Lane 13	CCC Run 2 (post UF)
Lane 14	CCC Run 3 (post UF)
Lane 15	Protein A purified IgG standard

Figure 8.3.5.2: Western blot, showing in' blue' the removal of HCPs. Samples following non synchronous CCC run at a Pr of 0.33. CCC samples that had not undergone sample clean up with 5KDa ultrafiltration column can be seen to appear smeared and are not clear showing interference with the assay.

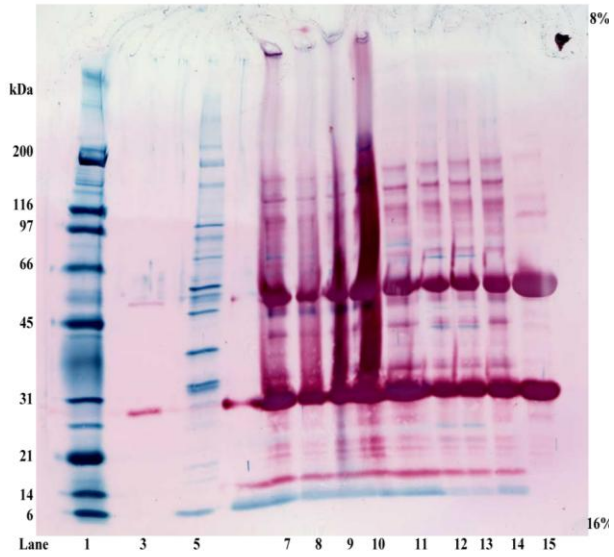

Lane	Sample ID
Lane 1	Molecular weight markers
Lane 3	BSA / IgG IAC
Lane 5	CHO HCP IAC
Lane 7	Cell culture supernatant
Lane 8	CCC Run 1
Lane 9	CCC Run 2
Lane 10	CCC Run 3
Lane 11	Cell culture supernatant (post UF)
Lane 12	CCC Run 1 (post UF)
Lane 13	CCC Run 2 (post UF)
Lane 14	CCC Run 3 (post UF)
Lane 15	Protein A purified IgG standard

Figure 8.3.5.3: Dual western blot, showing 'red' product related bands and the presence of any host cell proteins seen by the 'blue bands'. Samples following non synchronous CCC run at a Pr of 0.33. CCC samples that had not undergone sample clean up with 5KDa ultrafiltration column can be seen to interfere with the assay.

Following the Western blot to show the removal of HCP (Figure 8.3.5.2) it appeared that the CCC samples that had not undergone buffer exchange using ultrafiltration (lane 7 to 10) interfered with the assay. The phase system appeared to mask the IgG and smearing of the HCP band was evident. CCC samples post ultrafiltration however (lane 12-14) did not interfere with the assay and had a distinct banding profile. The necessity for sample clean up post CCC with ultrafiltration was demonstrated, to allow QC testing without any interference.

Results from the dual stain western blot (Figure 8.3.5.3) showed the presence of similar product related bands as shown in red, that was comparable to the Protein A purified IgG control. However it also showed the presence of many additional HCP bands (blue) that had not been removed by CCC processing, but were removed in the Protein A purified IgG control. Most specifically this was evident at 6kDa, additionally existing HCP could also be seen around 31-66kDa, this demonstrated that HCP proteins had not been removed to a comparable level to that of the Protein A purified IgG control.

2) Gel permeation HPLC

Gel permeation HPLC is used for the estimation of monomers and aggregates in IgG samples post purification. Structurally altered proteins which can arise during purification, processing and storage can lead to the formation of aggregates and precipitation. Stability

of proteins post purification is vital to avoid any major safety concerns in patients e.g. anaphylactoid reactions (Arakawa *et al*., 2006).

Gel permeation HPLC is based on the separation of molecules by their size or hydrodynamic volume, as opposed to their molecular weight. The column is packed with porous beads and molecule elution time is based on size. An example is shown in Figure 8.3.5.4, molecules of a larger hydrodynamic volume will elute first i.e. the aggregates followed by the monomer. The smaller anaylets i.e. fragment will be retained in the pores, thus eluted last with prolonged retention time. All components of the sample can consequently be separated out and the differing proportions of the sample calculated (aggregates, monomers and fragments).

The results of the non-synchronous CCC samples following gel permeation chromatography can be seen in Figure 8.3.5.5. The Protein A standard is compared to that of the CCS sample pre and post CCC. Samples are divided into the respective percentage of fragment, monomer and aggregates they contain. It can be seen that post CCC processing samples contained 84.01% monomers; this is compared to 99.45% seen with the protein A purified IgG standard. Post CCC processing samples also contained 2.04% of fragments. Aggregates levels however were higher than that of the protein A control at 10.96% following CCC processing, this compared to 0.55% with the protein A purified IgG control.

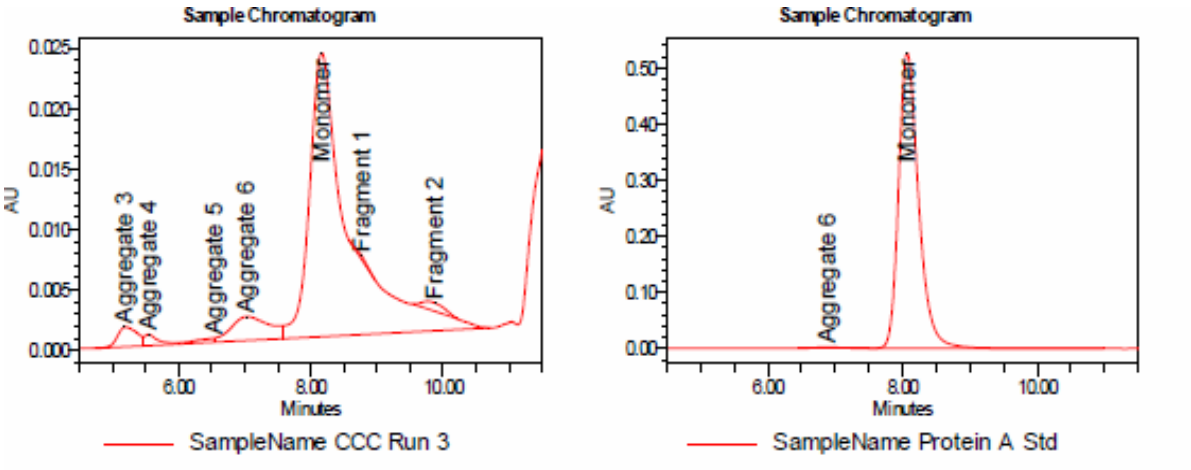

Figure 8.3.5.4: Example gel permeation HPLC chromatogram seen for CCC run 3 purified sample and the protein A purified IgG standard.

Sample name	Average (%)		
	Total fragment	Total monomer	Total aggregate
Protein A purified IgG standard	0.00	99.45	0.55
Control pre CCC	27.94	66.82	5.25
CCC purified sample post UF clean up	5.04	84.01	10.96

Figure 8.3.5.5: Gel permeation HPLC results averaged from triplicates from all samples tested post non synchronous CCC processing. Samples broken down into the respective percentages they contained of fragments, monomers and aggregates.

It could be seen that the CCS control prior to CCC had a low monomer percentage of 66.82 which could actually be due to the age of the sample. Ultimately it was seen that CCC processing, when compared to that of protein A HPLC, was producing aggregates and fragments not typically seen. The results were either due to the age of the samples or more likely the mixing and settling associated with CCC and the high PEG and salt concentrations.

3) Isoelectric focussing

Isoelectric focusing was used to determine if any structural changes had occurred during CCC processing which would be evident from the resulting banding pattern. With isoelectric focusing proteins are separated on the basis of their isoelectric point (pI), which is the pH at which the protein has no net charge.

To enable isoelectric focussing, proteins are loaded onto a polyacrylamide gel and an immobilised pH gradient strips containing a fixed pH gradient is affixed to the gel. By the use of an electrical field migration of proteins through the pH gradient is possible, until they reach their pI. The resolving power of isoelectric focusing has been demonstrated as much higher than normal electrophoresis, where proteins of the same size would be resolved as a single band (Maguire, 2006).

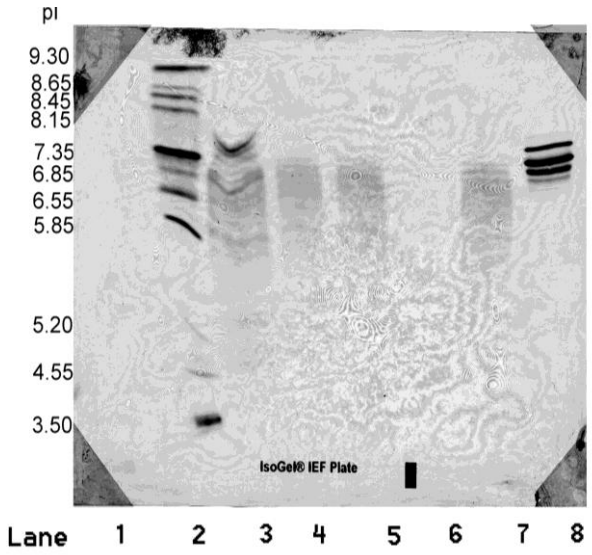

Lane	Sample ID	pI range
2	pI Markers	n/a
3	CCS	3.50-8.15
4	CCC post UF Run1	5.20-8.45
5	CCC post UF Run2	5.20-8.45
6	Blank	n/a
7	CCC post UF Run3	5.20-8.45
8	Protein A Standard	6.55-8.15

Figure 8.3.5.6: *Isoelectric focusing results using non synchronous CCC samples post ultrafiltration sample clean up from runs 1, 2 and 3. Samples separated according to their pI as labelled on the left hand side of the gel.*

Isoelectric focussing results and the respective pI range for each sample can be seen in Figure 8.3.5.6. With the CCC samples (Lane 4, 5 and 7) additional bands are present when compared to the PA purified IgG control. The pI range spans 5.20-8.45 with the CCC samples while only from 6.55-8.15 with the protein A purified IgG control. The presence of these additional bands seems to suggest that a structural change has occurred during the CCC purification run. A modification of amino acid residues on side chains, affecting protein charge could also have occurred.

4) qPCR

Quantitative PCR (qPCR) is used to demonstrate the removal of free DNA. Monoclonal antibody production is by recombinant DNA technology, where therapeutic proteins are secreted outside of mammalian cells into the surrounding culture medium. It is therefore a regulatory requirement to obtain a final product with less than 100 pg of cellular DNA per dose (as stated at Lonza). This is especially important as mAb are taken over prolonged periods of time with repeat injections. CCC samples were subject to qPCR and the resulting free DNA in corresponding samples is listed in Figure 8.3.3.8. The results showed that for all three runs the CCC samples showed the removal of free DNA to similar levels.

Sample	Protein Conc mg/ml	Results pg/ml	Results pg/mg
CCS Post UF	0.38	6949.7	18288.7
CCC Post UF Run 1	0.36	735.2	2042.2
CCC Post UF Run 2	0.32	1156.5	3614.2
CCC Post UF Run 3	0.41	1152.5	2811.1
STD error: CCC Post UF	0.03	139.77	453.83
Protein A IgG Standard	43.00		

Figure 8.3.5.7: qPCR results for the removal of free DNA post non synchronous CCC processing. The samples are compared to that of the protein A purified IgG standard.

Post CCC processing a tenfold drop in free DNA was seen (Figure 8.3.5.7). However when compared with the protein A purified IgG control (43pg/mg of free DNA) the CCC processing (average of 2822.5pg/mg of free DNA) had a difference of removal of >65 fold.

8.3.6 Summary of results

Results from the QC testing conducted for the non-synchronous CCC samples are tabulated in Figure 8.3.6.1 and compared to those routinely achieved for samples following Protein A purification. The table is listed such that each QC assay is described in terms of the reason for investigation and then the results achieved by both purification methods.

The non-synchronous CCC samples appeared out of the QC assay specification set by Lonza for samples tested following Protein A purification. The CCC samples had > 7 fold more HCP (measured in ng/ml) presents with those of a lower molecular weight (6kDa) persisting. By isoelectric focusing it was seen that the pI range of the CCC samples had been extended. By gel permeation chromatography monomer levels were at 84.01% as compared to the expect ≥98% seen post PA HPLC purification, furthermore a degree of aggregation was seen in samples (10.96%). Whilst a >281 fold difference in the removal of free DNA was seen when the samples were compared post qPCR.

QC assay	Investigation of	Non synchronous CCC QC results	Specification set at Lonza following protein A purification
HCP ELISA	Removal of host cell proteins (HCP)	• 27771 ng/mg	• ≤ 50 ng/mg
HCP western blot	Removal of host cell proteins (HCP)	• Removal of most HCP but low 6kDa HCP proteins still present. • 4 HCP bands still present	• Removal of all HCP bands
Isoelectric focussing	Structural changes	• pI range extended to 5.20-8.45 with the CCC sample from that of 6.55-8.51 for the PA purified IgG control. • Additional bands present suggest structural change had occurred.	• PI range from 6-8.5
Gel permeation chromatography	Aggregation	• Monomers: 84.01% • Fragments: 5.04% • Aggregates: 10.96%	• Monomers: ≥ 98% • Aggregates: ≤2%
qPCR	Removal of free DNA	• 2811.1 pg/mg remaining	• ≤10pg/ml

Figure 8.3.6.1: Comparison of QC results following non synchronous CCC processing to that of protein A purification.

Despite the clear need for optimisation of CCC samples to reach the required industry quality level, the results were promising. They showed a positive indication for the non-synchronous CCC for the separation of biologics. The reduction of aggregates formation during CCC runs however is critical. The focus of work now needs to be on assessing how CCC could be aligned with other techniques and then a re-evaluation of QC testing. As these non-synchronous CCC conditions have only been optimised to allow a separation that retains IgG biological activity many other lines of investigation e.g. use of differing phase systems such as ionic liquids etc must be considered, which may impact on QC data.

8.4 Conclusions

Following the development of fundamental operating parameters (Chapter 7) purified non synchronous CCC samples were characterised by a range of Lonza quality assurance assays. CCC fractions were prepared in triplicate and reproducibility was noted.

Sample clean up by the PD-10 columns, which function based on size exclusion, were seen to be unsuitable for the mAb and perhaps more suited to globular proteins. The PEG was seen to displace the IgG, resulting in the IgG being lost in the flow through rather than being retained by the pores and collected with elution buffers. A more suitable method of sample clean-up was found following investigation with Vivaspin ultrafiltration columns. These allowed buffer exchange of the IgG from the phase system to Lonza formulation buffer. Furthermore they also allowed > 100% IgG mass recovery when a 5kDa cut off size was used. These columns were demonstrated to sufficiently removed PEG as seen by Child's assay.

When CCC samples were analysed by QC assays, 96.11% of the HCP had been removed as demonstrated by the ELISA. The presence of the HCP bands that had not been removed during CCC processing were evident with the Western blot, most specifically a prominent band at 6kDa. In total 4 HCP bands were still present in the CCC samples, compared to all HCP being removed in the Protein A purified IgG control. A tenfold removal of free DNA was demonstrated by qPCR with the CCC samples (2811.1 pg/ml) as opposed to only 43pg/mg of free DNA being present in the Protein A purified IgG control.

Isoelectric focussing was used to detect any structural changes post CCC processing; the pI range for the CCC samples had been extended to 5.20-8.45 from that of 6.55-8.51 of the Protein A purified IgG control. The presence of these additional bands suggested structural changes had occurred. These results were further confirmed by gel permeation chromatography which showed the monomer levels (usually > 98% with Protein A HPLC purified IgG) was only 84.01% with the CCC samples and as a result gave rise to 10.96% aggregates and 5.04% fragments.

The initial QC assay data showed that impurity reduction is possible; however significant future optimisation work is required. The work within this project has

culminated in finding a biological operating condition that allows both IgG purification and the retention of biological activity. Further work is required to optimise these conditions such that purity can be increased. These fundamentals must primarily be addressed to allow the industrial uptake of the technique and future comparison with PA purification to be drawn.

CHAPTER 9: General discussion, conclusions and future work

9) General discussion, conclusions and future work

The work detailed within this thesis demonstrates for the first time the separation of monoclonal antibody from crude cell culture supernatant by CCC. Moreover the ability to attain a high resolution separation with the full retention of mAb biological activity has been shown. This fundamental work for the separation of biologics by CCC has allowed the determination of the required critical operating parameters. Furthermore the removal of most impurities has been demonstrated. Positive indications have been seen that further future optimisation would allow CCC purified samples the potential to approach industry standard. Ultimately CCC does not have to match Protein A purification, modification of the whole purification process would allow other remaining impurities to be removed. CCC also demonstrates a clear benefit compared to PA purification in terms of cost of goods. Protein A resin is currently priced around £10,000/L, with a maximum of 100 reuse cycles possible. Once the initial purchase and implementation cost of CCC had been considered all further expenditure would just be on consumables (e.g polymers and salt), that are considerable cheaper than the Protein A resin.

Key to a successful biological separation by CCC is the choice of phase system employed. The systematic and logical approach offered by a liquid handling program was used in this work, allowing the creation of an array of various ATPS, with the mAb incorporated. In comparison to previous robotic work with aqueous organic systems (Garrrard, 2005), significant changes were made to robotic programming, mainly due to the nature of the ATPS. A Protein A HPLC analytical method was developed to tolerate the phase system, allowing the respective partition coefficients (K) of the mAb within phase systems to be calculated. Partition coefficients (K) were calculated for each ATPS, by the ratio of the mAb partitioning between upper to lower phase. The PEG 1000 17.5%/17.5% sodium citrate system was highlighted as the most appropriate based on a high IgG recovery (>85% of that of the Protein A purified IgG control) and a partition coefficient in the range of 0.5-2.

It was previously highlighted in the literature review that column design was vital to permit high g force, high vigour mixing and sufficient stationary phase retention. These factors were thought imperative to accomplish protein separation by CCC. The majority of protein separation successes were therefore seen with hydrostatic machines, that permitted more vigorous cascade mixing. However, surprisingly and

completely against conventional wisdom, it was uncovered within this project that the choice of CCC machine affected the recovery of functional mAb. Hydrostatic CCC columns (CPC and TC CCC) with different degrees of mixing vigour were seen to cause IgG degradation. The highest IgG recovery seen with the hydrostatic machines was only 70%, despite separation from impurities being achieved, as shown by SDS PAGE and silver stain. A relatively higher recovery of 80% of IgG biological activity was seen with the hydrodynamic Mini CCC, however resolution of the IgG from impurities was lost with this wavelike mixing. Essentially a loss in the ability of IgG to bind to Protein A post CCC purification (in both hydrostatic and hydrodynamic machines) was seen. The CCC machine appeared to adversely affect IgG functionality, creating an unfunctional form termed Protein A non-binding IgG.

Auxiliary quantitative confirmation of the loss in IgG functionality by the use of Biacore analysis was obtained. Purified IgG following CCC had a reduced binding affinity to Protein A. The results indicated that only a weak binding association existed post CCC, rendering the IgG partially functional. In addition the degradation of model protein Myoglobin was seen post CCC with the production of Apomyoglobin, which was Myoglobin missing its haem group. The damage was thus confirmed and evident in more robust small protein molecules. Following a review of the literature, it appeared that biological recovery post CCC was frequently just assumed, and even those that did investigate it suffered losses.

Attempts at reversing or ceasing the production of this non-functional form by temperature, pH and sonication were not successful. Investigation into a number of stages of CCC processing was conducted including IgG phase system incubation and mixing within the machine itself. No loss in the IgG biological activity was seen following phase system incubation (up to 50ºC) and when samples were subject to spinning at a constant g force. A custom built shaker was designed and investigated to emulate the mixing occurring in a CCC machine. It allowed the relationship between the phase system, the shearing effect, mixing vigour and the sample itself (PA purified IgG and CCS) to be investigated without the additional complications of stationary phase retention and flow rate in a CCC machine. Loss in IgG functionality was seen to involve a combination of factors rather than a single underlying cause. The presence of other protein components (anti-foaming agents, host cell proteins) in the CCS, which increased the total protein concentration were seen to affect the retention of IgG functionality. The interface of the

phase system was also highlighted to cause a loss of the IgG functionality. Losses however were still seen when the IgG was processed in a single phase (most greatly in the salt phase), however not to the same level of degradation as in the phase system. The motion of mixing or agitation even within one phase was hence suggested sufficient to cause IgG damage, which would be exacerbated when both phases were mixed together.

Flow rate was determined as a foremost parameter in affecting IgG functionality. Increased flow rates allowed shorter CCC run times, consequently reducing the transit time of the IgG within the machine and significantly increasing the retention of functional IgG. However this increased flow rate conversely reduced IgG resolution from impurities. A reduction in rotational speed also improved the retention of IgG activity, but again to the detriment of the IgG peak width.

Such losses in IgG biological activity could not gain regulatory acceptance or be used to exhibit the potential of CCC processing for industrial uptake. The need for a modification in CCC design was demonstrated as crucial within this work. The instruments had clearly been designed for more robust small molecule separation, as opposed to fragile larger biologics. An optimal CCC mode, to allow the retention of IgG biological activity whilst attaining a separation, was found to be the non-synchronous CCC machine. The novel machine, when operated in a hydrodynamic mode, allowed the independent control of mixing and settling, which was exploited to allow increased rotor to bobbin rotations (Pr ratio). With a J type Mini CCC the Pr ratio is fixed at 1; with non-synchronous CCC this Pr ratio can be changed. As constraints were seen with this 1:1 ratio with the use of ATPS for protein separations, the Pr ratio was reduced to 0.33, allowing reduced mixing and increased settling time. Retention of IgG biological activity was seen with sharp, high resolution separation of the IgG from impurities. This was the first time this had been achieved with any CCC machine tested thus far. Improvements of loading capacity from 1.34mg to 20.26mg (tenfold) was additionally demonstrated with the maintenance of purity (>85%).

The most critical parameters noted in the study of this mAb separation and resulting CCC operational mode was settling time. Vigorous mixing was seen to be secondary to settling, despite mixing previously being considered in the literature as key, to allow sufficient mass transfer between the ATPS. Work within this project has shown vigorous mixing is not required due to the low interfacial tension, resultant from a minimal

density differences between phases. For aqueous organic systems, however, this is a critical requirement. However, adequate settling time, where IgG can experience mass transfer is vital. Which was further highlighted at a Pr ratio of 0.67, this level of settling for the amount of mixing offered was not sufficient. A loss in both IgG biological activity and resolution from impurities was seen. The use of the correct 0.33 Pr ratio, in the case of this mAb, has been seen to underpin the whole CCC separation. As a result the varying g force range associated with this machine was relatively much lower.

The clear relationship of increased g force ranges created by various machines (both hydrostatic and hydrodynamic) and degradation to IgG functionality were highlighted by the use of a g force program. A significantly lower g force was created with the non-synchronous machine especially at a Pr ratio of 0.33. IgG degradation was not resultant on a single parameter; however g force created within the machine itself was clearly a major factor.

Ultimately purified non-synchronous CCC samples using fundamentally determined operating parameters were characterised by a range of Lonza quality control. The necessity for sample clean up prior to the quality control analysis was seen and ultrafiltration columns at a cut off of 5kDa were used. The removal of PEG was further confirmed by the Child's assay. The QC assays demonstrated the removal of 96.11% of host cell protein (HCP) by ELISA. By Western blot, results were observed qualitatively, four HCPs post CCC processing were not removed. Most specifically a prominent band at 6kDa remained; this was in comparison to the Protein A purified IgG control where all bands were removed. A tenfold removal of free DNA was demonstrated by qPCR with the CCC samples (2811.1 pg/mg) as opposed to only 43pg/mg of free DNA being present in the Protein A purified IgG control. Structural changes in CCC purified IgG were also seen by isoelectric focussing, by the presence of additional bands. The pI range for the CCC samples had been extended to 5.20-8.45 from that of 6.55-8.51 of the Protein A purified IgG control. These results were further confirmed by gel permeation chromatography which showed monomer levels (usually > 98% with Protein A HPLC purified IgG) was 84.01% with the CCC samples and as a result gave rise to 10.96% aggregates and 5.04% fragments. The initial QC assay data has shown that impurity reduction is possible; however significant future optimisation work is required to allow purification of product to the required level.

All the aims and objectives outlined in Chapter 1 have been met. A multiprobe robotic programme was developed to allow the investigation of mAb partitioning in a number of varying ATPS. Furthermore by the development of a Protein A HPLC analysis method, for mAb partitioning in a variety of phase systems was analytically determined. The completely unexpected loss in IgG functionality by various CCC machines resulted in the initially predicted hydrostatic CCC machines for protein separation being inappropriate. An optimal non-synchronous CCC machine was found. With significant optimisation and insight obtained from previous CCC runs, operating conditions were determined. These optimal operation conditions culminated in developing a CCC mode that allowed the retention of IgG biological activity whilst attaining high resolution separation. Furthermore, this proof of concept work has been seen via Lonza quality control testing to allow the removal of some impurities. Further work is required to optimise these conditions such that purity can be increased and structural changes avoided. The resulting verdict from the studies in this chapter showed indications of promise for the non-synchronous CCC mode in monoclonal antibody separation from bioreactor cell culture supernatant.

Future work is required to focus on preventing the structural changes that have been indicated by CCC. These fundamentals must be studied primarily to allow industrial uptake of the technique and furthermore any future comparison with PA purification to be conducted.

Another area of future work is the sample loading capacity of the non-synchronous CCC. A major limiting factor with CCC is the requirement for the sample to be prepared in the ATPS, so as to not perturb the running of the machine. Consequently this adds a dilution effect and must be balanced with the effect this had on resolution of the IgG from impurities. However from an engineering stance, the non-synchronous CCC coils can be tailored to this particular separation to allow the efficient use of the coil, resulting in increased throughput. The non-synchronous CCC coils used for the studies in this thesis were based on an academic model. The beta values of the coil could be changed depending on the Pr ratio. Therefore it was estimated that currently with the use of this non-synchronous CCC at a Pr ratio of 0.33, that only one third of the coil was being actively used, the remaining coil was filled with mobile phase. By an engineering change, where the coils are constructed based on a specific Pr ratio such that the beta values are continual and not variable, all of the coil could be efficiently used. Future work would allow

consideration of this, such that future to maximum coil volume usage is possible, which will ultimately increase the sample throughput.

A key benefit of the non-synchronous CCC, when compared to that of the Protein A chromatography is the cost reduction it offers. After the initial purchase of the machine and implementation into a manufacturing facility the only major costs that will be incurred are the purchase of the PEG and salt components. When this is compared to the cost of the Protein A resin it is much more economical. Additionally, future work can be conducted into polymer recycling, thermo separating polymers and also the use of ionic liquids, to further reduce the cost. As this work has shown, this technique could be useful on a small scale for the purification of high value product such as growth hormones or factors.

In conclusion, this work has indicated that monoclonal antibody purification by CCC is possible and an economically feasible alternative to Protein A purification. Significant future work however, is needed to allow samples to reach industry standard.

Appendix

The presentation of aspects of this thesis at various conferences is detailed:

***1) Bioprocessing UK,* Glasgow, Dec 2011 (Poster, bursary prize winner)**

Finding the balance between the retention of monoclonal antibody (mAb) biological activity and attaining a separation using Counter Current Chromatography (CCC)

***2) Biopartitioning and purification,* Mexico, Sept 2011 (Oral platform presentation)**

Finding the balance between the retention of monoclonal antibody (mAb) biological activity and attaining a separation using Counter Current Chromatography (CCC)

***3) CCC 2010*, Lyon, France, Jul 2010 (Poster)**

Monoclonal antibody purification using robotic phase system selection coupled with counter current chromatography (CCC)

***4) Bioprocessing UK,* York, Nov 2009 (Poster, bursary prize winner)**

Monoclonal antibody purification using robotic phase system selection coupled with counter current chromatography (CCC)

***5) Biopartitioning and purification*, London, 2008 (poster)**

Rapid ATPS selection method based on a liquid handling robot

References

Ahlstedt, S., Holmgren, J. & Hanson, L.A. (1973) "The validity of the ammonium sulphate precipitation technique of estimation of antibody amount and avidity", *Immunology,* vol. 25, no. 6, pp. 917-922.

Ahmed Samatou, J., Engbert Wentink, A., Alexandra J.Rosa, P., Margarida Azevedo, A., Raquel Aires-Barros, M., Bäcker, W. & Górak, A. (2007) "Modeling of counter current monoclonal antibody extraction using aqueous two-phase systems" in *Computer Aided Chemical Engineering*, ed. Valentin Pleşu and Paul Şerban Agachi, Elsevier, , pp. 935-940.

Albertsson, P.-., Sasakawa, S. & Walter, H. (1970) "Cross partition and isoelectric points of proteins", *Nature,* vol. 228, no. 5278, pp. 1329-1330.

Aldington, S. & Bonnerjea, J. (2007) "Scale-up of monoclonal antibody purification processes", *Journal of Chromatography B: Analytical Technologies in the Biomedical and Life Sciences,* vol. 848, no. 1, pp. 64-78.

Alkan, S.S. (2004) "Monoclonal antibodies: The story of a discovery that revolutionized science and medicine", *Nature Reviews Immunology,* vol. 4, no. 2, pp. 153-156.

Andrews, B.A., Schmidt, A.S. & Asenjo, J.A. (2005) "Correlation for the partition behavior of proteins in aqueous two-phase systems: Effect of surface hydrophobicity and charge", *Biotechnology and bioengineering,* vol. 90, no. 3, pp. 380-390.

Arend, W.P. & Mannik, M. (1974) "Determination of soluble immune complex molar composition and antibody association constants by ammonium sulfate precipitation", *Journal of Immunology,* vol. 112, no. 2, pp. 451-461.

Asenjo, J.A. & Andrews, B.A. (2008) "Challenges and trends in bioseparations", *Journal of Chemical Technology and Biotechnology,* vol. 83, no. 2, pp. 117-120.

Asenjo, J.A. & Andrews, B.A. "Aqueous two-phase systems for protein separation: A perspective", *Journal of Chromatography A,* vol. In Press, Corrected Proof.

Azevedo, A.M., Rosa, P.A.J., Ferreira, I.F. & Aires-Barros, M.R. (2007) "Optimisation of aqueous two-phase extraction of human antibodies", *Journal of Biotechnology,* vol. 132, no. 2, pp. 209-217.

Azevedo, A.M., Rosa, P.A.J., Ferreira, I.F. & Aires-Barros, M.R. (2008) "Integrated process for the purification of antibodies combining aqueous two-phase extraction, hydrophobic interaction chromatography and size-exclusion chromatography", *Journal of Chromatography A,* vol. 1213, no. 2, pp. 154-161.

Azevedo, A.M., Ferreira, G.N.M. & Aires-Barros, M.R. (2009) "Advances in biopartitioning and purification", *Separation and Purification Technology,* vol. 65, no. 1, pp. 1-2.

Azevedo, A.M., Gomes, A.G., Rosa, P.A.J., Ferreira, I.F., Pisco, A.M.M.O. & Aires-Barros, M.R. (2009) "Partitioning of human antibodies in polyethylene glycol–sodium citrate aqueous two-phase systems", *Separation and Purification Technology,* vol. 65, no. 1, pp. 14-21.

Azevedo, A.M., Rosa, P.A.J., Ferreira, I.F. & Aires-Barros, M.R. (2009) "Chromatography-free recovery of biopharmaceuticals through aqueous two-phase processing", *Trends in biotechnology,* vol. 27, no. 4, pp. 240-247.

Azevedo, A.M., Rosa, P.A.J., Ferreira, I.F., de Vries, J., Visser, T.J. & Aires-Barros, M.R. (2009) "Downstream processing of human antibodies integrating an extraction capture step and cation exchange chromatography", *Journal of Chromatography B,* vol. 877, no. 1-2, pp. 50-58.

Baker, M. (2005) "Upping the ante on antibodies", *Nature biotechnology,* vol. 23, no. 9, pp. 1065 1072.

Balasubramaniam, D., Wilkinson, C., Van Cott, K. & Zhang, C. (2003) "Tobacco protein separation by aqueous two-phase extraction", *Journal of Chromatography A,* vol. 989, no. 1, pp. 119-129.

Becker, J.S., Thomas, O.R.T. & Franzreb, M. (2009) "Protein separation with magnetic adsorbents in micellar aqueous two-phase systems", *Separation and Purification Technology,* vol. 65, no. 1, pp. 46-53.

Benavides, J. & Rito-Palomares, M. (2004) "Bioprocess intensification: A potential aqueous two-phase process for the primary recovery of B-phycoerythrin from Porphyridium cruentum", *Journal of Chromatography B: Analytical Technologies in the Biomedical and Life Sciences,* vol. 807, no. 1, pp. 33-38.

Benavides, J., Aguilar, O., Lapizco-Encinas, B.H. & Rito-Palomares, M. (2008) "Extraction and purification of bioproducts and nanoparticles using aqueous two-phase systems strategies", *Chemical Engineering and Technology,* vol. 31, no. 6, pp. 838-845.

Bérot, S., Le Goff, E., Foucault, A. & Quillien, L. (2007) "Centrifugal partition chromatography as a tool for preparative purification of pea albumin with enhanced yields", *Journal of Chromatography B,* vol. 845, no. 2, pp. 205-209.

Berthod, A. & Carda-Broch, S. (2004) "Determination of liquid-liquid partition coefficients by separation methods", *Journal of Chromatography A,* vol. 1037, no. 1-2, pp. 3-14.

Berthod, A., Ruiz-Ángel, M.J. & Carda-Broch, S. (2008) "Ionic liquids in separation techniques", *Journal of Chromatography A,* vol. 1184, no. 1-2, pp. 6-18.

Berthod, A., Ruiz-Ángel, M.J. & Carda-Broch, S. (2009) "Countercurrent chromatography: People and applications", *Journal of Chromatography A,* vol. 1216, no. 19, pp. 4206-4217.

Bibila, T.A. & Robinson, D.K. (1995) "In pursuit of the optimal fed-batch process for monoclonal antibody production", *Biotechnology progress,* vol. 11, no. 1, pp. 1-13.

Binyamin, L., Borghaei, H. & Weiner, L.M. (2006) "Cancer therapy with engineered monoclonal antibodies", *Update on Cancer Therapeutics,* vol. 1, no. 2, pp. 147-157.

Birch, J.R. & Racher, A.J. (2006) "Antibody production", *Advanced Drug Delivery Reviews,* vol. 58, no. 5-6, pp. 671-685.

Bourton E. (2008) “Countercurrent chromatography of proteins using aqueous two-phase systems”, PhD thesis, Brunel institute for Bioengineering, Brunel university, UK.

Brekke, O.H. & Sandlie, I. (2003) "Therapeutic antibodies for human diseases at the dawn of the twenty-first century", *Nature Reviews Drug Discovery,* vol. 2, no. 1, pp. 52-62.

Cao, X., Hu, G., Huo, L., Zhu, X., Li, T., Powell, J. & Ito, Y. (2008) "Stationary phase retention and preliminary application of a spiral disk assembly designed for high-speed counter-current chromatography", *Journal of Chromatography A*, vol. 1188, no. 2, pp. 164-170.

Chen, J., Ma, G.X. & Li, D.Q. (1999) "HPCPC separation of proteins using polyethylene glycol-potassium phosphate aqueous two-phase", *Preparative Biochemistry and Biotechnology*, vol. 29, no. 4, pp. 371-383.

Chen, J., Tetrault, J. & Ley, A. (2008) "Comparison of standard and new generation hydrophobic interaction chromatography resins in the monoclonal antibody purification process", *Journal of Chromatography A*, vol. 1177, no. 2, pp. 272-281.

Chen, L., Zhang, Q., Yang, G., Fan, L., Tang, J., Garrard, I., Ignatova, S., Fisher, D. & Sutherland, I.A. (2007) "Rapid purification and scale-up of honokiol and magnolol using high-capacity high-speed counter-current chromatography", *Journal of Chromatography A*, vol. 1142, no. 2, pp. 115-122.

Chon, J.H. & Zarbis-Papastoitsis, G. (2011) "Advances in the production and downstream processing of antibodies", *New Biotechnolog*,.

Clausen, A.M., Subramanian, A. & Carr, P.W. (1999) "Purification of monoclonal antibodies from cell culture supernatants using a modified zirconia based cation-exchange support", *Journal of Chromatography A*, vol. 831, no. 1, pp. 63-72.

Conway, W.D. (1991) "Counter-current chromatography", *Journal of Chromatography A*, vol. 538, no. 1, pp. 27-35.

Conway, W.D. (2000) "chromatography| Countercurrent Chromatography and High Speed Countercurrent Chromatography: Instrumentation" in *Encyclopedia of Separation Science*, ed. Ian D. Wilson, Academic Press, Oxford, pp. 365-374.

D'Agostino, B., Bellofiore, P., De Martino, T., Punzo, C., Rivieccio, V. & Verdoliva, A. (2008) "Affinity purification of IgG monoclonal antibodies using the D-PAM synthetic ligand: chromatographic comparison with protein A and thermodynamic investigation of the D-PAM/IgG interaction", *Journal of immunological methods*, vol. 333, no. 1-2, pp. 126-138.

Dallora, N.L.P., Klemz, J.G.D. & Pessôa Filho, P.d.A. (2007) "Partitioning of model proteins in aqueous two-phase systems containing polyethylene glycol and ammonium carbamate", *Biochemical engineering journal*, vol. 34, no. 1, pp. 92-97.

de Belval, S., le Breton, B., Huddleston, J. & Lyddiatt, A. (1998) "Influence of temperature upon protein partitioning in poly(ethylene glycol)–salt aqueous two-phase systems close to the critical point with some observations relevant to the partitioning of particles", *Journal of Chromatography B: Biomedical Sciences and Applications*, vol. 711, no. 1-2, pp. 19-29.

Dembczynski, R., Bialas, W. & Jankowski, T. (2010) "Recycling of phase components during lysozyme extraction from hen egg white in the EO50PO50/K2HPO4 aqueous two-phase system", *Biochemical engineering journal*, vol. 51, no. 1-2, pp. 24-31.

Farid, S.S. (2007) "Process economics of industrial monoclonal antibody manufacture", *Journal of Chromatography B: Analytical Technologies in the Biomedical and Life Sciences*, vol. 848, no. 1, pp. 8-18.

, G. (2004) "Influence of high concentration monovalent cations on the protein partitioning in polyethyleneglycol 1500-phosphate aqueous two-phase systems", *Journal of Chromatography B: Analytical Technologies in the Biomedical and Life Sciences,* vol. 809, no. 2, pp. 301-306.

Fassina, G., Ruvo, M., Palombo, G., Verdoliva, A. & Marino, M. (2001) "Novel ligands for the affinity-chromatographic purification of antibodies", *Journal of Biochemical and Biophysical Methods,* vol. 49, no. 1-3, pp. 481-490.

Ferreira, I.F., Azevedo, A.M., Rosa, P.A.J. & Aires-Barros, M.R. (2008) "Purification of human immunoglobulin G by thermoseparating aqueous two-phase systems", *Journal of Chromatography A,* vol. 1195, no. 1-2, pp. 94-100.

Follman, D.K. & Fahrner, R.L. (2004) "Factorial screening of antibody purification processes using three chromatography steps without protein A", *Journal of Chromatography A,* vol. 1024, no. 1-2, pp. 79-85.

Garrard, I.J. (2005) "Simple approach to the development of a CCC solvent selection protocol suitable for automation", *Journal of Liquid Chromatography and Related Technologies,* vol. 28, no. 12-13, pp. 1923-1935.

Garrard I.J. (2005) "A systematic approach to the development of a countercurrent chromatography protocol with examples from polar, intermediate and non polar compounds". PhD thesis, Brunel institute for Bioengineering, Brunel university, UK.

Ghose, S., Hubbard, B. & Cramer, S.M. (2006) "Evaluation and comparison of alternatives to Protein A chromatography. Mimetic and hydrophobic charge induction chromatographic stationary phases", *Journal of Chromatography A,* vol. 1122, no. 1-2, pp. 144-152.

Ghosh, R. & Wang, L. (2006) "Purification of humanized monoclonal antibody by hydrophobic interaction membrane chromatography", *Journal of Chromatography A,* vol. 1107, no. 1-2, pp. 104-109.

Gopinath, S.C.B. (2010) "Biosensing applications of surface plasmon resonance-based Biacore technology", *Sensors and Actuators, B: Chemical,* vol. 150, no. 2, pp. 722-733.

Guan, Y., Lilley, T.H., Treffry, T.E., Zhou, C.-. & Wilkinson, P.B. (1996) "Use of aqueous two-phase systems in the purification of human interferon-α1 from recombinant Escherichia coli", *Enzyme and microbial technology,* vol. 19, no. 6, pp. 446-455.

Guan, Y.H., Fisher, D. & Sutherland, I.A. (2007) "Model for spiral columns and stationary phase retention in synchronous coil planet centrifuges", *Journal of Chromatography A,* vol. 1151, no. 1-2, pp. 136-141.

Guan, Y.H., Smulders, J., Fisher, D. & Sutherland, I.A. (2007) "Spiral coils for counter-current chromatography using aqueous polymer two-phase systems", *Journal of Chromatography A,* vol. 1151, no. 1-2, pp. 115-120.

Guan, Y.H., Bourton, E.C., Hewitson, P., Sutherland, I.A. & Fisher, D. (2009) "The importance of column design for protein separation using aqueous two-phase systems on J-type countercurrent chromatography", *Separation and Purification Technology,* vol. 65, no. 1, pp. 79-85.

Guan, Y.H., Fisher, D. & Sutherland, I.A. (2010) "Protein separation using toroidal columns by type-J synchronous counter-current chromatography towards preparative separation", *Journal of Chromatography A*, vol. 1217, no. 21, pp. 3525-3530.

Hober, S., Nord, K. & Linhult, M. (2007) "Protein A chromatography for antibody purification", *Journal of Chromatography B: Analytical Technologies in the Biomedical and Life Sciences*, vol. 848, no. 1, pp. 40-47.

Holschuh, K. & Schwammle, A. (2005) "Preparative purification of antibodies with protein A - An alternative to conventional chromatography", *Journal of Magnetism and Magnetic Materials*, vol. 293, no. 1, pp. 345-348.

Homola, J. (2003) "Present and future of surface plasmon resonance biosensors", *Analytical and Bioanalytical Chemistry*, vol. 377, no. 3, pp. 528-539.

Huang, Y., Hsu, H. & Huang, C.C. (2007) "A protein detection technique by using surface plasmon resonance (SPR) with rolling circle amplification (RCA) and nanogold-modified tags", *Biosensors and Bioelectronics*, vol. 22, no. 6, pp. 980-985.

Huddleston, J., Veide, A., Kohler, K., Flanagan, J., Enfors, S.-. & Lyddiatt, A. (1991) "The molecular basis of partitioning in aqueous two-phase systems", *Trends in biotechnology*, vol. 9, no. 11, pp. 381-388.

Huddleston, J., Abelaira, J.C., Wang, R. & Lyddiatt, A. (1996) "Protein partition between the different phases comprising poly(ethylene glycol)-salt aqueous two-phase systems, hydrophobic interaction chromatography and precipitation: a generic description in terms of salting-out effects", *Journal of Chromatography B: Biomedical Sciences and Applications*, vol. 680, no. 1-2, pp. 31-41.

Huse, K., Böhme, H.-. & Scholz, G.H. (2002) "Purification of antibodies by affinity chromatography", *Journal of Biochemical and Biophysical Methods*, vol. 51, no. 3, pp. 217-231.

Ibarra-Herrera, C.C., Aguilar, O. & Rito-Palomares, M. (2011) "Application of an aqueous two-phase systems strategy for the potential recovery of a recombinant protein from alfalfa (Medicago sativa)", *Separation and Purification Technology*, vol. 77, no. 1, pp. 94-98.

Ignatova, S., Hawes, D., van den Heuvel, R., Hewitson, P. & Sutherland, I.A. (2010) "A new non-synchronous preparative counter-current centrifuge-the next generation of dynamic extraction/chromatography devices with independent mixing and settling control, which offer a step change in efficiency", *Journal of Chromatography A*, vol. 1217, no. 1, pp. 34-39.

Ikehata, J., Shinomiya, K., Kobayashi, K., Ohshima, H., Kitanaka, S. & Ito, Y. (2004) "Effect of Coriolis force on counter-current chromatographic separation by centrifugal partition chromatography", *Journal of Chromatography A*, vol. 1025, no. 2, pp. 169-175.

Ikehata, J.-., Shinomiya, K. & Ito, Y. (2005) "Partition efficiencies of an eccentric coiled separation column for centrifugal partition chromatography", *Journal of Liquid Chromatography and Related Technologies*, vol. 28, no. 17, pp. 2807-2818.

Ito, Y. (1991) "Recent advances in counter-current chromatography", *Journal of Chromatography A*, vol. 538, no. 1, pp. 3-25.

Ito, Y. & Ma, Y. (1996) "pH-zone-refining countercurrent chromatography", *Journal of Chromatography A*, vol. 753, no. 1, pp. 1-36.

Ito, Y., Matsuda, K., Ma, Y. & Qi, L. (1998) "Toroidal coil counter-current chromatography study of the mass transfer rate of proteins in aqueous–aqueous polymer phase system", *Journal of Chromatography A,* vol. 802, no. 2, pp. 277-283.

Ito, Y. (2000) "Chromotography: Liquid | Countercurrent Liquid Chromatography" in *Encyclopedia of Separation Science*, ed. Ian D. Wilson, Academic Press, Oxford, pp. 573-583.

Ito, Y. (2000) "Ph-zone refining countercurrent chromtaography" in *Encyclopedia of Separation Science*, ed. Ian D. Wilson, Academic Press, Oxford, pp. 3815-3832.

Ito, Y. (2005) "Golden rules and pitfalls in selecting optimum conditions for high-speed counter-current chromatography", *Journal of Chromatography A,* vol. 1065, no. 2, pp. 145-168.

Ito, Y., Clary, R., Sharpnak, F., Metger, H. & Powell, J. (2007) "Mixer-settler counter-current chromatography with multiple spiral disk assembly", *Journal of Chromatography A,* vol. 1172, no. 2, pp. 151-159.

Ito, Y., Qi, L., Powell, J., Sharpnack, F., Metger, H., Yost, J., Cao, X., Dong, Y., Huo, L., Zhu, X. & Li, T. (2007) "Mixer-settler counter-current chromatography with a barricaded spiral disk assembly with glass beads", *Journal of Chromatography A,* vol. 1151, no. 1-2, pp. 108-114.

Ito, Y., Clary, R., Powell, J., Knight, M. & Finn, T.M. (2009) "Improved spiral tube assembly for high-speed counter-current chromatography", *Journal of Chromatography A,* vol. 1216, no. 19, pp. 4193-4200.

Ito, Y. (2010) "Spiral column configuration for protein separation by high-speed countercurrent chromatography", *Chemical Engineering and Processing: Process Intensification,* vol. 49, no. 7, pp. 782-792.

Jiang, Y., Li, F., Button, M., Cukan, M., Moore, R., Sharkey, N. & Li, H. (2010) "A high-throughput purification of monoclonal antibodies from glycoengineered Pichia pastoris", *Protein expression and purification,* vol. 74, no. 1, pp. 9-15.

Johansson, H., Karlström, G., Tjerneld, F. & Haynes, C.A. (1998) "Driving forces for phase separation and partitioning in aqueous two-phase systems", *Journal of Chromatography B: Biomedical Sciences and Applications,* vol. 711, no. 1-2, pp. 3-17.

Jungbauer, A. & Hahn, R. (2004) "Monoliths for fast bioseparation and bioconversion and their applications in biotechnology", *Journal of Separation Science,* vol. 27, no. 10-11, pp. 767-778.

Jungbauer, A. (2005) "Chromatographic media for bioseparation", *Journal of Chromatography A,* vol. 1065, no. 1, pp. 3-12.

Karakatsanis, A. & Liakopoulou-Kyriakides, M. (2007) "Comparison of PEG/fractionated dextran and PEG/industrial grade dextran aqueous two-phase systems for the enzymic hydrolysis of starch", *Journal of Food Engineering,* vol. 80, no. 4, pp. 1213-1217.

Kelley, B. (2007) "Very large scale monoclonal antibody purification: The case for conventional unit operations", *Biotechnology progress,* vol. 23, no. 5, pp. 995-1008.

Knight, M., Fagarasan, M.O., Takahashi, K., Geblaoui, A.Z., Ma, Y. & Ito, Y. (1995) "Separation and purification of peptides by high-speed counter-current chromatography", *Journal of Chromatography A,* vol. 702, no. 1-2, pp. 207-214.

Knight, M. (2007) "Separations of hydrophobic synthetic peptides in counter-current chromatography", *Journal of Chromatography A,* vol. 1151, no. 1-2, pp. 148-152.

Knight, M., Finn, T.M., Zehmer, J., Clayton, A. & Pilon, A. "Spiral counter-current chromatography of small molecules, peptides and proteins using the spiral tubing support rotor", *Journal of Chromatography A,* vol. In Press, Corrected Proof.

Knudsen, H.L., Fahrner, R.L., Xu, Y., Norling, L.A. & Blank, G.S. (2001) "Membrane ion-exchange chromatography for process-scale antibody purification", *Journal of Chromatography A,* vol. 907, no. 1-2, pp. 145-154.

Kobayashi, K., Ohshima, H., Shinomiya, K. & Ito, Y. (2005) "Analysis of acceleration produced by planetary motion in a nonsynchronous coil planet centrifuge", *Journal of Liquid Chromatography and Related Technologies,* vol. 28, no. 12-13, pp. 1839-1850.

Kumar, A., Srivastava, A., Galaev, I.Y. & Mattiasson, B. (2007) "Smart polymers: Physical forms and bioengineering applications", *Progress in Polymer Science (Oxford),* vol. 32, no. 10, pp. 1205-1237.

Lim, S., Manusu, H.P., Gooley, A.A., Williams, K.L. & Rylatt, D.B. (1998) "Purification of monoclonal antibodies from ascitic fluid using preparative electrophoresis", *Journal of Chromatography A,* vol. 827, no. 2, pp. 329-335.

Liu, C., Kamei, D.T., King, J.A., Wang, D.I.C. & Blankschtein, D. (1998) "Separation of proteins and viruses using two-phase aqueous micellar systems", *Journal of Chromatography B: Biomedical Sciences and Applications,* vol. 711, no. 1-2, pp. 127-138.

Low, D., O'Leary, R. & Pujar, N.S. (2007) "Future of antibody purification", *Journal of Chromatography B: Analytical Technologies in the Biomedical and Life Sciences,* vol. 848, no. 1, pp. 48-63.

Lu, M., Albertsson, P.-., Johansson, G. & Tjerneld, F. (1996) "Ucon-benzoyl dextran aqueous two-phase systems: Protein purification with phase component recycling", *Journal of Chromatography B: Biomedical Applications,* vol. 680, no. 1-2, pp. 65-70.

Luechau, F., Ling, T.C. & Lyddiatt, A. (2010) "A descriptive model and methods for up-scaled process routes for interfacial partition of bioparticles in aqueous two-phase systems", *Biochemical engineering journal,* vol. 50, no. 3, pp. 122-130.

Lyddiatt, A. (2002) "Process chromatography: current constraints and future options for the adsorptive recovery of bioproducts", *Current opinion in biotechnology,* vol. 13, no. 2, pp. 95-103.

Ma, J., Hoang, H., Myint, T., Peram, T., Fahrner, R. & Chou, J.H. (2010) "Using precipitation by polyamines as an alternative to chromatographic separation in antibody purification processes", *Journal of Chromatography B: Analytical Technologies in the Biomedical and Life Sciences,* vol. 878, no. 9-10, pp. 798-806.

Madeira, P.P., Xu, X., Teixeira, J.A. & Macedo, E.A. (2005) "Prediction of protein partition in polymer/salt aqueous two-phase systems using the modified Wilson model", *Biochemical engineering journal,* vol. 24, no. 2, pp. 147-155.

Magri, M.L., Cabrera, R.B., Miranda, M.V., Fernández-Lahore, H.M. & Cascone, O. (2003) "Performance of an aqueous two-phase-based countercurrent chromatographic system for horseradish peroxidase purification", *Journal of Separation Science*, vol. 26, no. 18, pp. 1701-1706.

Marchal, L., Foucault, A., Patissier, G., Rosant, J.M. & Legrand, J. (2000) "Influence of flow patterns on chromatographic efficiency in centrifugal partition chromatography", *Journal of Chromatography A*, vol. 869, no. 1-2, pp. 339-352.

Margraff, R., Intes, O., Renault, J.-. & Garret, P. (2005) "Partitron 25, a multi-purpose industrial centrifugal partition chromatograph: Rotor design and preliminary results on efficiency and stationary phase retention", *Journal of Liquid Chromatography and Related Technologies*, vol. 28, no. 12-13, pp. 1893-1902.

Marx, U., Embleton, M.J., Fischer, R., Gruber, F.P., Hansson, U., Heuer, J., De Leeuw, W.A., Logtenberg, T., Merz, W., Portetelle, D., Remette, J.-. & Straughan, D.W. (1997) "Monoclonal Antibody Production: The Report and Recommendations of ECVAM Workshop 23", *ATLA Alternatives to Laboratory Animals*, vol. 25, no. 2, pp. 121-137.

Matsuda, K., Matsuda, S. & Ito, Y. (1998) "Toroidal coil counter-current chromatography: Achievement of high resolution by optimizing flow-rate, rotation speed, sample volume and tube length", *Journal of Chromatography A*, vol. 808, no. 1-2, pp. 95-104.

Mattiasson, B., Dainyak, M.B. & Galaev, I.Y. (1998) "Smart polymers and protein purification", *Polymer - Plastics Technology and Engineering*, vol. 37, no. 3, pp. 303-308.

Mattiasson, B., Ling, T.G.I. & Ramstorp, M. (1982) "Binding assays involving separation in aqueous two-phase systems: partition affinity ligand assay (PALA).", *Enzyme Engineering: Proceedings of the International Enzyme Engineering Confrence*, pp. 359.

Menet, J., Shinomiya, K. & Ito, Y. (1993) "Studies on new cross-axis coil planet centrifuge for performing counter-current chromatography: III. Speculations on the hydrodynamic mechanism in stationary phase retention", *Journal of Chromatography A*, vol. 644, no. 2, pp. 239-252.

Merchuk, J.C., Andrews, B.A. & Asenjo, J.A. (1998) "Aqueous two-phase systems for protein separation: Studies on phase inversion", *Journal of Chromatography B: Biomedical Sciences and Applications*, vol. 711, no. 1-2, pp. 285-293.

Müller-Späth, T., Aumann, L., Ströhlein, G. & Morbidelli, M. (2009) "Improvement of specific monoclonal antibody (mAb) activity by reduction of the mAb heterogeneity using continuous chromatography (MCSGP)", *New Biotechnology*, vol. 25, no. Supplement 1, pp. S187-S187.

Müller-Späth, T., Krättli, M., Aumann, L., Ströhlein, G. & Morbidelli, M. (2010) "Increasing the activity of monoclonal antibody therapeutics by continuous chromatography (MCSGP)", *Biotechnology and bioengineering*, vol. 107, no. 4, pp. 652-662.

Müller-Späth, T., Ströhlein, G., Aumann, L., Kornmann, H., Valax, P., Delegrange, L., Charbaut, E., Baer, G., Lamproye, A., Jöhnck, M., Schulte, M. & Morbidelli, M. (2011) "Model simulation and experimental verification of a cation-exchange IgG capture step in batch and continuous chromatography", *Journal of Chromatography A*, vol. 1218, no. 31, pp. 5195-5204.

Murayama, W., Kobayashi, T., Kosuge, Y., Yano, H., Nunogaki, Y. & Nunogaki, K. (1982) "A new centrifugal counter-current chromatograph and its application", *Journal of Chromatography A,* vol. 239, pp. 643-649.

Pan, H., Chen, K., Pulisic, M., Apostol, I. & Huang, G. (2009) "Quantitation of soluble aggregates in recombinant monoclonal antibody cell culture by pH-gradient protein A chromatography", *Analytical Biochemistry,* vol. 388, no. 2, pp. 273-278.

Papalia, G.A., Baer, M., Luehrsen, K., Nordin, H., Flynn, P. & Myszka, D.G. (2006) "High-resolution characterization of antibody fragment/antigen interactions using Biacore T100", *Analytical Biochemistry,* vol. 359, no. 1, pp. 112-119.

Pei, Y., Wang, J., Wu, K., Xuan, X. & Lu, X. (2009) "Ionic liquid-based aqueous two-phase extraction of selected proteins", *Separation and Purification Technology,* vol. 64, no. 3, pp. 288-295.

Persson, J., Johansson, H.-. & Tjerneld, F. (1999) "Purification of protein and recycling of polymers in a new aqueous two-phase system using two thermoseparating polymers", *Journal of Chromatography A,* vol. 864, no. 1, pp. 31-48.

Peterson, E., Owens, S.M. & Henry, R.L. (2006) "Monoclonal antibody form and function: Manufacturing the right antibodies for treating drug abuse", *AAPS Journal,* vol. 8, no. 2, pp. E383-E390.

, G., Romanini, D., Nerli, B. & Farruggia, B. (2006) "Polyethyleneglycol molecular mass and polydispersivity effect on protein partitioning in aqueous two-phase systems", *Journal of Chromatography B: Analytical Technologies in the Biomedical and Life Sciences,* vol. 830, no. 2, pp. 286-292.

Platis, D. & Labrou, N.E. (2006) "Development of an aqueous two-phase partitioning system for fractionating therapeutic proteins from tobacco extract", *Journal of Chromatography A,* vol. 1128, no. 1-2, pp. 114-124.

Platis, D., Drossard, J., Fischer, R., Ma, J.K.-. & Labrou, N.E. (2008) "New downstream processing strategy for the purification of monoclonal antibodies from transgenic tobacco plants", *Journal of Chromatography A,* vol. 1211, no. 1-2, pp. 80-89.

Platis, D. & Labrou, N.E. (2009) "Application of a PEG/salt aqueous two-phase partition system for the recovery of monoclonal antibodies from unclarified transgenic tobacco extract", *Biotechnology Journal,* vol. 4, no. 9, pp. 1320-1327.

Przybycien, T.M., Pujar, N.S. & Steele, L.M. (2004) "Alternative bioseparation operations: Life beyond packed-bed chromatography", *Current opinion in biotechnology,* vol. 15, no. 5, pp. 469-478.

Qian, H., Li, C., Zhang, Y. & Lin, Z. (2009) "Efficient isolation of immunoglobulin G by paramagnetic polymer beads modified with 2-mercapto-4-mythyl-pyrimidine", *Journal of immunological methods,* vol. 343, no. 2, pp. 119-129.

Qu, F., Qin, H., Dong, M., Zhao, D.X., Zhao, X.Y. & Zhang, J.H. (2009) "Selective separation and enrichment of proteins in aqueous two-phase extraction system", *Chinese Chemical Letters,* vol. 20, no. 9, pp. 1100-1102.

Raghavarao, K.S.M.S., Rastogi, N.K., Gowthaman, M.K. & Karanth, N.G. (1995) "Aqueous Two-Phase Extraction for Downstream Processing of Enzymes/Proteins" in *Advances in Applied Microbiology*, ed. Saul L. Neidleman and Allen I. Laskin, Academic Press, , pp. 97-171.

Reichert, J. & Pavlou, A. (2004) "Monoclonal antibodies market. Market analysis", *Nature Reviews Drug Discovery,* vol. 3, no. 5, pp. 383-384.

Reichert, J.M. & Valge-Archer, V.E. (2007) "Development trends for monoclonal antibody cancer therapeutics", *Nature Reviews Drug Discovery,* vol. 6, no. 5, pp. 349-356.

Reichert, J.M. (2008) "Monoclonal antibodies as innovative therapeutics", *Current Pharmaceutical Biotechnology,* vol. 9, no. 6, pp. 423-430.

Rito-Palomares, M. & Lyddiatt, A. (2000) "Practical implementation of aqueous two-phase processes for protein recovery from yeast", *Journal of Chemical Technology and Biotechnology,* vol. 75, no. 7, pp. 632-638.

Rito-Palomares, M. & Lyddiatt, A. (2002) "Process integration using aqueous two-phase partition for the recovery of intracellular proteins", *Chemical Engineering Journal,* vol. 87, no. 3, pp. 313-319.

Roque, A.C.A. & Lowe, C.R. (2006) "Advances and applications of de novo designed affinity ligands in proteomics", *Biotechnology Advances,* vol. 24, no. 1, pp. 17-26.

Roque, A.C.A., Silva, C.S.O. & Taipa, M.A. (2007) "Affinity-based methodologies and ligands for antibody purification: Advances and perspectives", *Journal of Chromatography A,* vol. 1160, no. 1-2, pp. 44-55.

Rosa, P.A.J., Azevedo, A.M. & Aires-Barros, M.R. (2007) "Application of central composite design to the optimisation of aqueous two-phase extraction of human antibodies", *Journal of Chromatography A,* vol. 1141, no. 1, pp. 50-60.

Rosa, P.A.J., Azevedo, A.M., Ferreira, I.F., Sommerfeld, S., Bäcker, W. & Aires-Barros, M.R. (2009) "Downstream processing of antibodies: Single-stage versus multi-stage aqueous two-phase extraction", *Journal of Chromatography A,* vol. 1216, no. 50, pp. 8741-8749.

Rosa, P.A.J., Azevedo, A.M., Sommerfeld, S., Mutter, M., Aires-Barros, M.R. & Bäcker, W. (2009) "Application of aqueous two-phase systems to antibody purification: A multi-stage approach", *Journal of Biotechnology,* vol. 139, no. 4, pp. 306-313.

Rosa, P.A.J., Ferreira, I.F., Azevedo, A.M. & Aires-Barros, M.R. (2010) "Aqueous two-phase systems: A viable platform in the manufacturing of biopharmaceuticals", *Journal of Chromatography A,* vol. 1217, no. 16, pp. 2296-2305.

Rosa, P.A.J., Azevedo, A.M., Sommerfeld, S., Bäcker, W. & Aires-Barros, M.R. "Aqueous two-phase extraction as a platform in the biomanufacturing industry: Economical and environmental sustainability", *Biotechnology Advances,* vol. In Press, Corrected Proof.

Ross, K.C. & Zhang, C. (2010) "Separation of recombinant β-glucuronidase from transgenic tobacco by aqueous two-phase extraction", *Biochemical engineering journal,* vol. 49, no. 3, pp. 343-350.

Ruiz-Angel, M.J., Pino, V., Carda-Broch, S. & Berthod, A. (2007) "Solvent systems for countercurrent chromatography: An aqueous two phase liquid system based on a room temperature ionic liquid", *Journal of Chromatography A*, vol. 1151, no. 1-2, pp. 65-73.

Saravanan, S., Rao, J.R., Nair, B.U. & Ramasami, T. (2008) "Aqueous two-phase poly(ethylene glycol)–poly(acrylic acid) system for protein partitioning: Influence of molecular weight, pH and temperature", *Process Biochemistry*, vol. 43, no. 9, pp. 905-911.

Schwartz, W., Judd, D., Wysocki, M., Guerrier, L., Birck-Wilson, E. & Boschetti, E. (2001) "Comparison of hydrophobic charge induction chromatography with affinity chromatography on protein A for harvest and purification of antibodies", *Journal of Chromatography A*, vol. 908, no. 1-2, pp. 251-263.

Selber, K., Tjerneld, F., Collén, A., Hyytiä, T., Nakari-Setälä, T., Bailey, M., Fagerström, R., Kan, J., Van Der Laan, J., Penttilä, M. & Kula, M.-. (2004) "Large-scale separation and production of engineered proteins, designed for facilitated recovery in detergent-based aqueous two-phase extraction systems", *Process Biochemistry*, vol. 39, no. 7, pp. 889-896.

Selvakumar, P., Ling, T.C., Walker, S. & Lyddiatt, A. (2010) "A practical implementation and exploitation of ATPS for intensive processing of biological feedstock: A novel approach for heavily biological feedstock loaded ATPS", *Separation and Purification Technology*, vol. 75, no. 3, pp. 323-331.

Shen, C.-. & Yu, T. (2007) "Protein separation and enrichment by counter-current chromatography using reverse micelle solvent systems", *Journal of Chromatography A*, vol. 1151, no. 1-2, pp. 164-168.

Shibusawa, Y. & Ito, Y. (1991) "Protein separation with aqueous—aqueous polymer systems by two types of counter-current chromatographs", *Journal of Chromatography A*, vol. 550, pp. 695-704.

Shibusawa, Y., Mugiyama, M., Matsumoto, U. & Ito, Y. (1995) "Complementary use of counter-current chromatography and hydroxyapatite chromatography for the separation of three main classes of lipoproteins from human serum", *Journal of Chromatography B: Biomedical Sciences and Applications*, vol. 664, no. 2, pp. 295-301.

Shibusawa, Y., Mugiyama, M., Matsumoto, U. & ito, Y. (1995) "Complementary use of counter-current chromatography and hydroxyapatite chromatography for the separation of three main classes of lipoproteins from human serum", *Journal of Chromatography B: Biomedical Applications*, vol. 664, no. 2, pp. 295-301.

Shibusawa, Y., Eriguchi, Y. & Ito, Y. (1997) "Purification of lactic acid dehydrogenase from bovine heart crude extract by counter-current chromatography", *Journal of Chromatography B: Biomedical Applications*, vol. 696, no. 1, pp. 25-31.

Shibusawa, Y., Hagiwara, Y., Chao, Z., Ma, Y. & Ito, Y. (1997) "Application of high-speed counter-current chromatography to the separation of coumarin and related compounds", *Journal of Chromatography A*, vol. 759, no. 1-2, pp. 47-53.

Shibusawa, Y. (1997) "Lipoproteins: comparison of different separation strategies", *Journal of Chromatography B: Biomedical Sciences and Applications*, vol. 699, no. 1-2, pp. 419-437.

Shibusawa, Y., Eriguchi, Y. & Ito, Y. (1997) "Purification of lactic acid dehydrogenase from bovine heart crude extract by counter-current chromatography", *Journal of Chromatography B: Biomedical Sciences and Applications,* vol. 696, no. 1, pp. 25-31.

Shibusawa, Y., Kihira, S. & Ito, Y. (1998) "One-step purification of proteins from chicken egg white using counter-current chromatography", *Journal of Chromatography B: Biomedical Sciences and Applications,* vol. 709, no. 2, pp. 301-305.

Shibusawa, Y., Misu, N., Shindo, H. & Ito, Y. (2002) "Purification of lactic acid dehydrogenase from crude bovine heart extract by pH-peak focusing counter-current chromatography", *Journal of Chromatography B: Analytical Technologies in the Biomedical and Life Sciences,* vol. 776, no. 2, pp. 183-189.

Shibusawa, Y., Ino, Y., Kinebuchi, T., Shimizu, M., Shindo, H. & Ito, Y. (2003) "Purification of single-strand DNA binding protein from an Escherichia coli lysate using counter-current chromatography, partition and precipitation", *Journal of Chromatography B,* vol. 793, no. 2, pp. 275-279.

Shibusawa, Y., Fujiwara, T., Shindo, H. & Ito, Y. (2004) "Purification of alcohol dehydrogenase from bovine liver crude extract by dye–ligand affinity counter-current chromatography", *Journal of Chromatography B,* vol. 799, no. 2, pp. 239-244.

Shibusawa, Y., Takeuchi, N., Sugawara, K., Yanagida, A., Shindo, H. & Ito, Y. (2006) "Aqueous–aqueous two-phase systems composed of low molecular weight of polyethylene glycols and dextrans for counter-current chromatographic purification of proteins", *Journal of Chromatography B,* vol. 844, no. 2, pp. 217-222.

Shibusawa, Y., Takeuchi, N., Tsutsumi, K., Nakano, S., Yanagida, A., Shindo, H. & Ito, Y. (2007) "One-step purification of histone deacetylase from Escherichia coli cell-lysate by counter-current chromatography using aqueous two-phase system", *Journal of Chromatography A,* vol. 1151, no. 1-2, pp. 158-163.

Shinkazh, O., Kanani, D., Barth, M., Long, M., Hussain, D. & Zydney, A.L. (2011) "Countercurrent tangential chromatography for large-scale protein purification", *Biotechnology and bioengineering,* vol. 108, no. 3, pp. 582-591.

Shinomiya, K., Menet, J., Fales, H.M. & Ito, Y. (1993) "Studies on a new cross-axis coil planet centrifuge for performing counter-current chromatography: I. Design of the apparatus, retention of the stationary phase, and efficiency in the separation of proteins with polymer phase systems", *Journal of Chromatography A,* vol. 644, no. 2, pp. 215-229.

Shinomiya, K., Menet, J.-., Fales, H.M. & Ito, Y. (1993) "Studies on a new cross-axis coil planet centrifuge for performing counter-current chromatography. I. Design of the apparatus, retention of the stationary phase, and efficiency in the separation of proteins with polymer phase systems", *Journal of chromatography,* vol. 644, no. 2, pp. 215-229.

Shinomiya, K., Inokuchi, N., Gnabre, J.N., Muto, M., Kabasawa, Y., Fales, H.M. & Ito, Y. (1996) "Countercurrent chromatographic analysis of ovalbumin obtained from various sources using the cross-axis coil planet centrifuge", *Journal of Chromatography A,* vol. 724, no. 1-2, pp. 179-184.

Shinomiya, K., Kabasawa, Y. & Ito, Y. (1999) "Effect of elution modes on protein separation by cross-axis coil planet centrifuge with two different types of coiled columns", *Preparative Biochemistry and Biotechnology,* vol. 29, no. 2, pp. 139-150.

Shinomiya, K., Hirozane, S., Kabasawa, Y. & Ito, Y. (2000) "Protein separation by cross-axis coil planet centrifuge with two different positions of eccentric coil assemblies using polyethylene glycol- dextran solvent system", *Journal of Liquid Chromatography and Related Technologies*, vol. 23, no. 7, pp. 1119-1129.

Shinomiya, K., Kabasawa, Y., Yanagidaira, K., Sasaki, H., Muto, M., Okada, T. & Ito, Y. (2003) "Protein separation by nonsynchronous coil planet centrifuge with aqueous–aqueous polymer phase systems", *Journal of Chromatography A*, vol. 1005, no. 1-2, pp. 103-112.

Shinomiya, K. & Ito, Y. (2004) "Effects of the planetary motion of a coiled column on protein separation by the nonsynchronous coil planet centrifuge", *Journal of Liquid Chromatography and Related Technologies*, vol. 27, no. 20, pp. 3243-3255.

Shinomiya, K., Yanagidaira, K. & Ito, Y. (2006) "New small-scale cross-axis coil planet centrifuge: The design of the apparatus and its application to counter-current chromatographic separation of proteins with aqueous–aqueous polymer phase systems", *Journal of Chromatography A*, vol. 1104, no. 1-2, pp. 245-255.

Shinomiya, K., Kobayashi, H., Inokuchi, N., Kobayashi, K., Oshima, H., Kitanaka, S., Yanagidaira, K., Sasaki, H., Muto, M., Okano, M. & Ito, Y. (2007) "New small-scale cross-axis coil planet centrifuge: Partition efficiency and application to purification of bullfrog ribonuclease", *Journal of Chromatography A*, vol. 1151, no. 1-2, pp. 91-98.

Shinomiya, K., Kobayashi, H., Motoyoshi, N., Inokuchi, N., Nakagomi, K. & Ito, Y. (2009) "Countercurrent chromatographic separation and purification of various ribonucleases using a small-scale cross-axis coil planet centrifuge with aqueous–aqueous polymer phase systems", *Journal of Chromatography B*, vol. 877, no. 10, pp. 955-960.

Shinomiya, K. & Ito, Y. (2009) "Partition efficiency of newly designed locular multilayer coil for countercurrent chromatographic separation of proteins using small-scale cross-axis coil planet centrifuge with aqueous-aqueous polymer phase systems", *Journal of Liquid Chromatography and Related Technologies*, vol. 32, no. 8, pp. 1096-1106.

Shinomiya, K., Kobayashi, H., Inokuchi, N., Nakagomi, K. & Ito, Y. (2011) "Partition efficiency of high-pitch locular multilayer coil for countercurrent chromatographic separation of proteins using small-scale cross-axis coil planet centrifuge and application to purification of various collagenases with aqueous-aqueous polymer phase systems", *Journal of Liquid Chromatography and Related Technologies*, vol. 34, no. 3, pp. 182-194.

Shukla, A.A., Gupta, P. & Han, X. (2007) "Protein aggregation kinetics during Protein A chromatography. Case study for an Fc fusion protein", *Journal of Chromatography A*, vol. 1171, no. 1-2, pp. 22-28.

Shukla, A.A., Hubbard, B., Tressel, T., Guhan, S. & Low, D. (2007) "Downstream processing of monoclonal antibodies-Application of platform approaches", *Journal of Chromatography B: Analytical Technologies in the Biomedical and Life Sciences*, vol. 848, no. 1, pp. 28-39.

Shukla, A.A. & Thömmes, J. (2010) "Recent advances in large-scale production of monoclonal antibodies and related proteins", *Trends in biotechnology*, vol. 28, no. 5, pp. 253-261.

Sommerfeld, S. & Strube, J. (2005) "Challenges in biotechnology production - Generic processes and process optimization for monoclonal antibodies", *Chemical Engineering and Processing: Process Intensification*, vol. 44, no. 10, pp. 1123-1137.

Stein, A. & Kiesewetter, A. (2007) "Cation exchange chromatography in antibody purification: pH screening for optimised binding and HCP removal", *Journal of Chromatography B: Analytical Technologies in the Biomedical and Life Sciences,* vol. 848, no. 1, pp. 151-158.

Steinmeyer, D.E. & McCormick, E.L. (2008) "The art of antibody process development", *Drug discovery today,* vol. 13, no. 13-14, pp. 613-618.

Sticher, O. (2008) "Natural product isolation", *Natural product reports,* vol. 25, no. 3, pp. 517-554.

Sutherland, I.A. & Sharpe, J.E.E. (1976) "Counter-current chromatography using a new coil planet centrifuge", *Journal of Chromatography A,* vol. 122, no. C, pp. 333-344.

Sutherland, I.A. (2007) "Countercurrent chromatography" | Large-Scale" in *Encyclopedia of Separation Science*, ed. Ian D. Wilson, Academic Press, Oxford, pp. 1-11.

Sutherland, I.A. (2007) "Recent progress on the industrial scale-up of counter-current chromatography", *Journal of Chromatography A,* vol. 1151, no. 1-2, pp. 6-13.

Sutherland, I.A. (2007) "Review of centrifugal liquid-liquid chromatography using aqueous two-phase solvent systems: Its scale-up and prospects for the future production of high-value biologicals", *Current Opinion in Drug Discovery and Development,* vol. 10, no. 5, pp. 540-549.

Sutherland, I., Hewitson, P., Siebers, R., van den Heuvel, R., Arbenz, L., Kinkel, J. & Fisher, D. (2011) "Scale-up of protein purifications using aqueous two-phase systems: Comparing multilayer toroidal coil chromatography with centrifugal partition chromatography", *Journal of Chromatography A,* vol. 1218, no. 32, pp. 5527-5530.

Sutherland, I., Ignatova, S., Hewitson, P., Janaway, L., Wood, P., Edwards, N., Harris, G., Guzlek, H., Keay, D., Freebairn, K., Johns, D., Douillet, N., Thickitt, C., Vilminot, E. & Mathews, B. (2011)."Scalable Technology for the Extraction of Pharmaceutics (STEP): The transition from academic knowhow to industrial reality", *Journal of Chromatography A,* vol. In Press, Corrected Proof.

Sutherland, I., Hewitson, P. & de Folter, J. (2011)."Toroidal coil chromatography: The effect of scale-up and "g" field on stage efficiency", *Journal of Chromatography A,* vol. In Press, Corrected Proof.

Swinnen, K., Krul, A., Van Goidsenhoven, I., Van Tichelt, N., Roosen, A. & Van Houdt, K. (2007) "Performance comparison of protein A affinity resins for the purification of monoclonal antibodies", *Journal of Chromatography B: Analytical Technologies in the Biomedical and Life Sciences,* vol. 848, no. 1, pp. 97-107.

Tabrizi, M.A., Tseng, C.-.L. & Roskos, L.K. (2006) "Elimination mechanisms of therapeutic monoclonal antibodies", *Drug discovery today,* vol. 11, no. 1-2, pp. 81-88.

Thongborisute, J. & Takeuchi, H. (2008) "Evaluation of mucoadhesiveness of polymers by BIACORE method and mucin-particle method", *International journal of pharmaceutics,* vol. 354, no. 1-2, pp. 204-209.

Toueille, M., Uzel, A., Depoisier, J.-. & Gantier, R. (2011) "Designing new monoclonal antibody purification processes using mixed-mode chromatography sorbents", *Journal of Chromatography B: Analytical Technologies in the Biomedical and Life Sciences,* vol. 879, no. 13-14, pp. 836-843.

Trebak, M., Chong, J.M., Herlyn, D. & Speicher, D.W. (1999) "Efficient laboratory-scale production of monoclonal antibodies using membrane-based high-density cell culture technology", *Journal of immunological methods,* vol. 230, no. 1-2, pp. 59-70.

Trikha, M., Yan, L. & Nakada, M.T. (2002) "Monoclonal antibodies as therapeutics in oncology", *Current opinion in biotechnology,* vol. 13, no. 6, pp. 609-614.

, G. (2004) "Relationship between the protein surface hydrophobicity and its partitioning behaviour in aqueous two-phase systems of polyethyleneglycol- dextran", *Journal of Chromatography B: Analytical Technologies in the Biomedical and Life Sciences,* vol. 799, no. 2, pp. 293-301.

Uhlén, M., Lindberg, M. & Philipson, L. (1984) "The gene for staphylococcal protein A", *Immunology today,* vol. 5, no. 8, pp. 244-248.

van den Heuvel, R.N.A.M. & König, C.S. "Improved g-level calculations for coil planet centrifuges", *Journal of Chromatography A,* vol. In Press, Corrected Proof.

Walker, S.G. & Lyddiatt, A. (1999) "Processing of nanoparticulate bioproducts: Application and optimisation of aqueous two-phase systems", *Journal of Chemical Technology and Biotechnology,* vol. 74, no. 3, pp. 250-255.

Walter, H. & Widen, K.E. (1994) "Cell partitioning in two-polymer aqueous phase systems and cell electrophoresis in aqueous polymer solutions. Human and rat young and old red blood cells", *Biochimica et Biophysica Acta - Biomembranes,* vol. 1194, no. 1, pp. 131-137.

Wang, L., Kanani, D.M. & Ghosh, R. (2006) "Purification of humanized monoclonal antibodies by membrane-based hybrid bioseparation technique", *Journal of immunological methods,* vol. 314, no. 1-2, pp. 1-8.

Wang, L., Mah, K.Z. & Ghosh, R. (2009) "Purification of human IgG using membrane based hybrid bioseparation technique and its variants: A comparative study", *Separation and Purification Technology,* vol. 66, no. 2, pp. 242-247.

Wei, W. (2005) "Protein aggregation and its inhibition in biopharmaceutics", *International journal of pharmaceutics,* vol. 289, no. 1-2, pp. 1-30.

Wei, Y., Zhang, T. & Ito, Y. (2001) "Counter-current chromatographic separation of glycoprotein components from Morchella esculenta (L.) with a polymer phase system by a cross-axis coil planet centrifuge", *Journal of Chromatography A,* vol. 917, no. 1-2, pp. 347-351.

Weiner, L.M., Surana, R. & Wang, S. (2010) "Monoclonal antibodies: Versatile platforms for cancer immunotherapy", *Nature Reviews Immunology,* vol. 10, no. 5, pp. 317-327.

Wood, P., Ignatova, S., Janaway, L., Keay, D., Hawes, D., Garrard, I. & Sutherland, I.A. (2007) "Counter-current chromatography separation scaled up from an analytical column to a production column", *Journal of Chromatography A,* vol. 1151, no. 1-2, pp. 25-30.

Wu, S., Tai, Y., Pan, Y. & Sun, C. (2006) "Effect of gravitational force on type-J counter-current chromatography by mathematical analysis", *Journal of Chromatography A,* vol. 1103, no. 2, pp. 243-247.

Yanagida, A., Isozaki, M., Shibusawa, Y., Shindo, H. & Ito, Y. (2004) "Purification of glucosyltransferase from cell-lysate of Streptococcus mutans by counter-current chromatography using aqueous polymer two-phase system", *Journal of Chromatography B: Analytical Technologies in the Biomedical and Life Sciences*, vol. 805, no. 1, pp. 155-160.

Yang, Y., Aisa, H.A. & Ito, Y. (2009) "Flat-twisted tubing: Novel column design for spiral high-speed counter-current chromatography", *Journal of Chromatography A*, vol. 1216, no. 27, pp. 5265-5271.

Yang, Y., Aisa, H.A. & Ito, Y. (2009) "Mathematical model of computer-programmed intermittent dual countercurrent chromatography applied to hydrostatic and hydrodynamic equilibrium systems", *Journal of Chromatography A*, vol. 1216, no. 35, pp. 6310-6318.

Yang, Y., Gu, D., Aisa, H.A. & Ito, Y. (2010) "Novel designs for centrifugal countercurrent chromatography: V. comparative studies on performance of various column configurations", *Journal of Liquid Chromatography and Related Technologies*, vol. 33, no. 16, pp. 1542-1549.

Yin, L., Xu, L., Yu, K., Zhen, Y., Han, X., Xu, Y., Qi, Y., Peng, J. & Tan, A. (2011) "Orthogonal test design for optimization of suitable conditions to separate C-phycocyanin from Spirulina platensis by high-speed counter-current chromatography using reverse micelle solvent system", *Journal of Separation Science*, vol. 34, no. 11, pp. 1253-1260.

Yin, L., Sun, C.K., Han, X., Xu, L., Xu, Y., Qi, Y. & Peng, J. (2011) "Preparative purification of bromelain (EC 3.4.22.33) from pineapple fruit by high-speed counter-current chromatography using a reverse-micelle solvent system", *Food Chemistry*, vol. 129, no. 3, pp. 925-932.

Zaslavsky, A., Gulyaeva, N. & Zaslavsky, B. (2000) "Peptides partitioning in an aqueous dextran-polyethylene glycol two- phase system", *Journal of Chromatography B: Biomedical Sciences and Applications*, vol. 743, no. 1-2, pp. 271-279.

Zhang, Q., Chen, G., Liu, X. & Qian, Q. (2007) "Monoclonal antibodies as therapeutic agents in oncology and antibody gene therapy", *Cell research*, vol. 17, no. 2, pp. 89-99.

Zhi, W., Deng, Q., Song, J., Gu, M. & Ouyang, F. (2005) "One-step purification of α-amylase from the cultivation supernatant of recombinant Bacillus subtilis by high-speed counter-current chromatography with aqueous polymer two-phase systems", *Journal of Chromatography A*, vol. 1070, no. 1-2, pp. 215-219.

Zhi, W.B., Deng, Q.Y., Song, J.N. & Ouyang, F. (2005) "Purification of ovalbumin from hen egg white by high-speed counter-current aqueous two-phase chromatography", *Sheng wu gong cheng xue bao = Chinese journal of biotechnology*, vol. 21, no. 1, pp. 129-134.

Zhou, J.X., Dermawan, S., Solamo, F., Flynn, G., Stenson, R., Tressel, T. & Guhan, S. (2007) "pH-conductivity hybrid gradient cation-exchange chromatography for process-scale monoclonal antibody purification", *Journal of Chromatography A*, vol. 1175, no. 1, pp. 69-80.